

See discussions, stats, and author profiles for this publication at: <https://www.researchgate.net/publication/257544445>

Fundamental Questions in Astrophysics: Guidelines for Future UV Observatories

Book · January 2006

DOI: 10.1007/978-1-4020-4839-5

CITATIONS

2

READS

80

2 authors, including:



A. I. Gómez de Castro

Complutense University of Madrid

226 PUBLICATIONS 1,026 CITATIONS

[SEE PROFILE](#)

Some of the authors of this publication are also working on these related projects:



Ultraviolet astronomy [View project](#)

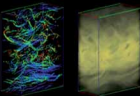
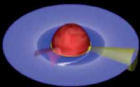
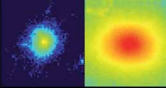
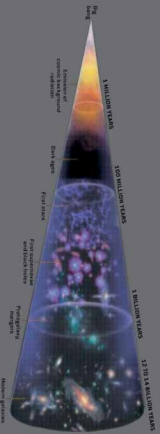


Fresnel imager [View project](#)

Fundamental Questions in Astrophysics: Guidelines for Future UV Observatories

Edited by

Ana I. Gómez de Castro
and Willem Wamsteker



FUNDAMENTAL QUESTIONS IN ASTROPHYSICS: GUIDELINES FOR FUTURE UV OBSERVATORIES

Edited by:

ANA I. GÓMEZ DE CASTRO and WILLEM WAMSTEKER

Reprinted from *Astrophysics and Space Science*
Volume 303, Nos. 1–4, 2006



Library of Congress Cataloging-in-Publication Data is available

ISBN 1-4020-4838-6 (hardbook)

ISBN 1-4020-4839-4 (eBook)

ISBN 978-1-4020-4838-6 (hardbook)

ISBN 978-1-4020-4839-4 (eBook)

Published by Springer,
P.O. Box 17, 3300 AA Dordrecht, The Netherlands.

Picture left: inserted as tribute to the late Willem Wamsteker who liked this image very much

Pictures right:

Top: Galaxy halo if the Universe reionized at redshift 15 or 6, by Kenji Bekki & Masashi Chiba, Tohoku University, Japan

Below: Sonic Point model of KiloHertz QPOs, by M. Colleman, F.K. Lamb & D. Psaltis

Below: Simulations of accretion disks, by J.F. Hawley, S.A. Balbus, J.M. Stone

Below: Simulations of the interaction of the accretion disk and the magnetized star in a T Tauri System, by Brigitta von Rekowsky & Axel Branderger

Bottom: Artist illustration of the evaporation of an exoplanet atmosphere, by European Space Agency and Alfred Vidal-Madjar (Institut d'Astrophysique de Paris)

Printed on acid-free paper

All Rights Reserved
© Springer 2006

No part of the material protected by this copyright notice may be reproduced or utilized in any form or by any means, electronic or mechanical, including photocopying, recording or by any information storage and retrieval system, without written permission from the copyright owner.

Printed in the Netherlands

TABLE OF CONTENTS

Foreword	1–2
M.A. Barstow and K. Werner / Structure and Evolution of White Dwarfs and their Interaction with the Local Interstellar Medium	3–16
Isabella Pagano, Thomas R. Ayres, Alessandro C. Lanzaflame, Jeffrey L. Linsky, Benjamín Montesinos and Marcello Rodonò / Key Problems in Cool-Star Astrophysics	17–31
Ana I. Gómez de Castro, Alain Lecavelier, Miguel D'Avillez, Jeffrey L. Linsky and José Cernicharo / UV Capabilities to Probe the Formation of Planetary Systems: From the ISM to Planets	33–52
Boris T. Gänsicke, Domitilla de Martino, Thomas R. Marsh, Carole A. Haswell, Christian Knigge, Knox S. Long and Steven N. Shore / Ultraviolet Studies of Interacting Binaries	53–68
Willem Wamsteker, Jason X. Prochaska, Luciana Bianchi, Dieter Reimers, Nino Panagia, Andrew C. Fabian, Claes Fransson, Boris M. Shustov, Patrick Petitjean, Philipp Richter and Eduardo Battaner / The Need for Ultraviolet to Understand the Chemical Evolution of the Universe, and Cosmology	69–84
Rosa M. González Delgado / Starbursts at Space Ultraviolet Wavelengths	85–102
Noah Brosch, John Davies, Michel C. Festou and Jean-Claude Gérard / A View to the Future: Ultraviolet Studies of the Solar System	103–122
Wolfram Kollatschny and Wang Ting-Gui / Active Galaxies in the UV	123–132
Ana I. Gómez de Castro, Willem Wamsteker, Martin Barstow, Noah Brosch, Norbert Kappelmann, Wolfram Kollatschny, Domitilla de Martino, Isabella Pagano, Alain Lecavelier des Étangs, David Ehenreich, Dieter Reimers, Rosa González Delgado, Francisco Najarro and Jeff Linsky / Fundamental Problems in Astrophysics	133–145
Norbert Kappelmann and Jürgen Barnstedt / Guidelines for Future UV Observatories	147–151
F. Najarro, A. Herrero and E. Verdugo / Massive stars in the UV	153–170

Foreword

© Springer Science + Business Media B.V. 2006

Modern astrophysics is a mature science that has evolved from its early phase of discovery and classification to a physics-oriented discipline focussed in finding answers to fundamental problems ranging from cosmology to the origin and diversity of life-sustainable systems in the Universe. For this very reason, progress of modern astrophysics requires the access to the electromagnetic spectrum in the broadest energy range. The Ultraviolet is a fundamental energy domain since it is one of the most powerful tool to study plasmas at temperatures in the 3,000–300,000 K range as well as electronic transitions of the most abundant molecules in the Universe. Moreover, the UV radiation field is a powerful astrochemical and photoionizing agent.

The impact of UV instruments in astronomical research can be clearly traced through the considerable success of the International Ultraviolet Explorer (IUE) observatory and successor instruments such as the GHRS and STIS spectrographs on-board the Hubble Space Telescope (HST), or the FUSE satellite operating in the far UV (90–120 nm range). Of particular importance has been access to high resolution $R \simeq 40,000$ –100,000 spectra providing an ability to study the dynamics of hot plasma and separate multiple galactic, stellar or interstellar spectral lines. Furthermore, the GALEX satellite is providing new exciting views of UV sources.

This book describes the fundamental problems in modern astrophysics that cannot progress without easy and widespread access to modern UV instrumentation. Three among them should be stressed by its relevance:

1. Extrasolar planetary atmospheres and astrochemistry in the presence of strong UV radiation fields.
2. Chemical evolution of the Universe and the diffuse baryonic content.
3. The physics of accretion and outflow: the astronomical engines.

The volume contains a series of review articles that analyze the scientific requirements for modern UV instrumentation. The first article summarizes the science case for UV astronomy. After, several articles targeting the major research fields of astrophysics from Solar System to cosmological research are included. These articles analyze why and which UV instrumentation is required to make progress in each field. The book ends with a summary of the UV instrumentation demanded by the community and a brief update on technological requirements. All articles in this volume have gone through the peer-review system of the journal “*Astrophysics and Space Science*.”

This book contains the thoughts and work of the Network for UV astrophysics (NUVA) and the UV community at-large. By the end of 2002, a group of European astronomers coming from a broad range of areas: from fundamental astrophysical research to observational expertise in the optical, UV and X-ray ranges, as well as space instruments development teams, joined efforts to evaluate the need to develop new UV instrumentation for the coming decade in order to achieve some of the major scientific objectives of the astronomical community and make full profit of the large astronomical facilities planned for other spectral ranges; this group set the seed for the Network for UltraViolet Astrophysics (NUVA). At that time, STIS was working in HST and the Cosmic Origins Spectrograph (COS) was being built for replacement; HST was thought to last till 2010/12, FUSE was working nominally and GALEX was close to be launched. However, the big space agencies had no plans for new UV spectroscopic missions unless the large optical/UV telescope included in the NASA Origins plan targeted to enter development phase in 2015–2020 and to be launched in the second quarter of this century. Unfortunately, on Friday 16 January 2004 NASA informed that the planned shuttle mission to service and upgrade HST (SM-4) including the substitution of STIS by

COS, had been cancelled. Just few months later STIS failed. No access to high resolution UV spectroscopy has been feasible during most of 2005 since FUSE resumed observations in November 2005 after the failure of the third of the four onboard reaction wheels in December 2004. The NUVA was officially established in January 2004. A key objective of the NUVA is to run an exploratory analysis to define the scientific requirements for future UV observatories. This book contains the first outcome of this work and its publication has been funded by the NUVA as a part of its activities. The NUVA is within the Optical Infrared Co-ordination Network for Astronomy (OPTICON) funded by the European Commissions 6th Framework programme under contract number RII3-Ct-2004-001566.

In these two years, some respected colleagues and dear friends who actively promoted and enthusiastically collaborated in this project have passed away.

Willem Wamsteker was the director of ESA's IUE Observatory until the mission terminated in 1996. After his direction, the IUE data archive became the first fully internet driven astronomical archive. Willem was a promotor of the NUVA and a key initiator of the World Space Observatory UV (WSO/UV) project; a 1.7 m UV telescope equipped with state of the art instrumentation providing a factor of 10 improvement on the high resolution spectroscopic capabilities of HST/STIS. WSO/UV will be launched in 2010 becoming

the only UV spectroscopic facility available world-wide. The project is driven by a broad international collaboration led by Russia (ROSCOSMOS); there is a significant European participation in the project. Willem Wamsteker was also co-editor of "*Astrophysics and Space Science*" and deeply involved in the edition of this volume.

Marcello Rodonó was director of the Obsservatorio Astrofisico di Catania and a very relevant member of the "cool stars" community. He was keen off multi-wavelength studies and an active promotor of the WSO/UV project.

Michel Festou was director of l'Observatoire de Besançon and a passionate researcher. His work on UV spectroscopy of comets is reknowned world-wide. He actively collaborated with the NUVA in the identification of the UV facilities needed to make progress on Solar System Research.

We would like to dedicate this book to their memory.

Finally, we would like to thank our OPTICON colleagues and very especially John Davies (OPTICON Project Scientist) and Gerry Gilmore (OPTICON P.I.) for their support. We also acknowledge the support of the Universidad Complutense de Madrid which is hosting and maintaining the NUVA site (www.ucm.es/info/NUVA).

Prof. Ana Inés Gómez de Castro
NUVA, chair
Madrid, March 1st, 2006

Structure and Evolution of White Dwarfs and their Interaction with the Local Interstellar Medium

M.A. Barstow · K. Werner

Received: 11 March 2005 / Accepted: 11 August 2005
© Springer Science + Business Media B.V. 2006

Abstract The development of far-UV astronomy has been particularly important for the study of hot white dwarf stars. A significant fraction of their emergent flux appears in the far-UV and traces of elements heavier than hydrogen or helium are, in general, only detected in this waveband or at shorter wavelengths that are also only accessible from space. Although white dwarfs have been studied in the far-UV throughout the past ~ 25 years, since the launch of *IUE*, only a few tens of objects have been studied in great detail and a much larger sample is required to gain a detailed understanding of the evolution of hot white dwarfs and the physical processes that determine their appearance. We review here the current knowledge regarding hot white dwarfs and outline what work needs to be carried out by future far-UV observatories.

Keywords Ultraviolet astronomy · Space missions · White dwarfs

1. Introduction

1.1. White dwarf stars and the local interstellar medium in astrophysics

Many white dwarfs are among the oldest stars in the Galaxy. Their space and luminosity distributions help map out the history of star formation in the Galaxy and can, in principle, determine the age of the disk by providing an important

lower limit to the age of the Universe. Recently, it has been suggested that cool white dwarfs may account for a substantial fraction of the missing mass in the galactic halo (Oppenheimer et al., 2001). White dwarfs are also believed to play a role in the production of type Ia supernovae, through possible stellar mergers or mass transfer. Although no candidate precursor system has yet been found, they are used as “standard candles” to measure the distances of the most remote objects in the Universe and to imply a non-zero value for the cosmological constant. It is intriguing that such local, low luminosity objects as white dwarf stars play a key role in some of the most important cosmological questions of our day, concerning the nature and fate of the Universe. To understand and calibrate cosmologically important aspects of white dwarfs, such as their cooling ages, masses and compositions, we require a thorough understanding of how their photospheric compositions evolve. Atmospheric metal abundances affect cooling rates and bias the determination of temperature and surface gravity. Reliable masses can only be derived from accurate effective temperature and surface gravity measurements. Importantly, metals are difficult to detect in cool white dwarfs but still play an important role in cooling. Therefore, abundances measured in hotter stars provide important data as to what species may be present and in what quantities.

Interstellar gas is a fundamental component of the Milky Way and other galaxies. The local interstellar medium (LISM) is particularly important because it is close enough to us for detailed examination of its structure. Indeed, it is the only part of the Universe, apart from the solar system, that we can study directly, from the penetration of neutral particles through the heliopause. Study of the composition of the local interstellar gas tells us about the evolution of the Universe and our galaxy. While modified considerably since the formation of the solar system, the processes that have shaped the ISM

M.A. Barstow (✉)
Department of Physics and Astronomy, University of Leicester,
University Road, Leicester LE1 7RH, UK
e-mail: mab@star.le.ac.uk

K. Werner
Universität Tübingen, FRG, Tübingen

must have also affected the solar system and possibly even the evolution of life. For example, the local radiation field and gas properties of the LISM set the boundary conditions for the heliosphere. Therefore, it regulates the properties of the interplanetary medium and the cosmic ray fluxes through the solar system (see Frisch et al., 2002), which may affect the terrestrial climate (Mueller et al., 2003).

The relationship between white dwarfs and the LISM is intimate. The process of producing white dwarfs in the disk substantially enriches the content of the local ISM (Margio, 2001) and white dwarfs contribute significantly to the total cosmic abundance of metals (Pagel, 2002). They also provide a significant fraction of the total flux of ionizing radiation within the LISM and will affect the ionization state of the interstellar gas, even if the LISM is not in ionization equilibrium. At the same time, white dwarfs may be accreting material from the denser clouds in the ISM, which will modify their photospheric abundances. Finally, white dwarfs are ideal background sources for direct study of the LISM.

1.2. Physical structure and classification of white dwarfs

Astronomers have known about the existence of white dwarf stars for 150 years, since the discovery of a companion to the brightest star in the sky, Sirius. Studying the regular wave-like proper motion of Sirius, Bessel revealed the presence of a hidden companion, with the pair eventually resolved by Clark in 1862 and the orbital period revealed to be 50 years. Later, the first spectroscopic study of the system by Adams revealed a great enigma. While the temperature of Sirius B was found to be higher than Sirius A, it was apparently 1000 times less luminous. This result could only be explained if Sirius B had a very small radius, $1/100 R_{\odot}$ and similar to that of the Earth. However, with a known mass of $\sim 1 M_{\odot}$ for Sirius B, the implied density of $1400 \text{ Tonnes m}^{-3}$ was well above that of any form of matter known to 19th and early 20th century physicists. Within a number of years, a handful of stars similar to Sirius B were found, mostly in binaries. The term “white dwarf” was coined later, on the basis of the visual color and small size, when compared to other stars.

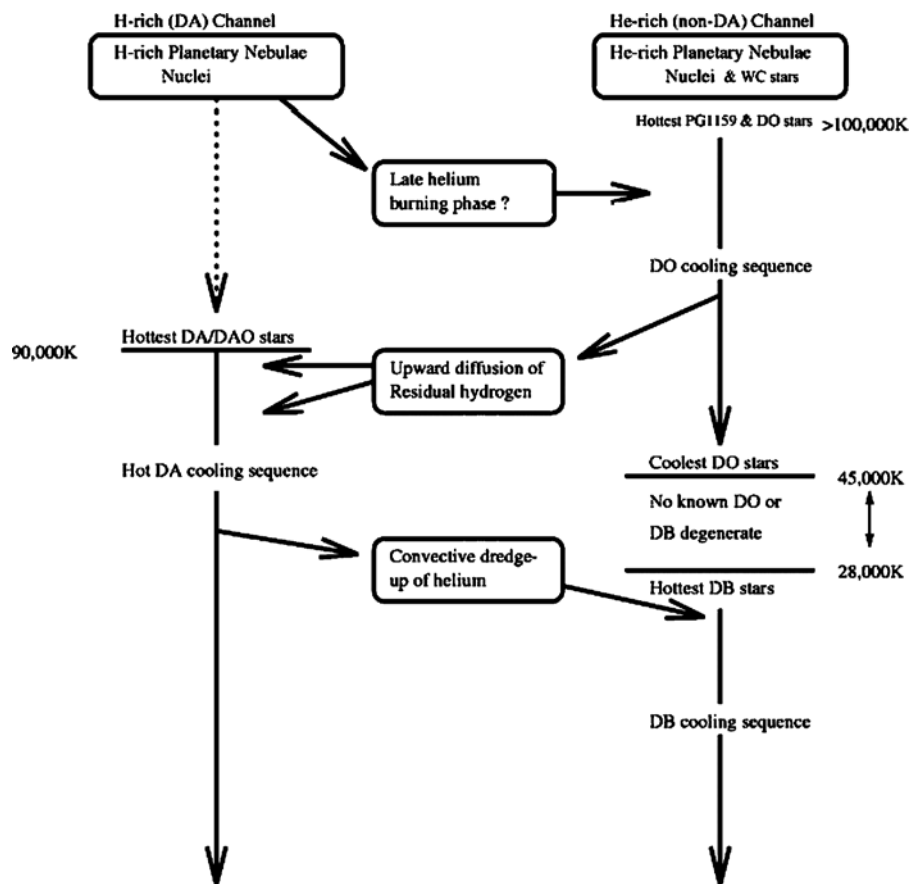
The answer to the riddle of their structure stems from the development of the quantum statistical theory of the electron gas by Enrico Fermi and Paul Dirac. When atoms in a material are sufficiently close together, their most weakly bound electrons move freely about the volume and can be considered to behave like a gas. Almost all the electrons in the gas will occupy the lowest available energy levels. Any states with the same energy are said to be “degenerate.” Hence, this gas is known as the “degenerate electron gas.” Under conditions of extreme pressure the electrons are forced to occupy space much closer to the nuclei of the constituent atoms than in normal matter, breaking down the quantised structure of

the energy levels. However, according to the Pauli Exclusion Principle, no two electrons can occupy the same quantum state, which has a finite volume in position-momentum space, so there is a limit where a repulsive force arising from this, the “electron degeneracy pressure”, resists further compression of the material. Fowler (1926) showed that this pressure could support a stellar mass against gravitational collapse and proposed that this might explain the existence of white dwarfs. Combining this insight with the equations of stellar structure, Chandrasekhar (1931, 1935) determined the mass-radius relation for white dwarfs and the maximum mass ($1.4 M_{\odot}$) that electron degeneracy pressure could support against gravity, the Chandrasekhar limit. As this Nobel Prize winning work has been extended by subsequent developments, the basic ideas remain unchanged. However, importantly, they have also hardly been tested by direct observation.

Theoretical and observational study of stellar evolution has placed white dwarfs as one possible end point of the process. In general terms, all stars with masses below about 8 times that of the Sun will pass through one or more red giant phases before losing most of their original mass to form a planetary nebula. The remnant object, a white dwarf, is the core of the progenitor star. In the absence of any internal source of energy, the temperature of a white dwarf, after its birth, is determined by how rapidly stored heat is radiated into space. Estimates of white dwarf cooling times indicate that it will take several billion years for the stars to fade to invisibility. Hence, white dwarfs are among the oldest objects in the galaxy. Since, the galaxy is younger than the cooling timescales; the lowest temperature (oldest) white dwarfs yield a lower limit to its age.

The basis for understanding the nature of most stars is analysis of their optical spectra and classification according to the characteristics revealed. A number of physical processes can alter the atmospheric composition of a white dwarf as it cools. As noted by Schatzmann (1958), the strong gravitational field ($\log g \sim 8$ at the surface) causes rapid downward diffusion of elements heavier than the principal H or He component. Hence, Schatzmann predicted that white dwarf atmospheres should be extremely pure. Consequently, the spectra should be devoid of most elements, showing signatures of only hydrogen and, possibly, helium. White dwarfs are thus divided into two main groups according to whether or not their spectra are dominated by one or other of these elements. The hydrogen-rich stars are given the classification DA, while the helium-rich white dwarfs are designated DO if HeII features are present (hotter than about 45,000 K) and DB if only HeI lines are visible. Small numbers of hybrid stars exist, with both hydrogen and helium present. In these cases, two classification letters are used, with the first indicating the dominant species. For example, DAO white dwarfs are mostly hydrogen but exhibit weak HeII features.

Fig. 1 Schematic description of the production of H-rich and He-rich branches of white dwarf evolution



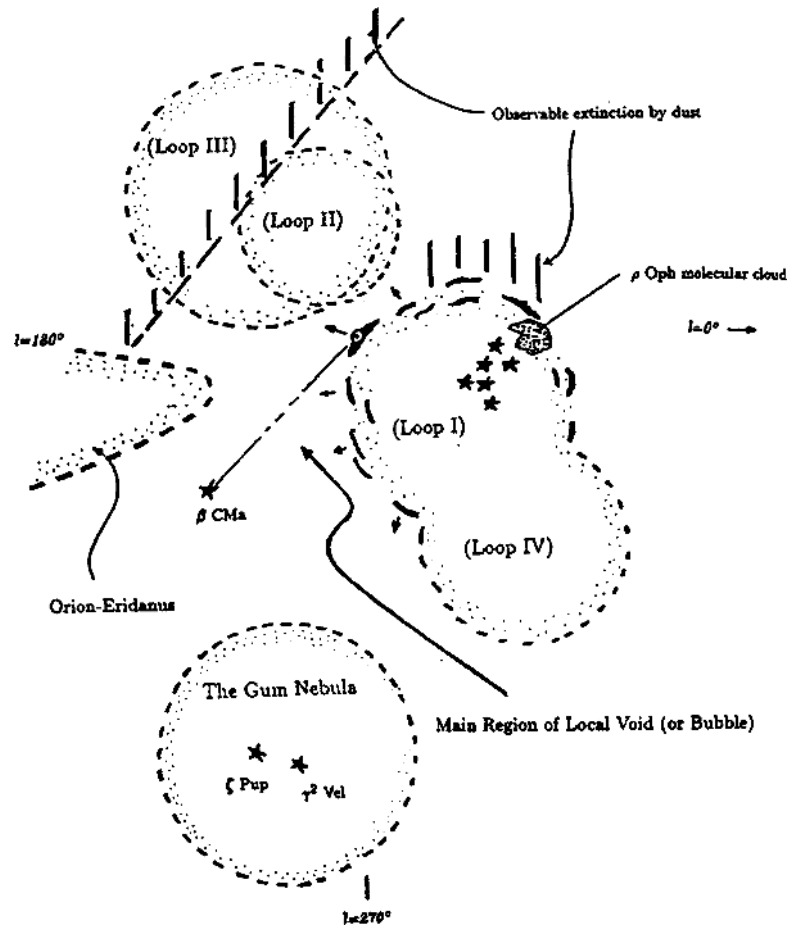
The above classification scheme applies only to white dwarfs with temperatures above $\sim 10,000$ K, when the H and He energy levels are sufficiently populated above the ground state to produce detectable features at visual wavelengths. At lower temperatures, although H and/or He may be present these elements are no longer directly detectable. Cool white dwarfs are divided into three main groups. DC white dwarfs have continuous, completely featureless spectra; DZ white dwarfs are He-rich and have only metal lines visible; DQ white dwarfs show carbon features. Figure 1 summarises the current thoughts regarding the relationships between the hot white dwarf groups along with the principal mechanisms that provide evolutionary routes between them.

Gravity is not necessarily the only influence on photospheric composition. It can be countered by radiation pressure which acts outward to support heavy elements in the atmosphere, a process termed “radiative levitation.” Another mechanism that can mix elements that have settled out in the stellar atmosphere is convection. If the convective zone reaches down to the base of the atmosphere then heavy elements can be dredged back up into the outer atmosphere. A further complication is that material can also be accreted from the interstellar medium.

1.3. The structure of the local interstellar medium

The Sun is embedded in the Local Interstellar Cloud (LIC), a warm ($T \sim 10,000$ K), low-density ($n \sim 0.1 \text{ cm}^{-3}$) region, which is observed in projection toward most, but not all, nearby stars. Models of the LIC (Redfield and Linsky, 2000) show the Sun located just inside the edge of the LIC in the direction of the Galactic Center and toward the North Galactic Pole (NGP). The LIC is surrounded by a hot 10^6 K substrate and appears to be part of the expanding cloud complex representing the Loop I radio shell, which is either a supernova remnant or a wind blown shell from the Sco-Cen Association (Fig. 2). Indeed, evidence for shocks in the LIC within the past 2 Myr is supported by EUV observations of ionized interstellar HeII (Lyu and Bruhweiler 1996; Barstow et al., 1997). Also, surrounding the LIC is the low density Local Bubble with dimensions of >200 pc. Soft X-ray and OVI observations imply this region is largely filled with a hot ($T \sim 10^6$ K), extremely low-density ($n \sim 10^{-2} \text{ cm}^{-3}$) plasma. Frisch (1995) and Bruhweiler (1996) discuss possible origins of Loop I and the Local Bubble, but we need to resolve two key questions. What is the geometry of the Local Bubble? What are the distribution, physical conditions, and kinematics of clouds in the Local Bubble? The answers

Fig. 2 View of the LISM within 400 pc of the Sun. The Sun is located at the end of the dashed line extending from the star β CMa. The dashed line is ~ 200 pc in length. The region of the Local Void or Local Bubble is denoted. Most of the volume of the LISM is composed of very low-density gas. The radio loop structures are further indicated. The stars of Sco-Cen are interior to Loop I. Regions of high dust extinction, regions where dense clouds are found, are also marked. From Bruhweiler (1996)



to these questions also bear directly on whether interstellar accretion is possible in specific white dwarfs.

2. The complex nature of the DA white dwarf population

2.1. Composition and structure of the stellar photospheres from UV spectroscopy

The emergence from the Asymptotic Giant Branch (AGB) of the two H- and He-rich groups, is qualitatively understood to arise from differences in precise evolutionary paths. The He-rich group undergoes a late helium shell flash, which causes convective mixing of the outer envelope. Hydrogen is ingested and burnt or diluted by this process (e.g., Herwig et al., 1999). The majority of young white dwarfs are of DA type, out numbering the He-rich objects by a ratio of $\sim 7:1$ (Fleming et al., 1986; Liebert et al., 2005). The more recent, deeper, Sloan Digital Sky Survey appears to yield an even higher value of 9:1 for the ratio of DAs to the total number of DO and DB white dwarfs (Kleinman et al., 2004). However, the complex relationships between these groups and a demonstrable temperature gap in the He-rich cooling se-

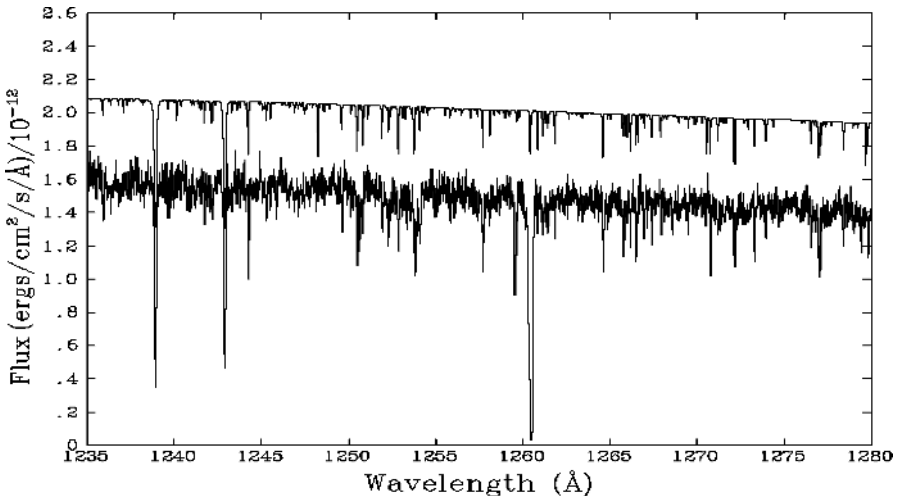
quence cannot yet be readily explained. For example, the ratio of H-rich to He-rich progenitors (4:1) is lower than that of the white dwarfs into which they evolve (Napiwotzki, 1999). Furthermore, a gap in the He-rich sequence, between ~ 45000 and 30000 K, separating the DO and DB white dwarfs (Wesemael et al., 1985; Liebert et al., 1986; Dreizler and Werner, 1996) implies that He-rich white dwarfs must temporarily be seen as DA stars due to some physical process.

It is well established that the hottest ($T \sim 50,000$ K) white dwarfs possess significant abundances of elements heavier than He in their atmospheres. Typical ranges are shown in Table I for the most important elements. Mass fractions are given, with respect to H for DAs and He for DOs, since they are essentially independent of nuclear burning, if the element does not participate in the process. Observed abundances may vary considerably with temperature, as discussed later. Hence, we list typical values and comment on the possible ranges in each white dwarf pathway. Studying how photospheric abundance patterns change as these stars cool can delineate the evolutionary pathways followed by white dwarfs. For example, abundance enhancements in C, N and O may be a sign of near exposure of the C–O core during the AGB phase or of a late He-shell burning episode.

Table 1 Abundances of important heavy elements observed in DA and DO white dwarfs

Note that the values are much more uncertain for the less well-studied DO stars

Element	DA		DO	
	Typical value	Comment	Typical value	Comment
C	10^{-6} to 10^{-5}	Zero in coolest	3×10^{-3}	
N	10^{-6}	From zero to 10^{-2} at extremes	5×10^{-5}	In a few cases
O	10^{-4}	Zero in coolest	10^{-5}	
Si	10^{-4}	Seen at most temps down to 10^{-8}	10^{-4}	
Fe	$2\text{--}5 \times 10^{-4}$	Zero in coolest	—	Not detected in any DOs
Ni	$1\text{--}2 \times 10^{-5}$	Zero in coolest	10^{-4}	

Fig. 3 1230 Å to 1280 Å region of the STIS spectrum of REJ0558-373, showing photospheric absorption lines of N V (1238.821/1242.804 Å) and large numbers of Ni lines. The best-fit synthetic spectrum is shown offset for clarity. The strong line near 1260 Å, present in the observation but not in the model, is interstellar Si II (from Barstow et al., 2003b)

Focused spectroscopic studies of the hottest white dwarfs have begun to establish the general pattern of abundance with respect to evolutionary status. Ultraviolet observations have played an essential role by providing access to absorption lines of elements heavier than H or He. Such features are not present in optical or IR data except where photospheric abundances are unusually high. Indeed, He is also hard to detect, requiring abundances in excess of a few times 10^{-3} in the visible band. Typical detection limits in the UV are two orders of magnitude lower. Therefore, the most important and useful transitions, particularly many resonance lines of elements heavier than H and He, lie in the far-ultraviolet (far-UV, 1000–2000 Å). However, since the lines are expected to be weak and narrow, they are only normally visible at high resolution ($R > 20,000$). An example is a small section of the high-resolution spectrum of the DA white dwarf REJ0558-373, recorded with the Space Telescope Imaging Spectrograph (STIS) onboard *HST* (Fig. 3), which shows the interstellar 1260.4 Å line of Si II together with photospheric NV.

A survey of 25 hot DA white dwarfs, based on IUE and HST data (Barstow et al., 2003b), shows that, while the presence or absence of heavy elements largely reflects what would be expected if radiative levitation were the support-

ing mechanism, the measured abundances do not match predicted values very well. These and earlier results are forcing us to confront complexities in the real physical structure of the stars. For example, it has become clear that the shape and strength of the Balmer line profiles, from which T_{eff} and $\log g$ (and, indirectly, mass) are measured, are dependent on the stellar photospheric abundances, requiring a self-consistent analysis of each individual star based on data acquired at all wavelengths (Barstow et al., 1998). Furthermore, we now have direct observational evidence (Barstow et al., 1999; Dreizler and Wolff, 1999) that photospheric heavy elements are not necessarily homogeneously distributed (by depth) and that more complex stratified structures must be considered. While almost all stars hotter than $\sim 50,000$ K contain heavy elements, as expected, there is an unexplained dichotomy at lower temperatures, with some stars having apparently pure H atmospheres and others detectable quantities of heavy elements (Barstow et al., 2003b, e.g., Fig. 4). In many of these objects the photospheric opacity does not reveal itself in EUV photometric or spectroscopic observations, implying that the observed material resides in a thin layer in the uppermost region of the photosphere (see Holberg et al., 1999; Barstow et al., 2003b). The effect of this stratification can be observed directly with high resolution UV spectroscopy. Figure 5 shows

Fig. 4 Measured abundances of nitrogen (number ratio with respect to hydrogen) as a function of T_{eff} for a sample of 25 DA white dwarfs (from Barstow et al., 2003b)

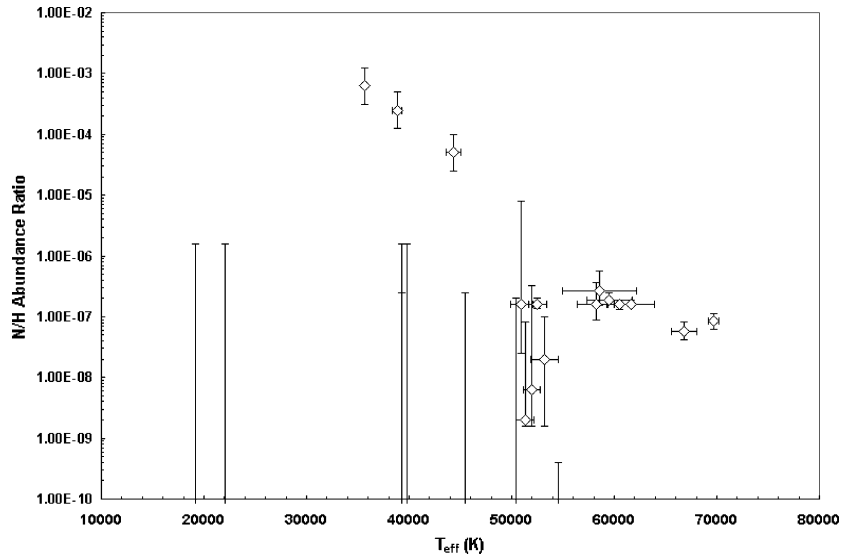
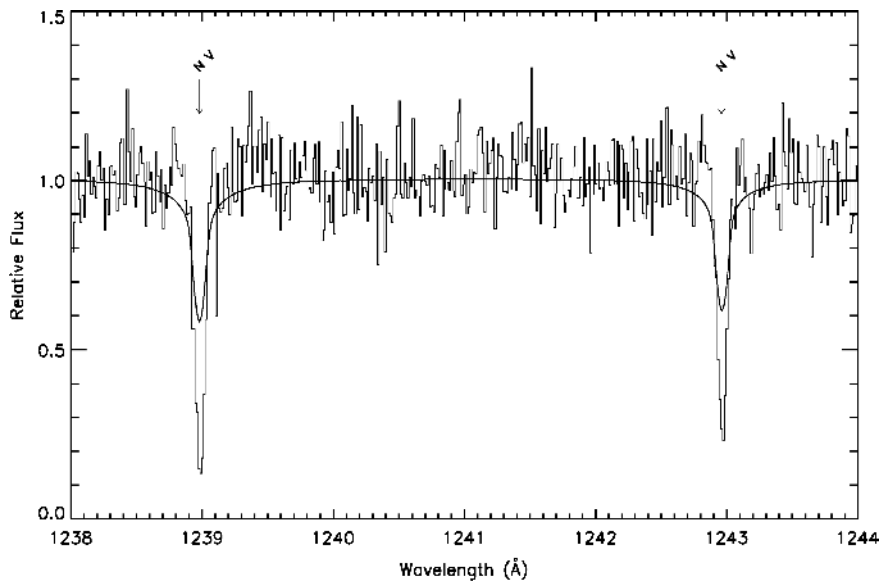


Fig. 5 The STIS E140M spectrum of REJ1032+532 in the region of the NV resonance doublet (histogram), compared to the predicted line profiles from a homogeneous model atmosphere calculation (from Holberg et al., 1999)



the HST/STIS spectrum of the white dwarf REJ1032+532, compared to that predicted by a homogeneous model stellar atmosphere. The N V line profiles in the model have significantly broader wings than are observed, while a stratified model (not shown) gives a much better match to the data.

Recently, important progress has been made in incorporating radiative levitation and diffusion self-consistently into the atmosphere calculations (Dreizler and Wolff, 1999; Schuh et al., 2002). This work reconciles the overall spectral distribution across the soft X-ray, EUV and far-UV bands with the models (a problem with homogeneously distributed elements) and explains the level of stratification inferred for various elements. However, the abundance predictions do not match observations for the known gravity of each star observed, and agreement requires a higher surface grav-

ity than allowed by the optical data. In particular, we cannot account for the large observed compositional differences between stars with identical temperature and surface gravity.

In almost all the hot DA white dwarfs observed, the high ionization resonance lines arising from photospheric heavy elements have blue-shifted components, indicating that there is some circumstellar gas present (Bannister et al., 2003). Whether or not this material is a remnant of the planetary nebula or due to ongoing mass-loss is unresolved. This has important consequences for our basic understanding of stellar composition. The effects of mass-loss, in the form of weak winds ejecting material into the local ISM, and direct accretion of material from the ISM are likely to be of great importance in providing a plausible framework that can explain measured abundances.

Hot He-rich DO white dwarfs are the progeny of stars which constitute an interesting spectral class. Much of the detailed physics involved in studying their atmospheres is similar to that of the DA white dwarfs. However, the levitation of heavy elements in these objects is far from understood. The DO progenitors are the so-called PG1159 stars, hot hydrogen-deficient objects, some of which represent the hottest white dwarfs known, while others are still burning helium in a shell.

Optical and UV spectral analyses have shown that the effective temperatures of PG1159 stars range between 75,000 and 200,000 K and the derived surface gravities are between $\log g = 5.5$ and 8 (Werner, 2001). They are probably the outcome of a late helium-shell flash, a phenomenon that drives the fast evolutionary rates of three well-known objects (FG Sge, Sakurai's object, V605 Aql). Flash-induced envelope mixing produces a H-deficient stellar surface (Herwig et al., 1999). The He-shell flash transforms the star back to an AGB star (born-again AGB star) and the subsequent, second post-AGB evolution explains the existence of Wolf-Rayet central stars of planetary nebulae (spectral type [WC]) and their successors, the PG1159 stars. The photospheric composition then essentially reflects that of the region between the H- and He-burning shells in the precursor AGB star. It is dominated by He, C, and O. Typical values are He = 33%, C = 50%, O = 17% (by mass), however, a considerable spread of abundance patterns is observed, pointing to complicated processes in the stellar interiors. Few stars show traces of nitrogen (1%) or considerable amounts of residual hydrogen (about 25%).

PG1159 stars provide the unique possibility of studying the chemistry in the intershell region between the H- and He-burning shells that is created after complicated and still poorly understood burning and mixing processes during the AGB phase. Usually the intershell material remains hidden within the stellar interior. During the third dredge-up on the AGB, however, intershell material can get mixed into the

convective surface layer and appears on the stellar surface, though in rather diluted abundances. Nevertheless, this process defines the role of AGB stars as contributors of nucleolarly processed matter to the Galaxy. The motivation to study PG1159 stars is based on the fact that these objects *directly* display their intershell matter. It can be expected that gravitational settling is not affecting the composition, because of ongoing mass-loss and convective motions. However, the quantitative interpretation of the abundance analyses is still premature because evolutionary calculations through a final He-shell flash including a full nuclear network are not yet available.

High-resolution UV spectroscopy was crucial in making surprising discoveries which provide essential constraints to calibrate theoretical modeling of stellar evolution. Generally, UV spectra of PG1159 stars show only few photospheric (absorption) lines, mainly from He II, C IV, O VI, and Ne VII. Some of them display shallow N V lines and in many of them we see sulfur. The S VI 933/944 Å doublet in K1-16, for example, suggests a solar abundance, which is in line with the expectation that S is not affected by nuclear processes. Silicon was also identified in some objects (Reiff et al., 2005), but detailed abundance analyses remain to be done.

A very surprising result of UV spectroscopy was the detection of a significant iron deficiency (1–2 dex) in the three best studied PG1159 stars (Miksa et al., 2002). Obviously, iron was transformed to heavier elements in the intershell region of the AGB star by n-captures from the neutron source $^{13}\text{C}(\alpha, n)^{16}\text{O}$ (Herwig et al., 2003). Subsequently, several other studies have also revealed an iron-deficiency in [WC]-type central stars, which matches our picture that these stars are immediate PG1159 star progenitors. Another important result was accomplished by the identification of one of the strongest absorption lines seen in FUSE spectra of most PG1159 stars, located at 973.3 Å. It is a Ne VII line (Fig. 6) that allowed us to assess the neon abundance in a large sample of objects (Werner et al., 2004).

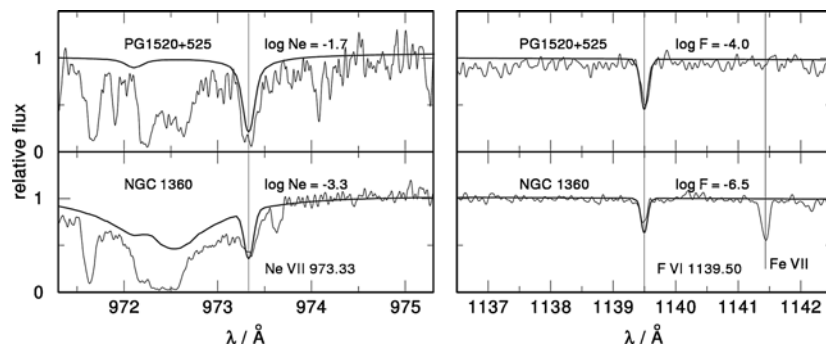


Fig. 6 Discovery of a neon line (left panels) and a fluorine line (right panels) in the hydrogen-deficient PG1159-type central star PG1520+525 (top panels) and in the hydrogen-normal central star of NGC 1360 (bottom panels). The neon and fluorine abundances in the PG1159 star (given as mass fractions in the panels) are strongly en-

hanced, namely 20 times and 250 times solar, respectively, whereas they are solar in NGC 1360. Note the strong Fe VII line (not included in the models) at 1141.4 Å in NGC 1360, which indicates a solar iron abundance (Hoffmann et al., 2005). It is not detectable in the PG1159 star, probably due to a subsolar Fe abundance (Werner et al., 2004)

It turns out that neon is strongly overabundant, (2%, i.e., 20 times solar). This result clearly confirms the idea that PG1159 stars indeed exhibit intershell matter. Neon is produced in the He-burning environment by two α -captures of nitrogen, which itself resulted from previous CNO burning: $^{14}\text{N}(\alpha,\gamma)^{18}\text{F}(\text{e}^+\nu)^{18}\text{O}(\alpha,\gamma)^{22}\text{Ne}$.

There are still many photospheric lines in UV spectra of PG1159 stars which remain unidentified. Some of them may stem from yet unknown Ne VII lines, or even of elements which have not been detected in these stars at all. The latest identification is that of a feature at 1139.5 Å, which appears rather strong in some objects. It is a line from highly ionized fluorine (Fig. 6) and large overabundances (up to 250 times solar) were derived for a number of PG1159 stars. This line was also identified in “normal” hydrogen-dominated central stars and, in contrast, solar fluorine abundances were found (Werner et al., 2005). This again is a clear proof that we see intershell matter on PG1159 stars. According to recent calculations by Lugardo et al. (2004), their stellar models show an effective fluorine production and storage in the intershell, leading to abundances that are comparable to the observed PG1159 abundances of fluorine. The general problem for fluorine production is that ^{19}F , the only stable F isotope, is rather fragile and readily destroyed in hot stellar interiors by hydrogen via $^{19}\text{F}(\text{p},\alpha)^{16}\text{O}$ and helium via $^{19}\text{F}(\alpha,\text{p})^{22}\text{Ne}$. The nucleosynthesis path for F production in He-burning environments of AGB and Wolf–Rayet stars is $^{14}\text{N}(\alpha,\gamma)^{18}\text{F}(\beta^+)^{18}\text{O}(\text{p},\alpha)^{15}\text{N}(\alpha,\gamma)^{19}\text{F}$.

All this underlines that AGB stars which dredge up material from the intershell are contributing to the Galactic fluorine content (together with Wolf–Rayet stars and type II SNe). This is completely in line with the detected fluorine overabundances (up to 30 times solar) found from IR spectra in AGB stars (Jorissen et al., 1992). To what extent PG1159 stars themselves return F to the ISM remains to be estimated. The life time of a born-again AGB star is short in comparison to a usual AGB star, however, the fluorine fraction in the mass lost by a wind of the former is much higher.

2.2. White dwarf masses and radii and the role of UV imaging observations

Two of the most important physical parameters that can be measured for any star are the mass and radius. They determine the surface gravity by the relation $g = GM/R^2$. Hence, if $\log g$ is measured the mass can be calculated provided the stellar radius is known. One outcome of Chandrasekhar’s original work on the structure of white dwarfs was the relationship between mass and radius, arising from the physical properties of degenerate matter. Further theoretical work yielded the Hamada–Salpeter zero-temperature mass-radius relation (Hamada and Salpeter 1961). However, white dwarfs do not have zero temperature, indeed

many are very hot. Hence, the Hamada–Salpeter relation is only a limiting case and the effects of finite temperature need to be taken into account. Evolutionary calculations, where the radius of a white dwarf of given mass decreases as the star cools, have been carried out by Wood (1992, 1995), Blöcker (1995), Blöcker et al. (1997) and others.

Measurements of the surface gravity of samples of white dwarfs show that the distribution of $\log g$ values and, therefore, of mass is very narrow (e.g., Bergeron et al., 1992; Napiwotzki et al., 1999), with a peak mass of $\sim 0.6 M_\odot$. This is a direct consequence of the evolution of single stars, with masses from $1 M_\odot$ up to $\sim 8 M_\odot$. While the details of the relationship between the initial mass of the progenitor star and the final white dwarf mass are not particularly well understood, it is clear that the small dispersion in the white dwarf masses is related to a similarly small range of stellar core masses and the fact that most of the outer stellar envelope is expelled through several phases of mass loss along the AGB. Importantly, any white dwarf with a mass outside the approximate range 0.4 – $1.0 M_\odot$ cannot arise from single star evolution and must have an origin in a binary, where mass exchange has taken place.

The basic model of the white dwarf mass-radius relation is often used to derive masses from the spectroscopic measurements of effective temperature and surface gravity (e.g., Bergeron et al., 1992; Napiwotzki et al., 1999). While this is not in serious doubt, opportunities for direct observational tests of the work are rare. This is particularly true of models that take into account the finite stellar temperature and details of the core/envelope structure, discussed above. Varying the assumed input parameters in these models can lead to quite subtle, but important differences in the model predictions. To test these requires independent measurements of white dwarf mass, which can be compared with the spectroscopic results. Such information can be obtained spectroscopically by measuring the gravitational redshift of absorption lines in the white dwarf atmosphere ($V_{\text{gr}}[\text{km s}^{-1}] = 0.636 M/R$, M and R in Solar units), but this is only possible if the systemic radial velocity is known as a reference point. Generally, this is only the case if the white dwarf is part of a binary system and then there is also the possibility of obtaining independent dynamical information on the white dwarf mass from the system orbital parameters. An additional important constraint is knowledge of the stellar distance.

The four best white dwarf mass determinations, where we have the most complete and accurate information, are for 40 Eri B, Procyon B, V471 Tauri B and Sirius B, where we can combine the assembled data with the *Hipparcos* parallax to test the mass radius relation (Fig. 7). While there is good agreement between the observation and theory, there nevertheless remains a high degree of uncertainty in the mass determinations. As a result, for example, it is not possible

Fig. 7 Comparison of mass estimates for 40 Eri B, Procyon B, V471 Tau B and Sirius B with the evolutionary models of Wood (1995), displayed at various temperatures and with “thin” and “thick” H envelopes. The solid limiting curve represents the Hamada–Salpeter zero temperature relation for a carbon core (figure produced by Jay Holberg)

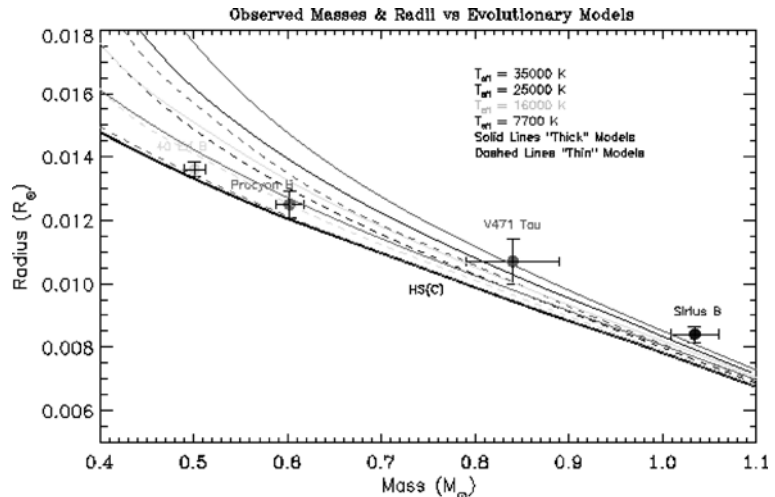
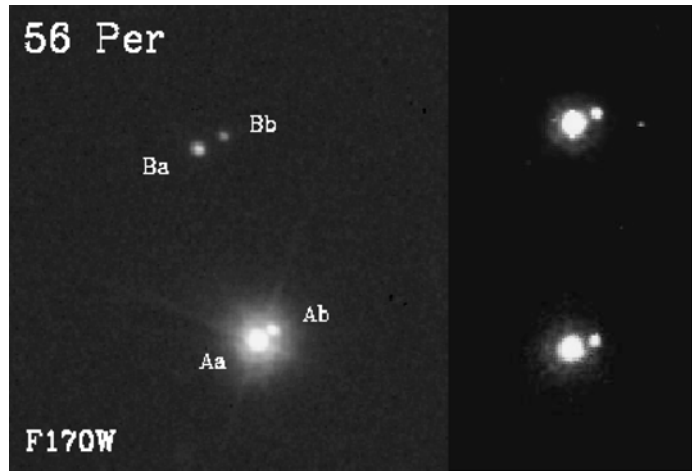


Fig. 8 Wide Field Planetary Camera image of the binary 56 Per, where each component (A & B) is itself resolved into a pair (left). (right) Successive images of the Aa/Ab pair taken \sim 18 months apart clearly show the orbital motion of the system



to distinguish between different models, such as those with “thin” or “thick” H envelopes.

We have such complete data (dynamical masses, gravitational redshifts and accurate parallaxes) for only a very few white dwarfs. Therefore, it is important to extend the sample of white dwarfs for which we have to more objects and, possibly, explore a wider range of masses and temperatures. The role of direct imaging in the UV as means of discovering new systems is particularly important. For example, a major result of the EUV sky surveys was the discovery of many unresolved binary systems containing white dwarfs and companion spectral types ranging from A to K (e.g., Barstow et al., 1994; Burleigh et al., 1997; Vennes et al., 1998). In visible light the presence of a companion of spectral type earlier than mid-K will swamp the signature of the white dwarf making it undetectable. In the EUV, where the companion flux is generally negligible, the white dwarf stands out very clearly. The UV wavelength range is an even more efficient way of searching for these binaries, as the interstellar opacity is much lower than in the EUV, and the GALEX sky survey is finding many examples.

The large difference in the visual magnitudes makes these systems generally impossible to resolve with ground-based observations. However, in the UV where the contrast is far better it is possible to measure their separations, or at least provide improved constraints. HST Wide Field Planetary Camera 2 images of 18 binary systems have resolved 9 objects (Barstow et al., 2001a). Figure 8 shows one of the most interesting examples, 56 Per, a known binary in which each component has been resolved into a pair, making it a quadruple star system. The white dwarf is a companion to 56 Per A and is labeled 56 Per Ab in the image. At a distance of 42 pc, the measured 0.39 arcsec separation indicates a binary period of \sim 50 years for the Aa/Ab system. Therefore, the orbital motion of the two stars should be readily apparent with repeated exposures on timescales \sim 1–2 years, from which a dynamical white dwarf mass can ultimately be obtained. This is clearly demonstrated in Fig. 8 which shows a zoomed view of the Aa/Ab pair from the main image and, on a similar scale, a second image obtained \sim 18 months after the first. Continued monitoring of systems like 56 Per will eventually yield the orbital parameters and dynamical determinations

of the component masses. This requires continued access to UV imaging.

3. Problems of white dwarf evolution

Clearly significant progress has been made in the study of white dwarf stars through ultraviolet observations. However, these have not yet given us access to a detailed understanding of the important physics because they have been limited in scope. First the total number of objects studied with the necessary spectral resolution and signal-to-noise is small. Therefore, we do not know how representative of the general population individual objects or small groups of objects may be. This is exacerbated by the fact that there are strong selection effects present within the existing samples. For example, most hot DA white dwarfs have been observed because of expectations that significant quantities of heavy elements were present in their photospheres, and, as a result are mostly stars with temperatures above 50,000 K. Therefore, a number of significant questions regarding the evolution of white dwarfs remain to be solved:

- What is the origin of the DO–DB gap and the relationship between the H- and He-rich white dwarf branches? For example, do DO white dwarfs appear as DAs through float up of residual H?
- What mechanisms determine the compositions of the DA white dwarfs as they cool? Radiative levitation and gravitational diffusion are clearly important, but why do some stars of the same apparent temperature and gravity have widely differing compositions? Is accretion (from the ISM or a companion) an important mechanism? Do the abundance differences reflect differences in progenitor composition/prior evolution of the progenitor?
- What are the metal abundances in the He-rich white dwarfs? Are the PG1159 stars and DOs part of a single sequence or do they represent the separate progenitor evolutionary paths. Do all hot He-rich white dwarfs eventually become DBs?
- What is the 3-D structure of the local ISM? How do white dwarfs interact with it and exchange material. Does mass-loss continue beyond the planetary nebula phase? Is apparently circumstellar material detected in some of the hottest white dwarfs evidence of such mass-loss or merely the residual signature of PN material?
- What is the initial-final mass relation for both H- and He-rich white dwarfs and what is the upper limit on the possible progenitor mass? Does the theoretical mass-radius relation for white dwarfs stand up to close scrutiny? Do the most massive white dwarfs have exotic core compositions beyond the C/O product of helium burning?

All white dwarfs that have ever been studied in the UV reside within our own galaxy and must have emerged from stellar populations with different ages and environments. To solve the outstanding problem and make significant further progress in the study of white dwarfs requires a substantial enlargement of the sample, to properly examine the full range of temperatures, gravities and possible environmental conditions.

- Expand the number of galactic white dwarfs by a factor 10 for which high resolution/high signal-to-noise UV spectra are available.
- Increase by a factor 10 the number of binary systems with white dwarf components for which astrometric masses can be obtained.
- Be able to study uniform, co-eval populations of white dwarfs in globular clusters, the Magellanic Clouds and nearby galaxies.

4. Future white dwarf research in the far ultraviolet

4.1. White dwarfs in the galaxy

A large-scale survey of the hot white dwarfs in the galaxy will provide observations which can simultaneously address two broad areas of astrophysics: the local interstellar medium, its composition, ionization and structure; and the degenerate stars, their origin and evolutionary history as well as the detailed modeling of critical physical processes in their photospheres. The primary broad scientific objectives would be following:

- Define the evolutionary history of the hot white dwarf stars through detailed modeling of their photospheric composition and structure.
- Study the occurrence of circumstellar material surrounding the white dwarfs and their interaction with the ISM.
- Map out the 3-D structure of the local interstellar medium (LISM) and determine its composition and ionization state.
- Use the morphology of the LISM and the estimated elemental diffusion (gravitational settling) times for white dwarf photospheres to provide a crucial test of the ability of interstellar accretion processes to explain abundance patterns in cooler white dwarfs.
- Identify and characterise new non-interacting white dwarf binary systems.
- Carry out a long-term astrometric programme to determine white dwarf masses.

4.1.1. White dwarf composition

Although there is a qualitative understanding of how the abundance patterns vary across the hot white dwarf

population, the detailed picture is quite confused and some very important questions need to be answered. The observed abundances will reflect the balance of several processes, including mass loss, radiative levitation, gravitational settling, and accretion from the LISM. DA white dwarfs have been selected for follow-up UV studies mainly on the basis of their EUV fluxes, low values indicating the presence of photospheric metals. Thus, the existing observational sample is strongly biased toward such stars. Few stars having apparently pure-H atmospheres have been observed. In addition, the existing data are highly non-uniform in wavelength coverage, signal-to-noise and spectral resolution, which yield non-uniform detection criteria for spectral features. Therefore, the apparent absence of metals may be as much a function of the weak detection limits and too few observations of appropriate stars than a real lack of metals. Hence, we have no idea whether the small group of heavy element-rich stars (see Fig. 4) are typical of the cooler group below 50,000 K, or whether they are truly unusual. Are there really two distinct groups of stars with and without metals? Or, is this an artifact of the small sample and in reality compositions range between the two extremes? It is hard to explain why any DA would have no heavy elements at all. Thus, establishing the frequency of pure-H envelopes is an important component of providing an answer to this problem. In particular, we need to properly sample the lower temperature white dwarfs, especially within the 20,000–35,000 K region, which are not well represented in earlier studies and existing data.

PG1159 stars are rare objects, about 40 are known. Only a few of them have been studied in detail in the UV. High-resolution UV observations are essential, because most diagnostic metal lines observed in these extremely hot stars are located in this wavelength region. The wide spread in element abundances, as well as the observed iron-deficiency and neon- and fluorine-overabundances show that PG1159 stars have a large, and unique, potential to study mixing and fusion processes whose consequences are usually unobservable in other stars. As a consequence of a late He-shell flash, PG1159 stars exhibit intershell matter that normally remains hidden in the stellar interior. In contrast to DA and DO white dwarfs, the observed element abundances in PG1159 stars are not affected by gravitational settling, hence, abundance patterns still do reflect the history of these stars.

4.1.2. Circumstellar material

What appears to be circumstellar gas has been detected in most of the white dwarfs observed in high resolution HST spectra. What is the nature of this material? Is it present in all white dwarfs with photospheric metals or is there a temperature cut-off? A lower temperature (greater age) limit would imply that we are looking at a nebular remnant, which disperses with time. Apportioning unresolved lines to circum-

stellar and photospheric components for the whole sample of stars is essential for correct atmospheric abundance measurements. For example, when observed by HST, the photospheric C abundance of G191-B2B was really found to be a factor 5 lower than the value obtained by IUE (see Barstow et al., 2003b).

4.1.3. 3-D structure of the ISM

High-resolution spectra of LISM absorption lines from abundant ionic species (C II, C II*, N I, O I, Si II-III, S II, Fe II, Zn II, Cr II, Mg I-II) will provide several quantitative measurements of nearby interstellar gas. We will be able to measure the line-of-sight densities and composition of the LISM, derive velocities, to probe the gas kinematics, and determine the ionization of the gas. It is important that the chosen white dwarf sample includes enough different lines-of-sight to provide a true 3-D picture. The high resolution of the echelle data for these white dwarfs will be instrumental in resolving the inherent complex velocity structure seen even in the very local gas within 15 pc (e.g., Lallement et al., 1986; Sahu et al., 2000a,b), and provide the means to obtain reliable ionic column densities for the individual velocity components in the LISM. Does a single bulk velocity vector fit all the lines of sight through a particular cloud, or is the gas fragmented into filamentary structures more characteristic of low velocity shocks? An adequate sample of white dwarfs will provide extensive sampling for distances out to 50–100 parsecs.

The problem of the variability of the D/H ratio in the LISM appears to be on the way to resolution, but there are many details that still need to be addressed (Moos et al., 2002; Sahu et al., 2000a,b). Specifically, obtaining reliable D/H ratios is not easy. Extreme care must be taken in data reduction and calibration and accounting for multiple velocity components along the line of sight. One must look at the heavy ions to determine what velocities are present, because they can be easily masked in the intrinsically broader profiles of light H I and D I.

Column densities, measured from high resolution far-UV spectra, will be useful for determining chemical abundances in the LISM clouds. Comparing the LISM abundances with those of Savage and Sembach (1996) would determine if the cloud has abundances and depletions similar to warm partially ionized gas observed in the more distant ISM.

Examination of the white dwarf data has revealed an unrecognized problem, namely the frequent occurrence of interstellar Si III $\lambda 1206$ in many lines-of-sight. This is difficult to reconcile, since this ion has a high charge-exchange rate with neutral hydrogen. Its presence suggests substantial amounts of warm ionized gas have been unaccounted for in the LISM. It is intriguing that low ionization species seen in G191-B2B (Sahu et al., 2000a,b) are close to the

velocity of interstellar Si III. An examination of S II/H I and C II/H I ratios compared to those found for the LIC at 19.3 km/s, suggests the H ionization fraction is near 0.7 for the 8.6 km/s gas. Another problem is that the shortward “circumstellar” components of C IV in G191-B2B also have a close velocity coincidence with the Si III and the 8.6 km/s low ionization species. Photoionization calculations find no way to have all of these ions in the same gas. High resolution ($R \sim 50,000\text{--}100,000$) data for other sightlines should be able to determine the origin of the Si III.

4.1.4. Interstellar accretion

For the cooler DAZ stars ($6000 < T_{\text{eff}} < 12,000$ K) the existence of heavy elements such as Ca, Mg and Fe has traditionally been attributed to interstellar accretion (e.g., Dupuis et al., 1993). For DA stars at intermediate temperatures ($20,000\text{K} < T_{\text{eff}} < 25,000$ K) the presence of heavy elements poses a dilemma.

In DAZ stars the retention times for high Z elements in the observable photospheres, while substantial (i.e., $\sim 10^4$ yr), remains short compared to the thermal (cooling) time scale of the photospheres. It is possible to imagine that DAZ white dwarfs represent stars passing through, or recently passed through, a diffuse interstellar cloud and having accreted heavy elements. As long as the fraction of DAZ stars remained small it was possible to entertain such views since the number of these stars were the result of infrequent encounters between diffuse clouds and white dwarfs. However, Zuckerman et al. (2003) have shown that the occurrence of cool DAZ stars approaches 25%, which is well in excess of the fraction that might be attributed to ISM accretion. Likewise, other possible explanations involving intrinsically rare events such as comet impacts are equally untenable. Yet, Zuckerman et al., were able to demonstrate a correlation between the presence of low mass companions and the DAZ phenomena.

Thus, some form of ongoing circumstellar accretion appears necessary to explain the bulk of the DAZ stars. Typically the DAZ stars are too faint and too cool to search for the UV presence of heavy elements. However, it is possible to investigate the DAZ phenomena in a hotter class of DA stars at UV wavelengths. In earlier work, there has been little evaluation of the actual conditions of the interstellar medium along the lines of sight to the known DAZ white dwarfs. Nevertheless, knowledge of the morphology of the LISM is necessary to evaluate and critically test the accretion model, since the local distribution of interstellar clouds directly determines the efficiency of interstellar accretion. In general, interstellar features can be distinguished from stellar features on the basis of velocity and the presence of excited fine-structure lines. We can use the several density sensitive indicators to

probe the gas phase density of any accreting medium in the vicinity of the star. For example, an important diagnostic tool is the presence of the collisionally excited C II* $\lambda 1335$ line, from which estimates of the ambient electron density can be determined (Holberg et al., 1999). The presence of ground state and excited C I lines indicate the presence of a medium, which is sufficiently dense to be effectively self-shielding with respect to UV radiation shortward of the C I ionization limit. Even if excited lines are not detected, the mere presence of significant column density, as evidenced by strong IS absorption, is important.

4.1.5. White dwarfs in binaries

Many new white dwarf binaries with main sequence companions are being discovered by the GALEX UV sky survey. In these systems the presence of the companion obscures the white dwarf at long wavelengths. Hence, for these objects, far-UV spectroscopy is essential to determine the basic physical parameters of the white dwarfs. For example, temperature and surface gravity can be determined from model atmosphere analyses of the hydrogen Lyman series lines (e.g., Barstow et al., 2003a), while photospheric composition can be determined from any heavy element lines present, as discussed above. Since many of the brighter companions will be members of the Hipparcos catalogue, and therefore have well-determined distances, the sample of binary white dwarfs can be used to study the mass-radius relation and the initial-final mass relation. The latter is extremely uncertain and is important in validating potential models for type Ia supernovae progenitors.

Only about half a dozen of the known binary systems have sufficiently short orbital periods for astrometric information to be obtained on sensible timescale. A subset of any newly discovered binaries will also fall into this group. Thus far astrometric orbits and directly determined masses are only available for three white dwarfs, Sirius B, 40 Eri B and Procyon B. All other WD masses are based on gravitational redshifts or spectroscopic log g determinations, which require theory-dependent assumptions, or on generally uncertain measurements of interacting close binaries. Knowledge of the masses is, in turn, vital in testing the theory of WD structure (e.g., the mass-radius-core composition relation), understanding the history of star formation in the solar neighbourhood, and setting limits on the age of the Galaxy.

4.2. White dwarfs outside the galactic disk

Imaging surveys of white dwarfs have been carried out in globular clusters, but most of the individual stars are only characterized by broad band photometry. This provides almost no information on the white dwarf masses and

weak temperature constraints. Knowledge of the white dwarf masses is essential for determining the cooling age of individual stars and interpretation of the observed luminosity functions. Study of white dwarfs in globular clusters yields a number of advantages compared to the galactic population.

- All the stars lie at the same, known distance.
- The stars are co-eval.
- The stars are all descendants of a uniform population.

Knowledge of white dwarf temperature and gravity (and, therefore mass) in globular clusters will provide a direct calibration of the initial-final mass relation. In particular, the upper limit of the progenitor mass will be reliably established for the first time, which has important implications for models of SNIa systems. In the galaxy most of the white dwarf progenitors for stars in the disk will probably have had population I metallicities. With all progenitors in a globular cluster being population II, the metallicity and, as result, their prior evolution will be well determined. Since post-main sequence evolution is affected by stellar metallicity, in particular in establishing core He burning, we would expect the resulting white dwarf population to have different characteristics to those in the galaxy.

5. The future need for far UV missions

In Section 4 we have outlined in detail the scientific goals for future studies of white dwarfs. This wealth of science is only possible through a programme of observations in the far ultraviolet waveband. The principal need is for high resolution spectroscopy, but diffraction limited imaging is also of importance. During the past 15 years, these joint capabilities have been provided by the Hubble Space Telescope, following on from 18 years of operations with IUE. Although of great importance, the relatively small aperture of IUE limited high resolution studies of white dwarfs to a handful of the brightest examples. Using a variety of instruments HST has provided us with a flow of high signal-to-noise and resolution ($R \sim 50,000\text{--}100,000$) spectra of white dwarfs and the first diffraction limited imaging of white dwarfs in binary systems. However, HST time has had to be shared across a wider range of wavelengths including the visible and IR bands. Since 1999, this has been complemented by the availability of the FUSE mission, working down to shorter wavelengths than HST (912 Å cf. 1050 Å), but with more modest spectral resolution ($R \sim 20,000$). Sadly, the STIS instrument on HST failed in August 2004, ending the UV spectroscopic capability for the foreseeable future. Also, FUSE is probably nearing the end of its lifetime. While operations have been maintained through the heroic efforts of the FUSE team, continued degradation of its attitude control system (through gyroscope and reaction wheel failures) will eventually lead

to its termination. Within current mission plans access to far UV spectroscopy is likely to end soon with no prospect of any replacement. It is astounding that, at a time when GALEX is opening up the discovery space in UV astronomy in a major way, that we will have no way of adequately following up its surveys.

The current situation regarding continued access to the far UV is full of complex programmatic and political issues which are making it difficult to plan ahead. For example, a shuttle mission to HST could carry out the installation of the Cosmic Origins Spectrograph (COS), which will operate in the far UV with $R \sim 20,000$, and (possibly) repair STIS. However, this is currently ruled out on safety grounds. A robotic alternative is being studied as an extension to the attachment of the de-orbit module (which must be carried out to control HST re-entry). If successful, any HST repair/servicing would resurrect the far UV capability and extend the mission lifetime to ~ 2012 . Alternatively, a new mission called the Hubble Origins Probe (HOP) is being studied as a way of placing COS into orbit (with the Wide Field Camera 3) using a new telescope and spacecraft.

Whatever is finally decided regarding HST and COS, the result will not be ideal. HST operations will still have a limited life and COS does not operate at the spectral resolution needed for the work proposed here. Furthermore, with its multi-waveband capability, HST has never provided as much UV observing time as is really needed. Therefore, there remains the problem of future provision for far UV spectroscopy. This can be divided into two: the replacement of 2-m class access to high resolution spectroscopy for the $\sim 2010\text{--}2015$ period and the long-term provision of a larger scale (4 to 6-m) facility beyond 2015.

There is an urgent need to provide a dedicated far UV mission to follow HST. To achieve this in a relatively short timescale requires the use of existing technology, but within these constraints it should be possible to provide an instrument with enhanced sensitivity through avoidance of complex relay optics and improved (but still current) grating and detector technology. A 2-m class telescope would be able to address many of the science goals relating to observation of white dwarfs in our own galaxy, provided the following technical capabilities are achieved:

- Galactic white dwarf spectroscopic survey
 - $\lambda\lambda \sim 912\text{--}3000 \text{ \AA}$, $R \sim 50,000\text{--}100,000$, $V_{\text{lim}} \sim 18$
- Astrometric white dwarf masses
 - Diffraction limited imaging to $V \sim 18$

The World Space Observatory (WSO, see e.g., Barstow et al., 2003c) is an example of a mission that could meet these aims on the necessary timescale. Plans for WSO have been developed over several years and phase A studies of the

concept and key instruments have been carried out. There is a good prospect that this mission will go ahead under the leadership of the Russian Space Agency, with contributions from many other countries.

In contrast, provision of a large (4 to 6-m) UV telescope is not in the plans of any space agency. Some US studies have been carried out on a large UV/optical space telescope but no concrete plans have yet emerged. However, as agencies begin to plan their programmes for the time-frame beyond 2015, it is absolutely essential that these should include a large UV facility. It would preferable that such a telescope should be UV only, but it may be inevitable that this would need to be UV/optical mission on cost grounds. For white dwarf research, the key requirements are for:

- Globular cluster/Magellanic Cloud white dwarf surveys
 - Integral field spectroscopy $\lambda\lambda \sim 912\text{--}1300\text{\AA}$, $R \sim 1000$, $V_{\text{lim}} \sim 28$
 - Wide field imaging (10 arcmin) to $V \sim 35$

References

- Bannister, N.P., Barstow, M.A., Holberg, J.B., Bruhweiler, F.C.: MNRAS **341**, 477 (2003)
- Barstow, M.A., Bond, H.E., Burleigh, M.R., Holberg, J.B.: MNRAS **322**, 891 (2001)
- Barstow, M.A., Good, S.A., Burleigh, M.R., Hubeny, I., Holberg, J.B., Levan, A.J.: MNRAS **344**, 562 (2003a)
- Barstow, M.A., Good, S.A., Holberg, J.B., Hubeny, I., Bannister, N.P., Bruhweiler, F.C., Burleigh, M.R., Napiwotzki, R.: MNRAS **341**, 870 (2003b)
- Barstow, M.A., Holberg, J.B., Cruise, A.M., Penny, A.J.: MNRAS **286**, 58 (1997)
- Barstow, M.A., Holberg, J.B., Fleming, T.A., Marsh, M.C., Koester, D., Wonnacott, D.: MNRAS **270**, 499 (1994)
- Barstow, M.A., Hubeny, I., Holberg, J.B.: **6C299**, 520 (1998)
- Barstow, M.A., Hubeny, I., Holberg, J.B.: **6C307**, 884 (1999)
- Barstow, M.A., Bannister, N.P., Crudace, R.G., Kowalski, M.P., Wood, K.S., Yentis, D.J., Gursky, H., Barbee, T.W., Jr., Goldstein, W.H., Kordas, J.F., Fritz, G.G., Culhane, J.L., Lapington, J.S.: Proc. SPIE **4864**, 640 (2003c)
- Bergeron, P., Saffer, R., Liebert, J.: ApJ **394**, 228 (1992)
- Blöcker, T.: A&A **297**, 727 (1995)
- Blöcker, T., Herwig, F., Driebe, T., Bramkamp, H., Schönberner, D.: in: J. Isern, M. Hernanz and E. Garcia-Berro (eds.), White Dwarfs, Kluwer, Dordrecht, p. 57 (1997)
- Bruhweiler, F.C.: Astrophysics in the Extreme Ultraviolet, C.S. Bowyer and R.F. Malina (eds.), p. 261 (1996)
- Burleigh, M.R., Barstow, M.A., Fleming, T.A.: MNRAS **6C287**, 381 (1997)
- Chandrasekhar, S.: ApJ **84**, 81 (1931)
- Chandrasekhar, S.: **6C95**, 226 (1935)
- Dreizler, S., Werner, K.: A&A **314**, 217 (1996)
- Dreizler, S., Wolff, B.: A&A **348**, 189 (1999)
- Fleming, T.A. et al.: ApJ **308**, 176 (1986)
- Fowler, R.H.: **6C87**, 114 (1926)
- Frisch, P.C.: Space Sci. Rev. **72**, 499 (1995)
- Frisch, P.C., Grodnicki, L., Welty, D.E.: ApJ **574**, 834 (2002)
- Hamada, T., Salpeter, E.E.: ApJ **134**, 683 (1961)
- Herwig, F., Blöcker, T., Langer, N., Driebe, T.: A&A **349**, L5 (1999)
- Herwig, F., Lugaro, M., Werner, K.: in: S. Kwok, M. Dopita and R. Sutherland (eds.), Planetary Nebulae, IAU Symp. 209, ASP, p. 85 (2003)
- Hoffmann, A.I.D., Dreizler, S., Rauch, T., Werner, K., Kruk, J.W.: in: D. Koester and S. Moehler (eds.), White Dwarfs, ASP Conf. Series, vol. 334, 321 (2005)
- Holberg, J.B., Bruhweiler, F.C., Barstow, M.A., Dobbie, P.D.: ApJ **517**, 850 (1999)
- Jorissen, A., Smith, V.V., Lambert, D.L.: A&A **261**, 164 (1992)
- Kleinman, S.J., Harris, H.C., Eisenstein, D.J., Liebert, J., Nitta, A., Krzesinski, J., Munn, J.A., Dahn, C.C., Hawley, S.L., Pier, J.R., Schmidt, G., Silvestri, N.M., Smith, J.A., Szkody, P., Strauss, M.A., Knapp, G.R., Collinge, M.J., Mukadam, A.S., Koester, D., Uomoto, A., Schlegel, D.J., Anderson, S.F., Brinkmann, J., Lamb, D.Q., Schneider, D.P., York, D.G.: ApJ **607**, 426 (2004)
- Lallement, R., Vidal-Madjar, A., Ferlet, R.: A&A **163**, 204 (1986)
- Liebert, J., Bergeron, P., Holberg, J.B.: ApJS **156**, 47 (2005)
- Liebert, J., Wesemael, F., Hansen, C.J., Fontaine, G., Shipman, H.L., Sion, E.M., Winget, D.E., Green, R.F.: ApJ **309**, 241 (1986)
- Lugaro, M., Ugalde, C., Karakas, A.I., et al.: ApJ **615**, 934 (2004)
- Lyu, Bruhweiler: ApJ **459**, 216 (1996)
- Margio, P.: A&A **370**, 194 (2001)
- Miksa, S., Deetjen, J.L., Dreizler, S., et al.: A&A **389**, 953 (2002)
- Moos, H.W., Sembach, K.R., Vidal-Madjar, A., York, D.G., Friedman, S.D., Hébrard, G., Kruk, J.W., Lehner, N., Lemoine, M., Sonneborn, G., Wood, B.E., Ake, T.B., André, M., Blair, W.P., Chayer, P.: ApJS **140**, 3 (2002)
- Mueller, H.R., Frisch, P.C., Zank, G.P.: American Geophysical Union, Fall Meeting (2003)
- Napiwotzki, R.: A&A **350**, 101 (1999)
- Napiwotzki, R., Green, P.J., Saffer, R.A.: ApJ **517**, 399 (1999)
- Oppenheimer, B.R., Hambly, N.C., Digby, A.P., Hodgkin, S.T., Saumon, D.: Science **282**, 698 (2001)
- Pagel, B.E.J.: Chemical enrichment of the intracluster and intergalactic medium, in: R. Fusco-Femiano & F. Metteucci (eds.), ASP Conf. Series, **253**, 489 (2002)
- Redfield, S. and Linsky, J.: ApJ **534**, 825 (2000)
- Reiff, E., Rauch, T., Werner, K. and Kruk, J.W.: in: D. Koester and S. Moehler (eds.), White Dwarfs, ASP Conf. Series, vol. **334**, 225 (2005)
- Sahu, M.S.: Proceedings of IAU 198, Light Element Abundances, Natal, Brazil (2001a)
- Sahu, M.S., Landsman, W., Bruhweiler, F.C., Holberg, J., Hubeny, I., Barstow, M., Linsky, J., Gull, T., Lindler, D., Lanz, T., Feggans, K.: Bull AAS **199**, 1101 (2001b)
- Savage, B. and Sembach, K.: ApJ **470**, 893 (1996)
- Schatzmann, E.: White Dwarfs, North Holland Publishing, Amsterdam (1958)
- Schuh, S., Dreizler, S., Wolff, B.: A&A **382**, 164 (2002)
- Vennes, S., Christian, D., Thorstensen, J.R.: ApJ **502**, 763 (1998)
- Werner, K.: in: T. Blöcker, L.B.F.M. Waters and A.A. Zijlstra (eds.), Low mass Wolf-Rayet stars: Origin and evolution, Ap&SS, **275**, 27 (2001)
- Werner, K., Rauch, T., Reiff, E., Kruk, J.W. and Napiwotzki, R.: 2004, A&A **427**, 685.
- Werner, K., Rauch and Kruk, J.W.: 2005, A&A **433**, 641.
- Wesemael, F., Green, R.F. and Liebert, J.: 1985, ApJS **58**, 379.
- Wood, M.A.: 1992, ApJ **386**, 539.
- Wood, M.A.: 1995, in: Koester D. and Werner K. (eds.), Lecture Notes in Physics, White Dwarfs. Springer, Berlin, p. 41.
- Zuckerman, B., et al.: 2003, ApJ **596**, 477.

Key Problems in Cool-Star Astrophysics

Isabella Pagano · Thomas R. Ayres ·
Alessandro C. Lanzaflame · Jeffrey L. Linsky ·
Benjamín Montesinos · Marcello Rodonò†

Received: 18 April 2005 / Accepted: 10 October 2005
© Springer Science + Business Media B.V. 2006

Abstract Selected key problems in cool-star astrophysics are reviewed, with emphasis on the importance of new ultraviolet missions to tackle the unresolved issues.

UV spectral signatures are an essential probe of critical physical processes related to the production and transport of magnetic energy in astrophysical plasmas ranging, for example, from stellar coronae, to the magnetospheres of magnetars, and the accretion disks of protostars and Active Galactic Nuclei. From an historical point of view, our comprehension of such processes has been closely tied to our understanding of solar/stellar magnetic activity, which has its origins in a poorly understood convection-powered internal magnetic dynamo. The evolution of the Sun's dynamo, and associated magnetic activity, affected the development of planetary atmospheres in the early solar system, and the conditions in which life arose on the primitive Earth. The gradual fading of magnetic activity as the Sun grows old likewise will have profound consequences for the future heliospheric environment. Beyond the Sun, the magnetic activity of stars can influence their close-in companions, and vice versa.

Cool star outer atmospheres thus represent an important laboratory in which magnetic activity phenomena can be

studied under a wide variety of conditions, allowing us to gain insight into the fundamental processes involved. The UV range is especially useful for such studies because it contains powerful diagnostics extending from warm ($\sim 10^4$ K) chromospheres out to hot (1–10 MK) coronae, and very high-resolution spectroscopy in the UV has been demonstrated by the GHRS and STIS instruments on *HST* but has not yet been demonstrated in the higher energy EUV and X-ray bands. A recent example is the use of the hydrogen Ly α resonance line – at 110 000 resolution with *HST* STIS – study, for the first time, coronal winds from cool stars through their interaction with the interstellar gas. These winds cannot be detected from the ground, for lack of suitable diagnostics; or in the X-rays, because the outflowing gas is too thin.

A 2 m class UV space telescope with high resolution spectroscopy and monitoring capabilities would enable important new discoveries in cool-star astronomy among the stars of the solar neighborhood out to about 150 pc. A larger aperture facility (4–6 m) would reach beyond the 150 pc horizon to fainter objects including young brown dwarfs and pre-main sequence stars in star-forming regions like Orion, and magnetic active stars in distant clusters beyond the Pleiades and α Persei. This would be essential, as well, to characterize the outer atmospheres of stars with planets, that will be discovered by future space missions like *COROT*, *Kepler*, and *Darwin*.

†Deceased October 23, 2005

I. Pagano (✉)
INAF, Catania Astrophysical Observatory, Italy

T. R. Ayres
CASA, University of Colorado, Boulder CO, USA

A. C. Lanzaflame · M. Rodonò
Department of Physics and Astronomy, Catania University, Italy

J. L. Linsky
JILA, University of Colorado & NIST, Boulder CO, USA

Benjamín Montesinos
IAA/CSIC, Granada and LAEFF/INTA, Madrid, Spain

Keywords Late-type stars · Magnetic activity · Chromospheres · Coronae · UV astronomy

1. Introduction

Magnetic activity signatures, analogous to well-known solar phenomena, are widely observed in cool stars. Dark cool

spots in the stellar photosphere produce modulations of optical light curves as the star rotates, and the migration of Doppler shifted features through the line profiles. Flares, coronal mass ejections (CME's), and stellar winds (of luminous cool stars) are commonly observed. Magnetic activity also is responsible for prominent emission-line spectra in the ultraviolet and far-ultraviolet (UV/FUV) regions, and for the entire stellar X-ray and radio emission.

In RS CVn-type binary systems, dMe stars, and young rapidly rotating dwarfs, magnetic activity is of paramount interest because of its extreme characteristics: in such stars more than 50% of the stellar photosphere can be spotted, chromospheric and transition region (TR) fluxes are so high that they have topped out at a saturation limit, and the X-ray luminosity can even reach a remarkable 10^{-3} of the stellar bolometric luminosity, ten thousand times larger than the equivalent solar ratio.

Thanks to long-term systematic monitoring programs of highly convective cool stars initiated in the mid sixties, notably at Crimea (Chugainov, 1966), Catania (Godoli, 1968) and Mt. Wilson (Wilson, 1978) and successively pursued worldwide at other Observatories (e.g., Vienna, Konkoly, Armagh, Potsdam and Fairborn), about forty years later we are now in a position to state with confidence that many cool stars show periodic variations of their emissions from almost all atmospheric layers with characteristics similar to the 11-year solar cycle (Wilson, 1978; Baliunas et al., 1995; Rodonò et al., 1995, 2000, 2002; Strassmeier et al., 1997; Lanza et al., 1998, 2002; Cutispoto et al., 2001, 2003; Olah and Strassmeier, 2002; Messina et al., 2001; Messina and Guinan, 2002, 2003; Favata et al., 2004). However, there are also phenomena that do not have analogues on the Sun: high-latitude (Rodonò, 1986) and polar spots (Strassmeier, 1990, Strassmeier et al., 1991), very hot (>10 MK) coronal components (Linsky, 2003; Audard et al., 2004), etc.¹ As for the Sun, however, the activity phenomena occurring in the different atmospheric layers of cool stars appear to be closely correlated (Catalano et al., 2000; Messina et al., 2002).

The Sun's contemporary magnetic activity affects the Earth's biosphere and human civilization through a variety of phenomena lumped under the heading "space weather." Furthermore, the Sun was considerably more active in its youth than today (e.g., Ribas et al., 2005), and had a correspondingly larger impact on the solar system, especially primitive planetary atmospheres and the environment in which life began on Earth. Given the importance of accurately forecasting solarrelated influences – now, in the past, and in the future

– it is essential to investigate how magnetic activity depends upon stellar parameters (mass, radius, rotation rate, binarity, evolutionary stage, etc.) if we ever want to develop a theory for these high-energy phenomena that has predictive power.

Hot plasma in magnetically disturbed cool-star outer atmospheres, with temperatures from 10,000 K to several millions, can be observed in a single ultraviolet spectrum, providing simultaneous information on thermal structures of a wide range of atmospheric components. As an example, Figure 1 illustrates the spectrum of α Cen A (G2 V) obtained with *HST/STIS* in the range 1140–1670 Å with a resolution $R \sim 114,000$ (E140H). In this spectrum Pagano et al. (2004) identify a total of 671 emission lines from 37 different ions, including low temperature chromospheric lines (e.g., C I, O I), TR lines (e.g., C II–IV, N IV, O III–V, Si II–IV), the coronal line Fe XII 1242 Å, a number of intersystem lines (e.g., [O IV]) that are useful for measuring electron densities, and two molecules (CO and H₂).

In what follows, we emphasize the importance of the ultraviolet for addressing unresolved issues in the study of cool stars and related objects.

2. A brief history of UV cool-star astronomy

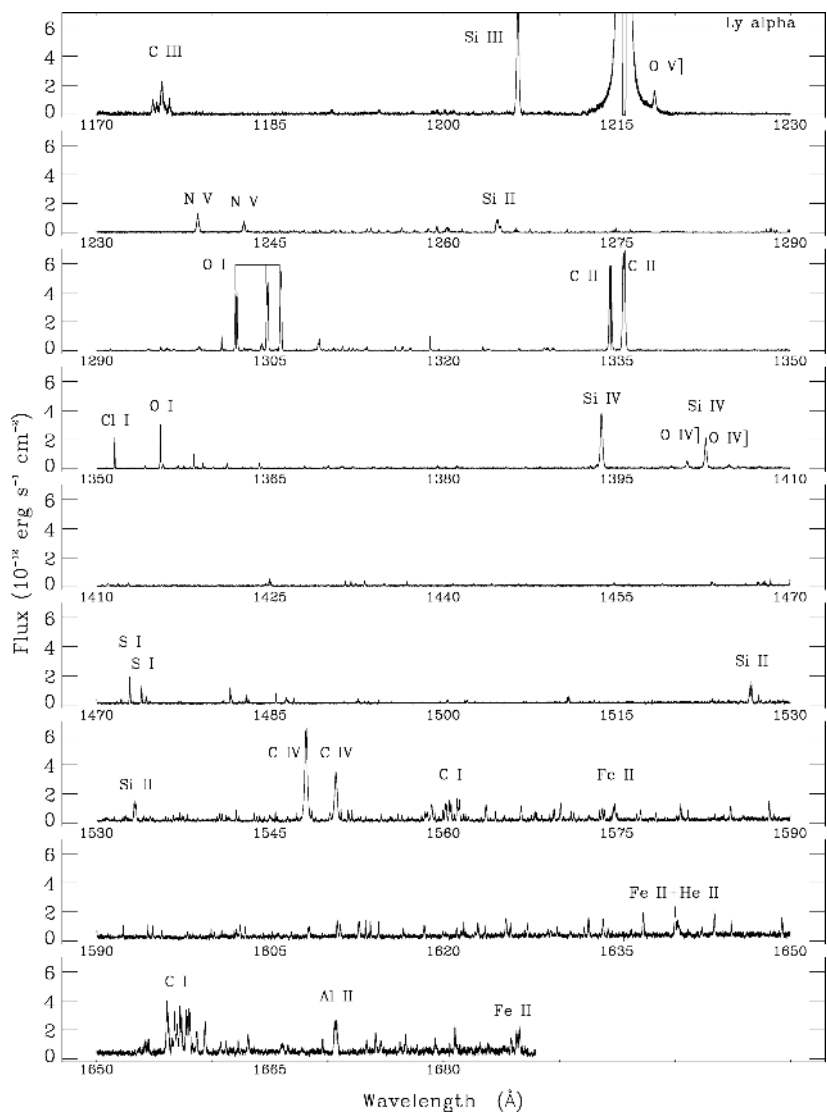
Ultraviolet astronomy has been crucial to the study of cool stars. Although the photospheric spectral energy distribution of this type of star peaks at red wavelengths, the presence of hot plasma in chromospheres, transition regions, and coronae reveals itself most prominently through emission at the shorter ultraviolet wavelengths, where conveniently the photospheric contribution typically is faint.

A comprehensive account of the development of UV astronomy from the pioneering rocket experiments of the 1960's until the era of the prolific International Ultraviolet Explorer (*IUE*) can be found in the review by Boggess and Wilson (1987). In summary, the first ultraviolet stellar spectra with sufficient resolution to detect emission lines were obtained during a rocket flight in 1965. In the nine years from 1964 to 1972, NASA's Orbiting Astronomical Observatories (*OAO*'s) constituted the first programme of space facilities designed specifically for ultraviolet astronomy. In particular, the final one, *OAO-C* – launched in 1972 and designated *Copernicus* – detected for the first time FUV emission lines in two UV-bright cool stars, namely Procyon (α CMi) and Capella (α Aur). In parallel, the first European satellite carrying several UV experiments was *TD-1*, launched in 1972.

The technological efforts and the scientific needs of the UV astronomical community crystallized in the joint NASA, ESA and British SERC *IUE* project, launched in January 1978 and finally terminated in September 1996, after an extraordinarily long and productive mission. The broad *IUE* coverage (1100–3200 Å), high spectral resolution (up to

¹ Detailed descriptions and references for all the phenomena mentioned above and the associated theoretical scenarios can be found in the Proceedings of the Cambridge Workshops "Cool Stars, Stellar Systems and the Sun", published in the Astronomical Society of the Pacific Conference Series.

Fig. 1 The spectrum of α Cen A, a twin of the Sun, as observed by *HST/STIS*. Only the strongest transitions are labelled. This spectrum contains a wealth of emission lines that probe the stellar atmosphere from the chromosphere to the coronae (from Pagano et al., 2004)



$R = \lambda/\Delta\lambda = 10000$ in its echelle modes), and higher sensitivity than previous UV missions provided numerous key discoveries in many different areas of cool-star science, from the atmospheres of T Tauri stars (Imhoff and Appenzeller, 1987), accretion processes in pre-main sequence stars, winds in Herbig Ae/Be stars, chromospheres and transition regions in all kinds of late-type stars (Jordan and Linsky, 1987), and Doppler imaging of the components (and atmospheres) of active binary systems, and stellar winds (Dupree and Reimers, 1987). Detailed summaries of the achievements in each of these fields at the end of the IUE mission can be found in the Proceedings of the Conference “Ultraviolet Astrophysics beyond the IUE Final Archive” (Wamsteker and González-Riestra, 1998).

Following IUE, three missions have made further and substantial contributions to UV astronomy of cool stars, namely the Hubble Space Telescope (*HST*), the Extreme Ultraviolet

Explorer (*EUVE*) and the Far Ultraviolet Spectroscopic Explorer (*FUSE*).

Three UV instruments on board *HST* have made pivotal discoveries in cool-star science. The Goddard High Resolution Spectrograph (GHRS) covered the interval 1150–3200 Å, with resolutions between 2000 and 80000. The companion Faint Object Spectrograph (FOS) covered the broad region from Ly α into the visible, although at relatively low resolution and with significant scattered light below 1900 Å. Nevertheless, FOS filled an important gap during the period when GHRS was not able to use its own low-resolution mode owing to an electrical failure (Ayres et al., 1996). The second-generation Space Telescope Imaging Spectrograph (STIS) covered the wavelength range 1150–10000 Å, with spectral resolving powers between 26 and 200 000. GHRS and FOS were in operation from 1990 until 1997; STIS carried on from then until a power supply failure in August

2004. The *HST* UV instruments covered the same range as *IUE*, but the much larger telescope aperture, higher spectral resolution in some of the observing modes, more sensitive digital cameras, and the ability to achieve high spatial resolution (in STIS long-slit modes) permitted observations of cool stars many magnitudes fainter than the targets accessible in the pre-*HST*era. A good example of the science added by the *HST* instruments is a survey of FUV coronal forbidden lines carried out by Ayres et al. (2003a) in a sample of F-M dwarfs, giants and supergiants, detecting faint lines from highly ionized species such as Fe XXI 1354 Å, formed at 10^7 K. The UV coronal forbidden lines are diagnostically unique because they can be recorded at high spectral resolution much more easily than their permitted counterparts in the X-ray region (where the current best resolution is only about 1,500). Contributions in all other UV fields, already opened by *IUE* were also remarkable and valuable.

EUVE was launched in 1992 and operated until January 2001. It covered the extreme ultraviolet wavelengths from 60 Å up to the Lyman continuum (LyC) edge at 912 Å (although in practice few stars were observable longward of ~ 400 Å owing to interstellar extinction). Of the 734 sources cataloged in *EUVE*'s all-sky survey, 55% were identified as late-type stars. *EUVE*'s ability to resolve spectral lines from a variety of high ionization stages was of tremendous value for modeling the temperature structure of stellar coronae, and many such studies of stars of different activity levels were carried out. *EUVE* also enabled for the first time the study of stellar coronal abundances and chemical fractionation phenomena such as the so-called FIP-effect (elements with First Ionization Potentials < 10 eV are overabundant in the solar corona compared with high-FIP counterparts, e.g. Osten et al., 2003). Equally important, the long continuous stares of days to weeks, motivated by operational considerations, made *EUVE* an ideal platform to study coronal variability, especially flare activity. An account of the achievements of *EUVE* can be found in Bowyer et al. (2000).

FUSE, launched in 1999, records the 912–1187 Å spectrum with four separate telescope/spectrograph channels (further subdivided by redundant detector segments). The *FUSE* range includes the strong Li-like O VI 1031,37 Å resonance doublet, formed at transition region (TR) temperatures around 300 000 K, as well as the very strong C III 977 Å resonance line, formed near 60 000 K. Like STIS, *FUSE* provides a link to coronal dynamics through the [Fe XVIII] 974 Å and [Fe XIX] 1118 Å forbidden lines (cf. Redfield et al., 2003). Molecular hydrogen absorption, and fluorescence of H₂ by H Ly α , add further diagnostics for determining plasma densities, temperatures, and structural constraints in, for example, circumstellar envelopes of Herbig Ae/Be and T Tauri stars. Two important papers are the surveys of cool dwarfs (Redfield et al., 2002) and giants (Dupree et al., 2005). Harper

(2004) and Ayres (2005) have reviewed recent *FUSE* results on cool stars.

3. Open issues

In the remainder of the paper we focus in the remainder of the paper on a few selected open issues in cool-star physics that can be addressed by new observations in the ultraviolet spectral range. These issues are, in our opinion, important topics in stellar physics and key ingredients for progress in the fields of “space weather,” “extrasolar planets,” and “life beyond Earth.”

- Stellar dynamos and the transport of magnetic energy in plasmas;
- Magnetic activity of stars hosting planets;
- Astrophospheres and solar-like stellar winds;
- Activity in young galactic clusters and star-forming regions.

3.1. Stellar dynamos and the transport of magnetic-energy in plasmas

In stars of spectral type early F and later, the coupling between differential rotation and turbulent convection in their subphotospheric layers generates strong magnetic flux ropes, by a mechanism known as “dynamo action”, first investigated for the stellar case by Belvedere et al. (1980a,b,c). The tubes buoyantly rise through the convection zone, penetrate the stellar surface, become braided and twisted by surface velocity fields, and ultimately reconnect releasing their magnetic free energy to power the nonclassical outer atmospheric activity that is a focus of much solar/stellar research today. Existing models of the dynamo are able to reproduce gross features of the 11-year sunspot cycle, and the 22-year period of the Sun's global magnetic field reversals. However, contemporary dynamo models cannot forecast the details of solar activity on short time scales of months to years (cf. review by Paternò, 1998).

One of the challenges of dynamo theory today is to explain the characteristic periods of the quasi-cyclic activity oscillations of stars and, in particular, the problem of the large observed ratio (> 100) of cycle times and correlation times of the turbulent eddies. While in an evolutionary scenario the actual picture of the dynamo action ranges from an α^2 in fully convective stars to $\alpha\Omega$ dynamo regime in solar-type stars, it has been recognized that a necessary ingredient to explain the observational features of magnetic activity in the Sun is the inclusion of the meridional circulation together with a small eddy diffusivity (Bonanno et al., 2005). In this case the magnetic Reynolds number reaches 100–1000 and the dynamo action correctly reproduces all the observation(cycle

times, butterfly diagram, sign of the current helicity, ratio of toroidal/poloidal field strengths) with a differential rotation profile as provided from helioseismology. Another key issue in understanding the “solar-stellar connection” in terms of dynamo theory, and more generally the evolution between α^2 regime and the $\alpha\Omega$ one, is the so-called “flip-flop” mechanism observed in some RS CVn’s and single young dwarfs (see also Section 3.1.1).

Only in recent decades have we begun to appreciate the effects of short-term solar variability on the Earth’s environment and human civilization. Major solar flares and CME’s can cause electronic failures in commercial and scientific satellites, disrupt long distance radio communications, and induce ground currents than can overload electricity transmission grids. Moreover, there is growing evidence that solar activity can, to a certain extent, influence the Earth’s climate.

For example, historical records of sunspot counts show that solar activity decreased for more than 50 years during the 17th century when Northern Europe was experiencing the “Little Ice Age.” On the other hand, a sustained increase of activity, in a modern version of the “Grand Maximum” that occurred during the 12th century, might cause climate warming and the increase in space storms and ultraviolet radiation, which is harmful to life, particularly if protective ozone layers continue to diminish as a consequence of anthropomorphic emissions.

Butler (1994) and Pallé Bagó and Butler (2001) have found quantitative evidence that much of the warming of the past century can be accounted for by the direct and indirect effects of solar activity. However, at the moment we cannot forecast long and short-term solar magnetic variability because we do not have a comprehensive understanding of their root causes: the dynamo mechanism and the physical processes that shape plasma structure and control dynamics in the solar outer atmosphere. One way to progress in this area is to step back from the Sun, and instead evaluate how magnetic activity phenomena depend on fundamental stellar parameters: mass, rotation rate, chemical composition, binarity, and so forth. The diverse stellar examples of activity might reveal insights into the underlying physical processes that observations of the singular example of our Sun cannot, no matter how detailed.

In what follows, potential new observational constraints on the stellar dynamo and the mechanisms of coronal heating are discussed.

3.1.1. Determining the locations and migration patterns of active structures

Observational constraints on stellar dynamos can be obtained by imaging the surface patterns of magnetic activity in large samples of stars. We already know that on other stars the mean locations of magnetic active regions and their migration

paths can be different from those observed on the Sun (Walter, 2003). In some cases, highly active stars show polar spots, migration of active regions toward the poles, preferred active longitudes, a “flip-flop” effect, i.e. sequential activation of a pair of active longitudes (see, e.g., Rodonò et al., 2000, Berdyugina and Tuominen, 1998).

Much of the existing work on surface patterns of stellar magnetic fields has involved optical observations of large dark starspots, the sites of concentrated strong (kilogauss) magnetic fields. However, there are important patterns of smaller-scale fields on the Sun-plage and supergranulation – that carry a large fraction of the global magnetic flux, and are present even at cycle minimum when few or no spots are on the disk. Just as the spots are associated with elevated chromospheric and coronal emissions (in the surrounding active region), so too are plage and the supergranulation network areas, of enhanced chromospheric and transition region emissions. For this reason, such areas show very large intensity contrasts in the ultraviolet, even though they are not easily distinguishable from the surrounding quiet photosphere at visible wavelengths.

There are two basic approaches that one might utilize to determine the migration patterns of active regions, plage, and supergranulation in the chromospheric and transition-region emissions of stars. The first is to obtain direct narrow-band images (like *TRACE* does for the Sun) at very high spatial resolution; the second is to use high-resolution spectroscopy to measure Doppler shifted signatures of active regions in time series of emission line profiles (so-called Doppler Imaging).

HST, which has about 50 milliarcsecond resolution in the mid-UV (Gilliland and Dupree, 1996), has successfully imaged in chromospheric light only star, α Ori. Even though the angular size of the chromosphere of a cool giant star can significantly surpass that of the photosphere—the diameter of Betelgeuse in Mg II 2800 Å light is four times larger than its optical size (Uitenbroeck et al., 1998) – the direct imaging of stellar outer atmospheres is a daunting task. In fact, to obtain a 100×100 pixel² UV map of the closest solar-like dwarf stars (sufficient to record small active regions and crudely image the supergranulation network) requires a spatial resolution of about a tenth of a milliarcsecond, 500× better than the best delivered by *HST*. Extending the sample to dwarfs within 100 pc would require *microarcsec* imaging. Reaching such an objective might seem to be far in the future. Nevertheless, one promising concept under study at the NASA GSFC is the *Stellar Imager* mission, a kilometer scale interferometer composed of ~30 small telescopes formation-flying in space (Carpenter et al., 2004).

Emission-Line Doppler Imaging, on the other hand, is a powerful contemporary tool for probing high-contrast surface structure or extended atmospheric zones in cool stars, strongly complementing optical and X-ray imaging—which preferentially maps the dark spotted areas, and the corona,

respectively. The reader is referred to Lanza et al. (1998) and Rice (2002) for the techniques to derive photospheric images, and to the reviews by (Güdel, 2004) and (Favata and Micela, 2003) for X-ray imaging techniques. Here we discuss chromospheric and TR Doppler imaging methods. Discrete features moving through the line profile, say, chromospheric Mg II h and k: 2800 Å or higher temperature C IV 1548 Å, can trace the locations of bright emission regions on the stellar surface, and help us understand how the activity is organized spatially and its relation to the dark starspots seen in optical Doppler images. A few maps of the chromospheres of RS CVn-type stars with rotation periods less than 3 days have been obtained by monitoring the Mg II h and k lines with *IUE* (Walter et al., 1987; Neff et al., 1989a; Busà et al., 1999; Pagano et al., 2001). In this way, cool prominences have been found at distances of 1–2 stellar radii, implying that multi-temperature plasmas thread the circumstellar environments of these systems. Spatially resolved surface fluxes in the chromospheric plage maps suggested that these regions are sites of “saturated heating” (Linsky, 1991) and that the relationship between radiative and magnetic flux densities valid for the Sun cannot be extrapolated to these extremely active stars (Schrijver and Zwaan, 2000). A related phenomenon is that of “super-rotational” broadening seen in the TR lines of certain types of rapidly-rotating giant stars. The observed line widths are up to twice that expected from the photospheric $v \sin i$, demonstrating that 100 000 K material is present at levels up to 10 pressure scale heights above its equilibrium altitude, raising questions as to how the gas got there and how it can remain (Ayres et al., 1998).

From a practical point of view, Doppler imaging typically requires spectral resolution $\geq 30\,000$ ($< 10\text{ km s}^{-1}$) to detect discrete emission components migrating through the line profile. An additional requirement is the ability to obtain a time series of spectra with sufficient cadence to avoid smearing the Doppler information, and long enough coverage to distinguish between persistent surface features and transient flare activity. In fact, the best targets for emission-line Doppler imaging are rapidly-rotating stars, and these by their nature are highly active and flare frequently. For example, the single attempt by *HST* to map a cool-star outer atmosphere, namely HD 155555 (Dempsey et al., 2001), covered one stellar rotation, and was only partially successful because flaring and non phase-dependent variability could not be separated from rotational modulation of unchanging active regions.

Another, more subtle, way to gain information on the small scale geometrical organization of a stellar atmosphere is to utilize fluorescent lines of molecules and atomic species. The molecular features further are a guide to the presence of very cool gas in the outer atmosphere, perhaps due to so-called molecular cooling catastrophes (Ayres, 1981). Fluorescent lines of molecules (e.g., H₂ and CO) and atomic species (e.g., Fe I & II, O I, Cl I) are particularly strong in T Tauri stars

(owing to their disks) and in red giants (owing to the generally tenuous atmospheres and the presence of “clouds” of very cool gas at high altitudes). For example, Herczeg et al. (2002, 2004) identified 146 emission lines of H₂ pumped primarily by Ly α in a STIS spectrum of the T Tauri star TW Hya. The fluorescent processes rely on the excitation of specific low-excitation lines by wavelength-coincident radiation fields produced in hotter, spatially separated regions of the stellar (or disk) atmosphere. In the case of the red giants, the dominant pumping lines are the resonance transitions of atomic oxygen and hydrogen, and the hot chromospheric layers in which these radiations form are too far removed from the cooler photosphere to properly excite the observed fluorescent transitions, at least if one considers traditional 1-D thermal models for such objects. The implication is that hot and cold gas are much more intimately associated in the outer atmospheres of these stars. It might be that magnetic processes (which tend to produce filamentary hot structures in an otherwise cool atmosphere) are more important in the red giants, for example, than previously thought; and that, in turn, might be an indication that the winds of such stars could have a magnetic origin. In short, fluorescent processes can be a guide to the geometrical organization of a stellar atmosphere (or accretion disk) on small physical length scales not accessible to direct telescope observations.

In this connection, it should also be mentioned that studies of the atmospheres of close-in exoplanets, through Doppler shifted Ly α and other fluorescence emissions, could be feasible with a sufficiently-sensitive next-generation UV spectrometer.

3.1.2. Velocity fields and plasma dynamics

The heart of understanding chromospheric and coronal heating – one of the major unsolved problems in solar and stellar physics – is mechanical energy transport and dissipation. In the outer convection zone, immediately beneath the photosphere, turbulence transforms gas kinetic energy into sound waves and propagating electrodynamic disturbances. Given the difficulty of transmitting sound waves through the steep TR temperature gradient, electrodynamic processes are thought to provide the bulk of coronal heating. However, the shock dissipation of pure acoustic waves probably is an important heating source for nonmagnetic portions of the chromosphere and the lower transition region. How sizeable this contribution is with respect to the magnetic mechanisms is not yet understood (c.f., Judge et al., 2004 and references therein), and the quantitative details of the energy transport and dissipation processes remain elusive. What is clear, however, is that plasma dynamics is an important byproduct of the heating mechanisms, and thus a potential window into their nature.

Observations of the Sun (e.g., Teriaca et al., 1999 and references therein) and late-type stars (e.g., Ayres et al., 1983, 1988, Wood et al., 1997, Pagano et al., 2004) have shown that transition region emission lines are, on average, redshifted, and the redshifts increase with increasing formation temperature up to about 10^5 K. This behaviour is not anticipated by models of upward propagating acoustic waves, for which both optically thin (e.g., Hansteen, 1993, Wikstöhl et al., 2000) and optically thick lines (Carlsson and Stein, 1997) are predicted to be blueshifted. On the other hand, statistically the observed solar redshifts are largest over active regions (Brynilsen et al., 1996; Peter, 2000), compared with quiet areas (Achour et al., 1995); and some TR models (Reale et al., 1996) predict larger redshifts in regions permeated by strong magnetic fields than in quiet regions.

The maximum redshift ($\sim 15 \text{ km s}^{-1}$) is reached at about $1 - 1.2 \times 10^5$ K (active regions and quiet Sun, respectively). At higher temperatures, the centroid velocities decrease, crossing over to blueshifts at $T \sim 10^6$ K (reaching about $\sim -10 \text{ km s}^{-1}$). A similar behaviour is seen in α Cen A (Pagano et al., 2004), α Cen B (Wood et al., 1997), ϵ Eri (Jordan et al., 2001), and Procyon (Wood et al., 1996), although the latter shows a maximum redshift at somewhat higher temperatures (Wood et al., 1997). On the other hand, the TR lines of the very active dM1e star AU Mic show hardly any redshifts, and certainly show no conspicuous trend of line shift versus formation temperature (Pagano et al., 2000; Redfield et al., 2002).

In addition to redshifts, stellar transition region emission lines also show a curious bimodal structure. AU Mic (dM1e) was the first star for which this behaviour was noticed (Linsky and Wood, 1994). The authors found that the Si IV and C IV lines have broad wings superimposed on a narrower central peak. The same bimodal structure of Si IV and C IV lines subsequently was detected in TR spectra of other stars covering a range of spectral types, luminosity classes, and activity levels, from RS CVn-type systems (e.g., HR 1099), to main sequence dwarfs (e.g., AU Mic, Procyon, α Cen A and B), and giants (Capella, 31 Com, β Cet, β Dra, β Gem, and AB Dor) (Linsky et al., 1995; Pagano et al., 2000, 2004; Linsky and Wood, 1994; Vilhu et al., 1998). The broad components have widths comparable to, or wider than, the broadened C IV profiles observed in solar transition-region explosive events (see Dere et al., 1989), small bursts thought to be associated with reconnections of emerging magnetic flux to overlying pre-existing canopy fields. Wood et al. (1997) showed that the narrow components can be produced by turbulent wave dissipation or Alfvén wave-heating mechanisms, while the broad components – whose strength correlate with activity indicators like the X-ray surface flux – can be interpreted as a signature of “microflare” heating. Alternatively, for the particular case of rapidly rotating AB Dor, Vilhu et al. (1998) suggested that broad wings can arise from a ring of hot gas

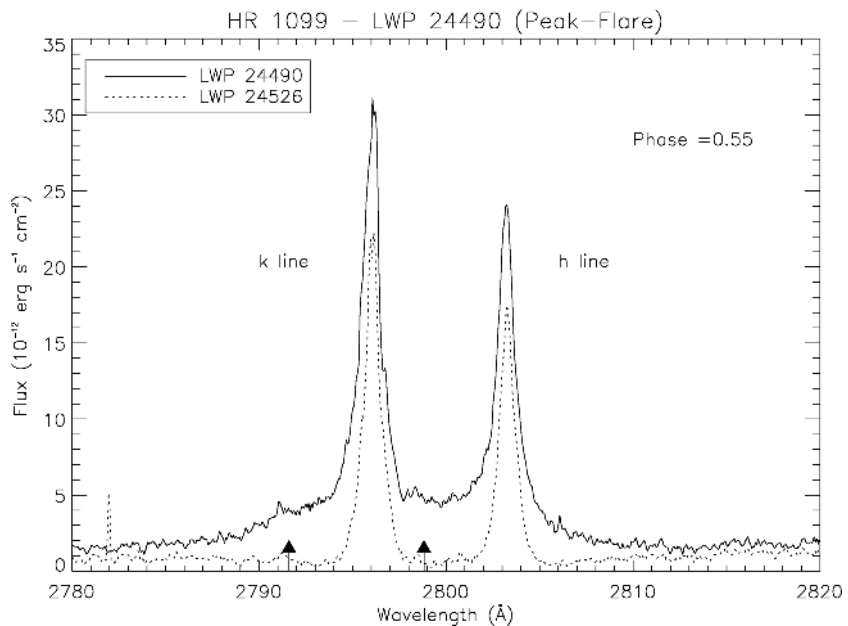
at 2–3 stellar radii, like the “slingshot prominences” seen in H α .

Using *SoHO/SUMER* data, Peter(2001) showed that broad components are a common feature in the thermal regime 40 000 K to 10^6 K above the magnetically dominated chromospheric network. The author presented evidence that the narrow line core and broad wings are formed in radically different physical settings: small closed loops and coronal funnels, respectively, the latter being the footpoints of large coronal loops. Non-thermal widths of the broad components follow a power-law distribution with respect to line-formation temperature, a signature of upward propagating magneto-acoustic waves (Peter, 2001). In stars other than the Sun, the broad components have been observed over formation temperatures of 40,000 K to 2×10^5 K.

Usually, chromospheric emission lines do not show broad wings in time-averaged spectra of normal stars, although very optically thick, opacity-broadened features like the Mg II h&k resonance lines would tend to mask such components if present. However, in extremely active stars, or during large stellar flares, chromospheric broad components occasionally are seen. For example, transient broad *redshifted* components of Mg II were recorded in the RS CVn binary AR Lac during a large flare event early in the *IUE* mission by Neff et al. (1989b). In another active binary, HR 1099, Busà et al. (1999) suggested that persistent broad components observed in Mg II h&k were associated with a large active region close to the pole. Subsequently, Lanzafame et al. (2000) employed a two-component NLTE model to synthesize the stellar H α and Mg II h&k lines, demonstrating that the broad component could be explained as an effect of elevated densities in the active region, while the narrow component would be formed in the surrounding lower density quiet chromosphere. This conceptually is a much different model than the dynamical origin proposed for the optically thin TR lines, but still potentially is a valuable indicator of local plasma conditions in active regions. Future observational and theoretical studies are needed to determine which is the more realistic model.

Extending the observational side of plasma dynamics to higher, coronal temperatures is relatively straightforward on the Sun, because many suitable strong coronal permitted lines (e.g., Mg $\times 610, 25 \text{ \AA}$) fall in the Lyman continuum region immediately below 912 Å, where high-resolution far-UV spectroscopy still is practical. Unfortunately, these key features are not accessible even in the nearest stars owing to interstellar extinction. Observing spatially-resolved profiles of permitted coronal X-ray lines, say in the important iron-L shell band at $\sim 1 \text{ keV}$, is not feasible at present, because contemporary high-energy missions like *Chandra* and *XMM-Newton* have inadequate spectral resolution by an order of magnitude, and there are no planned future missions that will push that limit.

Fig. 2 A very strong flare of the RS CVn-type system HR 1099 observed in the Mg II h&k lines by *IUE*. The dotted line is a spectrum obtained during quiescence. Arrows indicate the Mg II $3d - 3p$ subordinate lines (from Busà et al., 1999)



However, a number of coronal *forbidden* lines in the UV range long-ward of the Lyman continuum edge have been observed in the Sun (see for example Doschek et al., 1975; Feldman et al., 2000). On the stellar side, *HSTs* GHRS and STIS instruments, and *FUSE*, have been able to detect highly ionized iron forbidden lines in many cool stars (see for example Maran et al., 1994, Pagano et al., 2000, Ayres et al., 2003a, Redfield et al., 2003) with high spectral resolution (up to $R = 40000$).

The UV coronal forbidden lines detected in cool stars for the most part show negligible Doppler shifts from the photospheric radial velocities, suggesting that the emissions arise mainly from confined structures, analogous to magnetic loops on the Sun, rather than from a hot wind. Moreover, the Fe XII and Fe XXI line widths generally are close to their thermal values (FWHM 40–90 km s $^{-1}$ at $T \sim 10^{6.2} - 10^{7.0}$ K), except for the Hertzsprung-gap giants 31 Com (GO III) and Capella (G1 III) and the K1 IV component of HR 1099, all of which display excess broadening in Fe XXI. If the additional broadening is rotational, it would imply that the hot coronae of “X-ray deficient” 31 Com and Capella are highly extended, compared to the compact structures suggested by recent density estimates in a number of active coronal sources. On the other hand, the more common case of purely thermal line widths implies that supersonic turbulent motions are absent in the coronal plasma, eliminating shock waves as an important heating mechanism.

3.1.3. The physics of impulsive heating: Stellar flares and microflares

Flares, lasting from a few minutes to several days, are the most dramatic examples of transient energy release in so-

lar and late-type stellar atmospheres. A magnetic reconnection process is thought to power these events: magnetic free energy is converted – in thin current sheets – into thermal heating, Alfvén waves, and the acceleration of relativistic particles. Accordingly, the relaxation phenomenon is complex and fast, producing radiation across the whole electromagnetic spectrum from nonthermal radio synchrotron, to thermal emissions in the UV and X-ray ranges. In fact, the flare phenomenon involves the whole atmosphere, from the corona down to the lower chromosphere and photosphere, which are blasted by hard radiations and particle beams from the high-altitude flare kernel (Haisch et al., 1991). The investigation of detailed flare physics historically has relied on multiwavelength simultaneous observations, involving both spectroscopy and photometry.

Ultraviolet emission lines provide an important source of plasma cooling, as well as lower-atmospheric heating, during the gradual phase of stellar flares (e.g., Hawley et al., 2003), and thus are valuable diagnostics of the flare evolution. Figure 2 shows Mg II h & k line profiles from a flare on the RS CVn-type binary HR 1099 observed by *IUE*. At the flare peak, the Mg II lines display very broad wings, and the mid-UV continuum is enhanced. Busà et al. (1999) analysed this flare and concluded that material was ejected by the secondary star in the direction of the primary.

Although large flares are a conspicuous contributor to transient heating of stellar coronae, smaller scale events—so-called micro- and nano-flares—might play a key role in the “steady” heating of the outer layers of cool stars. Robinson et al. (2001) studied the statistics of transient bursts in high time resolution UV observations of AU Mic with *HST* STIS, and concluded that the power-law slope of the occurrence rate versus time-integrated flux was considerably steeper for

low-energy flares than for the rarer high-energy ones; implying that microflares potentially can account for a significant portion, if not all, of the coronal heating (see, e.g., Hudson, 1991 and Güdel, 2003). However, this is such an important issue that more conclusive evidence is needed: the investigation should be extended to a larger sample of flare stars with sufficient time resolution and sensitivity to collect a significant number of events for each target.

3.1.4. UV emissions from very late M dwarfs and brown dwarfs

Magnetic activity decreases for spectral types later than approximately M7. However, flares have been observed in the radio, optical, UV and X-rays from very late dM stars and brown dwarfs (e.g., Linsky et al., 1995, Rutledge et al., 2000). Several authors have suggested that hot gas in the atmospheres of very low mass main-sequence stars and brown dwarfs is present only during flares (Fleming et al., 2000, Rutledge et al., 2000, Mohanty et al., 2002, Berger et al., 2001, Berger, 2001). However, by recording UV spectra of a sample of these stars, Hawley & Johns-Krull (2003) showed that persistent quiescent chromospheres and transition regions, similar to those observed in earlier type dMe's, are present at least through spectral type M9. The existence of persistent magnetic activity in these fully convective stars poses challenges for contemporary $\alpha\Omega$ -type dynamo models that require a shear layer between the convective outer envelope and the radiative interior. The current thinking is that a "distributed dynamo" might be in play, one that operates directly on convective turbulence and does not require the catalyzing agency of differential rotation. Incidentally, this same " α^2 " dynamo process probably also is operating in the slowly rotating red giants, to account for the feable, but nonetheless present, coronal activity of the inhabitants of the so-called "coronal graveyard" (Ayres et al., 2003b), i.e. the region of the HR diagram near K1 III where stars were rarely detected in coronal proxy C IV ($T \sim 10^5$ K) lines and in X-ray surveys.

Extending this work—transient vs. persistent hot plasma—to the even lower mass range, and much cooler atmospheres, of the brown dwarfs will require significantly more sensitive UV spectroscopy than was available, for example, from *HST* STIS.

3.1.5. Composition anomalies in stellar outer atmospheres

Observations of solar and stellar coronae and of the solar wind provide evidence for plasma chemical composition anomalies with respect to the photosphere. The most famous of these is the so-called First Ion-ization Potential (FIP) effect: elements with low FIP (I.P.<10 eV) are overabundant

with respect to high-FIP (>10 eV) species, relative to photospheric ratios. This is the case, for instance, in closed magnetic flux regions on the Sun and in the slow solar wind (see Feldman and Laming (2000) for a review). On stars, a variety of behaviours are found, including the absence of any low-FIP bias, normal low-FIP enhancements, and even low-FIP abundance depletions (the so-called Metal Abundance Depletion [MAD] syndrome) seen in very active stars (Audard et al., 2003; Güdel, 2004).

The FIP chemical fractionation effect is thought to be a byproduct of the processes that heat and structure the chromosphere. For example, MHD waves passing through an ambient plasma with a temperature below about 7000 K, where low-FIP elements are the only ones ionized, could selectively sweep these ions into the corona, thereby boosting the local abundance. An important goal for future work would be to link stellar chromospheric spatial structure, as derived from UV Doppler images, to the coronal abundance patterns deduced from rotational modulations of suitable coronal X-ray lines, to constrain models of the FIP effect and its MAD syndrome cousin.

Recently, Laming (2004) has proposed models for abundance anomalies in the coronae of the sun and other late-type stars following a scenario first introduced by Schwadron et al. (1999). According to these models, the abundance anomalies are produced by the ponder-motive (proportional to the $\mathbf{j} \times \mathbf{B}$) force on ions arising as Alfvén waves propagate through the chromosphere and depends sensitively on the chromospheric wave energy density. The model can explain both the solar FIP effect and its variations as well as the inverse FIP effect observed in some stars. A better understanding of the coronal abundance anomalies may therefore offer a unique diagnostic of Alfvén wave propagation between the chromosphere and corona.

3.2. Magnetic activity of stars hosting planets

More than 130 extrasolar planets have been detected so far, mainly around solar-type stars. Most of these planets are massive Jovian-types, observationally favored by the currently popular Doppler-reflex observing techniques. However, space missions like *COROT* (Baglin, 2003), *Kepler* (Borucki et al., 2003), and *Darwin* (Fridlund, 2004) will discover—and eventually allow us to characterize—Earth-sized extra-solar planets.

How a planet might directly interact with its parent star is a new field of research, motivated by the tight orbits of some of the extreme "roasters." Cuntz et al. (2000) predicted that a giant planet orbiting close-by a star incites increased stellar activity by means of tidal and magnetospheric interactions. Experimental data supporting this prediction were reported by Shkolnik et al. (2001, 2005), who found the strength of the emission reversals in the Ca II H&K lines of a couple of

stars hosting **hot Jupiters** to be variable with the planet orbital period. The effects of the nearby planet should be exaggerated in the upper chromosphere, transition region, and corona; thus UV, and EUV, spectroscopy will certainly contribute importantly to exploring such planet-star interactions.

The other side of the story is to understand how stellar activity affects planets, especially habitable ones. The evolution of a planetary atmosphere under the joint erosive impacts of coronal ionizing radiations and wind from the parent star (e.g., Ayres, 1997), is an exciting scientific issue, with important ramifications for understanding the evolution of Earth's paleoclimate and the birth of life (see Lammer et al., 2003).

UV spectroscopy of the parent stars of planetary systems is feasible with a 2-m class telescope for most of the relatively nearby stars in contemporary planet searches by the Doppler reflex technique, as shown by *HST*. In fact, by using STIS on *HST*, Vidal-Madjar et al. (2003) found $\sim 15 \pm 4\%$ extra-absorption in the Ly- α emission line of HD 209458 (V = 7.6) during the transit of its *hot-jupiter* planet, which can be understood in terms of escaping hydrogen atoms from the planet atmosphere. Again looking at the UV stellar spectrum during the planetary transit, Vidal-Madjar et al. (2004) detected C and O in the atmosphere of HD 209458b. However, a more sensitive 4–6-m class UV facility would be needed to reach the next tier of fainter planet-stars that will be discovered in future surveys by *COROT* and *Kepler* exploiting the transit method.

In terms of detecting life on other worlds, we mention that there are useful biomarkers in the UV: for example ozone, O₂, H₂, CO⁺, CH₄. Gómez de Castro et al. in this volume has a more extensive description of these biomarkers, so we will not discuss them further.

3.3. Astrospheres and solar-like stellar winds

Winds of late-type stars are a byproduct of magnetic coronal activity, certainly in dwarf stars like the Sun, but perhaps also, to some extent, in red giants (e.g., Ayres et al., 2003b). The winds of low-mass cool stars feed back on their coronal evolution owing to the significant angular momentum carried away by a fast, magnetized outflow. In the evolved red giants, winds can potentially change the nuclear evolution of the star by removing significant mass from the surface layers (see e.g. Rauscher et al., 2002). Furthermore, as mentioned previously, coronal winds can erode volatiles from primitive planetary atmospheres by sweeping up charged molecules and ions from exospheric regions ionized by the stellar UV radiation field. Hence, exploring the winds of low-mass and evolved stars is of fundamental importance from a number of standpoints.

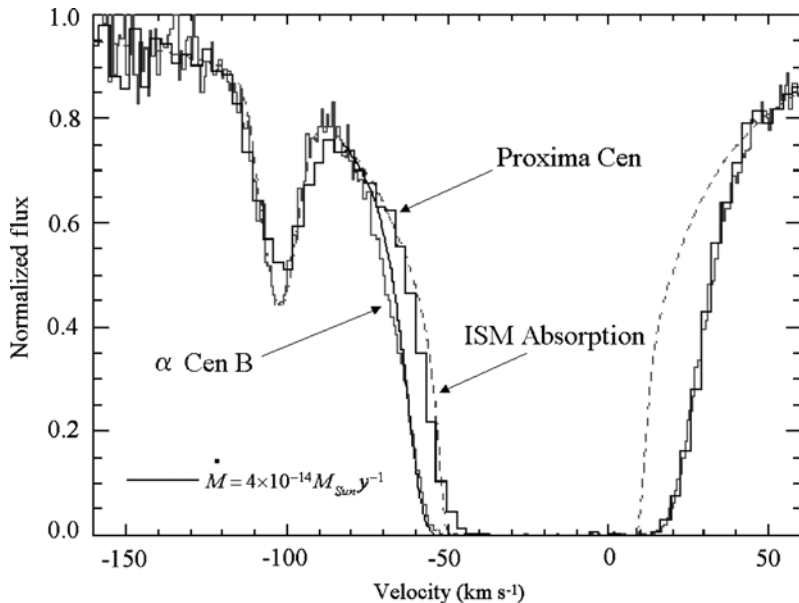
The velocity structure, mass loss rate, and ionization of the outflowing gas in the low-temperature ($\sim 10^4$ K) winds of late-type giants and supergiants can be inferred from high

resolution spectra of optically thick UV resonance lines (see e.g. Dupree et al., 2004, Young et al., 2005, Dupree et al., 2005). The UV provides unique access to the dominant circumstellar wind absorption species in the red giants: H I, O I, Mg II, and C II. Unfortunately, the winds of main sequence stars like the Sun are too hot and too thin to provide detectable UV or X-ray absorption (or emission) signatures, yet understanding these coronal outflows is of paramount importance to the wide range of issues described above. Fortunately, however, in a few favorable cases of nearby stars, coronal winds can be studied by subtle distortions of the H I Ly α line due to the “hydrogen walls” produced by the interaction of the stellar outflow with inflowing interstellar gas (cf. Wood et al., 2001, 2005a). In the stellar “astrosphere”, the stellar analog of the solar “heliosphere”, decelerated interstellar hydrogen (in the stellar rest frame) produces an absorption feature on the blue side of the interstellar absorption (seen in the observer's rest frame), as shown in Figure 3. By modeling these absorption features, Wood et al. (2002) performed the first quantitative measurements of mass loss rates for G and K dwarf stars. These authors found that the mass loss rates increase with activity, as measured by the X-ray surface flux, and thus with decreasing stellar age. By extending their investigation on a slightly large sample of dwarfs, Wood et al. (2005b) found evidence that winds suddenly weaken at a certain activity threshold. These authors suggest that in very active stars, winds may be inhibited by the strong magnetic fields associated with stellar spots that have a large filling factor on these stars. The sample of dwarfs for which an astrosphere has been detected thanks to high resolution profiles of their H I Ly α lines consists of 14 stars only. While it is necessary to consistently enlarge the number of studied stars in order to sample with a great significance each activity/age stage, the mass-loss/age relation inferred by Wood et al. (2005b) gives us an empirical estimate of the history of the solar wind. By implication, the solar wind might have been 1000 times stronger when the Sun was very young, and thereby likely played a major role in the evolution of planetary atmospheres, particularly the stripping of volatiles from primitive Mars.

3.4. Activity in young stellar clusters

The study of late-type stars in young (~ 50 –100 Myr) galactic clusters, and even younger star-forming regions (1–10 Myr), is a valuable window into not only the evolution of magnetic activity, but also its basic characteristics. In particular, within a given cluster or other coeval group of objects, the relationships between, for example, activity indicators and rotation periods for stars of different spectral types will not suffer a hidden age bias due to the common age and chemical composition of the stars.

Fig. 3 Comparison between the Ly α spectra of α Cen B (grey-tone histogram) and Proxima Cen (black-tone histogram). The inferred ISM absorption is shown as a grey-tone dashed line. The α Cen/Proxima Cen data agree well on the red side of the H I absorption, but on the blue side the Proxima Cen data do not show the excess absorption seen toward α Cen (i.e., the astrospheric absorption). The blue-side excess Ly α absorption is fitted by a model of the α Cen astrosphere, corresponding to a mass loss of $\dot{M} = 4 \times 10^{-14} M_{\odot} \text{ yr}^{-1}$ (adapted from Wood et al., 2001)



It is generally accepted that late-type stars undergo spin-down due to magnetic braking throughout their main-sequence phase, especially near the beginning when their angular momentum is highest thanks to spin-up by their natal disks (see, e.g., Jianke and Collier Cameron, 1993; Collier Cameron and Jianke, 1994 and references therein). Studies of the “Sun in time” (see Ribas et al., 2005; Guinan et al., 2003, Ayres, 1997, and references therein) have made use of observations of stars with different rotation periods and ages, but spectral types similar to the Sun to build a scenario of what might have happened to the Sun at different stages along its evolutionary path. These several efforts have used observations of activity tracers in the optical, ultraviolet and X-rays. In particular, in the ultraviolet domain *IUE* spectra were intensively exploited to extract information on chromospheric and transition region fluxes; while more recently *FUSE* observations were used to study the outer atmosphere (Guinan et al., 2003): emission features in the *FUSE* 920–1180 Å band probe hot plasma over three decades in temperature: from $\sim 10^4$ K for the H I Lyman series to $\sim 6 \times 10^6$ K for the coronal Fe XVIII 974 Å line.

The general activity-rotation-age relationship in stars also has been the subject of many studies. In one of the first efforts (Simon et al., 1985) utilized *IUE* data of a moderate size sample of solar-type field stars, compared with observations of T Tauri stars, in order to determine whether the pattern of main-sequence chromospheric decay shown by stars older than about 100 Myr extended back to earlier times. They showed that the activity-age relation for main sequence stars older than about 100 Myr can be modeled by an exponential law whose rate of decline depends on surface temperature.

Unfortunately, few subsequent extensive studies in this direction have been carried out using the much more sen-

sitive contemporary instruments of *HST* or other missions. Ayres (1999) obtained GHRS spectra (1150–1670 Å) of three solar-type dwarfs in the young clusters α Per (85 Myr) and the Pleiades (125 Myr) to complement an earlier FOS study of 10 cluster stars, including 5 in the Hyades (625 Myr); with the aim to investigate the behavior of the stellar activity and the dynamo at early ages (Ayres, 1997). Although the study drew important conclusions on the activity-age relationship for TR lines like C IV, these referred specifically to early G-type dwarfs, and generalization to other spectral types and luminosity classes was not possible. The lack of modern UV studies of the age-activity relation contrasts with the very extensive surveys accomplished in the optical (see e.g. Soderblom et al., 2001) and X-ray domains. In the latter, for example, Pizzolato et al. (2003) investigated the relationship between coronal X-ray emission and stellar rotation in a sample of 259 dwarfs in the *B–V* range 0.5–2.0 observed with *ROSAT*, including 110 field stars and 149 members of the Pleiades, Hyades, α Per, IC 2602 (30 Myr) and IC 2391 (30 Myr) open clusters. The “missing” UV part of the puzzle is extremely important to problems such as the radiative erosion of primitive planetary atmospheres by young hyperactive parent stars because the dominant ionizing radiations for abundant, atmospheric molecules like N₂ fall in the Lyman continuum (see Ayres, 1997); the crucial bright O v 629 Å feature, for example, cannot be observed directly in stars, but its strength can be inferred through measurements of O IV, O V, and O VI UV lines longward of the 912 Å H I edge.

At ages less than about 10^7 years, pre-main sequence T Tauri stars are located in star-forming regions. The UV is extremely valuable in studies of the less-obscured of the classical and “naked” T Tauri stars. For example, Herczeg et al.

Table 1 Instrumental requirements for research on cool stars in the UV domain

Issue	Telescope class	Spectroscopy or Imaging	Spectral resolution	Spectral resolution	Spatial monitoring	Time resolution
Doppler imaging of field stars	2 m	S	$\geq 35,000$		YES	minutes
Direct imaging of chromospheres and TRs	Interferometry (e.g. 20×1 m)	1		$\sim 50\text{--}100 \mu\text{as}$	YES	minutes
Plasma dynamics in chromosphere, TR and corona	2 m	S	≥ 35000		YES	minutes
Stellar activity of extrasolar planets' parent stars	2 m 4–6 m ^a	S	≥ 35000		YES	minutes
Astrospheres solar like stellar winds	2 m 4–6 m ^a	S	≥ 100000		YES	minutes
Flares	2 m	S	>10000		YES	seconds

^aTargets that will be explored by *COROT*, *Kepler*, and *Darwin*

(2004) has studied the fluorescent excitation of the Lyman bands of H₂ lines by H I Ly α to probe the physical conditions in the accretion disk. UV signatures of the hot splashdown point of the accretion stream can be exploited to estimate the accretion rate and geometry (Johns-Krull et al., 2000; Calvet et al., 2004). Furthermore, these very young objects, not surprisingly, are hyperactive in terms of the usual UV and X-ray indicators, and thus provide a laboratory for “magnetic activity in extreme environments”. The dissection of the highly complex TRs and coronae of these quite exotic objects is an important challenge for future emission-line Doppler imaging efforts.

4. Instrument requirements

Progress in exploring fundamental cool-star issues such as the dynamo and coronal heating benefits tremendously from high resolution UV spectroscopy. At a minimum, a resolution of $R = 30,000$ is sufficient to resolve most of the narrow chromospheric emission lines seen in dwarf stars, which typically have FWHM > 10 km/s. The hotter TR lines are broader owing to higher thermal velocities, but they also benefit from good resolution for deblending purposes, dynamical studies, and Doppler imaging. In addition to resolution, high sensitivity is needed to reach the faint, interesting objects beyond the solar neighborhood, out to at least 150 pc to include, for example, the important young galactic clusters a Per and the Pleiades, as well as the key TW Hya star-forming region.

For studies of cool winds and astrospheres, higher resolutions are needed: $R = 100,000$ has proved crucial in previous GHRS and STIS work, and certain ISM-oriented problems probably could benefit from $R = 200,000$, or more. Here,

however, sensitivity is less of an issue, because most of the key objects for wind studies are nearby bright red giants (or bright hot stars for ISM work). For some sources the lack of short-term variability (particular in the ISM background “light sources”) means that one can integrate for long periods to build up sufficient signal-to-noise in the high-resolution line profiles.

It also would be important to have a high sensitivity mode at lower resolution, to reach the next tier of interesting objects beyond the horizon accessible to the $R = 30,000$ mode and to study flares and other types of variability. Historically (e.g., for GHRS or STIS) this would be a $R = 1000$ resolution mode, but we would argue for at least 35000 (i.e., velocity resolution better than 100 km s^{-1}) because then one can have cleaner separation of close lines, some velocity discrimination in short-period binary systems, and the possibility of measuring hypersonic dynamics in large flare events. Furthermore, broad spectral coverage in the low-resolution and mid-resolution modes is essential, from the viewpoint of observing efficiency.

Together with point source spectroscopy, a long-slit imaging capability, in at least the low resolution mode ($R = 35000$) and possibly also the mid-resolution mode ($R = 35000$), would be especially valuable in studies of close binaries and the gaseous environments of PMS stars. In fact, a simple direct imaging system with suitable narrow-band filters tuned to important TR lines like C IV could be exploited to monitor flares and rotational modulations of active regions in dozens of late-type stars at the same time, for example, members of a compact galactic cluster or PMS candidates in a star-forming region. A beam splitter could divert visible light into a simple prism system that would record a low-res spectral energy distribution as well as key emission features

such as Ca II or H α . In this regard, the “Optical Monitor” on *XMM*-Newton has proven extremely valuable, although in the cool-star application one would want an optical system with a large dynamic range capable of recording bright nearby stars as well as much fainter distant objects.

In summary, research on cool stars would benefit enormously from a new 2 m class orbiting telescope feeding a high sensitivity, high resolution UV spectrometer, with an auxiliary strap-on optical/UV monitoring system. The telescope should be placed far from the Earth in a drift-away, L2, or Molniya-type high orbit suitable for long-duration uninterrupted observations of targets to obtain high quality Doppler maps, flare light curves and statistics, and for operational flexibility to allow rapid response to targets of opportunity. High wavelength accuracy is required by many of the topics we would address, hence a Pt-Ne calibration system—missing from FUSE, but which has been incredibly valuable for GHRS and STIS—is an essential component of such a facility.

A larger aperture telescope, of 4–6 m class, would allow the study of plasma dynamics and chromospheric/TR structures of fainter magnetic active stars, brown dwarfs, and cool stars in more distant stellar clusters and star-forming clouds beyond 150 pc: This more sensitive facility would also be able to characterize the outer atmospheres of parent stars of extrasolar planets that will be discovered by future space missions like *Corot*, *Kepler* or *Darwin*.

A summary of instrumental requirements discussed above is given in Table 1.

5. Conclusions

The term “stellar activity”, as applied to the Sun and other late-type stars, includes a very broad range of phenomena, such as starspots, plages, active regions, prominences, flares, coronal loops, winds, mass ejections, and so forth. These phenomena are observed directly on the Sun, and their existence on other stars is inferred by solar analogy from specific spectral properties or behaviors (following the so-called “solar-stellar” connection).

The driving mechanism for stellar activity is the magnetic field generated presumably by a dynamo process at the base of or embedded in the convection zone. The activity that we see in the outer atmospheres of late-type stars thus has its roots deep within the star. This activity is important in its own right, and also because of the influences of its ionizing radiations and wind on the heliosphere, or its extrasolar equivalent; as a model of magnetodynamic processes operating broadly in the cosmos; and as a window into the deep interior of the star.

Since in the near future, direct surface imaging of the morphology connected with activity will not be feasible for other

stars, the key information must be extracted from remote-sensing spectroscopy. The importance of the ultraviolet part of the electromagnetic spectrum in this regard has been emphasized: cool-star magnetic activity produces hot material above the stellar photosphere, from the chromosphere to the million degree, or hotter, corona. There are very few lines in the optical or infrared that are sensitive even to the cooler end of this range. On the other hand, emission lines formed at temperatures up to 10⁷ K are accessible in the UV longward of the LyC edge, and achieving high spectral resolution and large effective areas is much more feasible in this wavelength domain than in soft X-rays. From a practical point of view, cool stars usually have negligible photospheric emission below \sim 1900 Å, so the UV emissions from magnetically disturbed hot gas can be recorded with high contrast.

We can confidently say that ultraviolet astronomy is absolutely fundamental for understanding cool-star physics, and further progress in this area absolutely requires a new generation of UV observatories in space.

Acknowledgements IP thanks EU for supporting the Network for Ultraviolet Astronomy (NUVA) within the OPTICON program funded in the contest of its 6th Framework Program. The work of BM has been supported in part by the Spanish grant AYA2001-1124-C02, and TRA by NASA grant NAG5-13058. JLL thanks NASA for support through grant AR-09930 to the University of Colorado.

References

- Achour, H., Brekke, P., Kjeldseth-Moe, O., Maltby, P.: ApJ **453**, 945 (1995)
- Audard, M., Güdel, M., Sres, A., Rassen, A.J.J., Mewe, R.: A&A **398**, 1137 (2003)
- Audard, M., Telleschi, A., Güdel, M., Skinner, S.L., Pallavicini, R., Mitra-Kraev, U.: ApJ **617**, 531 (2004)
- Ayres, T.R.: ApJ **244**, 1064 (1981)
- Ayres, T.R.: JGR (Planets) **102**, 1641 (1997)
- Ayres, T.R.: ApJ **525**, 240 (1999)
- Ayres, T.R.: Astrophysics in the far-ultraviolet: five years of discovery with FUSE, in: Sonneborn, G., Moos, W., Andersson, B.-G. (eds.), ASP Conference Series, in press (2005)
- Ayres, T.R., Stencel, R.E., Linsky, J.L., Simon, T., Jordan, C., Brown, A., Engvold, O.: ApJ **274**, 801 (1983)
- Ayres, T.R., Jensen, E., Engvold, O.: ApJS **66**, 51 (1988)
- Ayres, T.R., Simon, T., Stauffer, J.R., Stern, R.A., Pye, J.P., Brown, A.: ApJ **473**, 279 (1996)
- Ayres, T.R., Simon, T., Stern, R.A., Drake, S.A., Wood, B.E., Brown, A.: ApJ **496**, 428 (1998)
- Ayres, T.R., Brown, A., Harper, G.M., Osten, R.A., Linsky, J.L., Wood, B.E., Redfield, S.: ApJ **583**, 963 (2003a)
- Ayres, T.R., Brown, A., Harper, G.M.: ApJ **598**, 610 (2003b)
- Baglin, A.: AdSpR **31**, 345 (2003)
- Baliunas, S.L., Donahue, R.A., Soon, W.H., Horne, J.H., Frazer, J., et al.: ApJ **438**, 269 (1995)
- Berger, E. et al.: Nature **410**, 338 (2001)
- Bogess, A., Wilson, R.: Exploring the Universe with the IUE satellite, in: Kondo, Y. (ed.), Kluwer Academic Publishers, Dordrecht, p. 3 (1987)

- Belvedere, G., Paternò, L., Stix, M.: *A&A* **86**, 40 (1980a)
- Belvedere, G., Paternò, L., Stix, M.: *A&A* **88**, 240 (1980b)
- Belvedere, G., Paternò, L., Stix, M.: *A&A* **91**, 328 (1980c)
- Berdyugina, S.V., Tuominen, I.: *A&A* **336**, L25 (1998)
- Bonanno, A., Elstner, D., Belvedere, G., Rüdiger, G.: *AN* **326**, 170 (2005)
- Borucki, W.J. et al.: *SPIE* **4854**, 129 (2003)
- Bowyer, S., Drake, J.J., Vennes, S.: *ARA&A* **38**, 231 (2000)
- Brynildsen, N., Kjeldseth-Moe, O., Maltby, P.: *ApJ* **462**, 534 (1996)
- Busà, I., Pagano, I., Rodonò, M., Neff, J.E., Lanzafame, A.C.: *A&A* **350**, 571 (1999)
- Butler, C.J.: *Sol. Phys.* **152**, 35 (1994)
- Calvet, N., Muñoz, J., Briceño, C., Hernández, J., Hartmann, L., Saucedo, J.L.: *AJ* **128**, 1294 (2004)
- Carlsson, M., Stein, R.F.: *ApJ* **481**, 500 (1997)
- Carpenter, K.G., Schrijver, C.J., Allen, R.J. et al.: SPIE astronomical telescopes and instrumentation, SPIE Paper #5491–28 (2004)
- Catalano, S., Rodonò, M., Cutispoto, G., Frasca, A., Marilli, E. et al.: in: Ibanoglu, C. (ed.), Variable stars as essential astrophysical tools, NATO ARW, 544, p. 687 (2000)
- Chugainov, P.F.: Comm. 27 IAU, Inf. Bull. Var. Stars 122 (1966)
- Collier Cameron, A., Jianke, L.: *MNRAS* **269**, 1099 (1994)
- Cuntz, M., Saar, S.H., Musielak, Z.E.: *ApJ* **533**, L151 (2000)
- Cutispoto, G., Messina, S., Rodonò, M.: *A&A* **367**, 910 (2001)
- Cutispoto, G., Messina, S., Rodonò, M.: *A&A* **400**, 659 (2003)
- Dempsey, R.C., Neff, J. E., Lim, J.: *AJ* **122**, 332 (2001)
- Dere, K.P., Bartoe, J.-D.F., Brueckner, G.E.: *Sol. Phys.* **123**, 41 (1989)
- Doschek, G.A. et al.: *ApJ* **196**, L83 (1975)
- Dupree, A.K., Reimers, D.: “Exploring the Universe with the IUE satellite”, in: Kondo, Y. (ed.), Kluwer Academic Publishers, Dordrecht, p. 321 (1987)
- Dupree, A.K.: *IAU Symp.* **219**, 623 (2004)
- Dupree, A.K., Lobel, A., Young, P.R., Ake, T.B., Linsky, J.L., Redfield, S.: *ApJ* **622**, 629 (2005)
- Favata, F., Micela, G.: *SSRv.* **108**, 577 (2003)
- Favata, F., Micela, G., Baliunas, S.L., Schmidtt, J.H.M.M., Güdel, M. et al.: *A&A* **418**, L13 (2004)
- Feldman, U., Laming, J.M.: *Phys. Scr.* **61**, 222 (2000)
- Feldman, U., Curdt, W., Landi, E., Wilhelm, K.: *ApJ* **544**, 508 (2000)
- Fleming, T.A., Giampapa, M.S., Schmitt, J.H.M.M.: *ApJ* **533**, 372 (2000)
- Fridlund, C.V.M.: *AdSpR* **34**, 613 (2004)
- Gilliland, R.L., Dupree, A.K.: *ApJ* **463**, L29 (1996)
- Godoli, G.: in: Oehman, Y. (ed.), Mass motion in solar flares and related phenomena, 9th Nobel Symp., p. 211 (1968)
- Güdel, M.: *A&ARv* **12**, 71 (2004)
- Güdel, M., Audard, M., Kashyap, V.L., Drake, J.J., Guinan, E.F.: *ApJ* **582**, 423 (2003)
- Guinan, E.F., Ribas, I., Harper, G.M.: *ApJ* **594**, 561 (2003)
- Haisch, B., Strong, K.T., Rodonò, M.: *ARA & A* **29**, 275 (1991)
- Hansteen, V.: *ApJ* **402**, 741 (1993)
- Harper, G.M.: in: Favata, F. et al. (eds.), Proc. of the 13th Cambridge Workshop on Cool Stars, Stellar Systems and the Sun. ESA SP-560, p. 51 (2004)
- Hawley, S.L. et al.: *ApJ* **597**, 535 (2003)
- Hawley, S.L., Johns-Krull, C.M.: *ApJ* **588**, L112 (2003)
- Herczeg, G.J., Linsky, J.L., Valenti, J.A., Johns-Krull, C.M., Wood, B. E.: *ApJ* **572**, 310 (2002)
- Herczeg, G.J., Wood, B.E., Linsky, J.L., Valenti, J.A., Johns-Krull, C.M.: *ApJ* **607**, 369 (2004)
- Hudson, H.S.: *Sol. Phys.* **133**, 357 (1991)
- Imhoff, C.L., Appenzeller, I.: Kondo, Y. (ed.), Exploring the Universe with the IUE Satellite, Kluwer Academic Publishers, Dordrecht, p. 295 (1987)
- Jianke, L., Collier Cameron, A.: *MNRAS* **261**, 766 (1993)
- Johns-Krull, C.M., Valenti, J.A., Linsky, J.L.: *ApJ* **539**, 815 (2000)
- Jordan, C., Linsky, J.L.: Exploring the Universe with the IUE Satellite, Kondo, Y. (ed.), Kluwer Academic Publishers, Dordrecht, p. 259 (1987)
- Jordan, C., Sim S.A., McMurry, A.D., Aruvel, M.: *MNRAS* **326**, 303 (2001)
- Judge, P.G., Saah, S.H., Carlsson, M., Ayres, T.R.: *ApJ* **609**, 392 (2004)
- Laming, J.M.: *ApJ* **614**, 1063 (2004)
- Lammer, H., Selsis, F., Ribas, I., Guinan, E. F., Bauer, S.J., Weiss, W.W.: *ApJ*, **598**, L121 (2003)
- Lanza, A.F., Catalano, S., Cutispoto, G., Pagano, I., Rodonò, M.: *A&A* **332**, 179 (1998)
- Lanza, A.F., Catalano, S., Rodonò, M., Ibanoglu, Tas, G. et al.: *A&A* **386**, 583 (2002)
- Lanzafame, A.C., Busà, I., Rodonò, M.: *A&A* **362**, 683 (2000)
- Linsky, J.L.: Mechanisms of Chromospheric and Coronal Heating, Ulmschneider, P., Priest, E.R., Rosner, R. (eds.), (Berlin: Springer-Verlag), 166 (1991)
- Linsky, J.L.: *Adv. Space Res.* **32**, 917 (2003)
- Linsky, J.L., Wood, B.E., Judge P., Brown, A., Andrusis, C., Ayres, T.R.: *ApJ* **442**, 381 (1995)
- Linsky, J.L., Wood: *ApJ* **430**, 342 (1994)
- Maran, S.P. et al.: *ApJ* **421**, 800 (1994)
- Messina, S., Guinan, E.F.: *A&A* **393**, 225 (2002)
- Messina, S., Guinan, E.F.: *A&A* **409**, 1017 (2003)
- Messina, S., Rodonò, M., Guinan, E.F.: *A&A* **366**, 215 (2001)
- Messina, S., Pizzolato, N., Guinan, E.F., Rodonò, M.: *A&A* **410**, 671 (2002)
- Mohanty, S., Basri, G., Shu, F., Allard, F., Chabrier, G.: *ApJ* **571**, 469 (2002)
- Neff, J.E., Walter, F.M., Rodonò, M., Linsky, J.L., 1989a, Solar and Stellar Magnetic Activity, Cambridge Astrophysics Series, 34.
- Neff, J.E., Walter, F.M., Rodonò, M., Linsky, J.L.: *A&A* **215**, 79 (1989b)
- Osten, R.A., Ayres, T.R., Brown, A., Linsky, J.L., Krishnamurthi, A.: *ApJ* **582**, 1073 (2003)
- Olah, K., Strassmeier, K.G.: *AN* **323**, 361 (2002)
- Pagano, I., Rodonò, M., Linsky, J.L., Neff, J.E., Walter, F.M., Kovářík, Zs., Matthews, L.D.: *A&A* **365**, 128 (2001)
- Pagano, I., Linsky, J.L., Carkner, C., Robinson, R.D., Woodgate, B., Timothy, G.: *ApJ* **432**, 497 (2000)
- Pagano, I., Linsky, J.L., Valenti, J., Duncan, D.K.: *A&A* **415**, 331 (2004)
- Pallé Bagó, E., Butler, C.J.: *IAU Symp.* **203**, 602 (2001)
- Paternò, L.: *Compt. Rend. Acad. Sci. Paris Ser. IIb* **326**, 393 (1998)
- Peter, H.: *A&A* **360**, 761 (2000)
- Peter, H.: *A&A* **374**, 1108 (2001)
- Pizzolato, N., Maggio, A., Micela, G., Sciortino, S., Ventura, P.: *A&A* **397**, 147 (2003)
- Rauscher, T., Heger, A., Hoffman, R.D., Woosley, S.E.: *ApJ* **576**, 323 (2002)
- Reale, F., Peres, G., Serio, S.: *A&A* **316**, 215 (1996)
- Redfield, S., Linsky, J.L., Ake, T.B., Ayres, T.R., Dupree, A.K., Robinson, R.D., Wood, B.E., Young, P.R.: *ApJ* **581**, 626 (2002)
- Redfield, S., Ayres, T.R., Linsky, J.L., Ake, T.B., Dupree, A.K., Robinson, R.D., Young, P.R.: *ApJ* **585**, 993 (2003)
- Ribas, I., Guinan, E.F., Güdel, M., Audard, M.: *ApJ* **622**, 680 (2005)
- Rice, J.B.: *AN* **323**, 220 (2002)
- Robinson, R.D., Linsky, J.L., Woodgate, B., Timothy G.: *ApJ* **554**, 368 (2001)
- Rodonò, M.: in: M. Zeilik and D. Gibson (eds.), Proc. of the 4th Cambridge Workshop on Cool Stars, Stellar Systems and the Sun. Lecture Notes in Physics **254**, 475 (1986)
- Rodonò, M., Lanzà, A.F., Catalano, S.: *A&A* **301**, 75 (1995)
- Rodonò, M., Messina, S., Lanza, A.F., Cutispoto, G., Teriaca, L.: *A&A* **358**, 624 (2000)

- Rodonò, M., Cutispoto, G., Lanza, A.F., Messina, S.: AN **322**, 333 (2002)
- Rutledge, R.E., Basri, G., Martn, E.L., Bildsten, L.: ApJ **538**, L141 (2000)
- Schrijver, C.J., Zwaan C.: ApJ **473**, 470 (2000)
- Schwadron, N.A., Fisk, L.A., Zurbuchen, T.H., 1999, ApJ **521**, 859.
- Simon, T., Herbig, G., Boesgaard, A.M.: ApJ 293, **551** (1985)
- Shkolnik, E., Walker, G.A.H., Bohlander, D.A.: AAS **33**, 1303 (2001)
- Shkolnik, E., Walker, G.A.H., Bohlander, D.A., Gu, P.-G., Kürster, M.: ApJ **622**, 1975 (2005)
- Soderblom, D., Jones, B.F., Fisher, D.: ApJ **563**, 334 (2001)
- Strassmeier, K.G.: ApJ **348**, 682 (1990)
- Strassmeier, K.G., Rice, J.B., Welhau, W.H., Vogt, S.S., Hatzes, A.P. et al.: A&A **247**, 130 (1991)
- Strassmeier, K.G., Bartus, J., Cutispoto, G., Rodonò, M.: A&AS **125**, 1 (1997)
- Uitenbroek, H., Dupree, A.K., Gilliland, R.L.: AJ **116**, 2501 (1998)
- Teriaca, L., Banerjee, D., Doyle, J.G.: A&A **349**, 636 (1999)
- Vidal-Madjar, A., Lecavelier des Etangs, A., Désert, J.-M., Ballester, G.E., Ferlet, R., Hébrard, G., Mayor, M.: Nature **422**, 143 (2003)
- Vidal-Madjar, A., Désert, J.-M., Lecavelier des Etangs, A., Hebrard, G., Ballester, G.E., Ehrenreich, D., Ferlet, R., McConnell, J.C., Mayor, M., Parkinson, C.D.: ApJ **604**, 69 (2004)
- Vilhu, O., Muhli, P., Huovelin, J., Hakala, P., Rucinski, S.M., Collier Cameron, A. 1998, AJ **115**, 1610 (1998)
- Walter, F.M.: The Future of Cool-Star Astrophysics: in: Brown, A., Harper, G.M., Ayres, T.R. (eds.), Proc. of the 12th Cambridge Workshop on Cool Stars, Stellar Systems, and the Sun, p. 14 (2003)
- Walter, F.M., Neff, J.E., Gibson, D.M. et al., A&A **186**, 241 (1987)
- Wamsteker, W., González-Riestra, R. (eds.) Proc. of the Conference “Ultraviolet Astrophysics beyond the IUE Final Archive”, ESA SP-413
- Wikstøl, Ø., Hansteen, V.H., Carlsson, M., Judge, P. G.: ApJ **531**, 1150 (2000)
- Wilson, O.C.: ApJ **26**, 379 (1978)
- Wood, B.E., Harper, G.M., Linsky, J.L., Dempsey, R.C.: ApJ **458**, 761 (1996)
- Wood, B.E., Linsky, J.L., Ayres, T.R.: ApJ **478**, 745 (1997)
- Wood, B.E., Linsky, J.L., Muller, H.-R., Zank, G.P.: ApJ **547**, L49 (2001)
- Wood, B.E., Müller, H.-R., Zank, G.P., Linsky, J.L.: ApJ **574**, 412 (2002)
- Wood, B.E., Redfield, S., Linsky, J.L., Muller, H.-R., Zank, G.P.: ApJS, **159**, 118 (2005)
- Wood, B.E., Muller, H.-R., Zank, G.P., Linsky, J.L., Redfield, S.: ApJL, **628**, 143 (2005)
- Young, P.R., Dupree, A.K., Espey, B.R., Kenyon, S.J., Ake, T.B.: ApJ, **618**, 891 (2005)

UV Capabilities to Probe the Formation of Planetary Systems: From the ISM to Planets

Ana I. Gómez de Castro · Alain Lecavelier ·
Miguel D'Avillez · Jeffrey L. Linsky · José Cernicharo

Received: 26 April 2005 / Accepted: 16 June 2005
© Springer Science + Business Media B.V. 2006

Abstract *Planetary systems* are angular momentum reservoirs generated during *star formation*. Solutions to three of the most important problems in contemporary astrophysics are needed to understand the entire process of planetary system formation:

The physics of the ISM. Stars form from dense molecular clouds that contain ∼30% of the total interstellar medium (ISM) mass. The structure, properties and lifetimes of molecular clouds are determined by the overall dynamics and evolution of a very complex system – the ISM. Understanding the physics of the ISM is of prime importance not only for Galactic but also for extragalactic and cosmological studies. Most of the ISM volume (∼65%) is filled with diffuse gas at temperatures between 3000 and 300 000 K, representing about 50% of the ISM mass.

The physics of accretion and outflow. Powerful outflows are known to regulate angular momentum transport dur-

ing star formation, the so-called accretion–outflow engine. Elementary physical considerations show that, to be efficient, the acceleration region for the outflows must be located close to the star (within 1 AU) where the gravitational field is strong. According to recent numerical simulations, this is also the region where terrestrial planets could form after 1 Myr. One should keep in mind that today the only evidence for life in the Universe comes from a planet located in this inner disk region (at 1 AU) from its parent star. The temperature of the accretion–outflow engine is between 3000 and 10^7 K. After 1 Myr, during the classical T Tauri stage, extinction is small and the engine becomes naked and can be observed at ultraviolet wavelengths.

The physics of planet formation. Observations of volatiles released by dust, planetesimals and comets provide an extremely powerful tool for determining the relative abundances of the vaporizing species and for studying the photochemical and physical processes acting in the inner parts of young planetary systems. This region is illuminated by the strong UV radiation field produced by the star and the accretion–outflow engine. Absorption spectroscopy provides the most sensitive tool for determining the properties of the circumstellar gas as well as the characteristics of the atmospheres of the inner planets transiting the stellar disk. UV radiation also pumps the electronic transitions of the most abundant molecules (H_2 , CO, etc.) that are observed in the UV.

Here we argue that access to the UV spectral range is essential for making progress in this field, since the resonance lines of the most abundant atoms and ions at temperatures between 3000 and 300 000 K, together with the electronic transitions of the most abundant molecules (H_2 , CO, OH, CS,

A. I. G. de Castro
Instituto de Astronomía y Geodesia (CSIC-UCM), Universidad Complutense de Madrid, Madrid E-28040, Spain

A. Lecavelier
Institute d'Astrophysique de Paris, Paris, France

M. D'Avillez
Department of Mathematics, University of Évora R. Romão Ramalho 59, 7000 Évora, Portugal; Institut für Astronomie, Universität Wien, Türkenschanzstr. 17, A-1180 Wien, Austria

J. L. Linsky
JILA, University of Colorado and NIST, Boulder, CO 80309-0440, USA

J. Cernicharo
DAMIR-IEM-CSIC, C/. Serrano 113 & 121, 28006 Madrid, Spain

$\text{S}_2, \text{CO}_2^+, \text{C}_2, \text{O}_2, \text{O}_3$, etc.) are at UV wavelengths. A powerful UV-optical instrument would provide an efficient mean for measuring the abundance of ozone in the atmosphere of the thousands of transiting planets expected to be detected by the next space missions (GAIA, Corot, Kepler, etc.). Thus, a follow-up UV mission would be optimal for identifying Earth-like candidates.

Keywords UV astronomy · ISM · Pre-main sequence stars · Jets · Winds · Accretion disks · Planets

1. Introduction

The formation of planetary systems covers a broad range of physical and astrophysical processes ranging from the physics of star formation (the interstellar medium (ISM), molecular clouds, and initial mass function), to the physics of accretion and outflow (accretion disk properties, winds generation, and disk instabilities) and finally, the formation of planets (dust nucleation, planetesimal and planet formation, planetary differentiation, planetary atmospheres and sustainable biological systems). The objective of this article is to summarize the reasons why access to the UV range is an essential requirement for making progress in these critically important areas of astrophysics.

For this reason, the article has been split into three key sections: physics of the ISM, physics of accretion and outflow, and planets and bio-markers. A summary has been added to the end of this contribution with the required UV capabilities to make progress in the field.

2. The physics of the ISM

Understanding the physics of the ISM is of prime importance not only for Galactic but also for extragalactic and cosmological studies. The ISM is everything observable in the Galaxy except for stars, e.g., gas (ionised, atomic and molecular), dust, high-energy particles (e.g., cosmic rays) and magnetic fields. The ISM is a very complex, highly non-linear dynamical system whose evolution controls star formation, gas mixing, and, therefore, the chemical enrichment of the Universe.

The ISM is often classified into five components: Hot Ionised Medium (HIM), Warm Ionised Medium (WIM), Warm Neutral Medium (WNM), Cold Neutral Medium (CNM) and dense Molecular Medium (MM) (see, e.g., Kulkarni and Heiles, 1988); the diffuse components (HIM, WIM, WHM and CNM) appear to be in approximate pressure equilibrium. The main properties of these components are summarized in Table 1. X-ray observations are most sensitive to the very hot gas with temperatures $T \geq 10^6$ K. IR and radio wavelength observations are the only tools for studying the dense molecular gas where stars form. UV spectroscopy is

the most sensitive tool for measuring the properties (column densities, temperatures, ionisation fractions, metallicity, depletions, etc.) of the diffuse gas in the 3000–300 000 K temperature range, the WNM and WIM.

In the last few years, old models, based on pressure equilibrium between the various ISM phases (e.g., McKee and Ostriker, 1977), have been replaced by detailed numerical simulations that allow studying the ISM as it is, a dynamical system. High-spatial resolution numerical simulations now permit addressing a set of problems simultaneously, encompassing both large and small scales, provided that the appropriate grid size, resolution and numerical tools (e.g., adaptive mesh refinement) are used. Among the most important of these problems are: (i) global modelling to yield information on the formation and lifetimes of molecular clouds, (ii) how star-forming regions are influenced by large-scale flows in the ISM, and (iii) the dynamic roles that SNe and superbubbles play in triggering local and global star formation (see Heyer and Zweibel, 2004).

Key problems in ISM physics include the determination of the relative contributions to the energy input from the various possible sources (SNe, massive star winds and radiation fields, mass infall from the halo, galactic dynamics, cosmic rays and magnetic fields) and the roles of MHD turbulence and shocks in the energy cascade and structure formation. During the last few years, a very efficient feedback loop has been operating between radio observations and numerical simulations to study the role of MHD turbulence in the energy cascade within the densest regions of the ISM (H I and molecular clouds). A similar feedback loop needs to be established with UV observations to understand the heating/cooling processes and the overall ISM evolution, including the formation of molecular clouds.

Numerical simulations predict that ~65% of the ISM volume (within the disk: $|z| < 250$ pc) is filled with gas at temperatures between 10^3 and $10^{5.5}$ K; in particular, the WIM ($10^4 < T < 10^{5.5}$ K) is expected to fill 25% of the disk volume, while the HIM filling factor is smaller (17%) because it escapes to the halo (de Avillez and Breitschwerdt, 2004). These predictions agree with recent observations. The Wisconsin H-Alpha Mapper (WHAM) has observed O III emission extending to Galactic latitudes as high as $|b| \sim 45^\circ$, and even He I (5876 Å) emission has been detected. However, X-ray and extreme UV observations now show that the filling factor of the HIM in the local ISM is small. Clearly, UV instruments are required to make progress in our understanding of the physics of the Galactic ISM. This physics can be studied at two scales:

Large scale (>kpc scale): At this scale, the prime objectives are understanding the overall star formation efficiency and which parameters control the disk–halo circulation (the Galactic fountain). The roles of supernova

Table 1 Components of the ISM (reference properties)

Component	n (cm $^{-3}$)	T (K)	Ionisation fraction	Spectral range
HIM	Few 10 $^{-3}$	(5–10) $\times 10^6$	1	X-ray, UV
WIM ^{a,b}	Few 10 $^{-1}$	10 4	1	UV, radio, optical
WNM	1–10	(3–8) $\times 10^3$	0.1	UV, optical, IR, radio
CNM	1–50	20–100	10 $^{-2}$	UV, IR, radio
MM	10 3 –10 6	10	<10 $^{-4}$	IR, radio

^aIn the last few years, a new sub-classification has been introduced to distinguish between the WIM envelope around molecular clouds, the so-called McKee & Ostriker WIM or MOWIM, and the other warm, ionised components, the so-called Reynolds WIM.

^bThis nominal temperature is often assigned because most of the observations come from H α emission. However, UV observations have pointed out the presence of significantly hotter gas traced by C IV or O VI

explosions, expanding H II regions and the overall Galactic dynamics (shear, spiral arm shocks, high velocity cloud shocks, etc.) is examined in detail. Some attention is also devoted to understanding Galactic magnetic fields and the Galactic dynamo.

Small scale (the Local Bubble scale): The Local Bubble represents the nearest region of the ISM and is thus an ideal laboratory to test the *details* of the ISM physics: dust depletion and abundances, non-equilibrium ionisation, shocks, turbulence, etc.

2.1. Halo–disk interaction in the Milky Way

The Milky Way is surrounded by a large halo of hot gas which must be replenished as the gas cools. The most direct evidence comes from the detection of high-ionisation UV resonance lines and of X-ray emitting gas surrounding the Galactic disk. The X-ray halo has a luminosity of $\sim 4 \times 10^{39}$ erg s $^{-1}$ and the thickness of the emission is probably a few kpc. The temperature of the X-ray emitting gas is $(1\text{--}2) \times 10^6$ K, well below the escape temperature, and therefore it is gravitationally bound to the Galaxy. The high temperatures of the gas in the halo must be explained by energetic processes, most likely occurring in the Galactic disk (though external sources could contribute). The most likely energy source for these processes are massive OB stars.

There is also evidence that hot halo gas has cooled, as provided by the presence of the high-ionisation UV resonance lines. Some of the UV resonance lines might be produced by photoionisation of gas near 10 4 K, but there is good evidence that the high-ionisation lines, such as Si IV, C IV and N V are due to gas that is cooling (Savage and Sembach, 1994). For the Si IV and C IV absorption lines it was found that the ratio of the column densities from these ions is almost a constant value, implying that the ionisation state of the gas is nearly identical in different parts of the halo. Benjamin and Shapiro (1993) argued that in a galactic fountain, gas cooling from 10 6 K would be opaque to its own radiation, causing it to

self-ionise, so that its ionisation state is determined by the cooling process itself. They also showed that the absorption strength of N V is reproduced by this model. Martin and Bowyer (1990) have shown that the emission from C IV and O III ions is consistent with being produced from a cooling Galactic fountain.

The cooling of the fountain flow, is dominated by collisional ionisation and radiative recombination as three-body recombination (the inverse process of collisional ionisation) is very unlikely to occur, because as the fountain gas, with a temperature in excess of 10 6 K, rises into the halo it expands and cools adiabatically. Hence, there is a reduction of the plasma temperature and density (to be of the order of 10 $^{-2}$ cm $^{-3}$). Furthermore, the cooling timescales at considerable heights above the disk can be much smaller than the dominant microphysical processes and therefore, recombi-

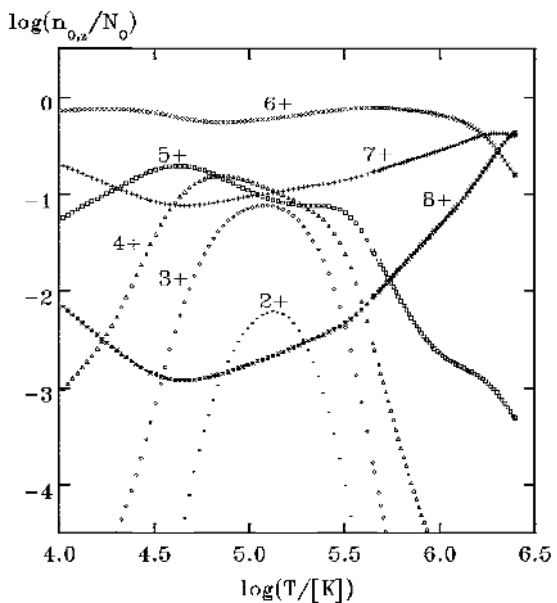


Fig. 1 Ionisation stages of oxygen in a self-consistent calculation of a galactic outflow (wind) (Breitschwerdt and Schmutzler, 1999). The initial temperature of the flow is $T = 2.5 \times 10^6$ K

nation of highly ionised species lags behind (Breitschwerdt and Schmutzler, 1999). An example is the O VI ion that is abundant over a large range of temperatures from 4×10^5 K to temperatures as low as 10^4 K (Fig. 1). Thus, care should be taken while using a single ion like O⁵⁺ as a diagnostic element for plasma temperature (see also Schmutzler and Tscharnutter, 1993).

Thus, measurements of the z -dependence of O VI, N V, C IV and Si IV emission are of prime importance for determining whether the gas is in collisional equilibrium ionisation, in non-equilibrium ionisation, or whether other relevant heating sources maybe present. These observations are critically needed to constrain numerical models of the ISM in disk galaxies to provide further clues concerning how matter and energy are transferred within the Galaxy. This is clearly displayed in Fig. 2; adaptative mesh simulations of the dynamical evolution of the ISM (Avillez and Breitschwerdt, 2004, in press) show that matter in the disk is concentrated in dense shells and filaments, while the halo acts as a pressure release valve for the hot ($T > 10^{5.5}$ K) phase in the disk thereby controlling its volume filling factor. The upper portions of the thick ionised disk form the disk–halo interface located about 2 kpc above and below the mid-plane. Here a large-scale fountain is set up by hot ionised gas injected from either the gas streaming out of the thick disk or directly from superbubbles in the disk underneath. The gas then escapes in a turbulent convective flow.

Radio observations can be used to map the clumpy distribution of matter in the disk, but the most important constraints will come from the study of the vertical distribution of warm gas, which is best studied with UV spectroscopy. This is also true for the high-velocity clouds (HVCs) detected by their H I 21 cm emission, which are surrounded by hot ionised envelopes as pointed out by new observations from the Far Ultraviolet Spectroscopic Explorer (FUSE) mission and the Space Telescope Imaging Spectrograph onboard the Hubble Space Telescope (HST/STIS). The detection of O VI, C IV and Si IV absorption indicates that many HVCs have a hot, collisionally-ionised component (Danly et al., 1992; Tripp et al., 2003). UV absorption lines provide detailed information on the physical conditions and abundances of the gas. Understanding the ionisation of such envelopes will permit us to constrain the properties of the Galactic corona and the Local Group medium. UV absorption lines are the most sensitive probes for determining the abundances (and hence their Galactic or extragalactic origin) of the HVCs (see, e.g., Richter et al., 2001). Note that the most robust specie for constraining the metallicity of HVCs is O I, since oxygen is only slightly depleted by dust grains (Moos et al., 2002) and the ionisation potential of O I is very similar to H I. Thus, oxygen abundances based on the O I/H I ratio depend only slightly on the ionisation of the gas for substantially ionised plasmas.

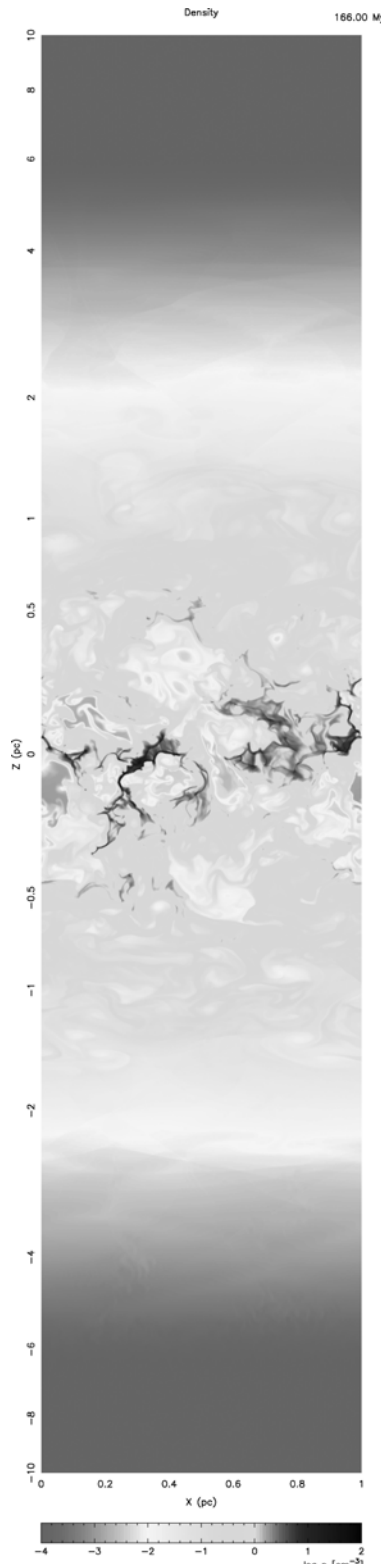


Fig. 2 Slice through the 3D data set showing the vertical (perpendicular to the mid-plane) distribution of the density at time 166 Myr. Red/blue in the colour scale refers to lowest/highest density (or highest/lowest temperature). The z -scale above 0.5 kpc and below -0.5 kpc is shrunk (in order to fit the paper size) and thus, the distribution of the labels is not uniform (from Avillez and Breitschwerdt, in press)

2.2. The local ISM

The Sun lies inside the Local Bubble, a large ionised gas bubble that extends outwards from the Sun to a neutral hydrogen column density $\log N(\text{H I}) \approx 19.2$ (cm $^{-2}$ units), corresponding to a geometrical size of 100–200 pc depending on the direction from the Sun. The Local Bubble's morphology has been identified by Na I absorption, which is formed in the cold gas than surrounds the Local Bubble and determines its shape (Lallement et al., 2003). The Local Bubble is thought to be an H II region formed by the explosions of supernovae and the strong winds of young hot stars in the Lower Centaurus Crux subgroup of the Scorpio–Centaurus Association (Maíz-Apellániz, 2001; Berghöfer and Breitschwerdt, 2002). The temperature of the gas in the Local Bubble is estimated to be about 10 6 K if most of the soft X-ray background is due to thermal emission from the Local Bubble gas. However, analysis of extreme ultraviolet emission obtained with the CHIPS satellite has not yet led to an accurate temperature or emission measure of the hot, low-density Local Bubble gas, which may be far out of collisional ionisation equilibrium.

Embedded in the Local Bubble are a number of warm gas clouds. The Sun is located inside one of these clouds called the Local Interstellar Cloud (LIC). The existence of the LIC was first suggested by Vidal-Madjar et al. (1978). The LIC was first identified by Lallement and Bertin (1992) on the basis of measured Doppler shifts of interstellar absorption lines in many directions that are consistent with a single velocity vector, implying that all of the gas in this cloud is moving with a common velocity away from the centre of the Scorpio–Centaurus Association. Analysis of interstellar UV absorption lines with the high-resolution echelle gratings in the GHRS and STIS instruments on HST enabled Redfield and Linsky (2000) to determine a temperature of the LIC gas (7000 ± 1000 K) and the morphology of the LIC. The LIC centre is located in the anti-Galactic centre direction. The maximum column density through the LIC is $\log N(\text{H I}) = 18.3$, the LIC's maximum dimension is about 6.8 pc, and its mass is about $0.32 M_{\odot}$. The main evidence for the Sun being located inside the LIC is that neutral helium flowing into the heliosphere, which is not influenced by the solar wind, has the same temperature and flow vector as the LIC (Bertin et al., 1993; Witte, 2004).

Slavin and Frisch (2002) computed the ionisation of many elements in the LIC taking into account UV and EUV radiation from the most important ionising source, the star ϵ CMa, hot white dwarfs and other stars, the diffuse UV background, and the estimated radiation from the putative conductive boundary between the warm clouds and the hot gas of the Local Bubble. More sensitive UV observations are required to study this boundary layer, if indeed it is present. Their models assumed ionisation equilibrium and realistic

H I column densities between the centre of the LIC and the external sources of ionising radiation. One of their models predicts the temperature, electron density, and ionisation of many elements in good agreement with observations. Dust, which is present in the LIC and other nearby warm clouds, plays an important role in cooling the gas and in depleting metals such as iron from the gas phase.

There are a number of other warm, partially ionised clouds in the solar neighbourhood, which are also located inside the Local Bubble. The so-called *G* cloud identified by Lallement and Bertin (1992), which is situated in the Galactic centre direction, is slightly cooler than the LIC and has a somewhat different velocity vector. The closest star α Cen (1.3 pc), which is located in the *G* cloud, shows no evidence for absorption by gas at the LIC velocity even in very high signal-to-noise GHRS echelle spectra. This places an upper limit of 0.05 pc on the thickness of the LIC in the direction of α Cen and a time of <3000 years for the Sun to leave the LIC and enter either the *G* cloud or an unknown interface region between the LIC and the *G* cloud.

The broad UV spectral coverage, high spectral resolution, and accurate wavelength scale of the STIS instrument allowed Redfield and Linsky (2004) to measure absorption line wavelengths, widths, and Doppler shifts for many atoms and ions including H I, D I, C II, N I, O I, Mg II, Al II, Si II and Fe II along 29 different lines of sight through warm clouds in the Local Bubble. They detected absorption at 50 different velocities along these lines of sight, indicating about 12 clouds with different velocity vectors. The observation of absorption lines from elements or ions with very different atomic weights (2 for deuterium compared to 56 for iron) allowed Redfield and Linsky (2004) to solve for the gas temperature and non-thermal motions (turbulence) separately for each velocity component. They found velocity components in the local ISM with temperatures as high as about 12 000 K and a few components with temperatures below 3000 K. The mean gas temperature is $T = 6680 \pm 1490$ K, which is characteristic of warm clouds, but there are some velocity components inside the Local Bubble that could be cold clouds. In almost all cases, the non-thermal motions are far smaller than the thermal motions. The mean thermal pressure in the clouds, $P_T/k = 2280 \pm 520$ K cm $^{-3}$. The magnetic fields in these clouds have not yet been measured.

While STIS spectra of interstellar absorption lines formed in the local ISM have begun to reveal its secrets, we have sampled far too few lines of sight to identify the structure of the local ISM in detail. In particular, we do not yet have a good understanding of the amount of gas at different temperatures in the local ISM, nor do we have a detailed understanding of how the ionisation and temperature of the gas depends on the radiation environment and past history. Understanding the physics of the local ISM is required if we are to have any confidence in understanding the physics of the Galactic

disk, halo, and ISM in other galaxies. Since most interstellar absorption lines are located in the UV and the absorption lines are typically narrow with multiple velocity components, a future sensitive high-resolution UV spectroscopic mission is needed to extend the preliminary work provided by the GHRS and STIS instruments on HST.

3. The physics of accretion and outflow

Understanding how stars form out of the contracting cores of molecular gas is a major challenge for contemporary astrophysics. Angular momentum must be conserved during gravitational contraction and magnetic flux is built up and dissipated in the process, but the underlying mechanisms are still under debate.

Solar-like protostars are an excellent laboratory for this purpose, since their pre-main sequence (PMS) phases last ~ 100 Myr. The collapse of low-mass protostars is sub-alfvénic, thus these protostars are expected to be magnetized. The detection of kG fields in stars as young as a few million years (Guenter et al., 1999; Johns-Krull et al., 1999) supports this assumption. In the last few years, a new paradigm has emerged to understand the basics of star formation. Protostars are assumed to be magnetized and star growth is regulated by the interaction between the stellar magnetic field and the disk. The physics of this interaction is outlined in Fig. 3. The disk–star interaction basically transforms the angular momentum of the disk (differential rotation) into plasmoids

that are ejected from the system. There is a current sheet that separates two distinct regions: an inner stellar outflow and an external disk flow. Magnetic flux dissipation should occur in the current layer producing the ejection of plasmoids, as well as the generation of high-energy particles (cosmic rays), X-rays, and ultraviolet radiation.

The phenomenon is non-stationary and is controlled by two different temporal scales: the rotation period and the magnetic field diffusion timescale. Stellar rotation is a well-known parameter that controls the opening of the field lines towards high latitudes. Plasmoid ejection, however, is controlled by field diffusion which is poorly determined (see, e.g., Priest and Forbes, 2000). All models can be fitted into this basic configuration (Uzdensky, 2004).

During the last 5 years, numerical research on this interaction region has gone into outburst (see, e.g., Goodson et al., 1997, 1999). So far, most studies have analysed the interaction between a dipolar stellar magnetic field and a Keplerian accretion disk. Numerical simulations show that the fundamental mechanism for jet formation is robust. The star–disk–outflow system is self-regulating when various initial disk densities, stellar dipolar field strengths, and primordial fields associated with the disk are tested (Matt et al., 2002), although strong stellar magnetic fields may disrupt the inner parts of the accretion disk temporarily (Kueker et al., 2003). Despite the numerical advances made so far, the real properties of the engine are poorly known because of the lack of observations to constrain the modelling. Very important open questions include the following:

1. How does the accretion flow proceed from the disk to the star? Is there any preferred accretion geometry like, for instance, funnel flows?
2. What roles do disk instabilities play in the whole accretion/outflow process?
3. What are the dominant wind acceleration processes? What are the relevant timescales for mass ejection?
4. How does this high-energy environment affect the chemical properties of the disk and planetary building?
5. How important is this mechanism when radiation pressure becomes significant as for Herbig Ae/Be stars?

Infrared and radio wavelengths cannot access this engine because the spatial scales involved are tiny (<0.1 AU or 0.7 mas for the nearest star-forming regions compared with ALMA's resolution of 10 mas) and the temperatures are too high (3000–300 000 K). High-resolution IR spectroscopy has indeed confirmed the presence of *warm* molecular gas with temperatures of 1500–3000 K in the innermost disk: both CO (fundamental and overtone) and H₂O emission have been detected (see Najita et al., 2000 for a review or Carr, Tokunaga and Najita, 2004 for more recent results). Fortunately, after 1 Myr, during the classical T Tauri Star (CTTS) phase, the circumstellar extinction becomes small ($A_V < 1$ mag)

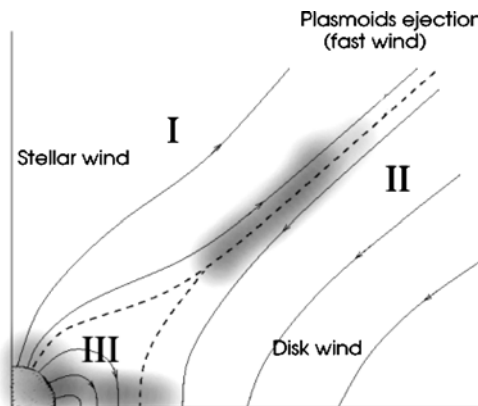


Fig. 3 The interaction between the stellar magnetic field and the disk twists the stellar field lines due to the differential rotation. The toroidal magnetic field generated out of the poloidal flux and the associated pressure tends to push the field lines outwards, inflating them, and eventually braking the magnetic link between the star and the disk (boundary between Regions I and II). Three basic regions can be defined: Region I dominated by the stellar wind, Region II dominated by the disk wind and Region III dominated by stellar magnetospheric phenomena. The dashed line traces the boundaries between this three regions. The continuous lines indicate the topology of the field and the shadowed areas represent regions where magnetic reconnection events are likely to occur, producing high-energy radiation and particles (from Gómez de Castro, 2004)

and the engine described above can be properly tested at ultraviolet wavelengths. The UV spectral range is the richest for diagnosing astrophysical plasmas in the 3000–300 000 K temperature range, since the resonance lines of the most abundant species are located in the UV. In addition, as the UV radiation field is strong in the circumstellar environment, fluorescence emission from the most abundant molecules (H_2 , CO, OH, CS, S₂, CO₂⁺, C₂, and CS) is observed. As a result, a single high-resolution spectrum in the 1200–1800 Å range provides information on the molecular content, the abundance of very reactive species such as the O I, and the warm and hot gases associated with the CTTSs. The potential of UV spectroscopy for studying the physics of accretion during PMS evolution is outlined in the following section.

3.1. UV observations of the jet engine in low-mass stars

The engine is a small structure (≤ 0.1 AU) with several different constituents (the accretion flow, stellar magnetosphere, winds, and inner part of the accretion disk) all radiating in the ultraviolet. The UV spectrum of the T Tauri Stars (TTSs) has a weak continuum and many strong emission lines. The continuum is significantly stronger than that observed in main sequence stars of similar spectral types (G to M); the so-called optical-veiling represents the low-energy tail of this excess UV emission (Hartigan et al., 1990). The underlying photosphere is barely detected, and only in warm (G-type) weak line TTSs (WTTSs) is the photospheric absorption spectrum observed. The UV continuum excess is significantly larger in CTTSs than in WTTSs, as is well illustrated in the colour (UV – V)-magnitude (V) diagram displayed in Fig. 4. Simple models of hydrogen free-free and free-bound emission

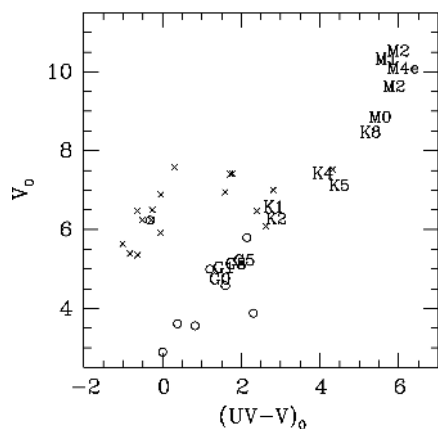


Fig. 4 The (UV – V, V) colour–magnitude diagram for the T Tauri Stars observed with the IUE satellite in the Taurus region (a distance of 140 pc to Taurus has been assumed). The crosses represent cool TTSs (spectral types later than \sim K3) and the open circles represent warm TTSs (spectral types earlier than \sim K3). The location of the main sequence is marked by the spectral types. The stars closer to the main sequence are the WTTTs (from Gómez de Castro, 1997)

added either to black bodies or to the spectra of standard stars reproduce the UV continuum reasonably well (Calvet et al., 1984; Bertout et al., 1988; Simon et al., 1990). The fits yield chromospheric-like electron temperatures of $(1\text{--}5) \times 10^4$ K. Three different mechanisms have been proposed to generate this hot plasma and its UV continuum: (1) a dense chromosphere (Calvet et al., 1984), (2) the release of the gravitational binding energy from the infalling material (Bertout et al., 1988; Simon et al., 1990; Gullbring et al., 2000), and (3) an outflow (Ferro-Fontán and Gómez de Castro, 2003; Gómez de Castro and Ferro-Fontán, 2005). This uncertainty in the formation of the UV emission points out why high-resolution UV spectroscopy and monitoring are so crucial for understanding and constraining the physics of the engine.

3.1.1. Signatures of accretion

The most obvious signature of accretion is the detection of narrow red-shifted absorption components on top of the emission profiles of singly ionised species such as Mg II or Fe II with strong transitions in the UV at 2600 and 2800 Å. It is widely accepted that this absorption is produced in funnel flows: magnetic tubes connecting the inner disk to the stellar surface. However, there are no detailed maps of the funnel flows except for some attempts made in the optical range (Petrov et al., 2001; Bouvier et al., 2003). UV mapping is crucial in determining the rigidity of the flux tubes and thus the possible distortions induced by differential rotation and the magnetic diffusivity of the disk.

Funnel flows are expected to radiate over a broad range of temperature, from 3000 K at the disk end to some 100 000 K at the stellar surface. Since infalling material is nearly in free-fall, its kinetic energy is finally released at the stellar surface in an accretion shock that reaches temperatures of 10^6 K. The dominant output radiation is produced by the photoionised pre-shock infalling gas (Gómez de Castro and Lamzin, 1999; Gullbring et al., 2000). Thus, the full accretion column could be tracked by monitoring CTTSs with a high spectral resolution UV instrument, but this observation has not yet been carried out! The only UV monitoring of CTTSs was by the IUE satellite with low dispersion due to the small effective area of its 40 cm telescope. Nevertheless, the results are very promising as rotational modulation of the UV continuum and line fluxes were detected in DI Cep and BP Tau (Gómez de Castro and Fernández, 1996; Gómez de Castro and Franqueira, 1997a). This modulation is caused by the small size of the accretion shock, which occupies only a small fraction of the stellar surface.

An important result of these campaigns is that only \sim 50% of the UV continuum excess is rotationally modulated. Thus, a significant fraction of the UV excess is not produced by the accretion shock. Whether the wind or an extended magneto-

sphere is responsible for the UV continuum excess remains a matter of debate. In fact, the coexistence of several funnel flows has been proposed to explain this fact (Muzerolle et al., 2001).

3.1.2. Signatures of disks

High-resolution HST/STIS spectra have revealed, for the first time, the rich UV molecular emission in CTTS. H_2 fluorescence emission has now been studied in detail in the nearest CTTS, TW Hya, and the richness of the spectrum is overwhelming: Herczeg et al. (2002) detected 146 Lyman-band H_2 lines, representing 19 progressions (see Fig. 5)! The observed emission is likely produced in the inner accretion disk, as are the infrared CO and H_2O lines. The excitation of H_2 can be determined from the relative line strengths by measuring self-absorption in lines originating in low-energy lower levels, or by reconstructing the $\text{Ly}\alpha$ emission line profile incident upon the warm H_2 using the total flux from each fluorescing upper level and the opacity in the pumping transition. Using this diagnostic technique, Herczeg et al. (2004) estimated that the warm disk surface has a column density of $N_{H_2} = 3.2 \times 10^{18} \text{ cm}^{-2}$, temperature of $T = 2500 \text{ K}$, and filling factor of H_2 as seen from the source of the $\text{Ly}\alpha$ emission of 0.25 ± 0.08 . The observed spectrum shows that some ground electronic state H_2 levels with excitation energies as large as 3.8 eV are pumped by $\text{Ly}\alpha$. These highly excited levels may be formed by dissociative recombination of H_3^+ , which in turn may be formed by reactions involving X-rays and UV photons from the star. A quick inspection of the UV spectra in the IUE and HST archives shows that fluorescent H_2 UV lines are observed in most of the TTSs (see also Gómez de Castro and Franqueira, 1997b; Valenti et al., 2000; Ardila et al., 2002).

The role of far-UV radiation fields and high-energy particles in the disk chemical equilibrium is now beginning to be understood. Bergin et al. (2003) showed how strong $\text{Ly}\alpha$ emission may contribute to the observed enhancement of CN/HCN in the disk. The penetration of UV photons coming from the engine in a dusty disk could produce an important change in the chemical composition of the gas, allowing the growth of large organic molecules. In this context, UV photons photodissociating organic molecules at $\lambda > 1500 \text{ \AA}$ could play a key role in the chemistry of the inner regions of the disk, while those photodissociating H_2 and CO will control the chemistry of the external layers of the disk directly exposed to the radiation from the central engine (see, e.g., Cernicharo, 2004). Ultraviolet radiation also plays a very important role in the evolution of the primary atmospheres of planetary embryos (Watson et al., 1981; Lecavelier des Etangs et al., 2004).

Strong continuum FUV emission (1300–1700 Å) has been detected recently from some stars with bright molecular disks

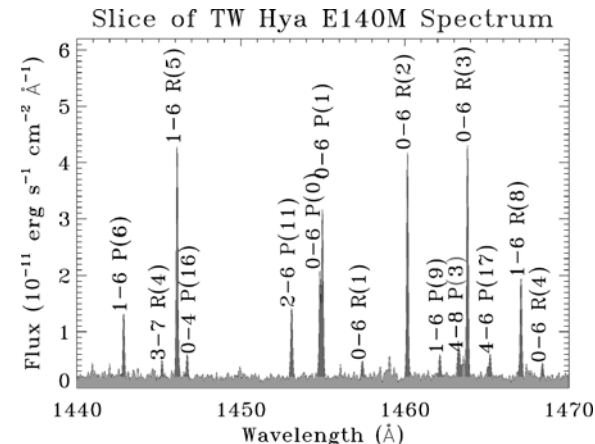


Fig. 5 A portion of the HST/STIS spectrum of the CTTS, TW Hya. The narrow H_2 emission lines originate in the B electronic state after being pumped by the $H I \text{ Ly}\alpha$ line (from Herczeg et al., 2002)

including GM Aur, DM Tau, and LkCa 15, together with inner disk gaps of few AU (Bergin et al., 2004). This emission is likely due to energetic photoelectrons mixed into the molecular layer that likely indicates the existence of a very hot component in the disk. This very hot component is probably created by X-ray and high-energy particle irradiation of the disk (Glassgold et al., 2004; Gómez de Castro and Antonicci, 2005).

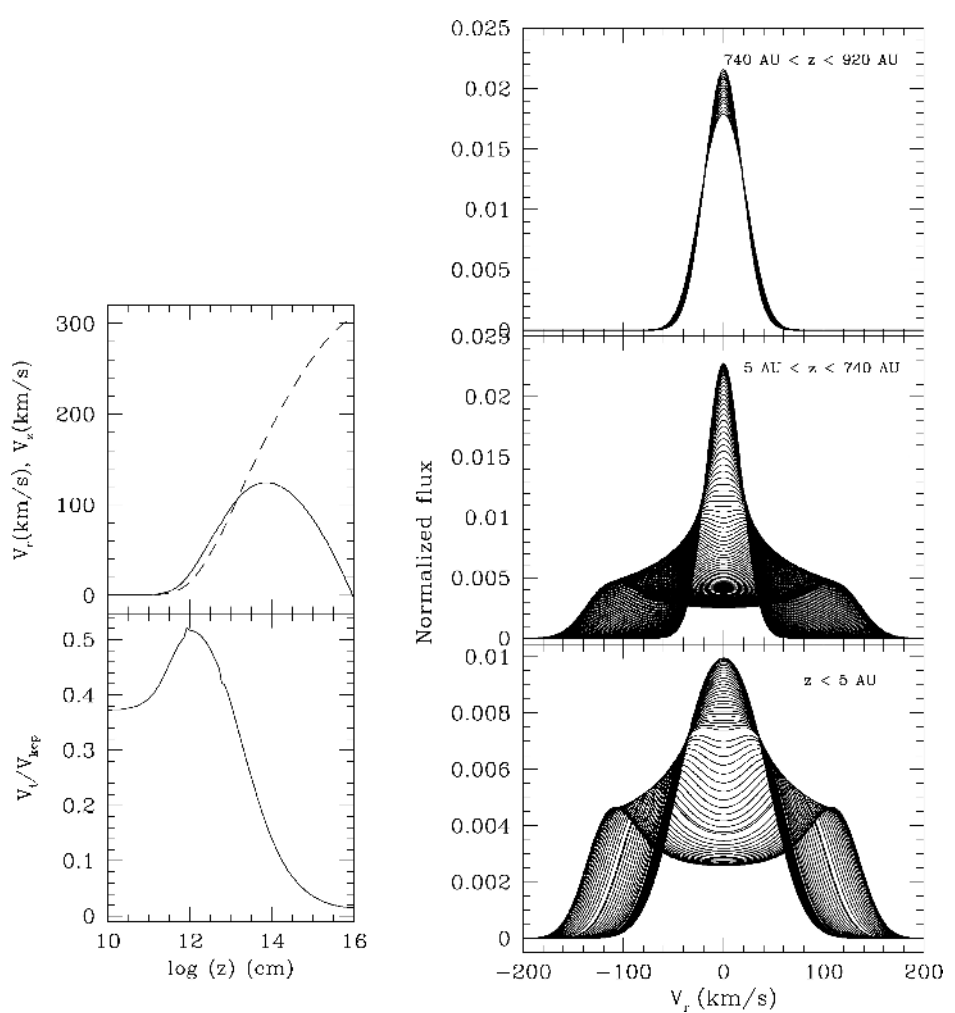
Spectroscopic observations of volatiles released by dust, planetesimals and comets provide an extremely powerful tool for determining the relative abundances of the vaporizing species and for studying the photochemical and physical processes acting in the inner parts of protoplanetary disks. The UV studies of β Pic-like systems illustrate the possibilities of this spectral range for this purpose (Vidal-Madjar et al., 1994, see also, Section 3.3). The relevance of UV observations to study comets is described in detail by Brosch et al. (2005) in the *Solar System* chapter of this volume.

3.1.3. Signatures of winds

Large-scale outflows are observed as collimated jets or Herbig-Haro objects in some TTSs (see Section 3.2). However, spectroscopic signatures of winds and outflows are detected in all the TTSs. Three types of signatures have been detected in the UV:

1. The emission profiles of the Mg II resonance lines (2796, 2803 Å) show pronounced broad absorption in their blue wing for the 16 TTSs observed with IUE or HST (see e.g., Gómez de Castro, 1997). Blue-wing absorption is also observed in $\text{Ly}\alpha$. Terminal velocities up to $\sim 300 \text{ km s}^{-1}$ are observed. Unfortunately, the interpretation of these profiles is very complex, since the Mg II and $\text{Ly}\alpha$ lines are optically thick and there is no unambiguous method

Fig. 6 Left: Variation of the three velocity components: rotation (V_t), radial expansion from the axis (V_r) and axial velocity (V_z) are represented. Top panel: V_z and V_r are represented with dashed and solid lines, respectively. Bottom panel: The ratio between V_t and the Keplerian velocity at 0.1 AU for a solar mass star (155 km s^{-1}) is plotted. Right: Disk wind kinematics as shown by the line profiles for an edge-on system. Each profile correspond to a ring of gas perpendicular to the outflow axis that is identified by its distance (z) to the disk plane. Bottom panel: Line profiles with $z < 5 \text{ AU}$ – the outflow passes from being rotationally dominated (inner broad or double peaked profile) to radial expansion dominated (double peaked profiles with peak velocity $\sim 120 \text{ km s}^{-1}$). Middle panel: Outflow passes from being radial expansion dominated to axial-acceleration dominated. Top panel: Outflow is dominated by axial acceleration and the line broadening is basically thermal (from Gómez de Castro and Ferro-Fontán, 2005)



for determining the underlying blue-shifted emission and thus the true wind absorption.

2. Narrow and blue-shifted C III] 1909 Å and Si III] 1892 Å emission has been detected at the same velocity as the optical jets in some TTSs (Gómez de Castro and Verdugo, 2003a). This emission is produced by unresolved jets and indicates that PMS star jets are hotter than previously inferred from the optical observations in agreement with the UV observations of protostellar jets and Herbig-Haro objects (see Section 3.2).
3. Optically thin semi-forbidden lines tracing warm plasma (C II] 2325 Å, O II], and, most prominently, C III] and Si III]) show long blueward-shifted tails with velocities up to -300 km s^{-1} as in RU Lup, together with slight shifts to the blue of the line peak (Gómez de Castro and Verdugo, 2003a).

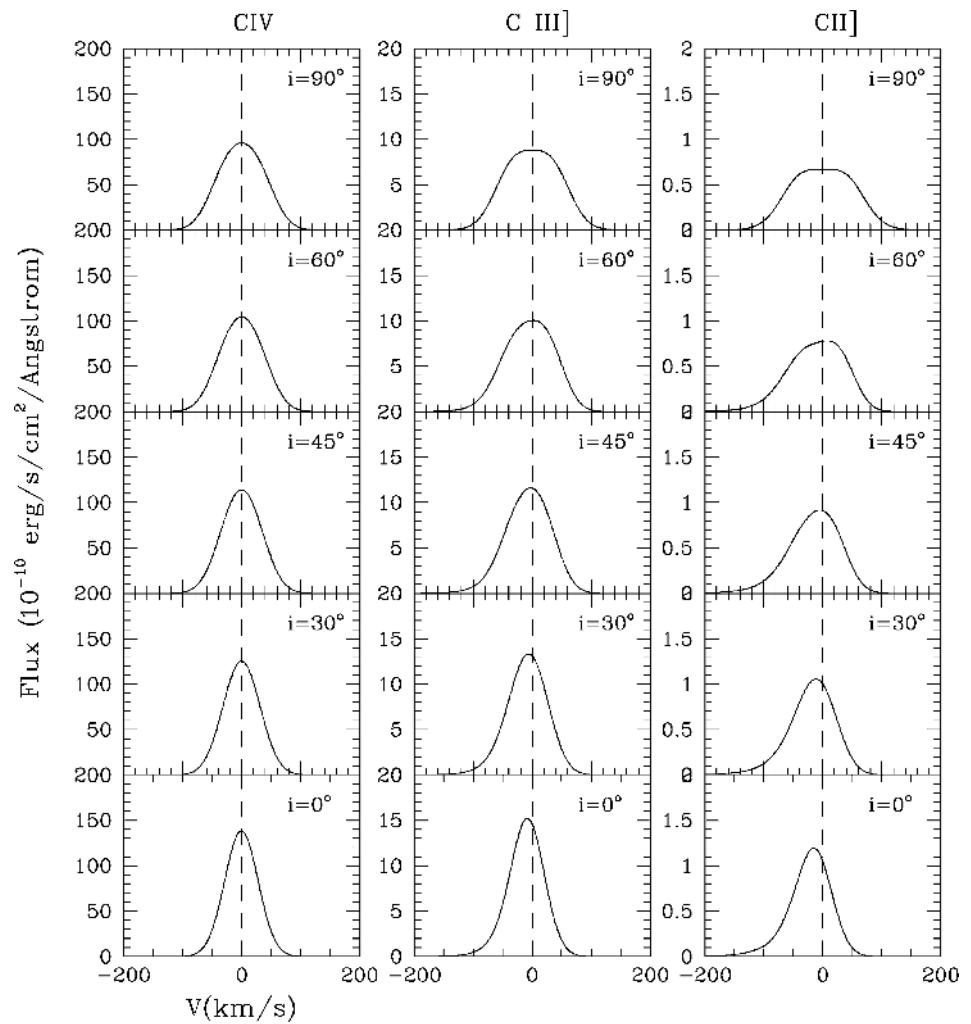
These data provide three key pieces of information: (i) there is a broad range of temperatures in the outflows (3000–30 000 K), (ii) outflows are not spherically symmetric, and (iii) their kinematics produce line broadenings/asymmetries

similar to the jet velocity (or terminal velocity of the outflow) in several sources.

The interpretation of the profiles requires a detailed comparison with theory, since the kinematics of MHD winds from rotating structures is very complex. Three basic motions overlap: rotation, acceleration along the axis, and radial expansion from the axis (see Fig. 6). Each kinematical component dominates at different locations in the outflow. Rotation is dominant close to the source of the outflow. Further out, radial expansion is the most significant component up to some height, z_0 , above the disk. For $z > z_0$, the dominant kinematical component is acceleration along the disk axis, e.g., a collimated outflow or jet. For standard parameters, the base of the wind is unresolved, $z_0 = 5 \text{ AU}$ (see Gómez de Castro and Ferro-Fontán, 2005). Thus, the only way to track the velocity law of the wind is by a clever selection of spectral indicators based on the thermal properties of the wind.

From a theoretical point of view, three possible types of outflows can be fitted into this broad context: a stellar wind, a disk wind, and an outflow driven from the interface. Either centrifugal stresses or magnetic/thermal pressure

Fig. 7 C IV, C III] and C II] line profiles for the unresolved $z < 12$ AU region. The profiles are plotted for inclinations 0° , 30° , 45° , 60° and 90° from bottom to top



are involved in the acceleration of the outflows, but it remains unclear which mechanism is dominant, whether it is universal, and how this mechanism acts when radiation pressure becomes significant as in Herbig Ae/Be stars. Numerical simulations predict temperatures between $\sim 10\,000$ K for the inner-disk winds up to $\sim 10^6$ – 10^7 K close to the magnetic reconnection boundary (Goodson et al., 1997). The X-rays (and the high-energy particles) produced in the reconnection areas will be redistributed towards lower energies due to the densities involved. Thus, the dominant radiative output from TTS winds is expected in the UV range, as is observed. UV line profiles calculated using a *simplified* warm disk wind model are shown in Fig. 7. Notice that very broad or double peaked profiles centered at the rest wavelength of the line can be produced in the wind (not only in the accretion disk) provided that the inclination is $\sim 90^\circ$. These type of profiles have been observed in some TTSs such as AK Sco or RW Aur. As shown in Fig. 7, a clever selection of the UV *spectral indicators* helps to dissect the kinematical structure of the wind. The effect of internal wind extinction by dust lifted from the

disk mid-plane can also be traced through the flux ratios of relevant lines.

Another important aspect of TTS winds is that a significant fraction of the mass outflow is ejected in a non-stationary manner. The timescales for these ejections range from a few hours (Alencar, 2001; Bouvier et al., 2003; Gómez de Castro and Verdugo, 2003b) to some 10 years (optical jets observations, see, e.g., López-Martín et al., 2003) or even to some hundreds of years (molecular gas bullets, see, e.g., Bachiller, 1996). Recent observations have established a *lower limit of about 1 h*, precluding the association of flares with the few hours timescale variability in RW Aur, since the characteristic decay time of flares in active stars is some few hundreds of seconds (Gómez de Castro and Verdugo, 2003b). Several ejection timescales typically coexist in the same object. For instance, timescales of ~ 1 h, ~ 5.5 days and ~ 20 years are observed in RW Aur. Despite the wealth of valuable information that HST/STIS could have obtained to determine the kinematics and properties of these outflows, *the available observations are few and not of long duration*.

3.2. UV observations of Herbig-Haro objects and jets

Observations of protostellar jets can provide important clues concerning the collimation mechanism: in particular, the role of episodic ejections or internal shocks in the jet, heat dissipation, and major heating sources. Also, such observations provide important clues concerning the interaction between the jet and the surrounding molecular gas, which helps to discriminate between radiation-induced (photodissociation) versus collision-induced (shocks) in the circumjet chemistry.

Since early in the IUE project, it has been known that protostellar jets and Herbig-Haro objects have a higher degree of ionisation than previously inferred from optical data (Bohm-Vitense, et al., 1982; Schwartz et al., 1985; see also Gómez de Castro and Robles, 1999 for a compilation). High-excitation objects like HH1 or HH2 produce strong emission lines of C IV 1548, 1550 Å, O III] 1664 Å, Si III] 1892 Å, and C III] 1909 Å (Ortolonai and D'Odorico, 1980). However, low-excitation objects like HH43 or HH47 are characterized by the presence of the H₂ Lyman band emission lines (Schwartz, 1983). H₂ emission lines, which are pumped by the UV radiation generated in the internal shocks of the jet, can measure the strength of the radiation field generated in the shock and the Ly α line strength.

UV lines are variable and the variations of the low-ionisation species are anticorrelated with the variations of the high-ionisation species and the short-wavelength continuum. A detailed study of HH29 combining optical and UV data led Liseau et al. (1996) to propose a two-phase model with a warm component ($T = 10^4$ K and $n_e = 10^3 \text{ cm}^{-3}$) and a hot, dense component ($T = 10^5$ K and $n_e = 10^6 \text{ cm}^{-3}$) with a very small filling factor (0.1–1%).

Using IUE, Bohm et al. (1987) and Lee et al. (1988) detected a variable and spatially extended short-wavelength (1300–1500 Å) UV continuum. At the end of the IUE mission, it was believed that the most likely mechanism for its formation was continuum H₂ emission formed when H₂ molecules are destroyed either by photodissociation by radiation shortwards of 912 Å or by collisions with low-energy thermal particles. This assumption was based on the absence of the dominant Lyman band features (at 1258, 1272, 1431, 1446, 1505, 1547 and 1562 Å), which are detected in such low-excitation objects as HH43 or HH47. The high-resolution spectra of HH2 obtained with the Hopkins Ultraviolet Telescope (HUT) showed that the UV emission below 1620 Å is mostly produced by H₂ Lyman bands detected below 1200 Å and at 1510, 1580 and 1610 Å (see Raymond et al., 1997). Unfortunately, this is the *only* high-resolution spectrum of a HH object obtained in the far UV. HH47 was observed with HST/GHRS but the spectral coverage was tiny 1262–1298 Å (Curiel et al., 1995). A low-dispersion (≈ 1000) spectrum of HH47 obtained with

HST/FOS/G270H shows no significant depletion of Fe in the outflow.

The existing UV observations have left open many important questions that cannot be solved without further UV observations. It is still unclear, how the kinetic energy of the flow is damped into radiation. The non-detection of O VI emission (Raymond et al., 1997) and the simultaneous detection of strong C IV and H₂ emission represent the strongest and most promising arguments against radiative cooling models. Another important question is how to understand the excitation mechanism of the H₂ line radiation, since H₂ band structure is observed in high-excitation HH objects. One proposed suggestion is collisional pumping of the H₂ levels (Raymond et al., 1997).

3.3. Herbig Ae/Be stars

Herbig Ae/Be stars are intermediate-mass (2–10 M_\odot) PMS stars. They are rather puzzling objects. Their larger masses suggest that the gravitational collapse is superalfvénic, so magnetic fields are not expected to be strong. However, Ae stars have a rich UV emission-line spectrum consistent with the presence of a chromosphere above the photosphere (Brown et al., 1996; Deleuil et al., 2005). Also, overionised species (transition region or corona-like) are observed; a marginal detection of magnetic fields has been reported for HD 104237 (Donati et al., 1997). Thus, observations point out that fields are present, at least, during the first $\sim 5 \times 10^6$ years of their PMS evolution.

UV-optical monitoring campaigns discovered azimuthal structures in the wind of AB Aur (Praderie et al., 1986). Subsequent optical monitoring campaigns, for example by the Multi-Site COntinuous Spectroscopic (MUSICOS) consortium, confirmed the presence of such azimuthal structures in the wind and in the chromosphere: the rotation period of the chromospheric structures is 32 h (the stellar rotation period), while the rotation period of the wind (traced by the UV Mg II lines) is 45 h (Bohm et al., 1996; Catalá et al., 1999). Further UV observations detected clumps of very hot gas, traced by N V emission, in the wind of AB Aur (Bouret et al., 1997). The generation of these azimuthal structures and the very hot clumps is often interpreted by means of a two-component wind model in some ways similar to the solar wind consisting of the following:

A “slow”, dense outflow reaching terminal velocities of $\sim 300 \text{ km s}^{-1}$, which produces the prominent P-Cygni profiles observed in the Ca II and Mg II[us1] lines and the broad, blue-shifted absorption observed in C IV[uv1]. Mass-loss rates derived from semi-empirical models are a few $\times 10^{-8} M_\odot$ per year (Bouret and Catalá, 1998; Catalá and Kunasz, 1987).

A “high” velocity component made by streamers of magnetically confined gas.

Since Herbig Ae/Be stars are fast rotators, gas in the streamers is forced to corotate up to the alfvén point and shocks are expected to occur between the “slow” and “fast” components. As a result, dense azimuthal structures are formed in the corotating interaction regions (CIRs). The existence of a magnetic collimator is further supported by the detection of low-density Ly α jets in HD 163296 and HD 104237 (Devine et al., 2000; Grady et al., 2004). Magnetic field dissipation also seems the most likely source for the radiative losses in the chromosphere/wind that represent 4–8% of the stellar bolometric luminosity according to Bouret and Catalá (1998), although accretion flows may be a non-negligible energy source (Blondel et al., 1983; Bouret and Catalá, 2000; Roberge et al., 2001). Accretion, however, may not be the driver of the outflow. Radiatively driven winds are able to produce collimated outflows provided there is a magnetic field (Sakurai, 1985; Rotstein and Giménez de Castro, 1996). The ultimate source of the field remains unidentified: turbulence and rotation could set up a dynamo in the outer layers. Turbulence can be generated by stellar pulsation; radial and non-radial modes have been detected with periods from some tens of minutes to hours (see Catalá, 2003 for a review). Also, the rotational braking produced by the strong stellar wind could induce turbulent motions below the stellar surface, forcing magnetic fields into the outer stellar layers (Lignières et al., 1996).

Future UV observations are required to characterize the winds, to study the evolution of the hot clumps (presumably shocks between the fast and slow components), and to study the physical conditions of the disks. Herbig Ae/Be stars are evolutionary precursors of the Vega-like stars, such as β Pictoris (Vidal-Madjar et al., 1998), and thus are ideal laboratories for studying planet formation. Radio and IR observations are well suited to map the extended disk structure. Optical and IR coronographic observations with the HST have provided high-quality images of the disk structure at large (e.g., Clampin et al., 2003). However, UV spectroscopy is the most sensitive tool for determining the column density of hydrogen and the fraction of hydrogen atoms in molecular form (see, for instance, Bouret et al., 2003; Grady et al., 2005). This high sensitivity is illustrated by the very low upper limits provided by FUSE to the H₂ abundance of the circumstellar disk surrounding β Pictoris (Lecavelier des Etangs, 2001). FUSE observations have allowed to detect H₂ in several disks surrounding Herbig Ae/Be stars, providing estimates of temperature, density and physical size of the emitting region (see, e.g., Roberge et al., 2001; Lecavelier des Etangs et al., 2003). Measurements of H₂ abundances can provide information on the rate of H₂ formation on dust grains and the strength of UV photoionising radiation.

3.4. In summary: The potentials of the UV

It is widely believed that infrared and radio wavelengths are the most appropriate regimes for studying the formation of stars. This perception is based on PMS stars typically being embedded in molecular clouds that strongly attenuate UV and optical radiation. This perception is true for the very early stages of star formation, but after about 1 Myr extinction generally is low and TTSs are accessible to the very powerful UV diagnostic tools. *To study the evolution of TTSs and Herbig Ae/Be stars after 1 Myr is very important*, because planets are formed at this time and the inner disk can be observed while the planets are forming. Also, the basic engine that regulates the formation of stars, the accretion–outflow engine, is naked at this time and can be properly observed.

Examples of some of the diagnostic capabilities of high-resolution UV spectroscopy and monitoring are outlined in Figs. 8 and 9.

UV line profiles can clearly disentangle accretion from outflow.

Figure 8 shows some UV lines in the spectrum of RY Tau. The Fe II] 2506 Å line shows a broad red-shifted profile with a sharp edge at zero velocity. Since this line is pumped by Ly α photons, it should be formed in the accretion flow. The [O II] 2471 Å line is blue-shifted and traces the wind (Gómez de Castro and Verdugo, 2005). Both lines are optically thin with no self-absorption. For comparison, the strong Mg II 2796, 2802 Å lines display absorption components at the wind velocity and an extended red wing associated with the accretion flow. These two physical components could not have been disentangled from the analysis of the Mg II profile alone. In fact, the long red-shifted tail would likely have been interpreted as a signature of line saturation.

UV monitoring can be used to study the distribution of matter in the circumstellar environment.

In the solar system, there are three very different types of “flares”, which are sudden increases of the high-energy radiation and high-energy particles flux: magnetic flares (magnetic reconnection events), corotating interaction regions or CIRs (shock fronts formed by the interaction between the slow and the fast component of the solar wind), and coronal mass ejections. This classification also applies to TTSs and their circumstellar environments. High-resolution UV spectroscopic monitoring is required to disentangle the possible mechanisms for flares in protostellar systems. This is feasible as shown in Fig. 9. AB Dor, a nearby 30 Myr old star, is the only young star that has been well monitored in the UV for flares. Nine events were detected during the roughly 10 h of monitoring with HST/GHRS! The C IV and Si IV UV line profiles produced by most of the events are narrow and red-shifted,

Fig. 8 Profiles of some relevant UV lines in the spectrum of RY Tau. The C II] lines are a multiplet with many transitions producing this peculiar profile. All of the lines, except for Mg II, are forbidden or semi-forbidden (from Gómez de Castro and Verdugo, 2005)

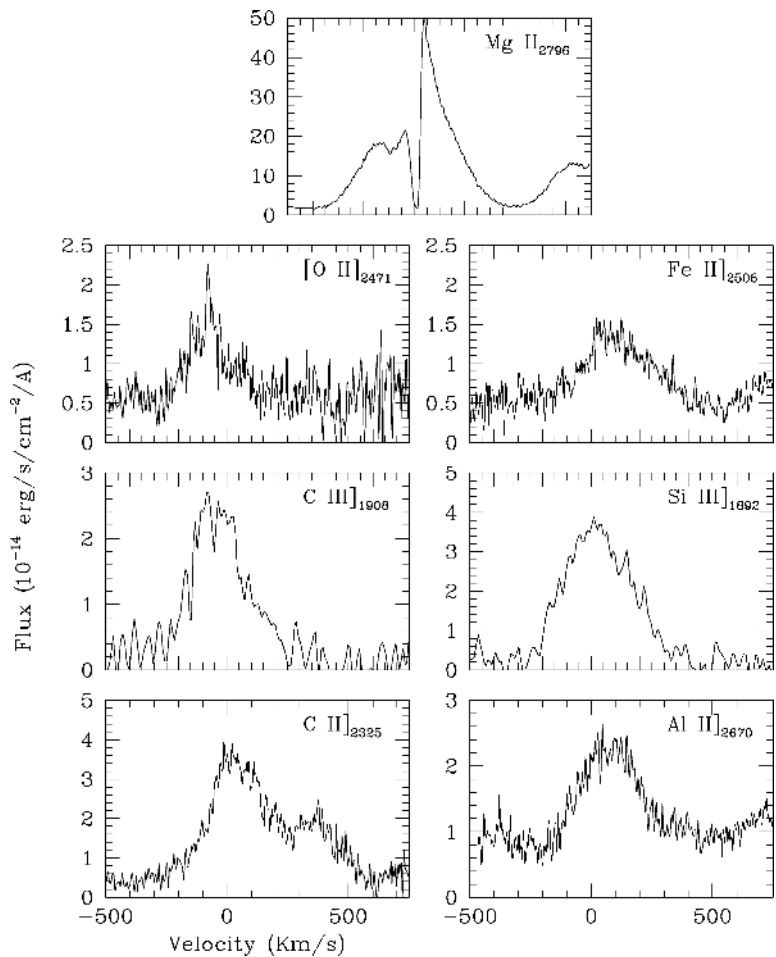
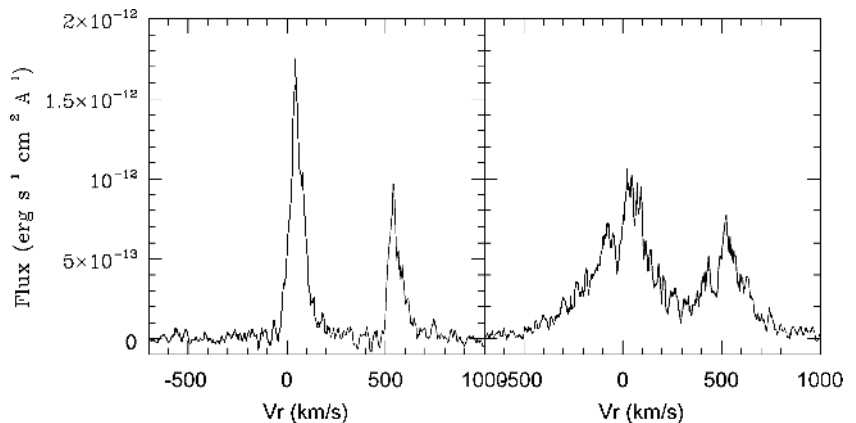


Fig. 9 The C IV 1548 Å profile of AB Dor during a normal stellar flare (left) and a transient feature probably associated with a CIR (right). Both events lasted several kiloseconds. The left profile is typical of three events that occurred during the short monitoring time, while the profile on the right was observed only once. Note the presence of a narrow absorption and the very broad line wings in the right panel profile (see Gómez de Castro, 2002 for more details)

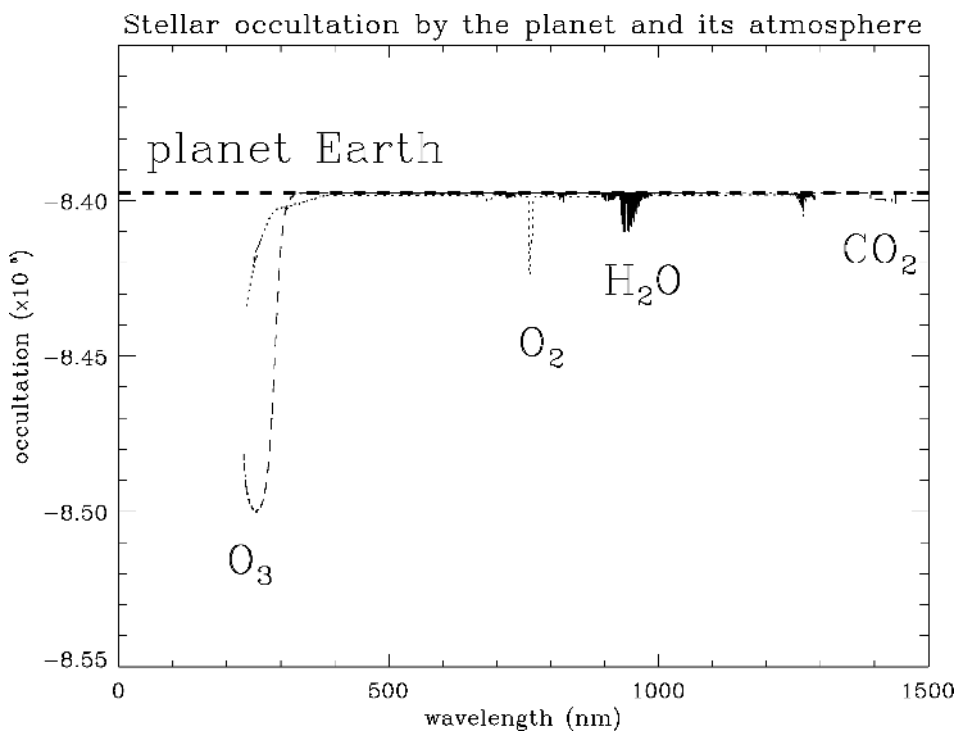


indicating hot gas falling onto the star during the flare. However, the strongest event produced a very broad profile with narrow absorption slightly blue-shifted. This profile lasted a few kiloseconds and thus the broad wings are most likely tracing the front shock of a CIR (Gómez de Castro, 2002).

In summary, IUE and HST (with its GHRS or STIS ultraviolet instruments) and FUSE have allowed us to begin to grasp the enormous potential of the UV spectral range for the

study of the physics of accretion and outflow, including the properties of the inner region of protoplanetary disks. Unfortunately, fewer than 10 TTSs were observed with spectral resolution $\sim 50\,000$ (6 km s^{-1}) during the lifetime of these instruments, partly because HST/STIS was not sufficiently sensitive. A UV instrument with sensitivity 50–100 times that of HST/STIS would permit observations of about 100 TTSs with magnitudes 10–13 located within 160 pc of the Sun. This sensitivity limit would permit observations of much fainter and more evolved WTTs than was possible with HST/STIS.

Fig. 10 Typical absorption spectrum of an Earth-like planet transiting in front of a solar-type star from the UV to the near infrared. We assumed the same atmospheric structure as for the Earth with, e.g., similar ozone content. Thin solid, dashed and dotted lines represent H_2O , O_2 and O_3 absorption. The vertical scale represents the occultation by the planet atmosphere of the stellar flux during the transit from Ehrenreich (2005)



4. Characterization of extrasolar planetary atmospheres and the search for bio-markers

Since the mid-1990s, more than 100 extrasolar planets (hereafter called “exoplanets”) have been discovered. In the coming decade, several observing programs will lead to the discovery of an extremely large number of exoplanets. To acquire a revealing picture of these new worlds, we need detailed observations of a large sample of these exoplanets to characterize planetary atmospheres well beyond the solar neighbourhood with reasonable exposure times. The observation of UV and optical absorption when an exoplanet transits its parent star is a very powerful diagnostic technique; in fact, the most powerful technique for detecting Earth-like planets because of the strong absorption of stellar UV photons by the ozone molecule in the planetary atmosphere (see Fig. 10). Near future space missions including Corot, Kepler or GAIA will lead to the discovery of a large number of exoplanets transiting their parent stars. An adequate capability for UV spectroscopic observations will be needed for detailed follow-up observations to characterize the exoplanets, their atmospheres, and their satellites.

4.1. The physical processes controlling the formation and evolution of exoplanets

Since the unexpected discovery of the first hot-Jupiter by Mayor and Queloz (1995), it is clear that exoplanets are an extremely diverse group. With the discovery of more than

100 exoplanets, this diversity is clearly seen in their orbital properties. We have “hot-Jupiters” with orbital periods as short as 3 days, and several “very hot-Jupiters” with orbital periods even shorter than 2 days. Less massive exoplanets have recently been discovered (Santos et al., 2004; McArthur et al., 2004; Butler et al., 2004), and the discussions on their true nature show that a large variety is now expected and certainly possible.

The same variety is also expected for the atmospheres of these exoplanets. A quick look at the atmospheric content and history of the solar system’s terrestrial inner planets shows that with four planets, we find four very different possibilities: Mercury has almost no atmosphere, Mars’ atmosphere is tenuous with atmospheric pressure about one-hundredth that of the Earth, and Venus is the extreme opposite with more than 90 times the atmospheric pressure of the Earth. Note that Titan, although much smaller than the Earth, also has an atmosphere of 1.5 bar and is very different from other giant planets satellites without atmospheres.

This diversity shows how difficult it is to predict what should be the content of an exoplanet’s atmosphere. In the solar system, the terrestrial atmosphere is unique with abundant O_2 and O_3 produced by biological activity. Another important characteristic of the terrestrial atmosphere is the significant amount of water. The Earth and Titan both have much N_2 in their atmospheres, but Titan has more methane and no O_2 . Mars and Venus have similar atmospheric composition, but their total amounts are in a ratio of more than 10^4 .

Thus, there is no simple answer to the question of the expected characteristics of planets and their atmospheres. On the one hand, the solar system planets provide a first hint of the expected diversity of the exoplanets and their atmospheres. On the other hand, observations of exoplanets and the detailed characterization of their atmospheres will help us better understand the physical processes at work in the building of a planet and its atmosphere.

It is clear that the detailed processes that created the solar system planets is still a matter of debate and the impact of many processes must still be clarified. In short, we do not yet know the key physical parameters that govern the formation, evolution and fate of a given planet and its atmosphere.

How do the properties (temperature, stellar type, high-energy particles, and metallicity) of the central star alter the evolution of its planetary system? What effects do a planet's orbital parameters (orbital distance and eccentricity) have on its size, mass and potential migration during the formation process? Are there volatile-rich planets like the proposed "Ocean-planets"? How do interactions with other planets and planetesimals in their environment influence the evolution of a planet? This last question is undoubtedly related to the origin of water on the Earth. Are water-rich planets in the "habitable zone" common, rare, or exceptions?

Several processes that are believed to play key roles in building a planet can now be identified. To begin, we can look at the best known planet, the Earth. Although still controversial, it is generally accepted that the Earth's original atmosphere was accumulated simultaneously with the planet's formation. However, the heating of the atmosphere by the young Sun's UV and X-ray flux led to the hydrodynamical escape of this primary atmosphere (as is observed on HD 209458b, Vidal-Madjar et al., 2003, 2004). Tectonics, volcanism and the planet out-gasing then formed the secondary atmosphere in which we now live. Late bombardment by planetesimals in the young planetary system contributed to a large fraction of the terrestrial water but the fraction of water coming from the Earth itself and the outside contribution is still a matter of debate. Finally, life enriched the atmosphere in O₂ and ozone, which are therefore considered as atmospheric bio-markers. The observation of O₂ and ozone in the atmosphere of the Earth or any exoplanet can lead to the conclusion that something very particular is happening there. Something which could suggest the presence of life.

It therefore appears that we will soon discover many more exoplanets, each one likely different from the others. As soon as we will be able to characterize them in detail, there will likely be many surprises. We cannot predict what will be discovered, but this will be an unprecedented opportunity to better understand the key processes at work in the shaping of planets and, in particular, to better understand the origin of our own Earth.

4.2. Ultraviolet observations of transiting planets

In the coming years, many exoplanets will be discovered through transits, for example, by the Corot, Kepler and GAIA missions. In particular, GAIA will likely identify thousands of exoplanets transiting bright stars. These will be prime targets for detecting the atmospheric constituents through absorption line spectroscopy, thereby characterising the chemical and physical properties of the atmosphere, including the search for bio-markers.

Many molecules have strong electronic transitions in the UV-optical domain. This wavelength range gives access to the most important constituents of the atmospheres. In particular, bio-markers like ozone (O₃) have very strong transitions in the ultraviolet (the absorption of UV radiation by the Earth atmosphere is primarily due to O₂ and O₃). The Hartley bands of O₃ are the main absorbers at 2000–3000 Å. O₂ has strong absorptions in the range 1500–2000 Å. CO has strong bands below 1800 Å, and weaker Cameron bands from 1800 to 2600 Å. The CO⁺ first negative bands are located in the 2100–2800 Å range. Finally, the presence of CO₂ can be detected through the CO₂⁺ Fox–Duffenback–Barker bands from 3000 to 4500 Å. We note also the important presence of O I and C II lines at 1304 and 1335 Å. Observation of these species can be done easily, demonstrating that these atoms and ions are present at very high altitude (several hundreds of kilometres) and providing large absorption depths.

The electronic molecular transitions are several orders of magnitude stronger than the vibrational or rotational transitions observed in the infrared or radio range. These transitions can be observed in absorption provided there is a sufficiently strong UV background source. For this reason, the observation of UV and optical absorption when a planet transits its parent star is intrinsically a more powerful diagnostic technique to characterize the atmospheres of the inner planets than infrared observations of planetary emission. This is especially true for studying small Earth-like exoplanets. It is far simpler to use the large number of photons in the stellar continuum that are absorbed in spectral lines or molecular bands by the planet's atmosphere than to attempt to cancel the huge stellar photon flux by a coronograph or interferometer to search for the faint infrared emission (thermal and scattered starlight) from the planet. In addition, the intrinsic faintness of the target sources enhances potential difficulties like confusion with exozodiacal light. Moreover, spectral observations of the atmospheres of satellites of giant planets, suspected to be numerous, are even more difficult in emission.

The first observations of the atmosphere of an exoplanet (HD 209458b, nicknamed Osiris) have been made through UV-optical spectroscopy (Charbonneau et al., 2002; Vidal-Madjar et al., 2003, 2004), demonstrating that it is an ideal tool for probing the atmospheric content of transiting planets.

It is noteworthy that we already have in hand four observations of the atmosphere of an exoplanet (including the detection of oxygen). All of these present detections have been performed: (1) in space, (2) in the UV-optical wavelength range, and (3) in absorption during planetary transits. This is not a coincidence but rather a consequence of this method being the most powerful and its presenting the best trade-off of scientific result versus technical feasibility.

4.2.1. Estimates of the expected detection rate for Earth-like exoplanets

For a typical life-supporting Earth-like planet, the ozone layer is optically thick to UV radiation incident at a grazing angle up to an altitude of about 60 km. This ozone layer creates an additional occultation depth of $\Delta F/F \sim 2 \times 10^{-6}$ over hundreds of Angstroms that can be compared to the 2×10^{-4} optical depth over 1 Å detected with HST on HD 209458. We can estimate the minimum brightness of the parent star (F_{\min}) relative to the brightness of HD 209458 ($F_{\text{HD 209458}}$) for a detection of the ozone absorption. We have:

$$F_{\min} = \left(\frac{\Delta F/F}{2 \times 10^{-4}} \right)^{-2} \left(\frac{\Delta \lambda}{1 \text{ \AA}} \right)^{-1} \left(\frac{S}{S_{\text{HST/STIS}}} \right)^{-1} F_{\text{HD 209458}}.$$

With a telescope 50 times as sensitive as HST/STIS, ozone can thus be detected in Earth-like exoplanets orbiting stars brighter than $V \approx 10$ (easily identified by GAIA). This magnitude corresponds to star at a distance $d \sim 50$ pc for the latest type stars considered (K V stars) and more than ~ 500 pc for the earliest stars (F V stars).

With this estimate of the minimum stellar brightness needed to detect a given species, we can evaluate the number of potential targets. The number of targets with exoplanets for which we can probe the atmospheric content, N_{pl} , is simply the total number of stars brighter than the limit N_* , multiplied by the fraction of stars having an identified transiting exoplanet at a given orbital range, P_{pl} .

$$N_{\text{pl}} = N_* \times P_{\text{pl}}.$$

To evaluate the total number of stars, we must select the stellar types to be included. The usual assumption is to limit the estimates by counting only K-, G- and F-type main sequence stars. This is a conservative assumption based on the bias of the present discoveries of exoplanets. We used the conservative estimate of

$$N_* = 48\,000 \times 10^{0.6*(V-10)}.$$

The second term of the equation, P_{pl} , is more difficult to quantify due to many unknowns: (i) there must be an exoplanet orbiting the star, (ii) this exoplanet must be identified,

and (iii) it must be transiting the stellar disk. We made the assumption that about 25% of stars will have identified orbiting exoplanets in the near future. The probability of a transit for a given exoplanet can be estimated to be $P_{\text{tr}} \approx a/R_*$, where a is the orbital distance and R_* is the stellar radius. For an exoplanet orbiting at 1 AU around a solar-type star, the probability is $P_{\text{tr}} \sim 0.5\%$. If we consider the habitable zone as the most interesting orbital range, this probability increases for the smaller and more numerous stars. $P_{\text{tr}} \sim 0.5\%$ can thus be considered as a conservative assumption for the habitable zone around solar-type stars.

Finally, we have an estimate of the number of targets with observable planets:

$$N_{\text{pl}} \approx 60 \times 10^{0.6*(V-10)}.$$

A combination of this last equation with the minimum brightness of the parent star needed to detect a given species, gives the size of the exoplanet sample that a telescope can analyse as a function of its sensitivity.

Similar calculations can be made for exoplanets very different from the Earth. The occultation depth is proportional to the planetary radius (R_p) multiplied by the atmospheric scale height (h), and the scale height is inversely proportional to the planet's gravity ($g \propto M_p/R_p^2$). These considerations determine that the occultation depth is related to the planet's density (ρ_p) by

$$\Delta F/F \propto R_p^3/M_p \propto \rho_p^{-1}.$$

Hence, low-density exoplanets and planetary satellites will give larger absorption depths than the high-density Earth (see Fig. 11). In short, it is easier to probe the atmosphere through transit spectroscopy in the case of Ocean-planets because they are larger, or in the case of Titan-like satellites, because they are less massive than the Earth and have larger atmospheric scale heights. With an ozone layer similar to that in the Earth's atmosphere, the occultation depth of an Ocean-planet, or a Titan-like satellite, will be $\Delta F/F \sim 5 \times 10^{-6}$. The resulting number estimates of possible detections as a function of the telescope sensitivity are given in Fig. 12.

Estimates of the minimum star brightness for detecting atmospheric signatures can be translated into the number of possible detections of such atmospheric signatures in transiting exoplanets (n_d). The number of possible detections is related to the number of stars brighter than the minimum brightness [$n(F > F_{\min})$], the probability of finding an exoplanet around these stars (P_p), and the transit probability at a given orbital distance [$P_t(d)$]. P_p is unknown and we consider $P_p = 0.25$ as a reasonable number. We also estimate the transit probability at 1 AU: $P_t(1 \text{ AU}) = 0.5\%$. For the number of stars at a given brightness, we restrict the sample to

Fig. 11 Typical absorption spectrum of an Ocean-planet as estimated by Leger et al. (2004) when seen transiting in front of a solar-type star. We assumed the same atmospheric structure as for the Earth but rescaled the structure to the size and density as presently expected for an 6 Earth mass and 2 Earth radius volatile-rich exoplanet from Ehrenreich (2005)

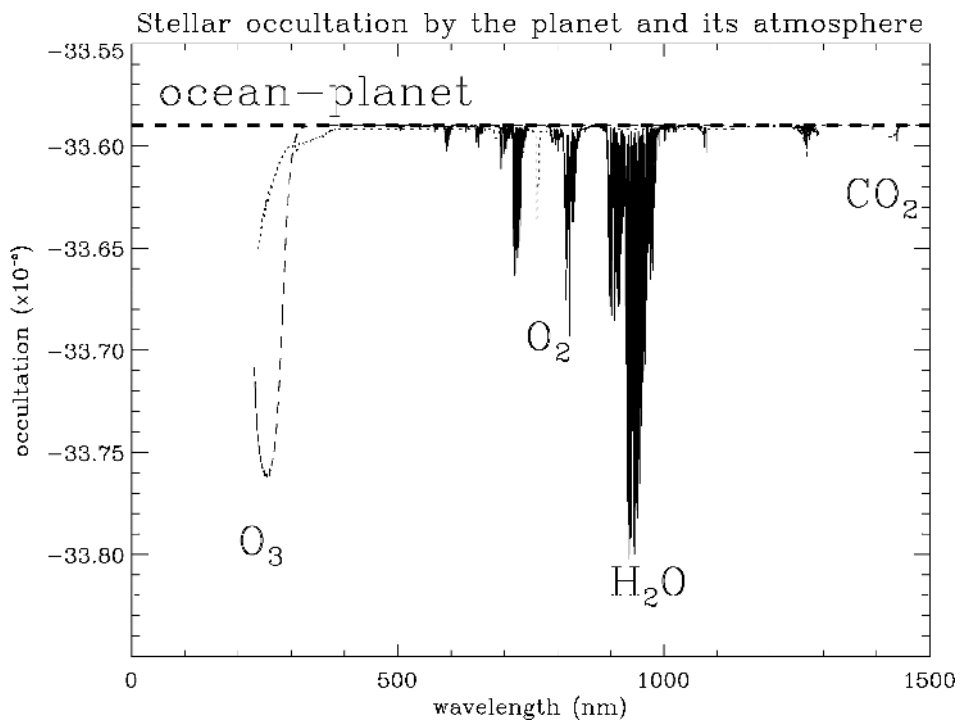
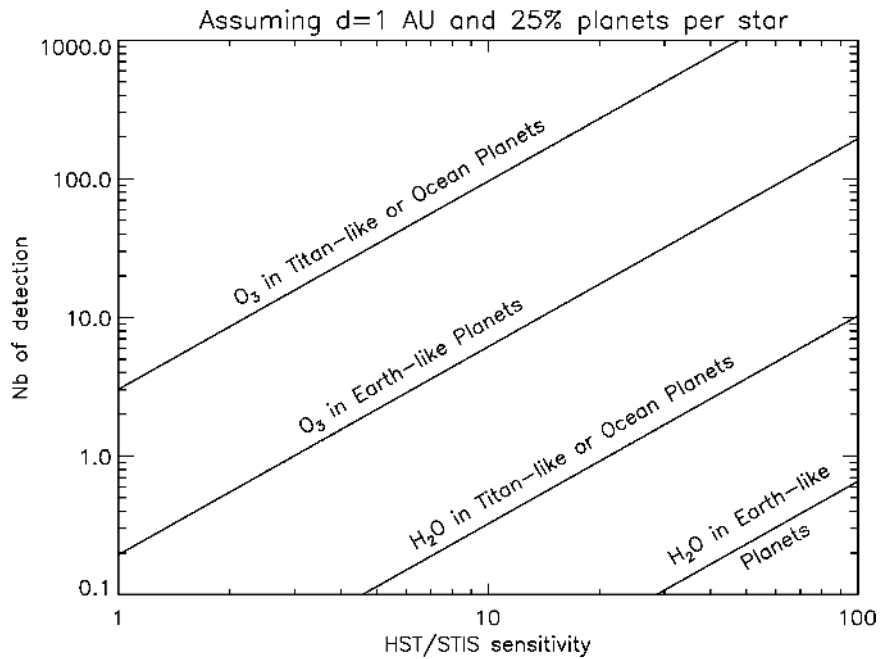


Fig. 12 Plot of the number of expected detections of atmospheric signatures as a function of telescope sensitivity for Earth-like and Ocean-like planets



K-, G- and F-type main sequence stars. With these numbers, we plot in Fig. 12 the number of possible detections of atmospheric signatures as a function of telescope sensitivity. For a UV telescope, the sensitivity depends on the mirror size and the spectrograph efficiency. From now on, we quote the telescope sensitivity (S) in units of HST/STIS sensitivity because planetary atmospheres have already been detected and studied with this instrument and, henceforth, we are not limited

to a theoretical calculation that may ignore some potential difficulties. We note that a 2-m class telescope including a spectrograph with the efficiency of the COS instrument leads to a sensitivity $S \sim 20$ HST/STIS.

We see that about 100 *exoplanets* are expected to transit in front of K-, G- or F-type main sequence stars brighter than $V = 10$. In conclusion, using the transit probabilities in the habitable zone, we find that the presence of bio-markers and

other constituents in the atmospheres can be searched for in more than about 100 Earth-like exoplanets orbiting K-, G- and F-type main sequence stars. Further considerations to be taken into account are given as follows:

The effect of stellar variety. The number estimates given earlier is probably conservative. Indeed, we neglected the stellar type in the estimates and considered the *real* observations of HD 209458b as a benchmark. However, HD 209458 is a G-type star. A very large number of targets will be exoplanets orbiting K-type stars. For these stars, the stellar radius is smaller and the absorption depth due to the transiting planets will be larger (as observed in the case of the recently discovered exoplanet TrES-1 transiting a K0 V star (Alonso et al., 2004)).

Moreover, late-type stars are expected to have habitable zones at orbital distances smaller than 1 AU assumed in the earlier calculation. With smaller orbital distances, the transit probability and the corresponding number of targets increase. Since the previous calculation was done for G-type stars, we expect a larger number of detections for K-type stars. The final number of possible detection of water bands should therefore be larger than is shown in Fig. 12. Water bands are likely detectable in a reasonable number of Earth-like exoplanets with a 50–100 HST/STIS sensitivity telescope.

The spatial structure of the atmosphere can be studied by time-tagged observations. Absorption spectroscopy of transiting planets can also provide *spatial* information on the physical and chemical properties of their atmospheres. During partial phases when the planet partially covers the observed stellar disk, time-tagged spectra provide a spatial scan of the exoplanet's atmosphere. The partial phase lasts about 10 min for an Earth-size exoplanet orbiting at 1 AU from its parent star. For the closest stars (≤ 100 pc), exposures of a few minutes will identify the atmospheric diagnostics of the most important constituents. Detailed time analysis of transit spectra can give information on the spatial distribution of atmospheric characteristics along the exoplanet's surface, for example, the difference between poles and equator or the spatial inhomogeneity of different chemical constituents.

5. Summary: The needed capabilities

The scientific program outlined in this article requires a broad range of instrumentation from imaging to spectroscopic capabilities.

5.1. Imaging

Two imaging instruments are required: a large field-of-view and a high-resolution imager.

The large field-of-view instrument will be used for two main purposes: mapping of protostellar jets and tracking flare timescales over large fields.

The high-resolution imager's primary use is to resolve the cooling structures of jets and to map protostellar disks. Coronography is required. UV observations provide the best contrast for detecting structures around young stars; for instance, a Herbig Ae/Be star is a 100 times fainter at Ly α than at H α . Narrow filters centered in the most prominent UV lines like Ly α , C IV, C III, C II, O I, He II or O VI are required.

5.2. Spectroscopy

Most of the science program is oriented towards spectroscopy. Two basic modes are required: high-resolution spectroscopy and medium-to-low long-slit spectroscopy.

High-resolution spectroscopy ($R \simeq 50\,000$) is required for the Doppler mapping of circumstellar structures, flares, winds and disks. It is also required for detailed studies of the ISM. The spectral resolving power required to observe the atmosphere of exoplanets is not a crucial capability. We have seen that $R = \lambda/\Delta\lambda = 10\,000$ is more than enough. Even lower resolving power, $R \lesssim 1000$, could be enough to detect the broad-band signatures of many molecules.

Note, however, that in some cases higher resolving power will resolve the thermal broadening of absorption lines in planetary exospheres (Vidal-Madjar et al., 2003). In that case, a high resolving power of $R \sim 100\,000$ will provide important constraints on the atmospheric structure.

Long-slit spectroscopy is required to map the spatially-resolved jet emission, disks and circumstellar envelopes. Spectral resolution as high as 10 000 is required.

Wavelength coverage. The target spectral range for the spectroscopic instruments goes from ~ 1000 Å (to include the O VI lines and the H₂ bands) to ~ 4000 Å to have some overlap with optical telescopes and to cover most of the molecular broad-band absorption expected from exoplanet atmospheres. Extension to 10 000 Å would provide access to the strong water band, which is of prime interest for the search, statistics and characterization of habitable exoplanets and, consequently, for exobiology.

Sensitivity. An improvement by a factor of 20–100 over HST/STIS capabilities will permit the study of the warm ISM beyond the Local Bubble and observe gas high in the halo towards the HVCs. It will also increase the sample of TTSs observed in the UV from some 10 to about 200 including the WTTSSs providing, for the first time, an unbiased view of the accretion–outflow engine during PMS evolution.

The sensitivity of the spectrograph should be high around prominent nebular lines like C III] 1909 Å, Si III] 1892 Å, and C II] 2325 Å.

Time-tagged observations. Accurate time information is essential. The absolute accuracy of the timescale needs to be precise to coordinate monitoring campaigns with other instruments or to study exoplanet transits. The accuracy and uniformity of the timing sets the spatial resolution for Doppler mapping. Time-tagged observations can be considered as a proxy for spatial resolution at the level of the exoplanet's size.

5.3. Orbit

The orbit should permit efficient observations. A long-period orbit will allow long uninterrupted observing with few Earth occultations, little airglow pollution, and minimal geocoronal emission. This will facilitate long-duration flare observations and Doppler mapping on timescales of 1 day. An L2 orbit is optimal for this purpose.

Acknowledgements This work has been supported by the European Commissions 6th Framework programme under contract number RII3-Ct-2004-001566 to the OPTical Infrared CO-ordination Network for Astronomy (OPTICON). The authors are member of the Network for UltraViolet Astrophysics (NUVA): this network is defined within the OPTICON activities to structure the European astronomy. AIGdC acknowledges support by the Ministry of Science and Technology of Spain through grants AYA 2000-966, ESP2001-4637E and ESP2002-10799-E. JLL acknowledges support by NASA through grant AR-09930. M.A. would like to thank Dieter Breitschwerdt for enlightening discussions on non-equilibrium ionisation.

References

- Alencar, S.H.P., Johns-Krull, C.M., Basri, G.: *Astrophys. J.* **122**, 3335 (2001)
- Ardila, D.R., Basri, G., Walter, F.M., Valenti, J.A., Johns-Krull, C.M.: *Astrophys. J.* **566**, 1100 (2002)
- Avillez, M., Breitschwerdt, D.: *A&A* **425**, 899 (2004)
- Avillez, M., Breitschwerdt, D.: *A&A* **436**, 585 (2005)
- Bachiller, R.: *Annu. Rev. Astron. Astrophys.* **34**, 111 (1996)
- Benjamin, R., Shapiro, P.: In: E. Silver and S. Kahn (eds.), *Ultraviolet and X-Ray Spectroscopy of Laboratory and Astrophysical Plasmas*, Cambridge University Press, Cambridge, p. 280 (1993)
- Bertout, C., Basri, G., Bouvier, J.: *Astrophys. J.* **330**, 350 (1988)
- Breitschwerdt, D., Schmitzler, T.: *A&A* **347**, 650 (1999)
- Berghöfer, T.W., Breitschwerdt, D.: *A&A* **390**, 299 (2002)
- Bertin, P., Lallent, R., Ferlet, R., Vidal-Madjar, A.: *J. Geophys. Res.* **98**(A9), 15193 (1993)
- Blondel, P.F.C., Talavera, A., Djie, H.R.E.T.A.: *A&A* **268**, 624 (1993)
- Boehm, T., Catala, C., Donati, J.-F., Welty, A., Baudrand, J., Butler, C.J., Carter, B., Collier-Cameron, A., Czarny, J., Foing, B., Ghosh, K., Hao, J., Houdebine, E., Huang, L., Jiang, S., Neffl, J.E., Rees, D., Semel, M., Simon, T., Talavera, A., Zhai, D., Zhao, F.: *Astron. Astrophys. Suppl.* **120**, 431 (1996)
- Boehm, K.-H., Buehrke, Th., Raga, A.C., Brugel, E.W., Witt, A.N., Mundt, R.: *Astrophys. J.* **316**, 349 (1987)
- Boehm-Vitense, E., Cardelli, J.A., Nemec, J.M., Boehm, K.H.: *Astrophys. J.* **262**, 224 (1982)
- Bouret, J.-C., Catala, C.: *A&A* **340**, 163 (1998)
- Bouret, J.-C., Catala, C.: *A&A* **359**, 1011 (2000)
- Bouret, J.-C., Catala, C., Simon, T.: *A&A* **328**, 606 (1997)
- Bouret, J.-C., Martin, C., Deleuil, M., Simon, T., Catala, C.: *A&A* **410**, 175 (2003)
- Bouvier, J., Grankin, K.N., Alencar, S.H.P., Dougados, C., Fernández, M., Basri, G., Batalha, C., Guenther, E., Ibrahimov, M.A., Magakian, T.Y., Melnikov, S.Y., Pelrov, P.P., Rud, M.V., Zapatero Osorio, M.R.: *A&A* **409**, 169 (2003)
- Calvet, N., Basri, G., Kuhi, L.V.: *Astrophys. J.* **277**, 725 (1984)
- Catala, C.: *A&SS* **284**, 53 (2003)
- Catala, C., Kunasz, P.B.: *A&A* **174**, 158 (1987)
- Cernicharo, J.: *Astrophys. J.* **608**, L41 (2004)
- Charbonneau, D., Brown, T.M., Noyes, R.W., Gilliland, R.L.: *Astrophys. J.* **568**, 377 (2002)
- Clampin, M., Krist, J.E., Ardila, D.R., Golimowski, D.A., Hartig, G.F., Ford, H.C., Illingworth, G.D., Bartko, F., Benétez, N., Biakeslee, J.P., Bouwens, R.J., Broadhurst, T.J., Brown, R.A., Burrows, C.J., Cheng, E.S., Cross, N.J.G., Feldman, P.D., Franx, M., Gronwall, C., Infante, L., Kimble, R.A., Lesser, M.P., Martel, A.R., Menanteau, F., Meurer, G.R., Miley, G.K., Postman, M., Rosati, P., Sirianni, M., Sparks, W.B., Tran, H.D., Tsvetanov, Z.I., White, R.L., Zheng, W.: *Astron. J.* **126**, 385 (2003)
- Curiel, S., Raymond, J.C., Wolfire, M., Hartigan, P., Morse, J., Schwartz, R.D., Nisenson, P.: *Astrophys. J.* **453**, 322 (1995)
- Danly, L., Lockman, F.J., Meade, M.R., Savage, B.D.: *ApJSS* **81**, 125 (1991)
- Deleuil, M., Bouret, J.-C., Catala, C., Lecavelier des Etangs, A., Vidal-Madjar, A., Roberge, A., Feldman, P.D., Martin, C., Ferlet, R.: *A&A* **429**, 247 (2005)
- Devine, D., Grady, C.A., Kimble, R.A., Woodgate, B., Bruhwiler, F.C., Boggess, A., Linsky, J.L., Clampin, M.: *Astrophys. J.* **542**, L115 (2000)
- Donati, J.-F., Semel, M., Carter, B.D., Rees, D.E., Collier Cameron, A.: *Month. Not. R.A.S.* **291**, 658 (1997)
- Ehrenreich, D.: PhD Thesis, Univ. de Paris VI (2005)
- Ferro-Fonán, C., Gómez de Castro, A.I.: *Month. Not. R.A.S.* **342**, 427 (2003)
- Glassgold, A.E., Najita, J., Igea, J.: *Astrophys. J.* **615**, 972 (2004)
- Grady, C.A., Woodgate, B., Heap, S.R., Bowers, C., Nuth, J.A., III, Herczeg, G.J., Hill, H.G.M.: *Astrophys. J.* **620**, 470 (2005)
- Grady, C.A., Woodgate, B., Torres, C.A.O., Henning, Th., Apai, D., Rodmann, J., Wang, H.S.B., Linz, H., Williger, G.M., Brown, A., Wilkinson, E., Harper, G.M., Herczeg, G.J., Danks, A., Vieira, G.L., Malumuth, E., Collins, N.R., Hill, R.S.: *Astrophys. J.* **608**, 809 (2004)
- Gómez de Castro, A.I.: *Month. Not. R.A.S.* **332**, 409 (2002)
- Gómez de Castro, A.I.: *A&SS* **292**, 561 (2004)
- Gómez de Castro, A.I., Verdugo, E.: APJ, submitte (2005)
- Gómez de Castro, A.I., Fernández, M.: *Month. Not. R.A.S.* **283**, 55 (1996)
- Gómez de Castro, A.I., Franqueira, M.: IUE-ULDA Access Guide No. 8: T Tauri Stars, ESA Scientific Publication, ESA-SP 1205 (1997a)
- Gómez de Castro, A.I., Franqueira, M.: *Astrophys. J.* **482**, 465 (1997b)
- Gómez de Castro, A.I., Ferro-Fontán, C.: *MNRAS* **362**, 569 (2005)
- Gómez de Castro, A.I., Lamzin, S.: *Month. Not. R.A.S.* **304**, L41 (1999)
- Gómez de Castro, A.I., Robles, A.: INES Access Guide No. 1: Herbig-Haro Objects, ESA Scientific Publication, ESA-SP 1237 (1999)
- Gómez de Castro, A.I., Verdugo, E.: *Astrophys. J.* **597**, 443 (2003a)
- Goodson, A.P., Boehm, K.-H., Winglee, R.M.: *Astrophys. J.* **524**, 142 (1999)
- Goodson, A.P., Winglee, R.M., Boehm, K.-H.: *Astrophys. J.* **489**, 199 (1997)

- Guenther, E.W., Lehmann, H., Emerson, J.P., Staude, J.: *A&A* **341**, 768 (1999)
- Gullbring, E., Calvet, N., Muzerolle, J., Hartmann, L.: *Astrophys. J.* **544**, 927 (2000)
- Haffner, L.M., Reynolds, R.J., Tufte, S.L., Madsen, G.J., Jaehnig, K.P., Percival, J.W.: *Astrophys. J. Suppl. Ser.* **149**, 405 (2003)
- Hartigan, P., Hartmann, L., Kenyon, S.J., Strom, S.E., Skrutskie, M.F.: *Astrophys. J.* **354**, L25 (1990)
- Heyer, M., Zweibel, E.: *A&SS* **292**, 9 (2004)
- Herczeg, G.J., Linsky, J.L., Valenti, J.A., Johns-Krull, C.M., Wood, B.E.: *Astrophys. J.* **572**, 310 (2002)
- Herczeg, G.J., Wood, B.E., Linsky, J.L., Valenti, J.A., Johns-Krull, C.M.: *Astrophys. J.* **607**, 369 (2004)
- Johns-Krull, C.M., Valenti, J.A., Koresko, C.: *Astrophys. J.* **516**, 900 (1999)
- Kueker, M., Henning, T., Ruediger, G.: *Astrophys. J.* **589**, 397 (2003)
- Kulkarni, S., Heiles, C.: *Galactic and Extragalactic Radio Astronomy*, Springer-Verlag, Berlin and New York, p. 95 (1988)
- Lallement, R., Bertin, P.: *A&A* **266**, 479 (1992)
- Lallement, R., Welsh, B.Y., Vergely, J.L., Cribo, F., Sfeir, D.: *A&A* **411**, 447 (2003)
- Lauroesch, J.T., Meyer, D.M., Blades, J.C.: *Astrophys. J.* **543**, L43, (2000)
- Lecavelier des Etangs, A., Deleuil, M., Vidal-Madjar, A., Roberge, A., LePetit, F., et al.: *A&A* **407**, 935 (2003)
- Lecavelier des Etangs, A., Vidal-Madjar, A., McConnell, J.C., Hébrard, G.: *A&A* **418**, L1 (2004)
- Lecavelier des Etangs, A., Vidal-Madjar, A., Roberge, A., Feldman, P.D., Deleuil, M., et al.: *Nature* **412**, 706 (2001)
- Lee, M.G., Bohm, K.H., Temple, S.D., Raga, A.C., Mateo, M.L., Brugel, E.W., Mundt, R.: *Astron. J.* **96**, 1690 (1988)
- Lignieres, F., Catala, C., Mangeney, A.: *A&A* **314**, 465 (1996)
- Liseau, R., Huldtgren, M., Fridlund, C.V.M., Cameron, M.: *A&A* **306**, 255 (1996)
- López-Martin, L., Cabrit, S., Dougados, C.: *A&A* **405**, L1 (2003)
- Maíz-Apellániz, J.: *Astrophys. J.* **560**, L83 (2001)
- Martin, C., Bowyer, S.: *Astrophys. J.* **350**, 242 (1990)
- Matt, S., Goodson, A.P., Winglee, R.M., Boehm, K.-H.: *Astrophys. J.* **574**, 232 (2002)
- McKee, C.F., Ostriker, J.P.: *Astrophys. J.* **218**, 148 (1977)
- Moos, H.W., Sembach, K.R., Vidal-Madjar, A., York, D.G., Friedman, S.D., Hébrard, G., Kruk, J.W., Lehner, N., Lemoine, M., Sonnenborn, G., Wood, B.E., Ake, T.B., André, M., Blair, W.P., Chayer, P., Gry, C., Dupree, A.K., Ferlet, R., Feldman, P.D., Green, J.C., Howk, J.C., Hutchings, J.B., Jenkins, E.B., Linsky, J.L., Murphy, E.M., Oegerle, W.R., Oliveira, C., Roth, K., Sahnow, D.J., Savage, B.D., Shull, J.M., Tripp, T.M., Weller, E.J., Welsh, B.Y., Wilkinson, E., Woodgate, B.E.: *Astrophys. J. Suppl. Ser.* **140**, 3 (2002)
- Muzerolle, J., Calvet, N., Hartmann, L.: *Astrophys. J.* **550**, 944 (2001)
- Ortolani, S., D'Odorico, S.: *A&A* **83**, L8 (1980)
- Petrov, P.P., Gahm, G.F., Gameiro, J.F., Duemmler, R., Ilyin, I.V., et al.: *A&A* **369**, 993 (2001)
- Praderie, F., Catala, C., Simon, T., Boesgaard, A.M.: *Astrophys. J.* **303**, 311 (1986)
- Priest, E., Forbes, T.: *Magnetic reconnection: MHD Theory and Applications*, Cambridge University Press, New York (2000)
- Raymond, J.C., Blair, W.P., Long, K.S.: *Astrophys. J.* **489**, 314 (1997)
- Redfield, S., Linsky, J.L.: *Astrophys. J.* **534**, 825 (2000)
- Redfield, S., Linsky, J.L.: *Astrophys. J.* **613**, 1004 (2004)
- Reynolds, R.J., Chaudhary, V., Madsen, G.J., Haffner, L.M.: *Astron. J.* **129**, 927 (2005)
- Richter, P., Savage, B.D., Wakker, B.P., Sembach, K.R., Kalberla, P.M.W.: *Astrophys. J.* **549**, 281 (2001)
- Roberge, A., Lecavelier des Etangs, A., Grady, C.A., Vidal-Madjar, A., Bourret, J.-C., et al.: *Astrophys. J.* **551**, L97 (2001)
- Rotstein, N., Giménez de Castro, C.G.: *Astrophys. J.* **464**, 859 (1996)
- Sakurai, T.: *A&A* **152**, 121 (1985)
- Savage, B.D., Sembach, K.R.: *Astrophys. J.* **434**, 145 (1994)
- Schmutzler, T., Tscharnutter, W.M.: *A&A* **273**, 318 (1993)
- Schwartz, R.D.: *Annu. Rev. Astron. Astrophys.* **21**, 209 (1983)
- Schwartz, R.D., Dopita, M.A., Cohen, M.: *Astron. J.* **90**, 1820 (1985)
- Shapiro, P.R., Moore, R.T.: *Astrophys. J.* **207**, 460 (1976)
- Simon, T., Vrba, F.J., Herbst, W.: *Astron. J.* **100**, 1957 (1990)
- Slavin, J.D., Frisch, P.C.: *Astrophys. J.* **565**, 364 (2002)
- Tripp, T.M., Wakker, B.P., Jenkins, E.B., Bowers, C.W., Danks, A.C., Green, R.F., Heap, S.R., Joseph, C.L., Kaiser, M.E., Linsky, J.L., Woodgate, B.E.: *Astron. J.* **125**, 3122 (2003)
- Valenti, J.A., Johns-Krull, C.M., Linsky, J.L.: *Astrophys. J. Suppl. Ser.* **129**, 399 (2000)
- Vidal-Madjar, A., Lagrange-Henri, A.-M., Feldman, P.D., Beust, H., Lissauer, J.J., Deleuil, M., Ferlet, R., Gry, C., Hobbs, L.M., McGrath, M.A., McPhate, J.B., Moos, H.W.: *A&A* **290**, 245 (1994)
- Vidal-Madjar, A., Laurent, C., Bruston, P., Audouze, J.: *Astrophys. J.* **223**, 589 (1978)
- Vidal-Madjar, A., Lecavelier des Etangs, A., Désert, J.-M., Ballester, G.E., Ferlet, R., Hébrard, G., Mayor, M.: *Nature* **422**, 143 (2003)
- Vidal-Madjar, A., Lecavelier des Etangs, A., Ferlet, R.: *Planet. Space Sci.* **46**, 629 (1998)
- Vidal-Madjar, A., Désert, J.-M., Lecavelier des Etangs, A., Hébrard, G., Ballester, G.E., Ehrenreich, D., Ferlet, R., McConnell, J.C., Mayor, M., Parkinson, C.D.: *Astrophys. J.* **604**, L69 (2004)
- Watson, A.J., Donahue, T.M., Walker, J.C.G.: *Icarus* **48**, 150 (1981)
- Witte, M.: *A&A* **426**, 835 (2004)

Ultraviolet Studies of Interacting Binaries

Boris T. Gänsicke · Domitilla de Martino ·
Thomas R. Marsh · Carole A. Haswell ·
Christian Knigge · Knox S. Long · Steven N. Shore

Received: 5 May 2005 / Accepted: 28 September 2005
© Springer Science + Business Media B.V. 2006

Abstract Interacting Binaries consist of a variety of stellar objects in different stages of evolution and those containing accreting compact objects still represent a major challenge to our understanding of not only close binary evolution but also of the chemical evolution of the Galaxy. These end-points of binary star evolution are ideal laboratories for the study of accretion and outflow processes, and provide insight on matter under extreme physical conditions. One of the key-questions of fundamental relevance is the nature of SN Ia progenitors. The study of accreting compact binary systems relies on observations over the entire electromagnetic spectrum and we outline here those unresolved questions for which access to the ultraviolet range is vital, as they cannot be addressed by observations in any other spectral region.

B.T. Gänsicke (✉) · T.R. Marsh
Department of Physics, University of Warwick, Coventry CV4
7AL, UK
e-mail: Boris.Gansicke@warwick.ac.uk

D. de Martino
INAF – Osservatorio di Capodimonte, Via Moiariello 16, 80131
Napoli, Italy

C.A. Haswell
Department of Physics and Astronomy, The Open University,
Milton Keynes MK7 6AA, UK

C. Knigge
School of Physics and Astronomy, University of Southampton,
Southampton SO17 1BJ, UK

K.S. Long
Space Telescope Science Institute, 3700 San Martin Drive,
Baltimore, MD 21218

S.N. Shore
Dipartimento di Fisica, Università di Pisa, Largo Pontecorvo 2,
56127 Pisa, Italy

Keywords Close binaries · Cataclysmic variables · Symbiotic stars · X-ray binaries · Evolution · Accretion discs · Winds · Magnetism

1. Scientific background and astrophysical context

The 20th century saw an impressive leap in the theory of stellar evolution – leading from not even knowing what source of energy powers the Sun to the extremely detailed models of stellar structure and evolution available today. A number of the present-day key research areas, e.g. galaxy evolution, are deeply rooted in our understanding of stellar evolution. However, while we may feel comfortable about our understanding of single stars, observational evidence collected throughout the last few decades makes it increasingly clear that the majority of all stars in the sky are born in binaries, of which many will interact at some point in their lives (Iben, 1991). Virtually all of the most exotic objects in the Galaxy are descended from such binary stars, including binary pulsars, all the galactic black-hole candidates, low-mass X-ray binaries (LMXB), millisecond pulsars, cataclysmic variables (CVs), symbiotic stars, and many others. Binary stars are important in many other contexts, too. Sub-dwarf B stars, which now appear to be another product of binary evolution, dominate the ultraviolet light of old galaxies. The Type Ia supernovae, among the most important ‘standard candles’ in the determination of extragalactic distances on a cosmological scale, are thought to arise from exploding white dwarfs driven over their Chandrasekhar mass limit by accretion from a companion star. Even the class of short gamma-ray bursts, the most powerful explosions in the Universe, may be related to the merging of two neutron stars, again products of binary star evolution.

Interacting binary stars are showcases of the processes of mass accretion and outflow, exhibiting a variety of phenomena such as accretion discs, winds, collimated jets and magnetically controlled accretion flows, thermal disc instabilities, and both stable and explosive thermonuclear shell burning. The plasma conditions in these accretion structures span a huge range of physical conditions, including relativistic environments and extreme magnetic field strengths. Consequently, interacting binaries are also extremely versatile plasma physic laboratories.

Despite their great importance for a vast range of astrophysical questions, our understanding of close binary stars and their evolution is still very fragmentary. The ultraviolet (UV) is of outmost importance in the study of interacting binaries, as a large part of their luminosity is radiated away in this wavelength range, and, more importantly, as the UV hosts a multitude of low and high excitation lines of a large variety of chemical species. These transitions can be used both as probes of the plasma conditions, as well as tracers of individual components within the binaries through time-resolved spectroscopy. Moreover, the physical status of the binary components and in particular the accreting white dwarf primaries in cataclysmic variables, symbiotic stars, and double-degenerate binaries can be easily isolated and studied in the UV range. Even though substantial scientific progress has been achieved throughout the last three decades, primarily using the *International Ultraviolet Explorer* (IUE), the *Hubble Space Telescope* (HST), and the *Far Ultraviolet Spectroscopic Explorer* (FUSE), these are still the early days of UV astronomy of interacting binaries, and many key questions are yet without answer. Here we outline the enormous potential that a major UV observatory has for our understanding of interacting binaries, and how the expected findings related to much wider astrophysical contexts, including galaxy evolution and cosmology.

2. Accreting white dwarfs

2.1. The complex interplay between stellar properties and binary evolution

Compared to their isolated relatives, the evolution of white dwarfs in interacting binaries is much more complex, and closely related to the evolution of the binary as a whole, and hence understanding close binary stellar evolution is impossible without detailed knowledge of the properties of the white dwarf components in these stars. The most abundant type of mass-transferring binaries containing a white dwarf are the cataclysmic variables (CVs), which have mass transfer rates in the range 10^{-11} – $10^{-9} M_{\odot}$ yr $^{-1}$. The accretion of this material and its associated angular momentum affects practically all fundamental properties of CV white dwarfs.

Compressional heating is depositing energy in the envelope and the core of the white dwarf, effectively compensating the secular cooling, with the result that accreting white dwarfs are substantially hotter than isolated white dwarfs of comparable age and mass. Townsley and Bildsten (2002, 2003) have shown that the white dwarf temperature can indeed be used to establish a measure of the long term average of the accretion rate sustained by the white dwarf. As the secular average accretion rate is directly related to the rate at which the binary is losing orbital angular momentum measuring this parameter is of fundamental importance for any theory of close binary evolution.

Accretion will increase the mass of the white dwarf. Eventually, if nothing else happens and the mass supply of the companion star is sufficient, this will drive the white dwarf over its Chandrasekhar mass limit, and it may turn in into a supernova Type Ia. Accreting white dwarfs as possible SN Ia progenitors are discussed in more detail in Section 2.2 below. However, in most CVs the accreted hydrogen layer will thermonuclearly ignite once the density and temperature exceed the critical condition. This hydrogen shell burning is typically explosive, observationally designated as a classical nova, and ejects a shell of material into space (see Section 2.3). As the critical mass of the accreted hydrogen-rich layer is fairly low ($\sim 10^{-5}$ – $10^{-3} M_{\odot}$), a CV will undergo hundreds to thousands of nova explosions. Currently, it is not clear what the mass balance during the nova event is, i.e. whether the amount of ejected material is equal to or even exceeds the mass of accreted material, and, hence, the long-term evolution of the white dwarf mass is not known.

Chemical abundances of white dwarf surfaces can be affected by accretion and greatly modified by nova explosions. While a roughly solar composition is expected for a freshly accreted white dwarf atmosphere, many CVs were recently found to possess an unexpected wide variety of departures from (solar) abundances (Sion, 1999), opening new horizons in the current understanding of binary evolution. Indeed while in single white dwarfs metallic species and their abundance reveal processes which oppose diffusion, those in cataclysmic variables show a mix of chemical species and abundances that cannot result from accretion from a normal secondary star, thus pointing towards a thermonuclear activity in their past evolution. The hypothesis of CNO processing as the source of the abundances has been further supported by the detection of proton-capture material by Sion et al. (1997). This has great implications for CV evolution and contributions to the heavy element content of the interstellar medium (see also Section 2.2).

Rotation rates of non-magnetic white dwarfs in CVs were unknown prior the HST era and its advent opened a new topic in close binary evolution. Global rotational velocities are now measured for a handful of dwarf novae systems (Sion, 1999) and were found to be much larger (300–1200 km s $^{-1}$) than

the few tens of km s^{-1} in isolated white dwarfs, implying that accretion efficiently spins-up the primaries. However the measured rates are much lower than expected on the basis of the amount of angular momentum accreted during their characteristic lifetimes (Livio and Pringle, 1998; King et al., 1991) suggesting that part of the accreted angular momentum is removed from the white dwarf during the expanded envelope mass loss phase which follows a nova eruption. This independently suggests that also dwarf novae experience nova outbursts and then return to be dwarf novae again, as suggested by the cyclic evolution scenario. Although this result has an enormous evolutionary implication, it is based on only 5 CV white dwarfs for which reliable rotation rates could be determined.

Whereas accretion alters the properties of white dwarfs in interacting binaries, some of the white dwarf characteristics will in turn deeply affect the accretion process – e.g. the mass of the white dwarf defines the depth of the potential well, and, thereby, the amount of energy released per accreted gram of matter, the rotation rate of the white dwarf determines the luminosity of the boundary layer, i.e. the interface between the inner accretion disc rotating at Keplerian velocities and the white dwarf itself, and finally the magnetic field of the white dwarf determines the accretion geometry.

The observational study of accreting white dwarfs can only be carried out in the UV, as the emission from the accretion flow dilutes or even completely outshines the white dwarf at optical wavelengths. Because of the faintness of most CV white dwarfs, the number of systems for which medium-resolution ($\simeq 1\text{--}2 \text{\AA}$) spectroscopic data, adequate for temperature measurements, has been obtained is $\simeq 35$ (Sion, 1999; Szkody et al., 2002; Araujo-Betancor et al., 2005) – out of a total of ~ 1000 CVs known (Downes et al.,

2001). High-resolution ($\simeq 0.1 \text{\AA}$) UV spectroscopy necessary for accurate abundance and rotation rate determinations has been obtained only for a handful of systems, most noticeably for the nearest CV, WZ Sge (Fig. 1, see e.g. Sion et al., 2001, 2003; Long et al., 2004; Welsh et al., 2003), at the expense of >20 *HST* orbits.

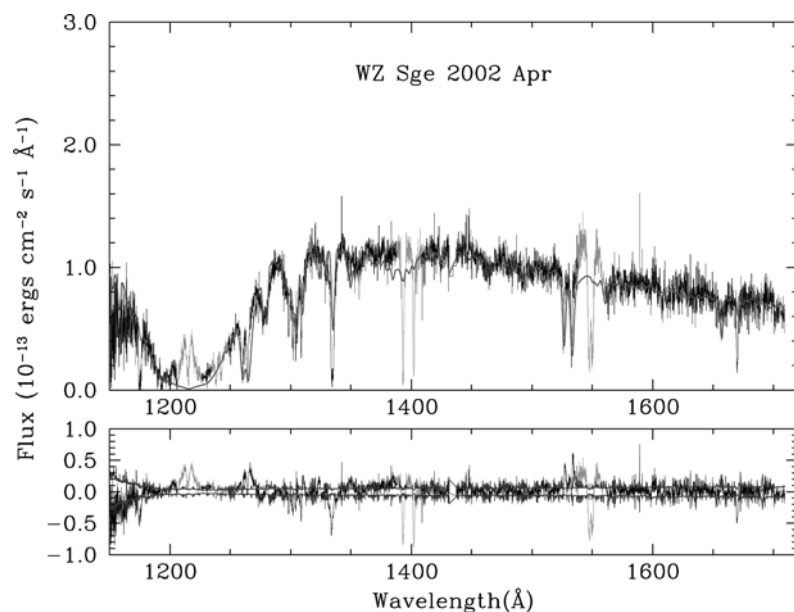
2.1.1. Future prospectives of UV astronomy

In order to fully assess the interrelation between the white dwarf properties and the evolutionary state of CVs, a sufficiently large number of systems has to be observed. Mapping out the parameter space (T_{wd} , M_{wd} , abundances and rotation rate of the white dwarf, as well as the binary orbital period) will eventually require adequate data for 100–200 systems. Temperature measurements need a broad UV wavelength coverage, optimally from the Lyman edge down to 3000\AA , at a low resolution ($R \simeq 1000\text{--}2000$). Abundance/rotation rate measurements rely on medium-resolution ($R \simeq 20000$) spectroscopy covering a sufficient number of transitions; the traditional range $1150\text{--}1900 \text{\AA}$ is adequate even though similar capabilities below $\text{Ly}\alpha$ would be desirable. Throughput is the crucial need for this science, as typical flux levels are a few $\simeq 10^{-16} \text{ erg cm}^{-2} \text{ s}^{-1} \text{\AA}^{-1}$.

2.2. Accreting white dwarfs as likely SN Ia progenitors

Whereas SN Ia are routinely used as beacons at cosmological distances (Filippenko, 2004), and generally associated with the thermonuclear disruption of a carbon-oxygen white dwarf (Livio, 2001), the nature of their progenitors remains elusive. Two different channels of SN Ia progenitors are currently most favoured (Yungelson and Livio, 2000).

Fig. 1 High-quality UV spectroscopy of accreting white dwarfs in CVs is necessary to determine their temperature, mass, rotation rate, and atmospheric abundances from detailed model atmosphere fits. Only a very limited number of CVs has been bright enough to be studied with the STIS high resolution grating, such as e.g. WZ Sge (from Long et al., 2004)



In the double-degenerate channel two white dwarfs spiral in under the effect of gravitational radiation until they finally merge, exceeding the Chandrasekhar mass limit. Intensive optical surveys have been carried out for this type of SN Ia progenitors, most recently by (Napiwotzki et al., 2001), identifying a few potential SN Ia progenitor candidates. In the single-degenerate channel a white dwarf accretes from a main-sequence companion. However, as outlined above, most white dwarfs accreting hydrogen-rich material will go through classical nova explosions and grow only little (or even shrink) in mass. Only if the white dwarf is accreting at a rate sufficiently high to sustain *steady-state hydrogen shell burning* – the accreted hydrogen is thermonuclearly processed at the rate it is accreted. These objects have been predicted (Shara et al., 1977; Iben, 1982; Fujimoto, 1982) and first found in the EINSTEIN X-ray survey of the Magellanic clouds (Long et al., 1981), even though it took a fair amount of time to identify their true nature (van den Heuvel et al., 1992). Based on their observational hallmark – a very large luminosity in soft X-rays, these objects are coined supersoft sources, or more appropriately supersoft X-ray binaries (Gänsicke et al., 2000). The high accretion rates that are necessary to fuel the steady-state shell burning in supersoft X-ray binaries can be provided by a Roche-lobe filling main sequence star if its mass is similar to or exceeds that of the white dwarf. As mass is transferred from the more massive to the less massive star, the binary period shrinks as a consequence of angular momentum conservation, stabilising or even enhancing the mass loss of the donor star. The mass transfer ensues on a time scale which is too short for the donor star to adjust its thermal structure, and in an evolutionary jargon supersoft X-ray binaries are known as thermal time scale mass transfer (TTSMT) CVs. In the absence of nova eruptions, the white dwarfs in TTSMT CVs grow in mass, and will, if the donor star provides a sufficient amount of material, surpass the Chandrasekhar limit and potentially explode in a SN Ia (Di Stefano, 1996; Starrfield et al., 2004).

If the donor star in a TTSMT runs out of fuel before the white dwarf reaches the Chandrasekhar mass limit, the mass ratio will eventually flip with the donor star being less massive than the white dwarf. Consequently, the mass transfer rate decreases and the shell burning ceases. From this point on, the system will evolve and look (at a first glance) like a normal CV – with the dramatic difference that normal CVs contain main-sequence donor stars, whereas post-TTSMT CVs contain the CNO processed core of the previously more massive star. Schenker et al. (2002) suggest that a significant fraction (up to 1/3) of all present-day CVs may actually have started out with a companion more massive than the white dwarf, and underwent a phase of TTSMT. A recent *HST/STIS* snapshot survey of 70 CVs showed that ~10% of the systems display a significantly enhanced N/C abundance ratio, which suggests that these systems went through a phase of TTSMT

(Gänsicke et al., 2003). So far, not a single *progenitor* of supersoft X-ray binaries/TTSMT CVs has been identified.

2.2.1. Future prospectives of UV astronomy

Mapping out the population of failed SN Ia = post-TTSMT CVs will require low ($R \simeq 1000$ –2000) resolution spectroscopy of several 100 CVs down to $\simeq 10^{-16}$ erg cm $^{-2}$ s $^{-1}$ Å $^{-1}$. Based this large sample, it will be possible to determine the orbital period distribution of post-TTSMT CVs with respect to the “normal” systems, model their evolution, and finally extrapolate these population models to the regime of true SN Ia progenitors. Follow-up the brighter ones at high resolution ($R \simeq 20000$) will be necessary in order to determine their detailed properties. This will also help to answer the very important question on whether the white dwarfs in these systems have grown in mass, i.e. are they more massive than in normal CVs?

Equally important is the search for true SN Ia progenitors. However, as the TTSMT phase is very short the chance of finding systems in this stage is small – in fact, in our Galaxy (where absorption in the plane further decreases the probability of finding such systems) only two supersoft X-ray binaries are known. Supersoft X-ray binaries can be located in local group galaxies using high spatial resolution ($\simeq 1''$) X-ray missions such as Chandra – however, X-ray data alone is typically insufficient to determine the properties of the objects. UV observations can substantially defeat crowding problems (see Section 7), and are well-suited to obtain fundamental parameters such as orbital periods. This implies large aperture high spatial resolution UV imaging capabilities (supersoft X-ray binaries in M31 have $V \simeq 23$).

A so far entirely unexplored potential is the search for *SN Ia pre-progenitors*, i.e. detached white dwarf/main sequence binaries with $M_{\text{sec}} > 1.6 M_{\odot}$ (Langer et al., 2000; Han, 2004). In the optical, these systems will be entirely dominated by the main-sequence star, and follow-up UV studies of main-sequence stars with UV excess (identified e.g. in the GALEX survey) will be necessary to identify them.

2.3. The nova phenomenon

Novae are the most spectacular phenomenon encountered in CVs and represent key objects to understand a wide variety of physical conditions of accreting matter including super-Eddington regimes and the interaction of ejecta in the interstellar medium and its chemical evolution. They are fundamental standard candles up to the Local Group, having hence important implications for cosmological distance calibrations.

Despite the enormous observational effort of the past 15 years, especially with multi-wavelength campaigns and

datasets, there remain two fundamental uncertainties: what are the masses and structures of the ejecta and what drives the mass loss during the outburst? Radiative processes, which might be the source of a stellar wind during the ejection phase (e.g. Hauschildt et al., 1994) depends on the abundances (and therefore the details of the spectral evolution during the initial stages) and the bolometric luminosity. Explosions are powered directly by decays of radioactive isotopes generated during the thermonuclear runaway following the initial envelope expansion, but any subsequent mass loss must be driven by the match of the flux distribution with the envelope opacities (Shore, 2002). The UV, now inaccessible to observation, is the driving spectral region for the phenomenological analysis of novae. Only in this region it is possible to directly probe the properties of the ejecta – abundances, structure, mass – and determine the energetics of the thermonuclear runaway. The reasons are simply that the photometric behaviour is driven at all wavelengths longer than the UV by bolometric flux redistribution from the evolving central remnant white dwarf and that in the UV we can measure the resonance transitions off the dominant ions throughout the first few months of outburst. To date, only novae in the Galaxy and the LMC have been observed.

Novae have been used as distance calibrators for nearly a century through the maximum magnitude – rate of decline (MMRD) relation, but the origin of this relation has only recently been understood. As the ejecta expand, the rapid and enormous increase in the opacity from recombination-driven strengthening of the line absorption redistributes flux into the optical. But the correspondence between these two regions, the completeness of the redistribution process, depends on the details of the ejecta *filling factors*. If the ejecta initially fragment and/or if they are not spherical in the earliest stages, the process will be less efficient and the observed maximum at longer wavelengths will be altered. Without the UV, it is impossible to determine the bolometric luminosity and therefore to constrain its constancy.

The two principal classes of *classical* novae are distinguished by their abundances, which reflect the composition differences of the accreting white dwarf (CO and ONe). The most extreme explosions may produce significantly altered abundance patterns and there is an indication that the ejecta for both of these types are also helium enriched. Without the UV to provide access to resonance lines for the relevant ions, abundance studies – and the determination of structure – are limited by uncertainties in the equation of state for the ejecta.

Among recurrent novae, the two classes; those in compact, cataclysmic-like systems and those with red giant companions, appear to have very low mass ejecta (in agreement with current models) but with abundance patterns that suggest helium enrichment. The UV is the only way to study the ejecta in the optically thick phases (which last only a matter of days) to obtain unambiguously the abundances. It also is

not clear whether these systems show discs, or winds, during quiescence. Finally, the interaction between the expanding ejecta and the winds in the symbiotic-like systems (with red giant companions) can only be studied effectively at high spectral resolution in the UV where the resonance lines and continuum of the white dwarf are accessible.

2.3.1. Future prospectives of UV astronomy

With increased aperture, especially in the 4–6 meter range, and high spectral resolution (10 000 or higher), it would be possible to study novae throughout the Local Group, especially M 31 in which the full range of novae appear to occur. Novae are important contributors to several rare isotopes, especially ^{22}Ne and possibly ^{22}Na , and also may be important in ionising galactic halos (thus being important for understanding the halo ionisation and properties of Ly α Forest systems formed therein). Since they are recurrent phenomena, on many timescales, and remain hot for long periods they may be important for understanding the UV upturn in elliptical galaxies (they can mimic post-AGB stars, for example). Finally, as bright, transient UV sources, they provide probes of the interstellar medium throughout their host galaxy. Also, the transition from the super-soft phase into the UV is essential but it has always been extremely difficult to determine. Furthermore the determination of chemical abundances in the ejecta is a fundamental parameter to test theories on the processes that lead to the nova phenomenon and to understand the state of the binary system. Indeed in no system these abundances were found to be solar-like (Selvelli and Gilmozzi, 1999) having important implications in the chemical evolution of interstellar medium.

2.4. Symbiotic stars

The symbiotic systems are exotic and intriguing interacting binaries. The nature of the accreting hot companion was longly debated and proofs that the hot accreting companion is most likely a white dwarf and not a main sequence star were provided by UV observations (e.g. Eriksson et al., 2004). These systems however differ from the CVs because of their wider orbits, with orbital periods from a few to a few dozen years, and because the white dwarf accretes from the stellar wind of a late-type giant rather than through Roche lobe overflow from a main sequence star. The wind from the cool star is ionised by the radiation from the white dwarf resulting in the characteristic combination of sharp nebular emission lines and molecular absorption bands in their UV and optical spectra (Birriel et al., 2000). An increasing number of symbiotic stars are also found to show nova outbursts. In these systems, despite the much smaller outburst amplitudes compared to those observed in novae, the total energy associated with the outburst may significantly exceed

that of a classical nova. Currently very little is known about the line-emitting regions associated with the outburst of a symbiotic nova because of the long timescales to reach the maximum and the very much slower decays (Rudy et al., 1999). Symbiotics also fall in the category of the supersoft X-ray sources (Greiner, 1996) making them potential SN Ia progenitors (Hachisu et al., 1999). Furthermore only a handful of symbiotics have been monitored through their outbursts in the UV, where the evolution of the hot accreting object can be best followed and from which the energetics of the process can be best studied and linked to the soft X-ray emission (González-Riestra et al., 1999).

Among the different classes of interacting binaries discussed in this paper, symbiotic stars are by far the physically largest objects, and future UV/optical interferometric missions with sub-milliarcsecond spatial resolutions will be able to resolve the two stellar components, as well as the wind / accretion flow from the companion star, and possibly an accretion disc around the compact star. Carrying out such studies in the different UV resonance lines will allow a detailed mapping of the ionization structure in the accretion flow.

2.4.1. Future prospectives of UV astronomy

To identify the hot accreting component and to determine the UV luminosity and its evolution during outbursts the construction of SED over a wide spectral range is necessary. This requires low dispersion (~ 2000) spectroscopy in the desirable range from the Lyman limit down to 3400 Å. Our knowledge of the population of symbiotic novae in our Galaxy and Local group will enormously improve with UV imaging capabilities as described in Sections 2.2 and 7. Furthermore the study of emission lines mapping a wide variety of physical conditions of the accreted matter and outflow need moderate-to-high dispersion spectroscopy ($R \sim 10\,000$ – $20\,000$) in the FUV range. UV imaging at sub-milliarcsec resolution is required to physically resolve the stellar components and accretion flow.

2.5. Accretion flows in magnetic systems

Accretion can be greatly influenced by the presence of magnetic fields of the primary star. In those CVs where the white dwarf is strongly magnetised ($B > 10^5$ – 10^8 G) important modifications of the accretion flow occur already at the distance of the donor star. The formation of an accretion disc is prevented in the high field systems ($B > 10$ MG) or truncation of the accretion disc can occur in moderately ($B < 5$ MG) magnetised CVs. Hence, the wide range of accretion patterns encountered in mCVs allows to test different physical conditions of accretion flow and X-ray irradiation. In particular, previous observations of magnetic systems have

shown that the FUV continuum is dominated by the X-ray irradiated white dwarf pole (Gänsicke et al., 1995), while the accretion funnel down to the post-shock regions contributes in the NUV continuum and in the FUV emission lines of CNO. The truncated disc is also a source of UV continuum (Haswell et al., 1997; de Martino et al., 1999; Eisenbart et al., 2002; Belle et al., 2003). However there are still important open questions on the physical conditions (kinematics, temperature and density) of the accretion flow:

- (1) A strong potential to diagnose ionised gas is provided by the resonance FUV emission lines (CNO), as their FWZI ~ 2000 – 3000 km s $^{-1}$ clearly indicates that they map the accretion flow down to the white dwarf surface. However, while past (low resolution) UV observations have allowed significant progress in the understanding of emission line formation ruling out collisional ionisation and strongly favouring photoionisation models (Mauche et al., 1997), there is still a great uncertainty in theory, as they cannot simultaneously account for all the line flux ratios observed in CVs. Among the magnetic systems there seems to be a higher ionisation efficiency in the hard X-ray intermediate polar systems with respect to the soft X-ray polar systems (de Martino, 1999) suggesting that the soft X-rays are efficiently absorbed likely due to larger absorption column densities. Contribution to the FUV lines can also arise from the X-ray irradiated hemisphere of the secondary star and from material located in different parts of the flow (Gänsicke et al., 1998), where plasma conditions can be very different from each other. An important improvement can be achieved by obtaining a systematic survey of phase-resolved (white dwarf spin and orbital period) of the FUV lines in magnetic CVs to perform Doppler tomogram analyses and to identify the kinematical properties of the accretion flow as well as to separate the different contributions of emission lines. This can allow a proper test of line formation theory as well as to understand the irradiation effects of the secondary star.
- (2) Magnetic systems have the most complex accretion geometry which is very difficult to parametrise. Spectral energy distributions (SEDs) from optical through the UV to the X-rays are necessary to determine the energy budget and to infer the mass accretion rates (Eisenbart et al., 2002). In the case of truncated discs as in the moderately magnetised systems, the UV SED is crucial to assess temperature profile and extension of disc down to the magnetospheric radius as the SED might show a turn-off in the UV range. Also, the X-rays can be substantially absorbed leading to accretion luminosities which can be much lower than those determined with combined UV and optical observations (Mukai et al., 1994). Up to date only a handful of bright magnetic CVs have been

observed in the UV so far, but a systematic UV study has the potential to infer the relation between mass accretion rate and system parameters such as inclination angle and magnetic moments.

Furthermore, it is of fundamental importance to separate the spectral contributions of the heated pole caps of white dwarfs in polars from the unheated underlying white dwarf, thereby determining both the effects of irradiation and the white dwarf temperature. In this respect an important issue is the tendency of white dwarfs in the magnetic CVs to be cooler than those in non magnetic systems (Sion, 1999; Araujo-Betancor et al., 2005) with significant differences at all orbital periods. This trend might reflect a difference in the mass transfer rate efficiency with respect to non-magnetic CVs as the systems evolve. In particular, the white dwarf magnetic field may reduce the secondary star magnetic braking efficiency (Wickramasinghe and Wu, 1994), a hypothesis which observations seem to confirm. However, a statistically significant sample of magnetic CVs is needed to be observed especially at periods above the orbital 2–3 hr period gap where only two systems have been covered so far with *HST*. This range of the period distribution is essential as it is dominated by angular momentum loss through magnetic braking. It is therefore important to determine the temperature of the unheated white dwarf atmosphere by means of low resolution UV spectroscopy over a wide wavelength range either when these systems are in a low accretion state or via phase-resolved observations which can allow to isolate the heated atmospheric pole from the unheated white dwarf atmosphere.

2.5.1. Future prospectives of UV astronomy

To map the accretion flow structure will need systematic phase-resolved UV spectroscopy at the orbital and white dwarf rotational periods in high and low dispersion to study the phase dependence of the FUV emission lines and of the SED. In particular the determination of kinematical properties of the accretion flow and the identification of the X-ray irradiated secondary star atmosphere require the coverage of the various FUV emission lines and hence a minimum range, of 1150–1800 Å (1000–1800 Å desirable) with a spectral resolution of $R \sim 20\,000$. Only for a handful of bright magnetic systems high resolution spectroscopy has been performed with *HST* and *FUSE*. Furthermore, the construction of SEDs over the widest spectral range from the Lyman edge down to 3400 Å is essential to determine simultaneously the different spectral components (disc, white dwarf, accretion funnels). This requires low resolution spectroscopy at $R \sim 2000$ and good quality spectra at levels of a few 10^{-16} erg cm $^{-2}$ s $^{-1}$ Å $^{-1}$. Phase – resolved spectroscopy also demands large through-

put in order to achieve reasonable signal-to-noise ratio with short exposure times. Timing capabilities of instrumentation (e.g. photon – counting systems) allowing to explore different types of variability (periodic, quasi-periodic and non periodic) on a wide range of timescales are essential. These can allow the access to the mostly unexplored temporal domain of UV emission in accreting magnetic systems.

3. Accretion discs

In order to form stars and galaxies, or to power active galactic nuclei and gamma-ray bursts, matter must be compressed by many orders of magnitude in size. This is possible while gravity dominates over thermal, magnetic and rotational energy. This can require the radiation of substantial amounts of thermal energy and the diffusion of magnetic field, but ultimately rotation always puts a brake upon this process because in a homologous collapse of a cloud of size R the rotation energy scales as R^{-2} while gravitational energy scales as R^{-1} . Nature's solution to this problem is to re-distribute the angular momentum in an accretion disc. In an accretion disc, gas travels in near-circular orbits gaining angular momentum from material at smaller radii, and losing it to matter at larger radii. The transport of angular momentum is driven by some form of viscosity, and only in recent years has a plausible candidate for this been identified in the magneto-rotational instability (Balbus and Hawley, 1998). Despite this progress, our understanding of the viscosity of accretion discs and precisely how energy is dissipated within them remain the central unanswered questions in the field. A major obstacle to making progress is that two important properties of discs, their luminosity and temperature distribution, are independent of viscosity in steady-state discs. Progress can only be made through the study of phenomena that change on the *viscous timescale*, $t_v \sim R^2/\nu$ where R is the size of a disc and ν is the kinematic viscosity or by examining the vertical temperature structure of discs through their spectra. The great advantage of close binary stars is their small scales which lead to viscous timescales of only a few days or weeks, making them amenable to direct observation.

The outbursts of dwarf novae are almost universally believed to be driven by changes in the viscosity of the material in their accretion discs. In the standard *disc instability model* developed in the 1980s, in the quiescent state, the viscosity ν is very low, and the viscous timescale, t_v , is so long that the disc cannot cope with the rate at which matter flows in at its outer edge. Instead, mass piles up in the outer parts of the disc until a critical point is reached and at some radius in the disc the viscosity (and therefore viscous dissipation rate) increases dramatically, by of order 100 times. This jump can take only a few minutes, with the outburst following as a heating wave propagates to all radii within the disc. A major

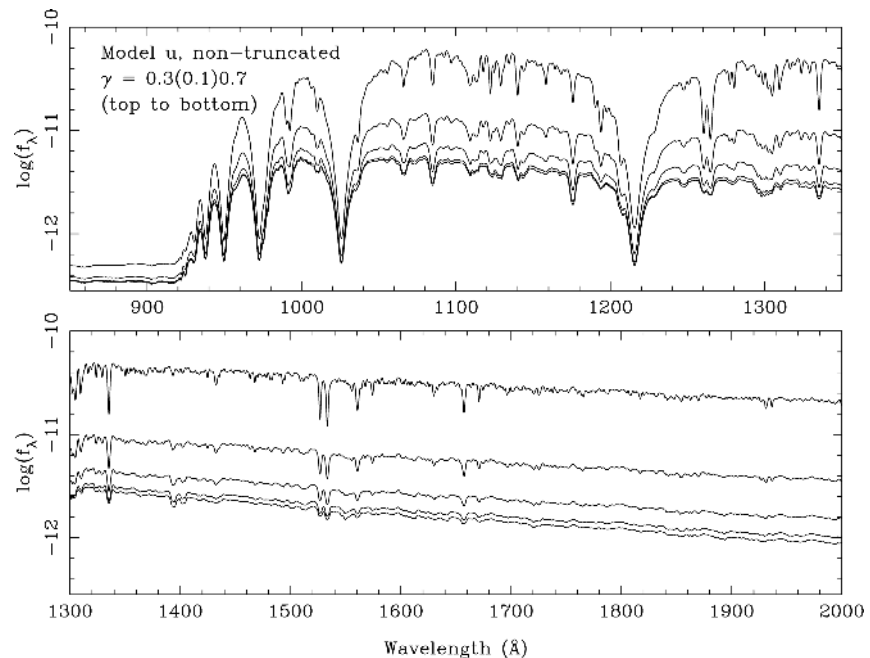
goal of the study of accretion discs is to understand these outbursts: how they propagate, what triggers them, but above all, why the viscosity ramps up so violently. This is thought to be rooted in the ionisation of hydrogen (or in ‘ultra-compact’ binary stars, helium), but we have no detailed physical mechanism from which we can compute the viscosity for a given composition, density and temperature. All current models, which have been applied to accretion discs in a wide variety of objects, are hence purely phenomenological.

The commonest, nearest and most easily studied accretion discs are those of the cataclysmic variable stars which have white dwarf accretors. Accretion discs around white dwarfs vary in temperature from $\sim 6\,000$ K in their outermost parts to over 100 000 K close to the white dwarf. The radius of the outer disc is typically 10 to 50 times that of the white dwarf, but it is from the hot, inner few white dwarf radii that most of the energy is released. The UV is the key waveband for seeing these regions. There are three other reasons for UV observation of accretion discs in these binaries. First, one can see absorption lines from the disc photospheres most easily in the FUV (Fig. 2). These give a handle upon ionisation state not available at optical wavelengths where emission from the (barely understood) disc chromosphere is always dominant and photospheric absorption lines are weak. Second, the UV is where disc model atmospheres currently seem to fail most severely, in general appearing too blue compared to observations (Orosz and Wade, 2003). The final unique feature of the UV is its sensitivity to the geometry of the disc because absorption of the inner by the outer disc is most easily seen in the UV and was first established from UV observations (Horne et al., 1994).

Fig. 2 Model spectra of accretion discs with a range of radial temperature profiles, $T_{\text{eff}} \propto R^{-\gamma}$ Orosz and Wade (2003)

3.1. Modelling the spectra of accretion discs

Since the early days of black-body models, followed by models based upon sums over standard stellar atmospheres (Wade, 1984), accretion discs models based upon modern model atmosphere codes have been developed (Wade and Hubeny, 1998; Orosz and Wade, 2003). Such models are however undermined by our ignorance of the mechanism of viscosity and hence of the vertical temperature structure of discs. In principle, spectra can be used in reverse to determine vertical structure, but, so far, little progress has been made in this area. A problem of long standing is that disc model atmosphere spectra do not work very well, especially at FUV wavelengths. This might be down to the vertical structure, or it could be that the steady-state (radial) temperature distributions used so far are not accurate (Orosz and Wade, 2003), even though it is hard to understand how this can be the case in systems that hardly change on many viscous timescales. The problem comes from the small size of accretion discs in close binary stars, with a typical radius of a few 10^{10} cm. While their sizes help keep viscous timescales small, so that thermal instabilities are easily observed over the course of days to months, it means that the discs are not spatially resolvable as they subtend at best a few $\simeq 0.01$ milli-arcseconds for the closest systems. Direct imaging of the accretion discs will be possible in the foreseeable future only in the much larger symbiotic stars (Section 2.4), in which, however, the viscous time scales are substantially longer, and the temporal variability of symbiotics in terms of disc instabilities is much less established compared to the situation in CVs. Thus the spectra we see are the integrated spectra from all radii in the



disc. This makes it hard to know whether it is the radial or vertical structure that is causing the problem. With integrated spectra, one cannot be sure whether all radii are poorly modelled or whether only specific effective temperatures are involved, and thus it is not clear how to adapt models. We need spatially resolved spectra, which can be achieved through a technique known as eclipse mapping (Horne, 1985). Applied at UV wavelengths, this technique has the capability to provide spatially resolved spectra of the inner parts of accretion discs where most energy is released. We can then see where it is in the discs that model atmospheres fail most severely.

The principle of eclipse mapping is as follows: in an eclipsing system, the light-curve of the disc as it is eclipsed depends upon how concentrated the surface brightness is. For instance a flat distribution of brightness leads to a shallow V-shaped light curve, whereas a distribution which is strongly peaked towards the centre of the disc has a deep U-shaped light curve (Fig. 3)

Thus, in essence, the light curves can be used to deduce the variation of surface brightness with radius. Eclipse mapping was developed by Horne (1985) for broad-band optical light curves. A significant step in eclipse mapping came with its extension to spectra (Rutten et al., 1993; Rutten et al., 1994). The simple, beautiful, idea was to carry out eclipse mapping on each pixel of low-resolution spectra to produce

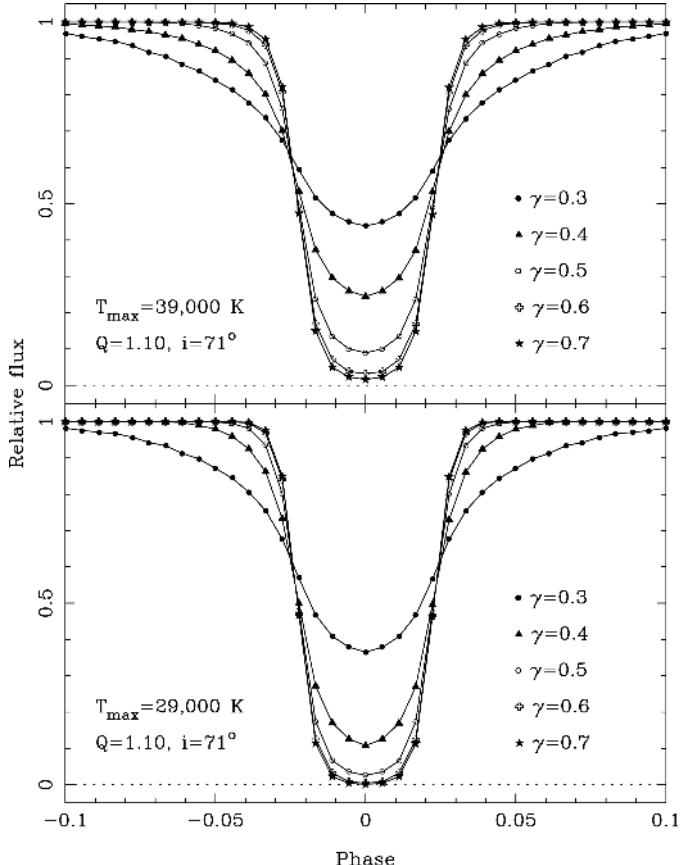
spectra at every point of discs. This technique applied to UV data has the capability of giving us spatially-resolved spectra of the inner accretion discs of close binary stars. Only one such analysis has been carried out in the UV with *HST/FOS* (Baptista et al., 1998; Fig. 4) of the brightest of all high-state systems, UX UMa.

Even on this, the brightest suitable system, the study was limited by signal-to-noise ratio, especially at FUV wavelengths, precisely the most important part of the spectrum. The signal-to-noise ratio in this region of the spectrum is a modest 10% and yet the radial resolution is still only ~ 4 white dwarf radii, which means that we are still seeing the integrated light from a region which varies by a factor of three in temperature from the inner to outer edge of the annulus. In other words the problem of integrated spectra is only partially solved in this study.

3.1.1. Future prospectives of UV astronomy

To substantially improve our ability to model the spectra of accretion discs requires a low resolution, wide wavelength coverage UV spectrograph of much greater sensitivity than has been available to date. Low resolution ($R \sim 300$) because the spectral eclipse mapping technique cannot resolve the $\sim 1000 \text{ km s}^{-1}$ motions within the disc. UV because, as

Fig. 3 Model eclipses in the continuum from 1410 to 1530 Å for black-body (top) and model atmosphere discs for a range of radial temperature profiles, $T_{\text{eff}} \propto R^{-\gamma}$ Orosz and Wade (2003)



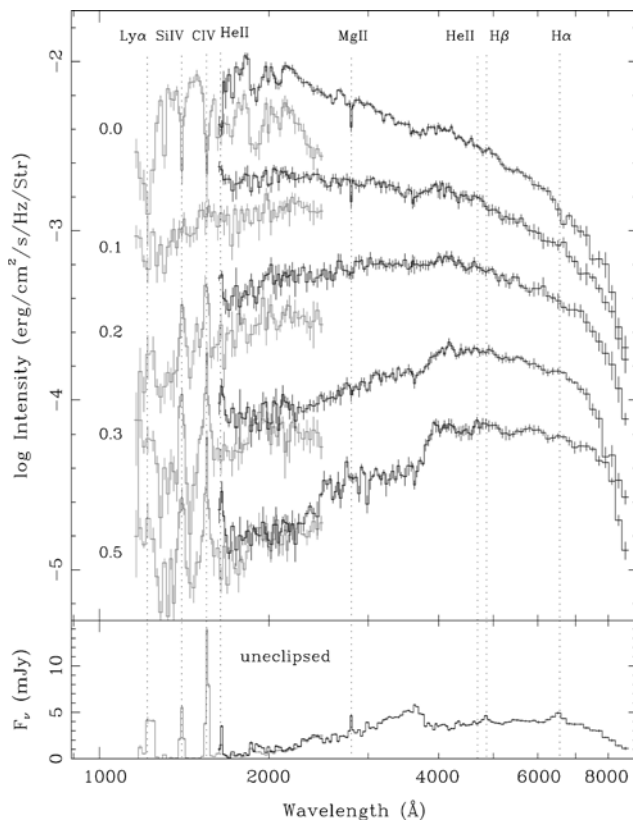


Fig. 4 The spectra of the steady-state system UX UMa as a function of radius deduced from *HST/FOS* observations of its eclipse (Baptista et al., 1998). The spectra are those of annuli with central radius indicated in units of the distance to the inner Lagrangian point. Note that the spectra are plotted in f_v ; the UV is dominant energetically

said before, this is where most luminosity is radiated and where the current disc atmospheres fail most severely. Wide wavelength coverage (at least 1000 to 3000 Å, and if possible extending to the Lyman edge) because it is the variation of continuum flux with wavelength which tells us most directly about the vertical structure in stellar atmospheres. Finally, and perhaps above all, in comparison to any UV mission to date, high sensitivity is needed in order to improve both the signal-to-noise ratio in the deconvolved spectra and their radial resolution down to of order a single white dwarf radius and so that the method can be applied to systems fainter than UX UMa. Two other requirements needed for this work are an ability to take short exposures (<2 seconds) which are accurately timed with absolute times good to better than one-hundredth of the exposure length.

Once progress in understanding gross properties of spectra has been made, there will be a need for higher resolution observations. Models can predict the changes in detailed line profiles expected during eclipse (Orosz and Wade, 2003). Again disc broadening means that moderate resolution is sufficient ($R \sim 5000$), but high-sensitivity in order to allow

short exposures and therefore high spatial definition of the disc are a must. The study of integrated spectra provides the most stringent requirement for spectral resolution because face-on discs (no eclipse) have significantly narrower line profiles and suffer less from blending. For these $R \sim 20\,000$ would be useful, covering from 900 to 1700 Å.

3.2. Disc instabilities

It is the study of dwarf nova outbursts that lead to the disc instability theory and the discovery of the strong dependence of viscosity with the physical conditions within the disc. The disc instability model has largely been used to explain the gross features of outbursts, such as their duration and amplitude, but there have not been convincing detections of the heating fronts which would allow us to confirm predictions of the models in detail. Attempts have been made from optical observations of eclipses, but these lose resolution in the inner disc because the outer disc dominates the light output at optical wavelengths. The propagation of the heating fronts into the inner disc is of particular interest because there is evidence to suggest that the inner disc is strongly depleted during quiescence (Schreiber et al., 2004). This is needed to prevent outbursts triggering in the inner disc, which in some systems would lead to too high an outburst rate. Propagation of heating fronts can be measured from the development of photospheric line profiles from the disc. As the front progresses inwards, the contribution from smaller radii in the disc will contribute to broadening the line profiles because Doppler broadening is largest in the inner disc. The photospheric lines are strongest by far in the UV and develop dramatically during outburst (Fig. 5).

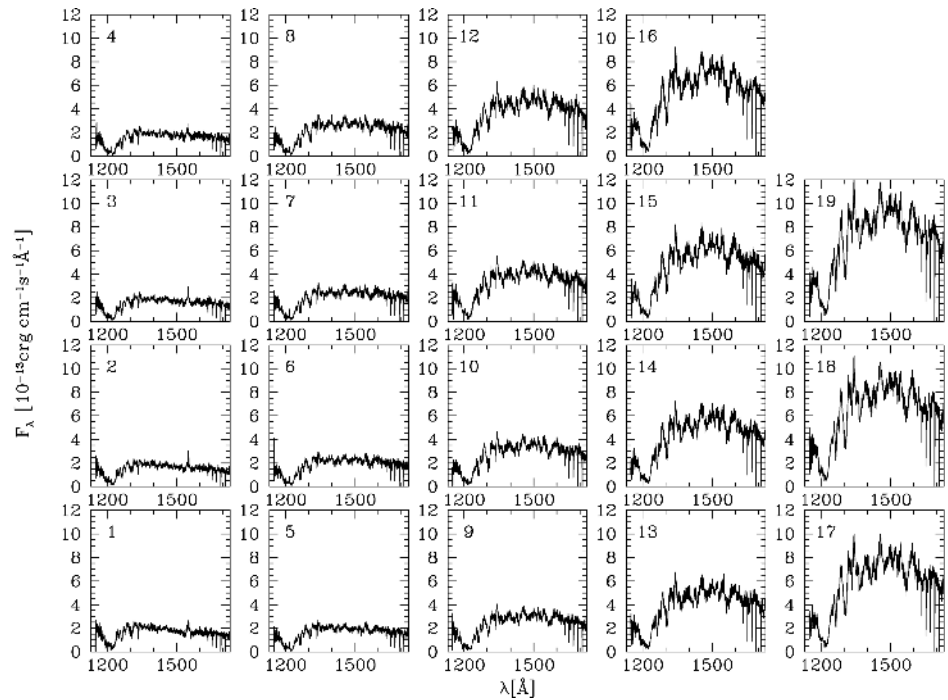
3.2.1. Future prospectives of UV astronomy

So far this sort of study has not been possible because of limited sensitivity at FUV wavelengths. It also requires a much higher duty cycle than possible with *HST* as outbursts take of order a few hours to a day to start. Observations such as these could also show the development of winds through the resonance lines which are only visible at UV wavelengths. A spectrograph covering 900 to 1700 Å with a resolution $R > 5000$ is needed for this work.

4. Hydrogen-deficient systems

A unique aspect of close binary stars is that owing to the evolution of their mass donor stars, some systems can show very unusual abundances, adding an extra dimension to the development of atmospheric models. The AM CVn systems for example have helium white dwarf donors and accretion discs which are >95% helium. Ultra-compact neutron star/white

Fig. 5 The spectra of the dwarf nova VW Hyi caught at the start of an outburst with *HST/STIS* (Sion et al., 2004). At first the spectra are dominated by the white dwarf but strong photospheric absorption lines develop as the heating front reaches the inner disc



dwarf binaries can have carbon-oxygen and oxygen-neon-magnesium donor stars. The element abundances are crucial to understanding the evolution that leads to such stars. For instance, an evolutionary path from cataclysmic variable stars to AM CVn stars typically leaves a small amount of hydrogen (Podsiadlowski et al., 2003), whereas a route via double white dwarf mergers does not. Similarly, the ratios of the CNO elements in such stars depends upon the initial mass of the donor stars. Such information is invaluable in pinning down evolutionary pathways, and therefore to predicting the numbers of systems. These binaries are so compact that they can fit comfortably inside the Sun. At the same time their short orbital periods means that gravitational radiation is strong (such systems will be significant sources for *LISA*) and mass transfer rates can be high. As a result, they emit mostly at UV wavelengths and the UV is where photospheric lines from the disc are strongest.

4.1. Future prospectives of UV astronomy

Over the next few years many more AM CVn systems are likely to be discovered, but as they are relatively rare, the majority will be faint. As for the hydrogen-rich systems, a $R \sim 20\,000$ spectrograph covering 900 to 1700 Å is needed, with high sensitivity the key feature.

5. Accretion winds

Mass loss is an ubiquitous feature of astrophysical systems and the evidence of mass loss in disc-dominated cataclysmic variables is unambiguous. In the wavelength range acces-

sible to *IUE* ($\simeq 1150$ – 3200 Å), the existence of outflows in systems observed a lower inclination is indicated by P-Cygni-like and/or blue shifted absorption profiles in resonance transitions of N v, Si iv, and most commonly C iv. Velocity widths of 3000 – 5000 km s $^{-1}$, comparable to the escape velocity from the primary, are regularly seen, especially in C iv. The features are understood to result largely from scattering of disc photons by the outflow. At low inclinations, the process removes photons along the line of sight to the disc; emission wings arise from photons scattered into the line of sight of the observer, just as in the stellar winds of massive stars. At higher inclinations, less direct light is observed from the disc, and the resonance lines generally appear as broad emission features. Indeed, after analysing 850–1850 Å spectra of Z Cam obtained with the *Hopkins Ultraviolet Telescope* Knigge et al. (1997) suggested that virtually all of the lines in the UV spectrum of a typical high-state CV are formed in the outflow, either in the supersonic portion of the wind or in a lower velocity portion of the wind near the interface with the disc photosphere.

Although the strong 1s–2p transitions of Li-like or Na-like ions dominate the line spectra of disc-CVs observed with *IUE* and *HST*, the FUV spectra obtained with *FUSE* often show narrower features from intermediate ionisation state transitions of abundant ions such as N iii, C iii, Si iii, and Si iv. These intermediate level ionisation state lines often show orbital phase dependent effects, even in systems of intermediate inclination such as Z Cam (Hartley et al., 2005) that suggest the effects of the accretion stream must be included to complete the picture of extra-planar gas in disc-dominated systems. In RW Sex and V592 Cas, enigmatic orbital variations in the

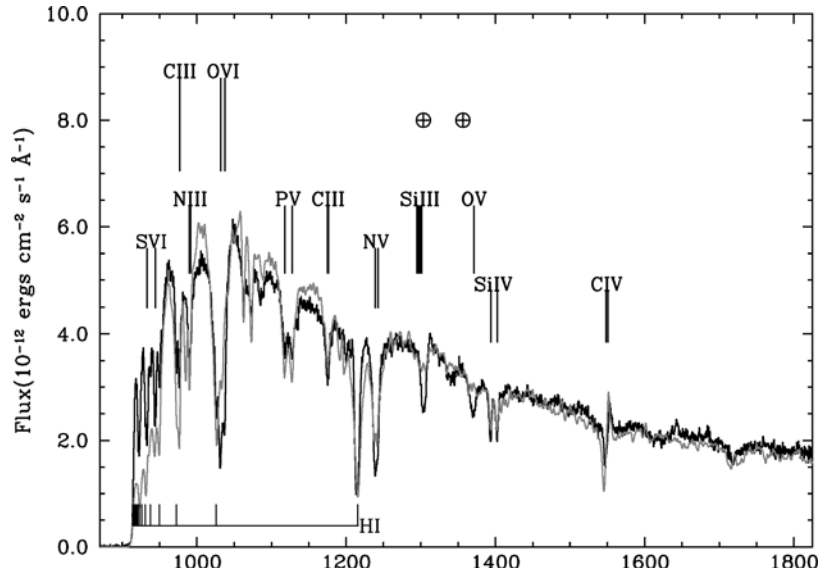
blue edges of broad C III profiles indicate departures from bi-conical symmetry in the high-velocity wind (Prinja et al., 2003, 2004). Whether these are associated with disc tilts or the accretion stream or some other mechanism is not understood. Unfortunately the number of systems in which appropriate studies have been undertaken is small, and generally speaking not intensive or lengthy enough to fully characterise the phenomenology of the effects.

Originally, the possibility that the wind was a radial wind was considered, but observations of eclipsing systems showed changes in profile shapes that are most straightforwardly interpreted as an indication of rotation, thereby indicating that the wind emanates from the inner disc (Drew, 1987). Consequently, our basic picture of the high velocity wind first observed with *IUE* is of a bi-conical flow emanating from the inner portion of the disc and/or rapidly rotating boundary layer. Vitello and Shlosman (1993) were the first to attempt to actually model the profile shapes of wind lines as observed in high state CVs in terms of kinematic prescription for a bi-conical wind. They found that the *IUE*-derived ($R = 200$) C IV profiles of three systems – RW Sex, RW Tri, and V Sge – could be reproduced with moderately collimated winds with the local mass loss rates of order 10% of the disc accretion rate and terminal velocities of 1–3 times the escape velocity at the footprint of each streamline. Subsequently, Knigge and Drew (1997) succeeded, using a somewhat different kinematic parameterisation for a bi-conical flow, in reproducing the C IV profile of UX UMa through an eclipse. This analysis was important, not only because it was the first attempt to model changes in the profile through eclipse, but also because it suggested, at least in UX UMa, the existence of a relatively dense, high column density, slowly outflowing transition region between the disc photosphere and the fast moving wind. Both the Vitello and Shlosman and Knigge

and Drew analyses suggested that the characteristic acceleration length for the high velocity winds observed in disc dominated CVs is quite long, or order $100 R_{\text{wd}}$. Most of the analyses of the spectra of disc winds were limited to single lines, but more recently Long and Knigge (2002) have developed Monte Carlo radiative transfer codes which in a few cases (see Fig. 6) are able to qualitative reproduce the full UV spectrum of a disc dominated CV. Hydrodynamical simulations of radiatively-driven CV winds are also been undertaken, and when combined with a radiative transfer code, these are also beginning to be compared to observed spectra with mixed results (see, e.g., Proga, 2003).

Although, modelling of CV winds has progressed, fundamental basic questions about the winds still remain. We are unable to measure basic parameters like the mass-loss rate, and although the wind is assumed to be radiatively driven, the observational and theoretical evidence for this is at best murky. For example, on the observational side, if the wind is radiatively driven, one might expect that the observational signatures of wind lines would be strongest when systems are brightest. But Hartley et al. (2002) found there was no correlation between the strength of wind features and continuum brightness in the spectra of three observations each of the two nova-like variables IX Vel and V3885 Sgr with *HST*. (Unfortunately, the number of high state systems that have been observed enough to begin to characterise their behaviour with time is quite limited.) And Drew and Proga (2000) have argued that the luminosity of discs is at best marginally enough to accelerate a high velocity wind. Thus, alternatives to the emission or additions to radiation pressure must be considered instead. These include viscous heating of the upper portion of the disc atmosphere (Czerny and King, 1989b), and irradiation (Czerny and King, 1989a) as well as magneto-centrifugal forces producing constant angular

Fig. 6 *HUT* spectrum of the wind dominated spectrum of IX Vel modelled compared to one of the models of Long and Knigge (2002)



velocity out to the Alven surface (Cannizzo and Pudritz, 1988).

5.1. Future prospectives of UV astronomy

As observations of high mass transfer discs and winds in CVs have improved, so has the complexity of phenomenological descriptions of the wind structures emanating from the disc, especially as the wavelength coverage has extended in the the UV. But very few systems have been studied in enough detail to isolate common from uncommon behaviour. Furthermore, it is quite clear that the appearance of disc dominated systems is strongly modified by inclination, and as a result one needs to observe a number of similar systems to the same level of detail to be able to go beyond the general variations that were observed with *IUE*. To carry out a study of this type higher sensitivity is required so that the pool of targets that can be studied is substantial and so that the observations can be made at the resolution needed to resolve the narrower lines that exist particularly in the FUV short-ward of 1200 Å.

Higher sensitivity observations are also required to obtain a better short term characterisation of the wind flow. Some systems seem to have little or no short term temporal variability, whereas others, e.g BZ Cam (Prinja et al., 2000) are highly variable. We do not know whether this is due to some fundamental difference in the systems – a magnetic white dwarf for example – or is it due simply to differences in the accretion rate. What is the role of outer disc in the creation of disc wind? Some hydrodynamical simulations show fast steady flows emanating from the inner disc, but complex time variable flows in the outer discs.

More systems need to be measured with high signal-to-noise ratio. The number of systems actually observed with *HST* were far fewer than observed with *IUE*, a fact that was partially a result of the way *IUE* was scheduled compared to *HST* and the fact that *HST* was never designed to be a dedicated UV observatory, but a multi-purpose / multi-wavelength facility. Instead the observations with *HST* have focused on a few key systems. Therefore it has been quite difficult to determine whether many of the phenomenological models proposed to explain the wind features of disc dominated features are founded on general characteristics of winds in disc dominated CVs and how many are due to individual systems.

To maximally constrain models of the wind, the wavelength coverage of a new mission should extend to the region containing O VI, and possible to the Lyman limit. Including O VI (along with N IV, Si IV, C IV, and He II) is important not only because O VI represents the next step up in the temperature space ladder, but also because the FUV below 1150 Å is rich in lines of intermediate ionisation states. These lines

establish stringent constraints on physical conditions in the region near the disc plane.

6. Black-hole binary stars

Most of the dynamically-confirmed black hole binaries are transients, which spend most of their time in a low-luminosity state. Recently there has been much debate surrounding comparison of these quiescent black holes with their neutron star analogues in the attempt to detect “direct” evidence of event horizons in the former systems. Neutron stars are brighter in X-rays, as might be expected if the black holes advect accretion energy through the event horizon. The theoretical models for low-luminosity accretion flows onto black holes, however, include variants where the flow is unbound so that much of the accretion energy may be carried away as kinetic energy of an outflow. Hence it is crucial to identify the correct theoretical model before claiming event horizons have been detected. The UV is a vital window for achieving this: almost any model can reproduce the X-ray data alone by varying the fit parameters, but simultaneously fitting the UV spectra is much more exacting while optical and infrared wavelengths are hopelessly contaminated by the donor star and outer disc. The problem is that these systems are faint in quiescence and only three quiescent UV spectra exist to date: of the black holes A 0620-00 and XTE J1118+480 and of the neutron star Cen X-4. The black hole spectra resemble each other and differ markedly from Cen X-4’s. This suggests a real physical difference, but clearly insufficient to decide definitively between models. We need to observe more systems, and obtain simultaneous X-ray and UV data.

In outburst, transients brighten by factors of ~1000 across the optical-UV-Xray spectra regions. This is attributed to the same disc instability that drives the outbursts of cataclysmic variable stars, but the black-hole binaries are complicated by (i) irradiation of the optical-UV emitting disc by the central X-ray source which changes the effective temperature distribution and causes warping of the disc, (ii) by large discs which have no global stable high-state configuration below the Eddington limit, (iii) for reasons which are not yet fully understood, the inner accretion disc is often missing, being replaced within a transition radius, R_{tr} , by an optically thin, inefficiently-radiating advective flow. These factors substantially alter the character of the sources: luminosity generation, outflows, duty cycle, and the mass accumulation by the black hole are all changed. To understand these complications, UV observations are essential: the optical is dominated by the outermost disc (which behaves more like CV discs) and by the donor stars. The UV is required to see unambiguously the signatures of irradiation in the SED, to detect self-occultation by warping, and to measure the transition radii.

6.1. Future prospectives of UV astronomy

Only a handful of black hole X-ray transient outbursts have had their SEDs monitored throughout the outburst, and their behaviour has been diverse. Transients outburst on time-scales of decades and there are many that we have yet to detect. To understand the outbursts in a systematic way, more SED monitoring, including the UV, is required. Broad wavelength coverage at low resolution and high throughput are essential for this kind of studies.

7. Star clusters as laboratories for close binary evolution

It has been known since the mid-1970s that there is a 100-fold or so overabundance of bright LMXBs in globular clusters (GCs), relative to the galactic field (e.g. Katz, 1975). This quickly led to the realization that the high stellar densities in the cores of GCs might open up entirely new *dynamical* channels for the formation of interacting close binaries. The most famous of these is tidal capture, a 2-body process resulting from a close encounter between a compact object (white dwarf or neutron star) and an “ordinary” cluster members (main sequence star or giant). During such an encounter, the latter star experiences tidal distortions. This dissipates orbital energy and can therefore lead to capture and binary formation (Fabian et al., 1975). However, interacting binaries can also be formed via 3- and 4-body interactions, i.e. processes involving existing binaries. For example, in a close encounter between a low-mass (e.g. MS/MS) binary system and a high mass (e.g. NS) single star, the most likely outcome is ejection of the lowest mass participant and formation of a NS/MS binary system (Sigurdsson and Phinney, 1993).

Interacting binaries in GCs deserve careful study for two basic reasons. First, they can in principle provide us with large, uniformly-selected samples of systems at known distances. This is precisely what is needed to test theoretical binary evolution scenarios. Second, close binaries are actually key players in controlling the late dynamical evolution of GC themselves. Thus interacting binaries can actually be used as tracers of the dynamically-formed close binary population in observational studies of GC evolution. In practice, the inevitable feedback between binary and cluster evolution will complicate things, but there is no doubt that interacting binaries in GCs can provide us with unique insights into both types of evolution.

UV astronomy has a key role to play in this area. Accreting binaries tend to have much bluer spectral energy distributions than the late-type main sequence stars that make up the bulk of stellar clusters and galaxies. This immediately implies that FUV observations should be an excellent way to find and study these populations, even in optically crowded fields, such as GC cores. This expectation is strikingly confirmed in Fig. 7, which shows FUV and U-band images of the same central regions of the GC 47 Tuc. The difference in crowding is obvious, and several CVs and new CV candidates pop up nicely in the FUV image. This image represents the deepest FUV survey of any GC carried out to date, and utilises observations obtained with STIS onboard *HST* (Knigge et al., 2002). Earlier generations of FUV/NUV detectors on *HST* have also been used to search for and study interacting binaries in GCs (e.g. Paresce et al., 1992; de Marchi et al., 1993; Ferraro and Paresce, 1993; de Marchi and Paresce, 1994, 1996; Paresce and de Marchi, 1994; Cool et al., 1995; Sosin and Cool, 1995). In the case of 47 Tuc, the lack of crowding in the FUV even makes it possible to carry out slitless, multi-object spectroscopy in the cluster core (Knigge et al., 2003; Knigge, 2004).

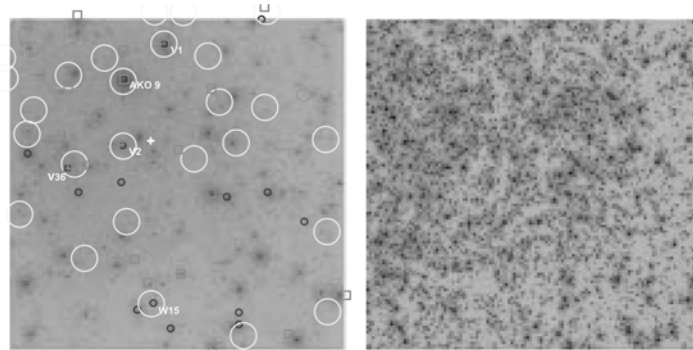


Fig. 7 *Left Panel:* A deep *HST*/STIS FUV image of the core of 47 Tuc. The image is approximately $25'' \times 25''$ in size and includes the cluster centre (marked as a white cross). For comparison, 47 Tuc’s core radius is $23''$. The positions of previously known blue objects (green squares), Chandra X-ray sources (large yellow circles) and CV candidates (small blue circles) are marked. The four confirmed CVs within the field of view are labelled with their most common designations. The

image is displayed on a logarithmic intensity scale and with limited dynamic range so as to bring out some of the fainter FUV sources. *Right Panel:* The co-added *HST*/WFPC2/F336W (roughly U-band) image of the same field. This image, too, is shown with a logarithmic intensity scale and limited dynamic range. Figure reproduced from Knigge et al. (2002) (© 2002 The American Astronomical Society)

In principle, open clusters and local group galaxies could also be used as binary evolution laboratories. However, open clusters contain fewer stars than GCs and are characterised by lower central densities. Thus interacting binaries are not as abundant in open clusters as in GCs, and the construction of a statistically interesting sample would probably have to involve studies of many such clusters. Local group galaxies obviously harbour large interacting binary population as well. However, even with a 4 m class space telescope, UV observations reaching the depths required to study the quiescent interacting binary populations will be extremely challenging for the Magellanic Clouds and probably impossible for all other local group galaxies.

7.1. Future prospectives of UV astronomy

Several additional galactic GCs have recently been imaged in the UV with *HST*, so the UV picture of their interacting binary populations will become clearer as soon as these new data sets have been analysed. However, all of these studies are seriously constrained by the small field of view of both the STIS and ACS UV detectors (roughly $30'' \times 30''$); this often makes it impossible to obtain a complete census of the interacting binary population. For example, the deep UV image of 47 Tuc in Fig. 7 covers only about 1/3 of the cluster core. GALEX will be of some use in this regard (e.g. to find sources in GC outskirts and open clusters), although the benefit of its larger field of view is partially offset by its poorer spatial resolution and lower sensitivity (relative to *HST*).

The optimal future UV imaging instrument would consist of a large (≥ 4 m) mirror feeding a large-format detector producing images with diffraction-limited spatial resolution. However, the ability to obtain spectral information is also crucial to allow secure classifications of the detected UV sources. Single-slit/single-object spectroscopy is an extremely inefficient way of obtaining this information in a cluster setting. As noted above, slitless spectroscopy may be used in special cases, but what is really needed is a more generally applicable way to carry out multi-object spectroscopy (MOS) in the UV. MOS using optical fibres is probably not an option, since fibre losses rise steeply towards short wavelengths (at least in the current generation of fibres). Configurable slit masks are probably also impractical in a space-based observatory, since their use would require a large number of delicate moving parts. A simple, low-tech solution is to provide a reasonably large selection of narrow-band filters. An intriguing high-tech solution might involve superconducting tunnel junction (STJ) detectors (e.g. Cropper et al., 2003; Verhoeve, 2002, see also Romani et al., 1999). These are able to provide an energy estimate for every photon detected, so imaging and spectroscopy could, in principle, be done in a single observation.

8. Requirements on future UV instrumentation

Here we summarise the instrumental requirements defined by the scientific goals above.

1. Low-resolution spectroscopy ($R \simeq 1000\text{--}2000$), with a wavelength coverage as large as possible. Optimum would be simultaneous data from Lyman edge down into the blue optical ($\simeq 5500 \text{ \AA}$). The first priority is the broadband coverage, and highest throughput. Continuum signal-to-noise ratio of $\simeq 10$ at flux levels of a few $10^{-16} \text{ erg cm}^{-2} \text{ s}^{-1} \text{ \AA}^{-1}$ should be achieved short exposures (10–30 min).
2. Medium-resolution spectroscopy ($R \sim 20\,000$). The “standard” wavelength range $1150\text{--}1800 \text{ \AA}$ would be adequate, covering the entire far UV down to the Lyman limit would be preferable.
3. Detectors. Both low and medium spectrographs should have photon counting detectors with absolute times accurate down to fractions of a second.
4. Large field-of-view UV imager (10 arcmin) with high spatial resolution (diffraction limited). Broad-band UV filters. Photon counting with accurate timing information. UV/optical interferometry providing sub-milliarcscale spatial resolution.

References

- Araujo-Betancor, S., Gänsicke, B.T., Long, K.S., Beuermann, K., de Martino, D., Sion, E.M., Szkody, P.: *ApJ* **622**, 589 (2005)
 Balbus, S.A., Hawley, J.F.: *Reviews of Modern Physics* **70**, 1 (1998)
 Baptista, R., Horne, K., Wade, R.A., Hubeny, I., Long, K.S., Rutten, R.G.M.: *MNRAS* **298**, 1079 (1998)
 Belle, K.E., Howell, S.B., Sion, E.M., Long, K.S., Szkody, P.: *ApJ* **587**, 373 (2003)
 Birriel, J.J., Espey, B.R., Schulte-Ladbeck, R.E.: *ApJ* **545**, 1020 (2000)
 Cannizzo, J.K., Pudritz, R.E.: *ApJ* **327**, 840 (1988)
 Cool, A.M., Grindlay, J.E., Cohn, H.N., Lugger, P.M., Slavin, S.D.: *ApJ* **439**, 695 (1995)
 Cropper, M., Barlow, M., Perryman, M.A.C., Horne, K., Bingham, R., Page, M., Guttridge, P., Smith, A., Peacock, A., Walker, D., Charles, P.: *MNRAS* **344**, 33 (2003)
 Czerny, M., King, A.R.: *MNRAS* **236**, 843 (1989a)
 Czerny, M., King, A.R.: *MNRAS* **241**, 839 (1989b)
 de Marchi, G., Paresce, F.: *A&A* **281**, L13 (1994)
 de Marchi, G., Paresce, F.: *ApJ* **467**, 658 (1996)
 de Marchi, G., Paresce, F., Ferraro, F.R.: *ApJS* **85**, 293 (1993)
 de Martino, D.: *Memorie della Societa Astronomica Italiana* **70**, 547 (1999)
 de Martino, D., Silvotti, R., Mouchet, M., Mukai, K., Buckley, D.A.H., Gänsicke, B.T. and Rosen, S.: in: Hellier, C., Mukai, K. (eds.), *Annapolis workshop on magnetic cataclysmic variables*, pp. 41–46, ASP Conf. Ser. 157 (1999)
 Di Stefano, R.: in Greiner, 1996, p. 193, Springer (1996)
 Downes, R.A., Webbink, R.F., Shara, M.M., Ritter, H., Kolb, U., Duerbeck, H.W.: *PASP* **113**, 764 (2001)
 Drew, J.E.: *MNRAS* **224**, 595 (1987)
 Drew, J.E., Proga, D.: *New Astronomy Review* **44**, 21 (2000)

The Need for Ultraviolet to Understand the Chemical Evolution of the Universe, and Cosmology

Willem Wamsteker · Jason X. Prochaska ·
Luciana Bianchi · Dieter Reimers · Nino Panagia ·
Andrew C. Fabian · Claes Fransson ·
Boris M. Shustov · Patrick Petitjean · Philipp Richter ·
Eduardo Battaner

Received: 25 May 2005 / Accepted: 31 August 2005
© Springer Science + Business Media B.V. 2006

Abstract We identify an important set of key areas where an advanced observational Ultraviolet capability would have major impact on studies of cosmology and Galaxy formation in the young Universe. Most of these are associated with the Universe at $z < 3\text{--}4$. We address the issues associated with Dark matter evidence in the local Universe and the impact of the Warm-Hot Intergalactic Medium WHIM on the local Baryon count. The motivations to make ultraviolet

W. Wamsteker[†]
INTA-LAEFF, Madrid, Spain

J.X. Prochaska (✉)
University of California, Santa Cruz, California, USA

L. Bianchi
GALEX, Space Research Lab., JHU, Baltimore, USA

D. Reimers
Remeis Sternwarte, Hamburg, Germany

N. Panagia
STScI, ESA-RSSD, Baltimore, USA

A.C. Fabian
IOA, Cambridge University, Cambridge, UK

C. Fransson
Stockholm University, Stockholm, Sweden

B.M. Shustov
INASAN, Russian Academy of Sciences, Moscow, Russia

P. Petitjean
Inst. D'Astrophys., Paris, France

P. Richter
Sternwarte, University of Bonn, Bonn, Germany

E. Battaner
Institute of Physics, University Granada, Granada Spain

(UV) studies of supernovae (SNe) are reviewed and discussed in the light of the results obtained so far by means of IUE and HST observations. It appears that UV studies of SNe can, and do lead to fundamental results not only for our understanding of the SN phenomenon, such as the kinematics and the metallicity of the ejecta, but also for exciting new findings in Cosmology, such as the tantalizing evidence for “dark energy” that seems to pervade the Universe and to dominate its energetics. The need for additional and more detailed UV observations is also considered and discussed.

Finally we show the enormous importance of the UV for abundance evolution in the Intergalactic Medium (IGM), and the importance of the He II studies to identify re-ionization epochs, which can only be done in the UV.

Keywords Ultraviolet astronomy · Chemical evolution · Cosmology · Galaxy formation · Supernovae · Intergalactic Medium

1. Introduction

Dramatic progress has been made during the past decade in the acquisition of observational evidence of the contents of our Universe at high redshift. Special mention can be made here of the coordinated efforts through the Hubble Deep Fields (HDF-N and HDF-S; Williams et al., 1996) and the associated Great Observatory Origins Deep Survey, GOODS (Giavalisco et al., 2004) multi-wavelength data collection effort. In addition to these, the results obtained from two major mapping efforts: the 2dF survey at the Anglo-Australian Telescope (Hawkins et al., 2003) and the Sloan Digital Sky Survey (SDSS; York et al., 2000), have supplied new insights in the stellar and galaxy content of the Universe, in

a redshift range extending from 0 to $z > 6$ and higher. The results on the structure of the Cosmic Background (CMB) by the Wilkinson Microwave Anisotropy Probe (WMAP) mission (Bennet et al., 2003) have, at the same time, allowed a much more detailed evaluation of the formation of structure after the first inflationary phases of Big Bang Cosmologies (Tegmark et al., 2004). However, all these efforts did not succeed to give a definite answer to the structure formation epoch, scale and evolution. These questions can not be answered from the high z side alone, because the consequences for the present state of the Universe are rather different for different cosmologies. Tegmark et al. (2004) have shown that the recent WMAP CMB studies appear to be best compatible with a Λ CDM cosmology (i.e. “vanilla type models with 6 parameters). Further new data on the small scale fluctuations and the polarization characteristics of the CMB are expected to be found by ESA’s Planck mission and from the various studies made from Antarctica.

A complete new window on the high redshift Universe can be expected to be opened up through the James Webb Space Telescope mission (JWST; NASA/ESA foreseen to be launched in 2012) and its precursor mission the Wide-Field Infrared Survey Explorer (WISE; NASA; launch in 2008), which will perform a new high sensitivity IR sky survey. Some of the infrared veils appear to be lifted by the Spitzer Space Telescope Observatory from NASA. Quite interesting results have been obtained already (e.g. Eyles et al., 2005). Further progress in this area is expected from the Herschel mission of ESA expected to be launched in 2007.

All these surveys and future missions characterize the history of star formation, the evolution of galaxy morphology and distribution in space, and in combination with the CMB data, give information on large-scale structure. These results will have a major effect on our understanding of the part of the baryonic material which has passed through the process of Galaxy and star formation in the Universe at all redshifts. There remain however some fundamental issues which can not be addressed through any of the observatories foreseen for the future either on the ground, or in space.

One needs to evaluate how the Universe evolved over its lifetime, after the first ionization phase. This requires a proper understanding of the variation in time of a number of different observables, such as abundance evolution, star formation rate changes with time, identification of possible re-ionization phases etc. All of these can only be addressed by observations of baryonic matter out to redshifts of $z \approx 3\text{--}4$.

The main questions can be summarized as follows:

1. All luminous material in the Universe has been formed from the gaseous matter in the Interstellar Matter and the Intergalactic matter, and little data are available to describe how this gas is cycled to feed star and galaxy formation.

2. Any self-consistent theory of Star Formation and Galaxy Formation will need an understanding of the Star Formation Rate (SFR) including UV data. This will allow us to incorporate the most massive and most rapidly evolving stars. They play a critical role in the recycling of matter in the Universe and are an important factor in the energy cycling in galaxies. An understanding of these processes is very important to clarify the nature and extent of “dark matter”. Similarly, the possible existence and effects of a major pressure associated with “dark energy” can be expected to be addressed through adequate observations in the UV. Due to cosmological redshift we can observe objects emitting or absorbing in FUV (at $z < \sim 2$) only with a space telescope.
3. The important task is to establish the connection between the nearby ($z < \sim 2$) Universe, covering 80% of the cosmic time and containing most of the baryonic matter, and the early Universe which is being studied in great detail at the redshifted UV wavelengths with the new generation of ground based telescopes.

From the results of observations related to the early phases (CMB and high z quasars and ultraluminous galaxies at $z > 3$) the following constituents of the Universe have been derived ($\Omega = \rho/\rho_{\text{crit}}$ with $\rho_{\text{crit}} = 3H_0/8\pi G = h^2 \times 1.88 \times 10^{-29} \text{ g/cm}^3$ and $H_0 = h \times 100 \text{ km/s Mpc}^{-1}$):

Total density of matter-energy	$\Omega = 1.02 \pm 0.02$
Dark energy density	$\Omega_\Lambda = 0.70 \pm 0.03$
Dark matter density	$\Omega_m = 0.27 \pm 0.07$
Baryonic matter density	$\Omega_b = 0.044 \pm 0.01$
Hubble constant	$h = 0.72 \pm 0.05$

Most of these parameters are referred to, and obtained from observations related to the first 3 Gyr of the Universe and therefore are based on strong assumptions and priors. For example, a major assumption underlying the quoted errors above, is the adoption of the errors associated with each prior. In particular, primordial gaussian adiabatic, scale-invariant density fluctuations are adopted. If, for example, an admixture of 30 per cent isocurvature fluctuations is included, consistency with CMB data is still obtained, but the error bars are up to an order of magnitude larger. Thus, many of these assumptions have strong affects on the above indicated constituent distribution in the Universe.

The very information on the (re)cycling of the IGM and population evolution over 90% of the lifetime of the baryonic Universe is an essential requirement for the understanding of the a physical transition from the early universe to the current epoch (14 Gyr) *in which we exist*.

One of the most direct tests of the standard big bang nucleosynthesis (SBBN) is the determination of the primordial abundances of the different light elements, especially H, D,

and ${}^4\text{He}$. The astration (destruction) of deuterium as gas is cycled through stars will then give also a strong constraint on the history of star formation (see Epstein et al., 1976). Various high redshift D/H ratios have been established through ground-based and HST observations of Lyman limit systems (and damped Ly- α systems) of QSO's with $z > 2.0$. Many attempts have been made in the recent years to establish the primordial D/H ratio. Unfortunately the values derived for D/H show a considerable spread for systems with $z_{\text{abs}} > 2$ (e.g. Pettini and Bowen, 2001). The prediction from SBBN for the ${}^4\text{He}$ abundance is $Y = 0.247 \pm 0.02$ and a present day baryon density of $\Omega_b h^2 = 0.0193 \pm 0.0014$ (Burles and Tytler, 1998), implying a surprisingly high baryon-to-photon ratio $\eta = 5.3 \pm 0.4 \times 10^{-10}$.

The interesting problem remains that FUSE observations have shown for the Local Bubble a relatively constant value For $D/H \approx 1.5 \times 10^{-5}$ while for somewhat more distant stars values extending from 7 ppm to 25 ppm are derived for D/H . It remains therefore an important challenge to find the “exact” value of Ω_b , i.e. to obtain an independent estimate amount of ordinary (baryonic) matter. The required D/H values can only be established if enough objects are used in the redshift range between 0 and 2, as that will allow to establish the validity of the astration model in the context of SBBN. A large amount of work is done in the theoretical aspects of the outstanding cosmological questions, but without good observational evidence to guide the theories for the time interval between $0 < z < 3$ -which spans 80% of the age of the Universe- no real choice can be made between the different models. Independent of the different models for the early Universe the major baryonic component of the Universe at $z < 3$ must be associated with the Inter Galactic Medium (IGM).

In the following sections we will illustrate the critical role of the UV domain to clarify the questions raised by this theoretically exciting, but observationally very unsatisfactory situation. We will evaluate the new observational capabilities needed to address the physical properties of the Intergalactic Medium (IGM) such as metallicity, dust content, ionization state, temperature. These will lead to a much improved determination of the total baryonic mass Ω_{bar} in the present day Universe and its state evolution during the expansion phase.

In this discussion we will not introduce different shades of baryonic matter such as concept of “dark baryonic matter” (Combes, 2003), but will confine ourselves to the distinction between baryonic matter and the generic term for non-baryonic matter, i.e. dark matter. The possibility for a non-zero cosmological constant is maintained conceptually as “dark energy”, but a detailed discussion of the various models which can be invoked introducing non-standard physics, is beyond the scope of this paper. As most accessible diag-

nostics for baryonic matter associated with the IGM lie in the UV for redshifts $z < 2$, new space missions will be required.

In Section 2 we will discuss the issues associated with the baryonic mass fraction Ω_{bar} . In Section 3 we will discuss the relevance of SN as probes of the Universe. In section 4 we will discuss the IGM cycling aspects and abundance issues. In section 5 the ionization state and the re-ionization epoch(s). Finally in section 6 the instrumental requirements for future instruments will be outlined. All this should be seen in the context of the results from the Galactic Evolution Explorer (GALEX; launch April 2003) which makes the first sensitive UV Sky Survey ever (Martin et al., 2005). The complete results catalogue of GALEX is expected to be ready in 2007.

2. Baryonic content of the universe (Weighing the universe)

2.1. What part of baryons do we observe?

The most direct way is to estimate relevant contributions from observations of all baryonic components. However this requires that we have identified all baryonic constituents. Even for those baryonic matter constituents we know, we can only observe part. From the mass-luminosity relation for galaxies the luminous matter density is estimated as $\Omega_{\text{lum}} h = 0.002\text{--}0.006$ i.e only up to 30% of Ω_b .

This implies that apart from the fact that a large fraction of the Universe is made up of Dark Matter and Dark Energy we do not even have a certainty about the baryons beyond 30%. The primary question to be addressed than is: where are missing baryons? (Carr, 1994). The known phases of baryonic matter are:

- **Condensed:** Stars and gas in or near galaxies; Easily observed
- **Very hot** ($10^{7\text{--}8}$ K): intracluster and intragroup gas: X-ray observations
- **Diffuse** (Warm 10^4 K) photoionized gas: Ly-alpha absorbers
- **Warm-hot:** intergalactic medium (WHIM) at $10^{5\text{--}7}$ K: Difficult to observe – highly ionized low density gas.

(C)DM is required to trigger the formation of structure after the inflationary phase in BB cosmologies. Support for the existence of DM has been found in the consistency of the Ly- α forest results with the predictions from CDM cosmologies. It must however be kept in mind that most these results have been obtained from the ground and thus are related to the distribution at $z > 2$ (i.e. where redshifted Ly- α enters the optical passbands). Only very few sightlines have been studied in the range from $0 < z < 2$. This has been

mainly caused by a lack of dedicated observing capabilities, but also by the lack of identified background UV sources. A new UV mission would, with the expected 10^5 QSO's in the GALEX catalogue, allow immediately sufficient statistics to determine both the distribution and evolution of Ly- α forest with redshift.

It has been well established that CDM is distributed in different ways throughout the Universe. While at high redshifts the DM appears to supply the separation between the individual Ly- α filamentary structures, in the massive clusters of galaxies strong gravitational lensing requires a distribution closely following the luminous matter. This would naturally lead to the idea that the DM distribution must show a strong evolution over the time from $z = 3$ to the current epoch. As the evidence in the last 10 Gyr for DM is all associated with observables in a semi-indirect way, it is clear that a firm understanding of the dominant component of the baryonic content of the Universe will have a direct and very important influence on the verification of DM evolution, and supply the, currently poorly understood, evolution of the Universe after structure formation.

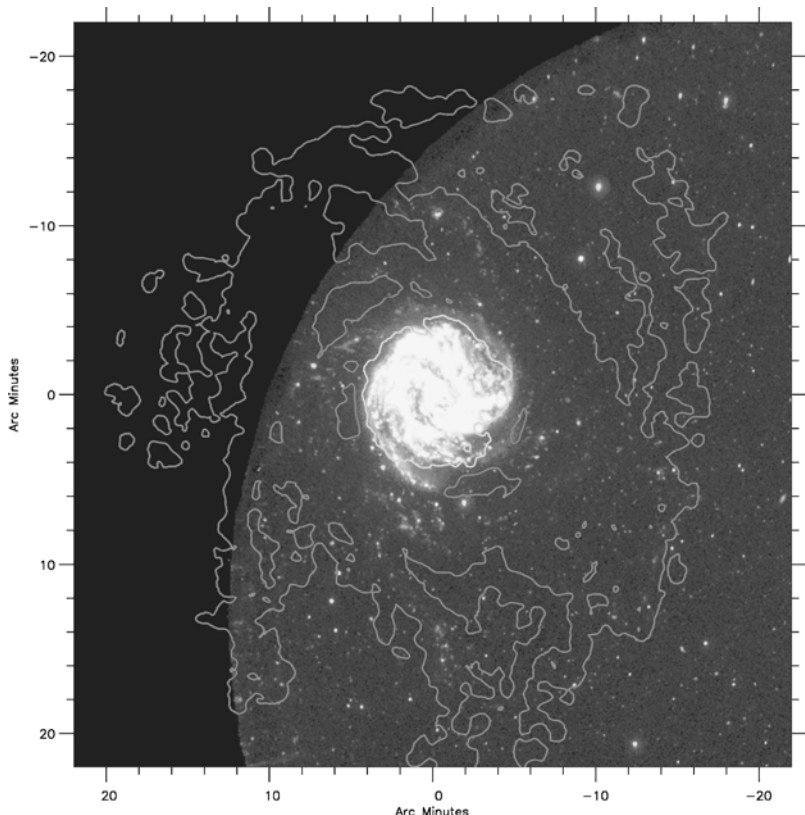
We will here only comment on the low redshift evidence for non-baryonic DM and the damped Ly- α systems (DLA). As it is uncertain that observables can be defined to identify the DM associated with Gravitational Lensing and the virial masses of large clusters, we will not discuss those further here.

Fig. 1 GALEX Color image of M83 (NGC 5236) showing star forming regions in the far outer disk extending to $R \sim 20$ Kpc from Thilker et al. (2005). This is nearly 4 times the radius where the majority of HII regions are detected. The normal size of galaxies is indicated by the contour just touching the outline of the galaxy body. The deep 21 cm contours are from Rogstad et al. (1974) and extend to a limit of $10^{21} n_{\text{HI}}/\text{cm}^2$

2.2. Damped Ly- α systems and their origin

We would like to comment on the conclusions derived from the observations of the damped Ly- α systems (DLA) and the Lyman forests. Especially the first are strongly influenced by the definitions of galaxy sizes, mainly on the basis of the very nearby galaxies as studied at optical and radio (21 cm) wavelengths. However, with the higher sensitivity supplied by the Ly- α absorption in the UV and the information on the ionization conditions supplied by the other strong UV lines (CIV, NIII, He II, NII etc.) a completely new view can be expected to be derived from the availability of a large number of background sources from the GALEX survey. Already early GALEX results on M83 (NGC 5236) have shown that the galaxy extent can be much larger than assumed in the normal DLA evaluations (Fig. 1). Also star formation may take place in much more rarified surroundings than was considered feasible till now (Thilker et al., 2005). The fact that only a limited number of galaxies can be expected to be discovered could limit the statistical value of such studies. On the other hand even a few galaxies will allow us to study the equivalent of many sightlines.

Through objects like M83, we will be able to study the environment giving rise to the DLA systems, not only through the absorption characteristics, but we will also be able to evaluate the nature of the stars formed in such rarified media, which is important for the interpretation of the DLA systems



at higher redshifts. Finally it will be possible to extend the empirical mass function of the Lyman forest to much lower surface densities than is possible by any other means. This as a consequence of the high sensitivity to relatively low densities of the Ly- α line in the UV.

2.3. Baryons in the warm-hot intergalactic medium

While the diffuse photonionized ionized intergalactic medium that gives rise to the Ly- α forest is expected to account for ~ 30 percent of the baryons at $z = 0$, the so-called Warm-Hot Intergalactic Medium (WHIM) at temperatures $T = 10^5\text{--}10^7$ K most likely contributes at a similar level to the cosmological mass density of the baryons in the local Universe, as predicted by cosmological simulations (e.g., Cen and Ostriker, 1999). The WHIM is believed to emerge from intergalactic gas that is shock-heated to high temperatures as the medium is collapsing under the action of gravity.

Directly observing this gas phase is a challenging task, as the WHIM represents a low density ($n_{\text{H}} \sim 10^{-4}\text{--}10^{-6}$ cm $^{-3}$), high-temperature ($T \sim 10^5\text{--}10^7$ K) plasma, primarily made of protons and electrons together with traces of some highly ionized heavy elements. The most promising approach to study the WHIM is the search for absorption features from the WHIM in the FUV and in the X-ray regime. Five-times ionized oxygen (OVI) currently is the most important high ion to trace the WHIM at temperatures of $T \sim 3 \times 10^5$ K in the FUV regime. Recent measurements indeed imply that intervening OVI absorbers contribute with $\Omega_{\text{bar}}(\text{OVI}) \sim 0.002$ to the cosmological mass density at $z = 0$ (e.g., Savage et al., 2002). Next to high-ion absorption from oxygen and other metals (e.g., NeVIII; Savage et al., 2005), observations with STIS (Richter et al., 2004) suggest that WHIM filaments can be detected in FUV Ly α absorption of neutral hydrogen (Fig. 2).

Although the vast majority of the hydrogen in the WHIM is ionized, a tiny fraction (typically $< 10^{-6}$) of neutral hydrogen should be present if the gas stays in collisional ionization equilibrium. Depending on the total gas column density of a WHIM absorber and its temperature, weak but broad HI Ly- α absorption at column densities $12.5 < \log N(\text{HI}) < 14.0$ may arise from WHIM filaments and can be used to trace

Fig. 2 The broad Ly- α absorber (BLA) at $z = 0.18047$ in the STIS spectrum of H1821+643 is shown (Richter et al., 2005). As clearly visible, the shape of this BLA differs significantly from the shape of the narrow $z = 0.17924$ Ly- α forest absorption near 1433.5 Å

the ionized hydrogen component. Recent STIS observations imply a mass density of the broad Ly- α absorbers (BLAs) of $\Omega_{\text{bar}}(\text{BLA}) > 0.003$. These absorbers therefore represent a significant baryon reservoir in the low-redshift Universe.

The STIS FUV measurements of the WHIM are encouraging, as they demonstrate that a large fraction of the baryons at $z = 0$ indeed is hidden in a highly-ionized, high-temperature intergalactic medium. However, to more precisely pinpoint the baryon budget of the WHIM and to explore its physical state, a FUV instrument more sensitive than STIS is required. Such a new FUV instrument would be of crucial importance

- to significantly improve the statistics of intervening OVI and broad Ly- α absorbers, and
- to achieve a higher S/N in QSO FUV absorption line data.

The latter point is particularly important to beat down the detection limit for FUV WHIM absorbers and to provide a more reliable estimate of the ionization conditions in the WHIM.

These considerations will lead to a dramatically improved determination of the baryonic content of the Universe in the range of $0 < z < 3$, and will supply new and important constraints to which cosmological theories will have to match.

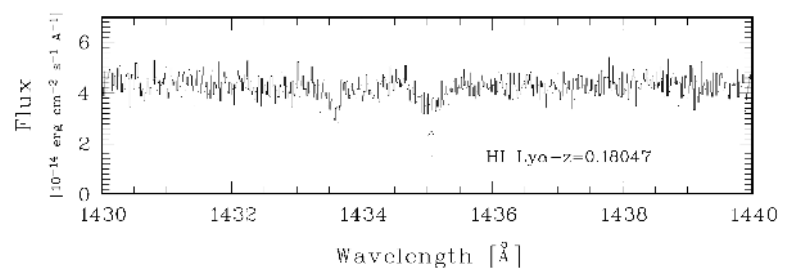
UV spectroscopic observations will be able to put strong constraints on the interpretation of the cosmological observations made of the CMB. Therefore less reliance on priors is needed for the analysis of structure formation, as derived from the data on the cosmic background.

With an improved baryonic mass content, we can expect to be able to make the connections needed for a Universe in which the CMB and other data on the early Universe can be understood in a coherent framework of physics *in which we can also exist*.

3. Ultraviolet studies of supernovae

3.1. Introduction

Supernovae (SNe) are the explosive death of massive stars and moderate mass stars in binary systems. They enrich the interstellar medium of galaxies with most heavy elements (only C and N can efficiently be produced and ejected into



the ISM by red giants winds and by planetary nebulae, as well as pre-SN massive star winds). The nuclear detonation supernovae, i.e. Type Ia SNe (SNIa; see Section 3.2.1 below) provide mostly Fe and iron-peak elements, while core collapse supernovae, i.e., Type II (SNII) and Type Ib/c (SNIb/c), mostly O and alpha-elements (see section 3.2.2 below). Through the interstellar medium (ISM) enrichment they are the primary drivers of the chemical evolution of the Universe. Additionally, SN ejecta deposit approximately 10^{51} ergs in the form of kinetic energy into the ISM of a galaxy. This compares with the total mechanical energy of a Milky Way class galaxy, which is approximately given by the product (galaxy mass) \times (rotation velocity) $^2 \sim 10^{43} \times 4 \times 10^{14} = 4 \times 10^{57}$ ergs, approximately equivalent to 4 million SN events. At a SN rate of 4 SNe/century, these explosions double the energy of a galaxy in about 100 Myrs (if there were no losses and dissipation phenomena). It is quite obvious that one can not ignore this energy input for the evolution of the entire galaxy, both dynamically and, through cloud compression/energetics, for star-formation.

SNe are bright events that can be detected and studied up to very large distances. Therefore they can be used for many different approaches to trace the evolution of the Universe. The general feasibility of these different techniques has been amply and very successfully demonstrated (e.g. Blades et al., 1988; Sonneborn et al., 1997; Gilmozzi et al., 1987) by the extensive UV observations of SN1987A with the International Ultraviolet Explorer (IUE). Ultraviolet spectroscopy is crucially important in order to:

- (1) Study the metallicity of individual SNe
- (2) Study the metallicity of the intervening ISM/IGM
- (3) Study the kinematics of the fast moving (i.e. the outermost layers) of the ejecta through the analysis of strong UV lines with P Cyg profiles
- (4) Study the overall energetics of the SN explosion at early phases (from shock breakout to optical maximum for types of SNe, but most importantly for SNII).
- (5) Study the strong emission lines produced in the interaction of the ejecta with pre-SN circumstellar material, e.g. NV1240 Å and collisionally excited CIV1550 Å, NIV] 1470 Å, OIII] 1665 Å, NIII] 1750 Å, CIII] 1909 Å, etc.

3.2. Types of supernovae

3.2.1. Nuclear Detonation Supernovae: Type Ia

Type Ia supernovae are characterized by a lack of hydrogen in their spectra at all epochs and their optical spectra are characterized by a number of broad, deep absorption bands, most notably the Si II 6355 Å feature (actually the blue-shifted absorption of the 6347–6371 Å Si II doublet; see e.g. Filippenko, 1997), which dominate their spectra at early epochs. SNIa

are found in all types of galaxies, from giant ellipticals to dwarf irregulars. However, the SNIa explosion rate, normalized relative to the galaxy luminosity (H or K band) and, thus relative to the galaxy mass, is much higher -up to a factor of 16 for the extreme cases of irregulars and ellipticals-in late type galaxies than in early type galaxies (Panagia, 2000; Mannucci et al., 2005). This suggests that, contrary to common belief, a considerable fraction of SNIa belong to a relatively young (age $\ll 1$ Gyr), moderately massive stellar population of $3.5M_{\odot} < M(\text{SNIa progenitor}) < 8M_{\odot}$, and that in present day ellipticals, SNIa are most likely the explosion in stars resulting from the capture of dwarf galaxies by massive ellipticals.

Classical Type Ia supernovae are important objects throughout many fields of astrophysics. They are believed to result from the explosion of an accreting white dwarf (WD) in a binary system. They can be used to probe the physics of thermonuclear burning in degenerate or partially degenerate matter, under conditions not achievable in the laboratory. The heavy elements they produce play a key role in the chemical evolution of galaxies, and details of the burning front influence the elemental relative abundances. SNIa are especially important because of their possible use as cosmological candles: one uses their observed light curve shape and color to standardize their luminosities.

3.2.2. Core Collapse Supernovae: Types II and Ib/c

Massive stars ($M_* > 8M_{\odot}$) end their evolution by collapsing onto their inner Fe core and producing an explosion by a gigantic bounce that launches a shock wave which propagates through the star and eventually erupts through the photosphere. In this ejection several solar masses of material are thrown into the surroundings at velocities of thousands of km/s. The current view is that single stars explode as type II supernovae, while the supernovae of types Ib and Ic originate from massive stars in interacting binary systems. Although the explosion mechanism is essentially the same in both types, the spectrum and light curve evolution are markedly different for each.

3.3. Ultraviolet observations

The launch of the International Ultraviolet Explorer (IUE) satellite in early 1978 marked the beginning of a new era for SN studies because of its capability to measure the ultraviolet emission of objects as faint as $m_B = 15$. Moreover, just around that time, other powerful astronomical instruments became available, such as the Einstein Observatory for X-rays, the VLA in the radio domain, and a number of telescopes with new and highly efficient IR instrumentation (e.g. UKIRT, IRTF, AAT and ESO). As a result a wealth of new multi-wavelength information became available in the early

1980's. The coordinating efforts of astronomers operating at widely different wavelengths, have provided us with fresh insights in the properties and the nature of supernovae of all types. Eventually, the successful launch of the Hubble Space Telescope (HST) could have opened new possibilities for the study of considerably fainter supernovae, allowing us to study SN spectra with a high accuracy and to reach beyond the local supercluster.

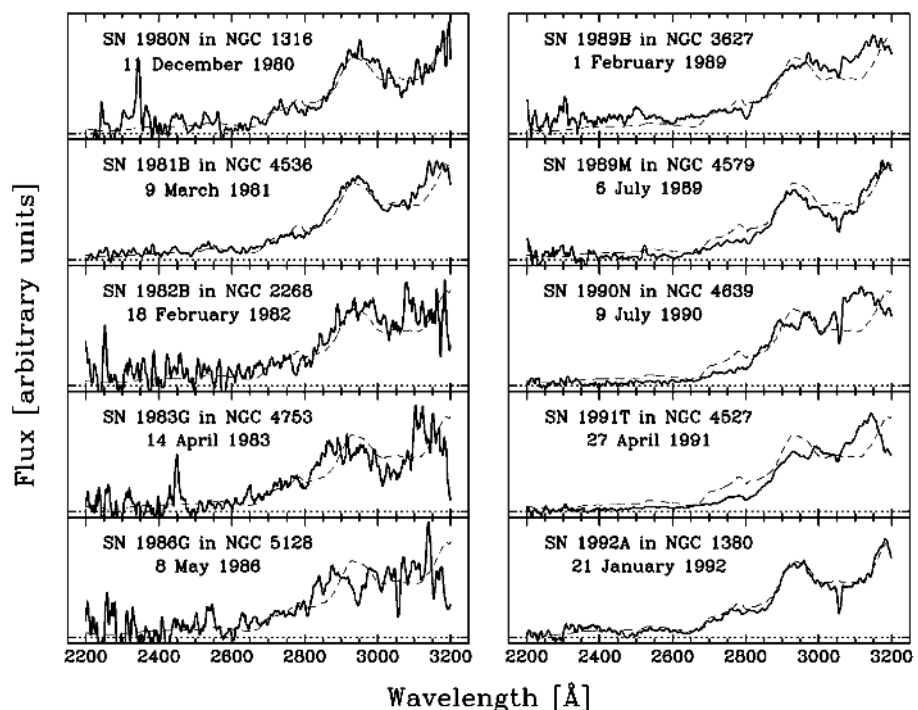
From 1979 through 1996 all bright supernovae, and a number of fainter ones have been observed with IUE. A total of 25, out of which 8 are of Type II, 12 Type Ia and 5 Type Ib/c. Of these 25 only 7 SNe (1979C, 1980K, 1981B, 1983N, 1987A, 1990N, and 1992A) were bright enough to obtain fair quality ultraviolet spectra and/or to follow their time evolution (Cappellaro, Turatto and Fernley, 1995). However even after 18 years of IUE observations and 14 years of HST observations, the number of SN events that have been studied in detail with UV spectroscopy remains quite small (no more than two objects per SN type with high quality spectra for more than three epochs). As a consequence, we still know very little about the properties and the evolution of the ultraviolet emission of SNe. On the other hand, the Ultraviolet observations of SN1987 (Pun et al., 1995) have shown that it is just the UV spectrum of a SN, especially at early epochs, that contains a wealth information that cannot be obtained at other wavelengths. A full review on the Ultraviolet observations of Supernovae can be found in Panagia (2003).

3.3.1. What we Know and Can Learn from UV Spectra of SNIa

The UV spectra of type Ia SNe decline rapidly with frequency, making them hard to detect at short wavelengths ($\lambda < 2500 \text{ \AA}$). This aspect is illustrated in Fig. 3, which displays the $\lambda > 2200 \text{ \AA}$ spectra of a sample of 10 type Ia SNe observed with IUE. In all cases, the observing epoch is within three days of the optical maximum. The spectra do not have a smooth continuum but rather consist of a number of "bands" with somewhat different strengths. The most prominent feature is the apparent emission at $\lambda \sim 2950 \text{ \AA}$ with a half-power width of $\sim 100 \text{ \AA}$, i.e. $\Delta v \sim 10^4 \text{ km/s}$. This band is likely to be the result an opacity minimum between strong absorptions on both sides i.e. Mg II centered at $\sim 2800 \text{ \AA}$ and Fe II $\sim 3060 \text{ \AA}$, each with half-power widths corresponding to the expansion velocity of $\sim 10^4 \text{ km/s}$. Several other absorption features can be recognized, which are present at all epochs of observation. Some of them are most likely associated with multiplets of Fe I, Fe II and Mg II, but the majority of these absorptions have not been unambiguously identified. The very fact that the spectra are so similar for the first three SNe in Fig. 3 and also at all epochs, is an important result. This supports the concept of homogeneity in the properties of all type Ia SNe.

On the other hand, some clear deviations from "normal" can be recognized in Fig. 3. While the UV spectra of most SNIa shown in Fig. 3 are quite similar, and virtually indistinguishable from the spectrum of SN1992A near maximum

Fig. 3 Ultraviolet spectra of a sample of Type Ia supernovae observed with IUE around maximum light. For comparison (see text) we show the spectrum of SN1992A at maximum as a dotted line



light, one notices that both SN1983G and SN1986G display excess flux around 2850 Å, and a flux deficiency around 2950 Å. This suggests that the Mg II resonance line is consistently weaker and may indicate a lower abundance of Mg in these two SNIa. They were characterized by a fast-decline and some under-luminosity. Contrary, SN1990N, SN1991T, and, possibly, SN1989M show excess flux around ~ 2750 Å and ~ 2950 Å and a clear deficit around ~ 3100 Å, possibly due to enhanced Mg II and Fe II features and showed a slow-decline and over-luminosity.

The best studied SNIa is the “normal” type Ia supernova SN1992A in the S0 galaxy NGC1380, that was observed both with IUE and HST (Kirshner et al., 1993). The FOS spectra of HST from 5 to 45 days past maximum light, are the best UV spectra available for any SNIa and reveal, with good signal to noise ratio also the spectral region at below $\lambda \approx 2650$ Å. The UV photometry taken with the FOC of HST in the F175W, F275W, and F342W bands shows light curves that resemble the SNIa template U-band light curve (Leibundgut, 1988). Using data from SN1992A and SN1990N, Kirshner et al. (1993) constructed a SNIa template light curve for the flux region near 2750 Å (Fig. 4) that is quite detailed from 14 days before maximum light to 77 days after maximum light. This light curve resembles the template U-band light curve although it drops off a bit faster.

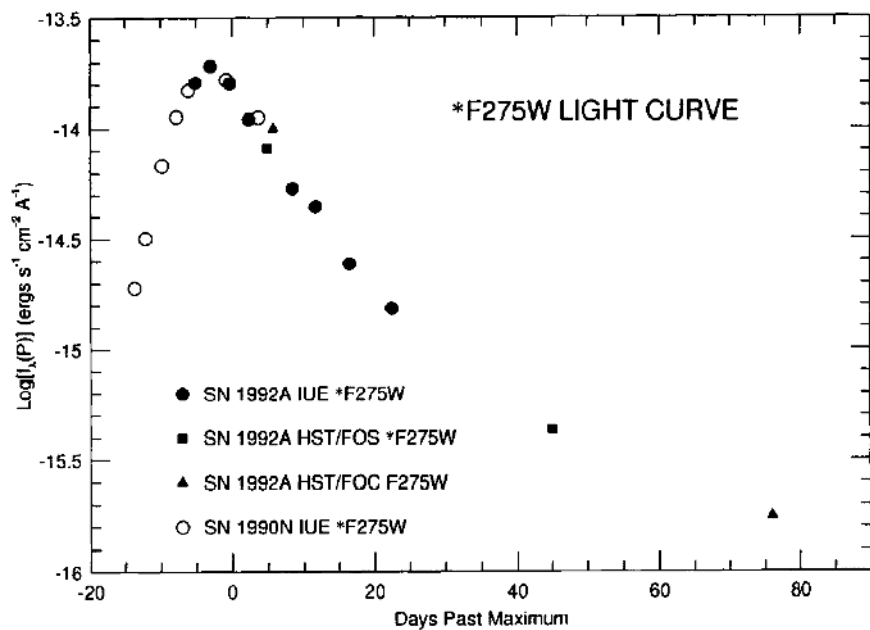
It is thus clear that type Ia supernovae are consistently weak UV emitters, and even at maximum light their UV spectra fall well below a blackbody extrapolation of their optical spectra. Broad features due to P Cygni absorption of Mg II and Fe II are present in all SNIa spectra, with remarkable similarity for normal SNIa and systematic deviations for slow-decline, over-luminous SNIa (enhanced Mg II and Fe II

absorptions) and fast-decline, under-luminous SNIa (weaker Mg II lines).

Despite the fact that SNIa are relatively weak UV emitters, obtaining UV spectroscopy of them is of fundamental importance for at least three reasons:

- (a) *Definition of the UV Luminosity/Light Curve Shape/Color Relations for Cosmological Applications:* At optical wavelengths SNIa are remarkably uniform in luminosity (0:16 mag), once corrected for the light curve shape and color. Recent work suggests the existence of a general correlation between the U-band light curve width and luminosity. Almost nothing is known, however, about SNIa behavior at space-UV wavelengths.
- (b) *The Nature of the Progenitors and Explosion Mechanisms of SNIa:* We have no idea how a white dwarf (WD) reaches the Chandra limit (e.g mass accretion from a main-sequence star, a subgiant, a red giant, or a merger with another WD), or whether it even reaches the Chandra limit, and how it explodes (off-center detonation, deflagration, or pulsed delayed detonation). Establishing the SNIa progenitor systems and explosion mechanisms are essential to a reliable use of SNIa as cosmological probes, and will allow to determine evolutionary trends from the progenitor age and its initial composition.
- (c) *Determination of the Metallicity and Other Effects in SNIa:* Given that the main dust extinction related issues surrounding high-z SNIa appear to be largely resolved possible evolutionary effects such as metallicity are now the major unresolved aspect of using SNIa as cosmological distance indicators.

Fig. 4 The light curve of SN1992A in the near ultraviolet



For cosmological studies the apparent brightness of high-z SNIa must be compared to those of low-z SNIa in order to measure accurate relative distances. Moreover, the physical understanding of SNIa, as well as techniques for standardizing SNIa and correcting for host galaxy dust extinction come from detailed observations of low-z SNIa.

Even more importantly, modern observations of high-redshift SNIa have provided evidence for a recent (past several billion years) acceleration of the expansion of the Universe, pushed by “dark energy”. If confirmed, this exciting result may require new physics (Panagia, 2005 and references therein; see also Section 1).

Thus, an efficient strategy to elucidate all relevant aspects about SNIa is:

- (a) To study the brightest, closest SNIa to make maximum progress in advancing our understanding of the physics of SNIa,
- (b) to utilize Hubble flow SNIa, where accurate relative luminosities can be determined, to search for, and constrain subtle effects that can affect precision cosmology measurements, and
- (c) to compare high-z SNIa to local Universe SNIa to determine cosmological parameters accurately and confidently.

As the UV spectra of type Ia SNe decline rapidly with frequency and time prompt, early UV observations are of paramount importance

3.3.2. Type Ib/c Supernovae

Type Ib/c supernovae (SNIb/c) are similar to SNIa in not displaying any hydrogen lines in their spectra. They are also dominated by broad P Cygni-like metal absorptions, but they lack the characteristic 6150Å trough of SNIa. The finer distinctions between SNIb and SNIc were introduced by Wheeler and Harkness (1986) and are based on the strength of He I absorption lines: the spectra of SNIb display strong He I absorptions and those of SNIc do not. SNIb/c have been found only in spiral galaxies associated with spiral arms and/or H II regions and seem associated with the evolution of massive stars in close binary systems.

The best observed SNIc is SN1994 both with IUE and with HST- FOS. The high quality UV spectra were remarkably similar to those obtained for SN1983N and were taken only at two epochs well past maximum light (10 days and 35 days). Synthetic spectra matching inferred a photospheric velocity decrease from 17, 500 to 7, 000 km/s (Millard et al., 1999). The kinetic energy carried by the ejected mass is near the canonical supernova energy of 10^{51} erg. Such velocities and kinetic energies for SN1994I are “normal” for SNe and are much lower than those found for the peculiar type Ic SN1997ef and SN1998bw (see, e.g. Branch, 2000)

which appear to have been hyper-energetic. Type Ib/c supernovae are, like type Ia, weak UV emitters with the UV much weaker than blackbody extrapolations of the optical and NIR spectra. Their typical luminosity is about a factor of 4 lower than that of SNIa, and thus the mass of ^{56}Ni synthesized in a typical SNIb/c is only $\sim 0.15 \text{ M}_\odot$.

3.3.3. Type II Supernovae

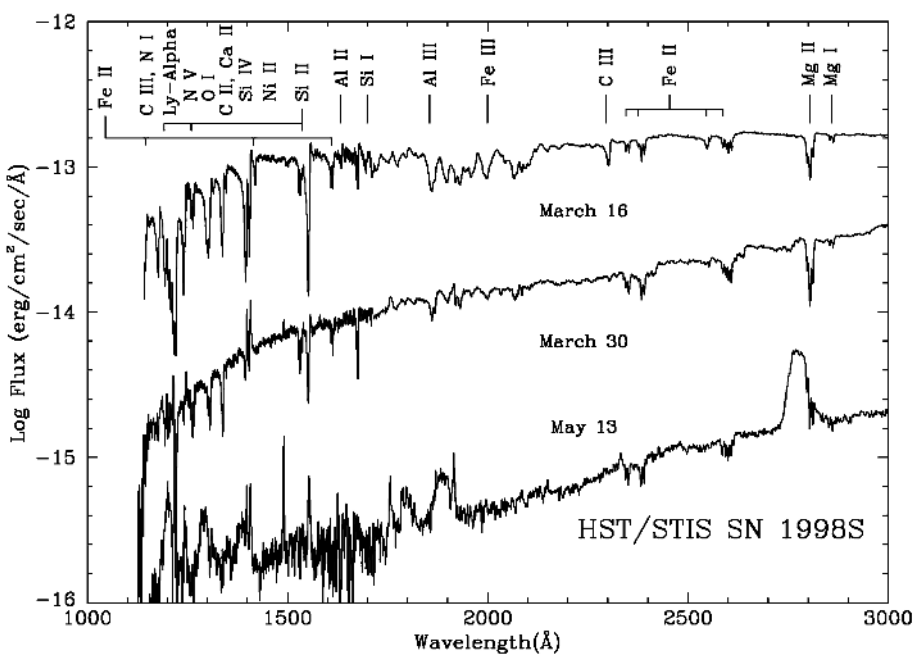
Type II supernovae display prominent hydrogen lines (Balmer series in the optical) with a strong continuum and broad P Cygni lines superimposed. SNII are considered to be the result of a core collapse of massive stars exploding at the end of their RSG phase. SN1987A was both a confirmation and an exception to this model (see Arnett et al., 1989; Panagia, 2003; Pun et al., 1995 for details on SN1987A). There are two types of SNII, the so-called “linear” type (SNIIL), which are characterized by an almost straight-line decay of the B and V-band light curves, and the more common “plateau” type (SNIIP) which display a flattening in their light curves a few weeks after maximum light.

The SNII studied best in the UV, is SN1998S, a type II with relatively narrow emission lines. SN1998S was discovered several days before maximum. The UV spectral evolution of SN1998S (Fig. 5) showed the spectrum to become gradually steeper in the UV, from near maximum light on 16 March 1998 to about two weeks past maximum on 30 March, and the blue absorptions weaken or disappear completely. About two months after maximum (13 May 1998) the continuum was much weaker, although its UV slope had not changed appreciably, and it had developed broad emission lines, the most noticeable being the Mg II doublet at about 2800 Å. This type of evolution is quite similar to that of SN1979C (Panagia et al., 1980).

Type II plateau (SNIIP) supernovae account for a large fraction of all SNII. However, the only SNIIP that has been studied in some detail in the ultraviolet is SN1999em. An analysis of the early optical and UV spectra (Baron et al., 2000) indicates that, spectroscopically, this is a normal type II. Very early spectra combined with sophisticated spectral modeling can supply an independent estimate of the total reddening of the supernova. When the spectrum is very blue, dereddening leads to changes in the blue flux that cannot be reproduced by altering the “temperature” of the emitted radiation. Thus, detailed modeling of the early spectra allows us to determine both the abundance and total extinction of SNII.

Another sub-type of the SNII family is the so-called type IIb SNe, which display strong Balmer lines early on, but later the Balmer lines weaken significantly or disappear altogether (e.g. Filippenko et al., 1997). At this point their spectra become more similar to type Ib SNe. The prototype this class is SN1993J. An HST-FOS UV spectrum of SN1993J

Fig. 5 UV spectral evolution of SN1998S (SINS project, unpublished). Shown are spectra obtained near maximum light (March 16, 1998), about two weeks past maximum (March 30, 1998), and about two months after maximum (May 13, 1998)



was obtained about 18 days after explosion, and close to maximum light. This spectrum (Jeffery et al., 1994) shows that the region between $\sim \lambda\lambda 1650\text{--}2900\text{ \AA}$ is smoother than observed for SN1987A and SN1992A and lacks strong P Cygni lines absorptions from iron peak element lines. The UV spectrum of SN1993J is appreciably fainter than observed in most SNII, thus revealing its “hybrid” nature and some resemblance to a SNIb. Synthetic spectra calculated using a parameterized LT procedure and a simple model atmosphere do not fit the UV observations. Radio observations suggest that SN1993J is embedded in a thick circumstellar medium envelope (Van Dyk et al., 1994). The UV spectra of other supernovae that are believed to have thick circumstellar envelopes also have the $\lambda\lambda 1650\text{--}2900\text{ \AA}$ regions lacking strong P Cygni absorptions. Interaction of supernova ejecta with circumstellar matter may be the origin of the smooth UV spectrum. UV observations of such supernovae provides insight in the circumstellar environment of the supernova progenitors.

Thus, despite their different characteristics in the details of the UV spectra, all type II supernovae of the various subtypes appear to provide clear evidence for the presence of a dense circumstellar medium and enhanced nitrogen abundance. They are important as background UV sources at early phases with the strong UV excess relative to a blackbody extrapolation of their optical spectra.

3.4. Cosmological applications

As mentioned before, SNIa are very good standard candles (e.g. Macchett and Panagia, 1999) to measure distances of

distant galaxies, currently up to redshift $z \approx 1$ and, considerably more in the foreseeable future. HST observations of Cepheids in the parent galaxies of SNIa have lead to very accurate determinations of their distances and the absolute magnitudes of normal SNIa at maximum light (e.g. Sandage et al., 1996; Saha et al., 2001). With these calibrations it is possible to determine the distances of much more distant SNIa. The Hubble diagram of distant SNIa ($30,000\text{ km/s} > v > 3,000\text{ km/s}$) gives a Hubble constant of $H_0 = 59 \pm 6\text{ km/s/Mpc}$ (Saha et al., 2001) while the independent HST calibration of SNIa absolute magnitudes at maximum light from Freedman, Kennicutt, Mould and collaborators (Freedman et al., 2001) gave a Hubble constant of $H_0 = 71 \pm 8\text{ km/s/Mpc}$.

Studying the more distant SNIa (i.e. $z > 0.1$) it has been possible to extend our knowledge to other cosmological parameters. These results (Perlmutter et al., 1998, 1999; Riess et al., 1998; Knop et al., 2003; Tonry et al., 2003; Riess et al., 2004) suggest a non-empty inflationary Universe, which is characterized by $\Omega_M \approx 0.3$ and $\Omega_\Lambda \approx 0.7$. Correspondingly, the age of the Universe can be bracketed within the interval 12.3–15.3 Gyrs to a 99.7% confidence level (Perlmutter et al., 1999).

However systematic uncertainties are uncomfortably large and observations of more high- z SNIa are absolutely needed. This is a challenging proposition, both for technical reasons, in that searching for SNe at high redshifts one has to make observations in the near IR (because of redshift) of increasingly faint objects (because of distance) and for more subtle scientific reasons, i.e. one has to verify that the discovered SNe are indeed SNIa and that these share the same properties as their local Universe relatives. One can only discern

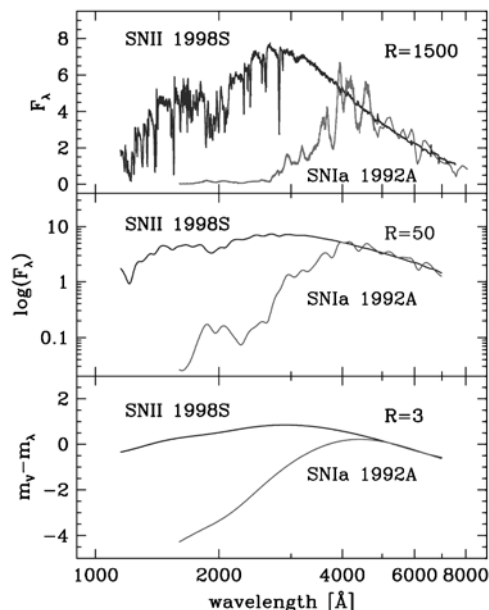


Fig. 6 Spectra of Type Ia SN1992A and Type II SNe SN1998S near maximum light, normalized so as to have the same average flux in the rest-frame V band. Upper panel: Linear flux scale, original spectral resolution $R \sim 1500$. Middle panel: Resolution degraded to $R = 50$ (low resolution spectroscopy). Lower panel: Magnitude scale ($m_\lambda = -2.5\log(F_\lambda) + \text{const}$), resolution $R = 3$ (broad-band photometry)

Type I from Type II SNe on the basis of the overall properties of their UV spectral distributions (Panagia, 2003, 2005), because Type II SNe are strong UV emitters, whereas all Type I SNe, irrespective of whether they are Ia or Ib/c, have spectra steeply declining at high frequencies, as illustrated in Fig. 6 for SNIa 1992A and SNII 1998S. Figure 6 also shows the same spectra that have been degraded to a resolution of $R = 50$ (low resolution spectroscopy), and to $R = 3$ (broad-band photometry, expressed in magnitude difference relative to the V-band; bottom panel). We see that while the characteristic spectral features are still easily recognized in the $R = 50$ spectra, the only property that in the $R = 3$ spectra distinguish a SNIa from a SNII is the UV slope. This technique of recognizing SNIa from their steep UV spectral slope was first suggested by Panagia (2003), and has been successfully applied by Riess et al. (2004a,b).

4. The state, abundances and distribution of the IGM at $0 < z < 3$

4.1. HI and metal-enrichment

Damped Ly- α systems derive their name from the observed quantum mechanical damping of the Ly- α transition relating to their very large HI column density N(HI). Because the Ly- α profile is dominated by this damping, a standard fit to the observed profile has two free parameters: (i) the centroid or

z_{abs} ; and (ii) N(HI). Therefore, accurate measures of N(HI) can be acquired with modest resolution and S/N data. and his collaborators initiated surveys for these galaxies 20 years ago (e.g., Wolfe et al., 1986; Storrie-Lombardi and Wolfe, 2000) and the majority of research has been performed on 4 m-class telescopes. The principal results from these HI surveys are: the cosmic evolution of Ω_{DLA} , the universal mass density of neutral gas in units of the critical density. The uncertainties in the each of the data sets obtained with IUE and HST are very large and there exists a stark disagreement between the central values of the two surveys. The uncertainties emphasize the current challenge of studying HI gas at $z < 2$ with existing UV spectrographs. While HST/COS would enable a modest survey of DLA at $z < 0.6$, the parameter space $z = 0.6–1.7$ will require a next generation space telescope simply to survey Ly- α .

Aside from the HI content, the most basic measure of the DLA is metallicity. Because of the large HI surface density of DLA, ionization corrections are generally small (e.g. Vladilo et al., 2001) and measurements of low-ions like Fe^+ , Si^+ , and Zn^+ yield accurate measures of the metallicity, i.e., $[\text{Zn}/\text{H}] \sim [\text{Zn}^+/\text{H}^0]$. The only serious systematic error is dust depletion; refractory elements like Fe and Si might be depleted from the gas-phase such that Si^+/H^0 and Fe^+/H^0 are lower limits to the true metallicity. In general, the depletion levels of the DLA are small (Pettini et al., 1997; Prochaska and Wolfe, 2002) and the basic picture is well revealed by any of these elements at high z . Metallicity observations of a large sample of DLA present two main results: (1) an N(HI)-weighted mean $\langle Z \rangle$, which is the cosmic mean metallicity of neutral gas; and (2) metallicities for a set of galaxies which presumably span a large range of mass, morphology, and luminosity.

Figure 7 presents over 50 metallicity measurements from $z \sim 2–4.5$ (Prochaska and Wolfe, 2002). The principal results are: (1) the mean metallicity (weighted or unweighted) is significantly sub-solar; (2) there is little evolution in the mean metallicity over this redshift range with the possible exception of a modest decrease at $z > 3.5$; (3) no galaxy exhibits a metallicity lower than 1/1000 solar. These optical observations constrain models of chemical evolution at these epochs (e.g., Pei et al., 1999) and give the first glimpse into metal production in the early universe. It is crucial, however, to press to lower redshift. The time encompassed by the redshift interval $2 < z < 4.5$ pales in comparison with $z < 2$. Of immediate concern is to determine how the mean metallicity rises to the enrichment level observed today.

4.2. Relative abundances: Dust and nucleosynthesis

High resolution ($R > 30000$), high S/N (> 30 per resolution element), observations of the damped Ly α systems enable detailed studies of nucleosynthetic enrichment and dust properties in the early universe. This level of data quality is crucial

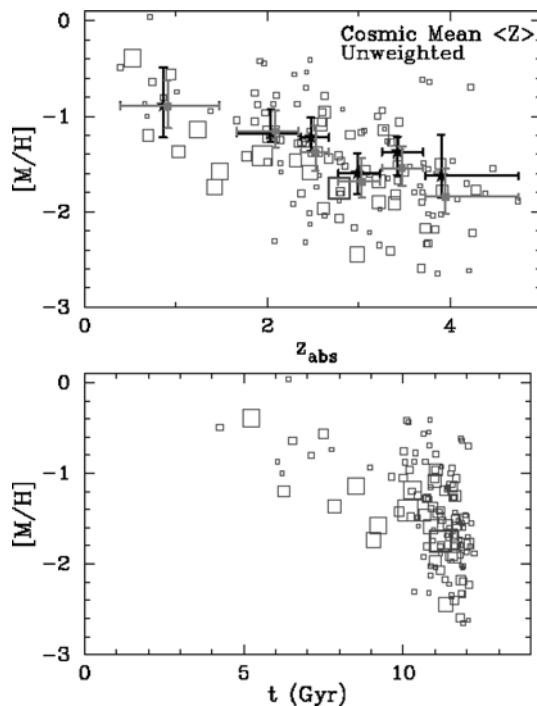


Fig. 7 The upper panel shows metallicity measurements versus redshift for some 100 DLA. Overplotted are the HI-weighted and unweighted means in several redshift bins. The lower panel presents the same measurements against cosmic time. It is clear that the cosmic enrichment history of the universe is severely undersampled over the past 10 Gyr

to achieving the better than 10% precision required by relative abundance studies. Currently, there is an entire ‘cottage industry’ focused on this area (Lu et al., 1996; Prochaska and Wolfe, 1999; Molaro et al., 2000; Pettini et al., 2000; Ledoux et al., 2002). Figure 8 presents two of the principal results from these efforts: (a) [Si/Fe] and (b) [N/α] measurements against [Si/H] metallicity.

The super-solar Si/Fe ratios presented in panel (a) highlight the greatest obstacle to interpreting relative abundance measurements from gas-phase abundances: the competing effects of nucleosynthetic enrichment and differential depletion. In terms of dust depletion, one observes Si/Fe enhancements in depleted gas owing to the differential depletion of these two refractory elements. Regarding nucleosynthesis, Si/Fe enhancements suggest Type II SN nucleosynthesis (e.g., Woosley and Weaver, 1995), whereas solar ratios would imply Type Ia SN enrichment patterns. Currently, we interpret the plateau of Si/Fe values at low metallicity as the primary result of nucleosynthesis. The mean enhancement matches the Galactic halo-star observations at the same metallicity (e.g., McWilliam, 1997) and it would be difficult to understand why differential depletion would imply such a uniform enhancement. In contrast, the rise in Si/Fe at $[Si/H] > -1$ is highly suggestive of differential depletion. One expects a decrease in Si/Fe from nucleosynthesis at higher metallicity due to the increasing contribution from

Type Ia SN. Furthermore, larger depletion levels are expected at higher metallicity. Investigating evolution in abundance ratios like these at $z < 2$ would reveal the detailed enrichment history of galaxies and the evolution of dust formation.

Overcoming this dust/nucleosynthesis degeneracy is among the most active areas of DLA research. One avenue is to focus on special pairs of elements which are largely non-refractory. Panel (b) is an excellent example of this; plotted are N/α pairs from recent compilations by Prochaska et al. (2002), Pettini et al. (2002) and Centurión et al. (1998). For N, S, and Si (the latter two are α-elements), depletion effects are small and the results show the nucleosynthetic history of N in the DLA. For comparison, we also plot [N/α], [α/H] pairs for $z \sim 0$ HII regions and stars (see Henry et al., 2000). The majority of DLA observations fall along the locus of local measurements, in particular the plateau of N/α values at $[Si/H] < -1$. In contrast, a sub-sample of low metallicity DLA exhibit much lower N/α values which Prochaska et al. (2002) interpret these in terms of a truncated or top-heavy initial mass function (IMF). These observations have important implications for the processes of star formation in the early universe and measurements at $z < 2$ would assess the timescale of star formation in these galaxies and further elucidate the nucleosynthesis of nitrogen.

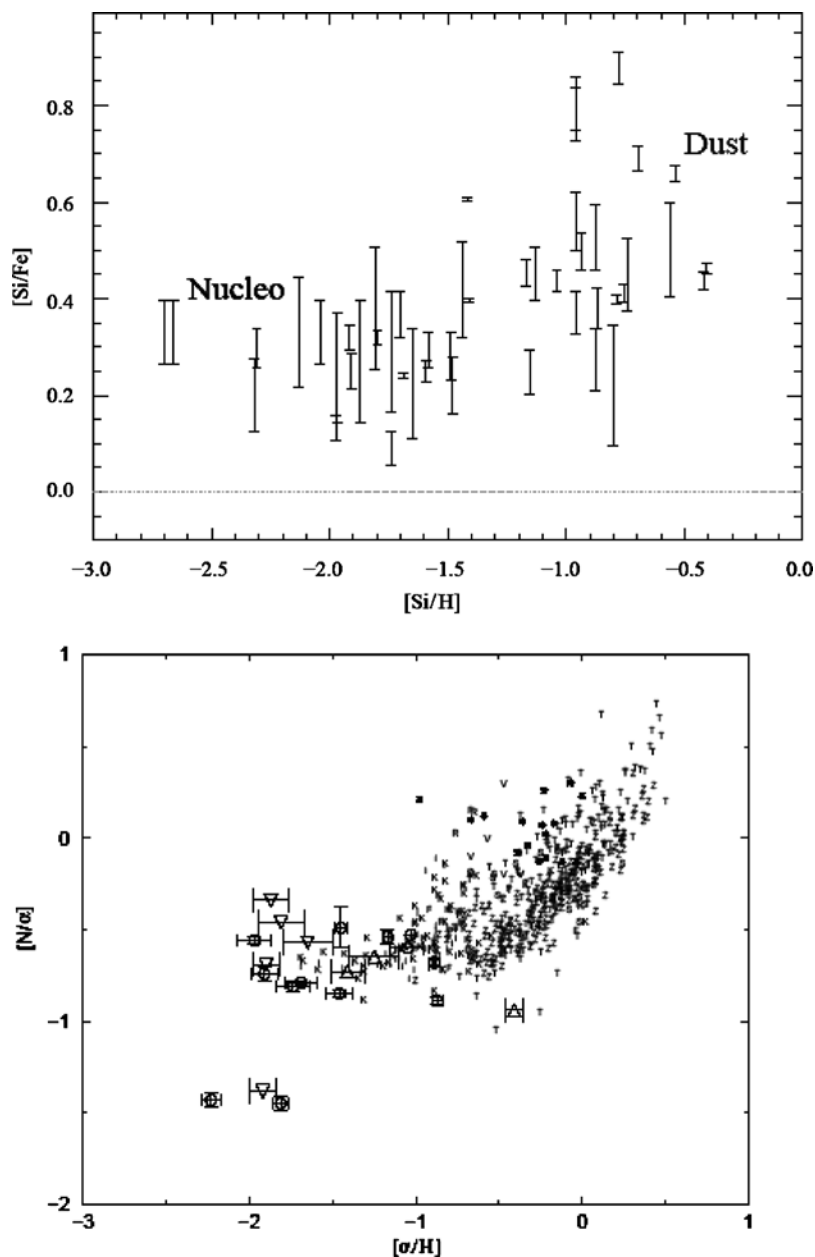
Finally, we wish to emphasize that a subset of DLA (<15%) exhibit very strong metal absorption (Prochaska et al., 2003). These metal-strong DLA allow the measurement of over 20 elements in a single galaxy including B, Fe, Ge, Pb, and Sn. At low redshift, the incidence of metal-strong DLA is presumably higher as the mean metallicity approaches the solar value. Furthermore, confusion with the Ly- α forest is minimized and high precision measurements of transitions with $\lambda_{rest} < 1200 \text{ \AA}$ are possible. This analysis would require high S/N, high resolution observations, yet the impact on studies of nucleosynthesis is extremely impressive.

5. HeII in the intergalactic medium

When the first generation of massive stars had been formed, the up to then cold and dark universe was ionized and heated (epoch of reionization). This happened at redshifts $z > 6$. After the reionization epoch, completely ionized intergalactic Hydrogen gives rise to the so called Ly- α forest. Spectroscopic observations of the Ly- α forest confirm the general theoretical picture of an intergalactic medium as a fluctuating distribution of baryons organized by the cosmic web of dark matter and photoionized by high-redshift starburst galaxies and later also by QSOs.

Observations of the HeII 304 Å Lyman α line in the line of sight of a handful of bright QSOs have added to this picture that HeII is reionized much later at redshift $z = 2.9$ (Reimers et al., 1997, 2005). This delayed reionization of HeII

Fig. 8 Relative abundances of (a) Si/Fe and (b) N/ α versus Si/H and α /H where α refers to either Si or S for the DLA. The upper panel highlights the competing effect of nucleosynthesis and dust depletion in interpreting the gas-phase abundances. We interpret the plateau of [Si/Fe] at $[\text{Si}/\text{H}] < -1.5$ as the result of nucleosynthesis in Type II Supernovae. The rise in Si/Fe at $[\text{Si}/\text{H}] > -1$ is associated with differential depletion (Prochaska and Wolfe, 2002). UV observations would allow one to trace these two processes at $z < 2$. The lower panel compares DLA (circles and triangles; the latter are upper/lower limits) against N/ α measurements for HII regions and stars at $z \approx 0$ (Prochaska et al., 2002; Henry et al., 2000). Although the majority of the DLA lie on a N/ α plateau associated with metal-poor HII regions, a significant sub-sample is identified at $N/\alpha < -1$. This sub-sample could present evidence for a truncated or top-heavy IMF (Prochaska et al., 2002). Observations of N/ α at $z < 2$ would be able to confirm this result



compared to HI had been predicted by theoreticians as caused by the later appearance of AGN (only their hard, nonthermal radiation can ionize HeII) compared to stars and by the 5–6 times higher HeIII recombination rate. The apparent 1.4 Gyr lag between HI and HeII reionization carries information on the relative beginnings of galaxy (stars) and AGN formation. Its quantitative understanding will pin down the first epoch of star formation, independent of direct detection methods.

The HeII Ly- α forest has been observed and spectroscopically resolved in the line of sight of two bright QSOs with FUSE (Kriss et al., 2001; Reimers et al., 2004). The earlier finding of a transition from continuous optically thick HeII 304 Å absorption for $z > 2.9$ (HeII Gunn-Peterson trough) to a resolved HeII Ly α forest at $z < 2.9$ has been confirmed,

i.e. the epoch of HeII reionization is in fact around $z = 3$. For $z < 2.9$, the resolved HeII 304 Å forest lines are observed to be generally much stronger than the HI Ly α forest by the factor $\eta = N(\text{HeII})/N(\text{HI})$. The factor η depends mainly on the ratio of the intensities of the ionizing radiation at the Lyman edge to the HeII 228 Å edge $J(911 \text{ Å})/J(228 \text{ Å})$ and is roughly 80. However, its value and correspondingly the shape of the ionizing radiation field appears to vary strongly between $\eta \sim 1$ and 400 on the scale of 1.3 Mpc h^{-1} , much smaller than the typical mean distances between AGN at $z = 3$ of roughly 30 Mpc (Shull et al., 2004). If these fluctuations are real, this would have considerable implications for elemental abundances in the diffuse IGM. Part of the fluctuations can possibly be explained by a combination of the

large range of EUV spectral shapes of AGN with additional filtering (softening) by absorption through the IGM.

Future observations of the HeII 304 Å forest at high spectral resolution and S/N have the potential to map both the Intergalactic Matter and Radiation Field in very much detail. At first, since the Ly- α forest “clouds” have kinetic temperatures of $\sim 10^4$ K, the lines are largely thermally broadened (with an additional turbulent/expansion component). This means that from a comparison of line widths of HI with HeII (the thermal widths of HeII lines are 2 times smaller) the kinetic temperature of the Ly- α forest gas can be measured directly with high spatial resolution. From theoretical modelling of the IGM we know that after reionization, the IGM cools by expansion, is reheated by the delayed HeII reionization at $z=3$ and continues to cool with decreasing redshift z . Observations of the HeII Ly- α forest over the redshift range $2.1 \leq z \leq 2.9$ will test this in the most direct way. Besides observing the evolution of the mean IGM temperature, we will observe its fluctuations and the latter’s relation to the fluctuating radiation field. Both IGM temperature, density and the ionizing background radiation field can be measured at a spatial resolution of less than 1 Mpc (co-moving).

Having measured these quantities, the existing theoretical models of the IGM can be tested with much more detail than possible today, when basically only the statistical properties of theoretical Ly- α forests are compared with observations.

Due to the possibility to observe simultaneously HI and HeII spectroscopically, the redshift range $2.1 \leq z \leq 2.9$ covers the only cosmic epoch where the IGM and its evolution can be studied in detail. As such, this is a test bed for theoretical modelling of the IGM. If successful, it can be applied to the epoch $1 \leq z \leq 2$ where the major star formation takes place. By-products will be improved determinations of the cosmic baryon density (at $z = 3$ more than 95% of the baryons are not in stars). Studies of the distribution of galaxies close to the lines of sight of QSO’s with HeII forest observations will allow to study the influence of galactic winds, SN explosions as well as UV radiation of starburst galaxies and AGN on the temperature and density of the IGM.

For $z < 2.1$ information on the shape of the ionizing background will never be available from HeII/HI due to absorption by interstellar HI in our galaxy. This means that the composition of most of the baryonic matter in the universe for $z < 2.1$ will be difficult to measure. On one hand, DLAs where abundance studies are easy contain only of the order of 5% of the baryonic component. On the other hand, the determination of the composition of the remaining 95%, the diffuse highly ionized component, requires knowledge of the shape of the ionizing background. Therefore, the only way to study heavy element abundances and the physical state of this component is to observe simultaneously several ionization stages of abundant elements, e.g. OIII-OVI, CIII, CIV, SIII-SVI, NeIII-NeVII, with the aim to model the ion-

izing UV background radiation field and the physical status in absorption systems. Except a few single ions like SiIV, CIV, and OVI observable from the ground and which are not sufficient to determine the state of ionization, all relevant lines are in the intrinsic EUV at rest wavelengths between 300 and 900 Angstroms. Consequently, quantitative information on the bulk of baryons in the diffuse IGM for $z < 2$ is only available by UV spectroscopy of QSO’s in the satellite UV. In fact, most of the mentioned ions have been observed in the UV in a few bright QSO’s like HS 1700+6416 with the Hubble Space Telescope (Reimers et al., 1992).

6. Instrumentation roadmap for the cosmological questions

We will here try to give first approach to the instrumental requirements needed to address the questions which have been raised in Sections 2–5. As the roadmap concept pursued under NUVA is solely related to the UV, we will only address globally the needs and requirements. As the most developed technique for UV astrophysics are spectroscopy and quantitative imaging (i.e. photometry), we will confine ourselves to these two. And since the only way to make UV observations is from space, The options are limited to those associated with a *telescope in space*.

Independently of the technique – photometry or spectroscopy- the requirements space can essentially be split into two different groups distinguished by some very primary technical constraints and a major difference in cost. The fundamental difference of the two approaches is in the size of the associated telescopes. One can essentially separate this in two major classes:

1. The 2-m class and
2. The 6-m class.

One can then try to establish the reachable goals for each of these and evaluate the importance of each of these through the net effect of being able to go to fainter flux levels. Although the possibility exists with the larger telescopes to obtain higher resolution this will require a major technology development programme.

Examples for each of these two classes have been discussed on various occasions in the scientific literature and at various workshops (e.g. Wamsteker and Shustov, 2004 for the 2-m class and Shull, 2003 for the >4-m class). In practice there are not very many differences in the type requirements for the instrumentation. The main difference in capabilities between the two classes is given by the about 10-fold increase in sensitivity between group 1 and group 2. A second also important difference is the cost. A rough estimate of the cost ratio of the two classes is a factor of 5, in the sense that the cost for a 6-m class mission is at least 5 times the

cost of a 2-m class mission. This is mainly associated with technology developments which are required before a high quality UV telescope with a diameter larger than 4 m can be expected to be successfully launched. Therefore there is a clear need for a roadmap in the UV, since otherwise no coherent planning and technology development will be implemented in the expectation that at some stage the results of this are sufficient that a major (6-m class) UV mission can be realistically considered.

Taking the position that a, in the UV, diffraction limited 6-m telescope will allow the range over which objects can be studied to be some ten times more distant, the science questions to be addressed with a 2-m class are very similar at the current stage of knowledge.

Although the requirements for the various subject areas considered in this paper are not completely identical the restraining properties of the instrumentation on a UV space telescope can be summarized as follows:

- a resolution $R \sim 1000$ is recommended for spectroscopic studies of SN ejecta.
- For ISM studies, a resolution $R > 50,000$, and possibly as high as $R \sim 100,000$ is recommendable.

Wavelength coverage. For the majority of QAL research, coverage from Ly- α (1215 Å) to 2000 Å rest-frame is essential. One of the problems associated with the wavelength coverage in the UV is that in the FUV (i.e. $\lambda < 1200$ Å) completely different technology is required than for the longer wavelengths. Many projects (e.g. D/H measurements, photo-ionization assessment, H₂ observations) need coverage down to 900 Å rest-frame. Therefore we are not only considering a single instrument but the full package of science described here would need an instrument which covers both the far UV and the near UV domain with associated increase in complexity and cost.

Resolution to examine the DLA or perform QAL studies in general is dependent on the specific research area. Nevertheless, we can lean on our extensive experience with high z QAL studies with optical spectrographs from the ground. For the majority of scientific applications $R = 30,000$ is a bare minimum. Only at this resolution can one confidently distinguish Ly- α clouds from metal lines in the Ly- α forest, obtain abundance measurements to greater than 0.1 dex precisions, resolve velocity fields, and investigate a multi-phase medium.

S/N, a good lower limit is 30 per resolution element (i.e. S/N=15 pix⁻¹ for 4 pixel sampling). At such level, one can carefully address systematic effects like continuum placement and analyze the absorption line diagnostics with a large dynamic range (e.g. Si II 1808, C IV 1550, O VI 1030). As is obvious, higher S/N is desirable and many applications would depend on higher sensitivity.

Observing power. To allow observations of a large enough sample for QSO's at $Z < 2$, a UV telescope must achieve the above resolution, S/N, and wavelength coverage for a QSO at $V \approx 18$ in a reasonable exposure time (< 10 h = 36 Ksec). This would provide enough targets to examine the physical conditions at similar levels as achieved at $z > 2$.

References

- Arnett, W.D., Bahcall, J.N., Kirshner, R.P., Woosley, S.E.: ARA&Ap **27**, 629 (1989)
- Baron, E., et al.: ApJ **545**, 444 (2000)
- Bennet, C.L., et al.: ApJ Suppl. Ser. **148**, 1 (2003)
- Blades, J.C., Wheatley, J.M., Panagia, N., Grewing, M., Pettini, M., Wamsteker, W.: ApJ **332**, L75 (1988)
- Branch, D.: in Livio, M., Panagia, N., Sahu, K. (eds.), The largest explosions since the big bang: Supernovae and gamma ray bursts, Cambridge University Press, Cambridge, p. 96 (2000)
- Burles, S., Tytler, D.: ApJ **499**, 699 (1998)
- Cappellaro, E., Turatto, M., Fernley, J.: ESA SP-1189, IUE-ULDA Guide No. 6, Supernovae, Ed. W. Wamsteker (1995)
- Carr, B.: ARA&A **32**, 531 (1994)
- Cen, R., Ostriker, J.: ApJ **514**, 1 (1999)
- Centurión, M., Bonifacio, P., Molinaro, P., Vladilo, G.: ApJ **509**, 620 (1998)
- Combes, F.: New Astr. Review **46**, 755 (2003)
- Epstein, R.I., Lattimer, J.M., Schramm, D.N.: Nature **268**, 198 (1976)
- Eyles, L.P., et al.: MNRAS, Mon. Not. Roy. Astron. Soc. **364**, 443–454 (2005)
- Filippenko A.: ARA&A **35**, 309 (1997)
- Freedman, W.L., et al.: ApJ **553**, 47 (2001)
- Giavalisco, M., et al.: ApJ **600**, L93 (2004)
- Gilmozzi, R., et al.: Nature **328**, 318 (1987)
- Hawkins, E., et al.: MNRAS **346**, 78 (2003)
- Henry, R.B.C., Edmunds, M.G., Köppen, J.: ApJ **541**, 660 (2000)
- Jeffery, D.J., et al.: ApJ **421**, L27 (1994)
- Kirshner, R.P., et al.: ApJ **415**, 589 (1993)
- Knop, R.D., et al.: ApJ **598**, 102 (2003)
- Kriss, G.A., Shull, J.M., Oegerle, W., et al.: Science **293**, 1112 (2001)
- Ledoux, C., Bergeron, J., Petitjean, P.: A&A **396**, 429 (2002)
- Leibundgut, B.: PhD Thesis, University of Basel (1988)
- Lu, L.-M., et al.: ApJ. Suppl.Ser. **107**, 475 (1996)
- Mannucci F. et al.: A&A, in press [astro-ph/0411450] (2005)
- Martin, D., et al.: ApJ **619**, L1 (2005)
- Millard, J., et al.: ApJ **527**, 746 (1999)
- McWilliam, A.: ARAAp **35**, 503 (1997)
- Molaro, P., et al.: ApJ **541**, 54 (2000)
- Panagia, N.: in Weiler, K.W. (ed.), Supernovae and Gamma-Ray Bursters, Springer-Verlag, Berlin, pp. 113–144 (2003)
- Panagia, N.: in Calamai, G., Mazzoni, M., Stanga, R., Vetrano, F. (eds.), Experimental Physics of Gravitational Waves, World Scientific, Singapore, p. 107 (2000)
- Panagia, N.: in Giovannelli, F., Mannocchi, G. (eds.), Frontier Objects in Astrophysics and Particle Physics, It. Phys. Soc., in press [astro-ph/0502247] (2005)
- Panagia N. et al.: MNRAS **192**, 861 (1980)
- Pei, Y.C., Fall, S.M., Hauser, M.G.: ApJ **522**, 604 (1999)
- Perlmutter S. et al.: Nature **391**, 51 (1998)
- Perlmutter S. et al.: ApJ **517**, 565 (1999)
- Pettini M., Bowen, D.V.: ApJ **560**, 41 (2001)
- Pettini, M., Ellison, S.L., Bergeron, J., Petitjean, P.: A&A **391**, 21 (2002)
- Pettini, M., Ellison, S.L., Steidel, C.C., Shapely, A.L., Bowen, D.V.: ApJ **532**, 65 (2000)

- Prochaska, J.X., Wolfe, A.M.: *ApJS* **121**, 369 (1999)
- Prochaska, J.X., Wolfe, A.M.: *ApJ* **566**, 68 (2002)
- Prochaska, J.X., Henry, R.B.C., O'Meara, J.M., Tytler, D., Wolfe, A.M., Kirkman, D., Lubin, D., Suzuki, N.: *PASP* **114**, 933 (2002)
- Prochaska, J.X., Howk, J.C., Wolfe, A.M.: *Nature* **423**, 57 (2003)
- Pun, C.S.J., et al.: *ApJ. Supp.Ser.* **99**, 223 (1995)
- Reimers, D., Fechner, C., Kriss, G.A., Shull, J.M. et al.: Proceed. FUSE Conf. Victoria, [astro-ph/0410588v1] (2004)
- Reimers, D., Vogel, S., Hagen, H.-J. et al.: *Nature* **360**, 561 (1992)
- Reimers, D., Fechner, C., Hagen, H.-J., Jakobsen, P., Tytler, D. and Kirkman, D.: *A&A*, in press [astro-ph/0507178] (2005)
- Richter, P., Savage, B.D., Tripp, T.M., Sembach, K.R.: *ApJS* **153**, 165 (2004)
- Riess A.G. et al.: *AJ* **116**, 1009 (1998)
- Riess A.G. et al.: *ApJ* **600**, L163 (2004a)
- Riess A.G. et al.: *ApJ* **607**, 665 (2004b)
- Rogstad, D.H., Lockart, I.A., Wright, M.C.H.: *ApJ* **193**, 309 (1974)
- Saha, A., Sandage, A., Tammann, G.A., Dolphin, A.E., Christensen, J., Panagia, N., Macchetto, F.D.: *ApJ* **562**, 314 (2001)
- Sandage, A., Saha, G.A., Tammann, L., Labhardt, N., Panagia, F.D., Macchetto: *ApJ* **460**, L15 (1996)
- Savage, B.D., Sembach, K.R., Tripp, T.M., Richter, P.: *ApJ* **564**, 631 (2002)
- Savage, B.D., Lehner, N., Wakker, B.P., Sembach, K.R., Tripp, T.M.: astro-ph 0503051 (2005)
- Shull, J.M.: in Sembach, K.R., Blades, J.C., Illingworth, G.D., Kennicutt, R.C. (eds.), *Hubble's Science Legacy; Future Optical – Ultraviolet Astronomy from Space*, ASP Conf series Vol. 291, p. 17 (2003)
- Sonneborn, G., et al.: *ApJ* **477**, 848 (1997)
- Storrie-Lombardi, L.J., Wolfe, A.M.: *ApJ* **543**, 552 (2000)
- Tegmark, M., et al.: *ApJ* **606**, 702 (2004)
- Thilker, et al.: *ApJ* **619**, L79 (2005)
- Tonry, J.L.: *ApJ* **594**, 1 (2003)
- Van Dyk, S., et al.: *ApJ* **432**, L115 (1994)
- Vladilo, G., Centurión, M., Bonifacio, P., Howk, J.C.: *ApJ* **557**, 1007 (2001)
- Wheeler, J.C., Harkness R.P.: in *Galaxy Distances and Deviations from Universal Expansion* (1986)
- Wamsteker, W., Shustov, B.M., in: Wamsteker, W., Albrecht, R., Haubold, H.J. (eds.), *Developing Basic Space Science Worldwide*, Kluwer Acad. Publ., p. 373 (2004)
- Williams, R.E., et al.: *AJ* **112**, 1335 (1996)
- Wolfe, A.M. et al.: *ApJS* **61**, 249 (1986)
- Woosley, S.E., Weaver, T.A.: *ApJS* **101**, 181 (1995)
- York, D., et al.: *AJ* **120**, 1579 (2000)

Starbursts at Space Ultraviolet Wavelengths

Rosa M. González Delgado

Received: 8 July 2005 / Accepted: 2 December 2005
© Springer Science + Business Media B.V. 2006

Abstract Starbursts are systems with very high star formation rate per unit area. They are the preferred place where massive stars form; the main source of thermal and mechanical heating in the interstellar medium, and the factory where the heavy elements form. Thus, starbursts play an important role in the origin and evolution of galaxies. The similarities between the physical properties of local starbursts and high- z star-forming galaxies, highlight the cosmological relevance of starbursts. On the other hand, nearby starbursts are laboratories where to study violent star formation processes and their interaction with the interstellar and intergalactic media, in detail and deeply. Starbursts are bright at ultraviolet (UV) wavelengths, as they are in the far-infrared, due to the ‘picket-fence’ interstellar dust distribution. After the pioneering IUE program, high spatial and spectral resolution UV observations of local starburst galaxies, mainly taken with HST and FUSE, have made relevant contributions to the following issues:

- *The determination of the initial mass function (IMF)* in violent star forming systems in low and high metallicity environments, and in dense (e.g. in stellar clusters) and diffuse environments: A Salpeter IMF with high-mass stars constrains well the UV properties.
- *The modes of star formation*: Starburst clusters are an important mode of star formation. Super-stellar clusters have properties similar to globular clusters.
- *The role of starbursts in AGN*: Nuclear starbursts can dominate the UV light in Seyfert 2 galaxies, having bolometric

luminosities similar to the estimated bolometric luminosities of the obscured AGN.

- *The interaction between massive stars and the interstellar and intergalactic media*: Outflows in cold, warm and coronal phases leave their imprints on the UV interstellar lines. Outflows of a few hundred km s^{-1} are ubiquitous phenomena in starbursts. These metal-rich outflows and the ionizing radiation can travel to the halo of galaxies and reach the intergalactic medium.
- *The contribution of starbursts to the reionization of the universe*: In the local universe, the fraction of ionizing photons that escape from galaxies and reach the intergalactic medium is of a few percent. However, in high- z star-forming galaxies, the results are more controversial.

Despite the very significant progress over the past two decades in our understanding of the starburst phenomenon through the study of the physical processes revealed at satellite UV wavelengths, there are important problems that still need to be solved. High-spatial resolution UV observations of nearby starbursts are crucial to further progress in understanding the violent star formation processes in galaxies, the interaction between the stellar clusters and the interstellar medium, and the variation of the IMF. High-spatial resolution spectra are also needed to isolate the light from the center to the disk in UV luminous galaxies at $z = 0.1\text{--}0.3$ found by GALEX. Thus, a new UV mission furnished with an intermediate spectral resolution long-slit spectrograph with high spatial resolution and high UV sensitivity is required to further progress in the study of starburst galaxies and their impact on the evolution of galaxies.

R.M. González Delgado
Instituto de Astrofísica de Andalucía (CSIC), Apdo. 3004, 18080
Granada, Spain

Keywords UV astronomy · Starburst galaxies · Galaxy evolution

1. Introduction

1.1. Starburst galaxies: Definition and general properties

Starbursts are a very significant component of the universe. They are the preferred place for the formation of massive stars, and hence they are a relevant energy source that drives the cosmic evolution of galaxies. Heckman (1998) finds that in the local universe, within 10 Mpc, the four most luminous starburst galaxies (M82, NGC 253, NGC 4945, M83) account for about 25% of the recent star formation rate in this volume. Massive stars have a significant impact on the evolution of galaxies. They are responsible for the thermal and mechanical heating of the interstellar medium. They are the factory where most of the heavy elements form; which are dispersed throughout the interstellar medium when massive stars explode as supernovae. From this enriched gas, new stars will form.

Starburst galaxies are systems with a high star formation rate. However, this rate can be sustained for much less than a Hubble time, because the gas reservoir in a galaxy may only last for a few 10^8 yr (the gas consumption time). Starbursts have a significant large population of massive stars that are able to produce large numbers of Lyman continuum photons to ionize the interstellar medium. When the gas cools down, hydrogen Balmer and other recombination lines form with intensities that can exceed 10^{39} erg s $^{-1}$. A fraction of the Lyman continuum photons are, however, absorbed by dust grains and their energy is re-emitted at far-infrared wavelengths.

Starburst galaxies are mainly selected on the basis of their strong continuum at ultraviolet (UV) wavelengths (defined here simply as the range 900 Å–3300 Å), their nebular optical emission lines, and/or strong far-infrared radiation. Due to these selection criteria, starbursts constitute a mixed type of star-forming systems, which include:

- Giant-extragalactic HII regions, such as 30 Doradus in the Large Magellanic Cloud, which is considered by Walborn (1991) as a Rosetta Stone. These star-forming regions are regarded as ministarbursts.
- Starburst dwarf galaxies, such as IZw 18. They have blue colors and an optical HII region spectrum, but with signs of an underlying stellar population older (a few 10^8 yr to 1 Gyr) than the ionizing population. They include HII galaxies (Terlevich et al., 1991), blue compact galaxies, and blue irregular galaxies, such as NGC 1569.
- Nuclear starbursts, such as the prototype NGC 7714 (Weedman et al., 1981). They have a strong UV continuum, and strong optical emission lines. Their hosts are spiral galaxies. Balzano (1983) found that about 40% of

the Markarian galaxies can be classified as nuclear starbursts.

- Very luminous infrared galaxies. The IRAS satellite has discovered many of these galaxies. They have far-infrared luminosities larger than $10^{11} L_\odot$. In most of these galaxies, the far-infrared flux is thermal emission by dust grains heated by massive stars. A typical very luminous far-infrared starburst is NGC 1640.
- Lyman break galaxies (LBG). They are star-forming galaxies at cosmological distances ($z \geq 2$) (Steidel et al., 1996; Williams et al., 1996) that provide a significant fraction of the global star formation rate of the universe (Madau et al., 1996). LBG show a strong rest-UV continuum with absorption lines very similar to those of local UV-bright starburst galaxies (Meurer et al., 1997; González Delgado et al., 1998a; Heckman et al., 2005). The most famous LBG is MS1512-cB58 at $z = 2.7276$, known simply as cB58.

Terlevich (1997) proposed to distinguish between starburst galaxy and starburst region. The former is when the galaxy luminosity is totally provided by the starburst, while in a starburst region, the starburst luminosity is substantial but smaller than the galaxy luminosity. So, starbursts may simply be defined as compact ($10\text{--}10^3$ pc) sites of recent star formation ($10^6\text{--}10^8$ yr), that often show dust obscuration.

In the conference ‘Starbursts – From 30 Doradus to Lyman break galaxies’ (de Grijs and González Delgado, 2005), Heckman (2005) has argued against the gas consumption time definition of starburst, proposing an alternative definition. The inverse of the consumption time, b , is related to the birth-rate parameter; b is the ratio between the current and the past average star formation. This parameter varies significantly and systematically with the properties of the galaxy, and leads to a steep decline in the fraction of starbursts with increasing galaxy mass, and a strong redshift dependence. For this reason, Heckman proposes a more physically meaningful definition, which is based on the star formation intensity. Starbursts are defined as systems that have a star formation rate per unit area which is much larger than that in the disks of normal galaxies. Nearby starbursts have star formation intensities ranging from 1 to $100 M_\odot \text{ yr}^{-1} \text{ kpc}^{-2}$, and similar values are found for LBG (Meurer et al., 1997).

The Galaxy Evolution Explorer (GALEX) satellite (Martin et al., 2005) has already made a significant contribution to establish the physical properties of starburst galaxies. Two categories of local ($0.1 \leq z \leq 0.3$) UV luminous galaxies (UVLG) have been found (Heckman et al., 2005). The main differences arise from the different UV luminosity per unit area, i.e., the variation in the star formation intensity. The large UVLG ($I_{\text{FUV}} \leq 10^8 L_\odot \text{ kpc}^{-2}$) are not starburst galaxies. They are massive, late-type disk galaxies that

have star formation rates sufficient to build their stellar mass in a Hubble time. In contrast, compact UVLG, which can clearly be classified as local starbursts, are low-mass galaxies ($M_{\text{star}} \sim 10^{10} M_{\odot}$) with half-light radii less than a few kpc. They have large enough star formation rates to build the present galaxy in $\sim 1\text{--}2$ Gyr.

1.2. The relevance of space UV observations of starburst galaxies

UV observations of starbursts are relevant because:

- This range is very sensitive to the star formation history. In fact, the UV energy distribution shows a strong evolution from very young to intermediate age (~ 1 Gyr) stellar populations.
- The UV light allows a direct detection of massive stars, thus, it provides a direct measurement of the star formation rate.
- UV wavelengths contain valuable tracers of the cold and molecular phases of the interstellar medium, and are an important probe of the ionized interstellar medium in starburst galaxies. Low and high-ionization absorption lines allow us to study the interaction of the starburst with the interstellar medium in an ample range of physical (density and temperature) conditions.

We owe much of our understanding of the starburst phenomenon to the International Ultraviolet Explorer (IUE) which provided the first UV (1200–3300 Å) spectra of star-

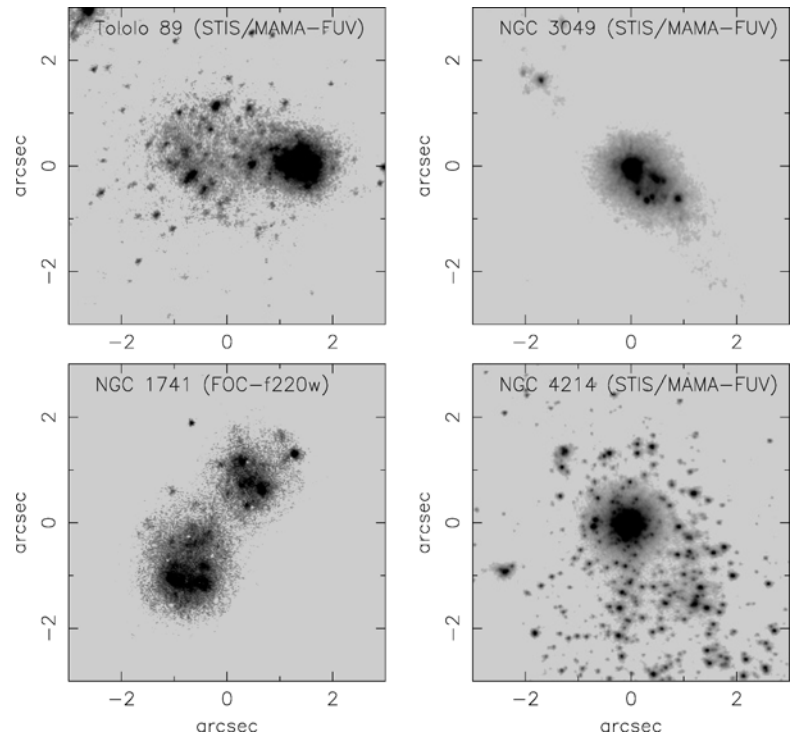
burst galaxies (Kinney et al., 1993); the Hubble Space Telescope (HST), for its impact with UV high spatial resolution images and spectra of starbursts (Meurer' et al., 1995; Leitherer et al., 1996); the Hopkins Ultraviolet Telescope (HUT) and FUSE for collecting spectra of starbursts below Ly α , down to the Lyman limit (Leitherer et al., 1995b). The impact of the GALEX mission has just started (see the first results in ApJL, volume 619), but there is no doubt about its important contribution to our understanding of the cosmic evolution of galaxies and, in particular, of starbursts.

Along this paper, we discuss the relevance of high spatial and spectral resolution observations of starbursts at space UV wavelengths and their impact on the following issues: the stellar content of starbursts, the interaction of massive stars with the interstellar medium, the relation between starburst clusters and the formation of globular clusters, the role of starbursts in AGN, and the contribution of starbursts to the reionization of the universe.

2. UV imaging morphology

HST has been the first telescope to provide UV high spatial resolution images of nearby starbursts. FOC, WFPC2, STIS and ACS/HR on board HST have been able to dissect the anatomy of nearby starbursts with a spatial sampling better than 0.025 arcsec/pixel (Fig. 1). Other instruments, on board UIT, FOCA and now GALEX, are quite useful to study the general UV morphology of galaxies at intermediate resolution (e.g. Bianchi et al., 2005) and

Fig. 1 UV images of starburst galaxies taken with HST+FOC (NGC 1741), and HST+STIS/MAMA (NGC 4214, NGC 3049 and Tololo 89) with a spatial sampling of 0.014 and 0.0244 arcsec, respectively; 1 arcsec corresponds to 260 pc (NGC 1741), 25 pc (NGC 4214), 80 pc (NGC 3049) and 100 pc (NGC 3049). Clusters and diffuse extended emission are detected.



to map the extended outflows in starbursts (Hoopes et al., 2005), but they have much less spatial resolution than HST.

In a pioneer work, Meurer et al. (1995) obtained HST/FOC images (at 2200 Å with a spatial sampling of 0.014 arcsec/pixel) of a sample of 9 starbursts, selected for their high UV flux in the IUE aperture (Kinney et al., 1993). All galaxies show an irregular UV morphology, but they reveal two important structural characteristics: compact knots embedded in a diffuse UV background.

Compact knots are marginally resolved stellar clusters and provide about 25% of the total UV emission. These clusters are distributed irregularly over the UV background, but the brightest ones are located in the center of the starburst. Their UV absolute magnitude ranges from –19 to –10, and their sizes are less than 10 pc. Their masses, estimated from the UV luminosity, range from 10^4 to $10^7 M_{\odot}$. These knots have ages of a few Myr to ~ 100 Myr, and they may be formed in bursts. The brightest knots are named super-stellar clusters (SSCs). The luminosity function (LF) of the stellar clusters follows a power law, $dN/dL \sim L^{-\alpha}$, with index $1.5 \leq \alpha \leq 2$, similar to that found in merger systems observed at optical wavelengths (Whitmore et al., 1993). Meurer (1995) argues that SSCs have properties similar to globular clusters if fading and a spread of the star formation time is taken into account.

The UV diffuse emission accounts for about 75% of the total UV flux from the starburst. It extends about a few 100 pc. Several origins have been proposed: (a) Continuous star formation (csf) lasting for a few 100 Myr; originally, the stars form in clusters over the last few 100 Myr, but clusters dissolve with age and disperse across the field. (b) The UV radiation originates in dusty compact stellar clusters, but it is scattered by dust to the field. (c) Individual massive stars, unresolved even at the HST spatial resolution. Long-slit UV

spectra of starbursts taken with STIS point to the csf origin, so that the UV field light is created via dissipation of aging star clusters (Tremonti et al., 2001; Chandar et al., 2005).

3. UV spectral morphology

Starbursts are recognized at optical wavelengths by their nebular emission line spectrum. In contrast, in the UV, starbursts show a continuum filled with absorption lines (Figs. 2 and 3). This spectral dichotomy is caused in part by the massive stars that power the starburst. Massive stars emit photons with energies of several eV that are absorbed and re-emitted in their stellar winds, producing ultraviolet resonance transitions. However, stellar winds are optically thin to most high energy (≥ 13.6 eV) ultraviolet photons, that can travel tens of parsecs from the star before they are absorbed and photoionize the surrounding interstellar medium. Subsequently, this ionized gas cools down via an emission spectrum. Beside the stellar wind origin, absorption lines can also form in the photosphere of massive stars, and in the interstellar medium. The wind and the interstellar absorption lines are resonant transitions. Usually, low-ionization lines have an interstellar origin, but high-excitation lines can be wind lines with some interstellar contribution.

The most important characteristics of these lines are described below, and labeled in Figs. 2 and 3.

– *Photospheric:* These lines form in layers that are in hydrostatic equilibrium. Mainly from C, N, O, S, Si and Fe ions of low and high-excitation potential, they originate from excited levels, so they are not resonant transitions, and thus not contaminated by interstellar components. Although much weaker, they are not too much affected by stellar wind lines. These lines are useful to constrain the age of the starburst, but also the metallicity (de Mello

Fig. 2 UV spectra of starburst galaxies taken with HST+STIS/MAMA (NGC 3049 and Tololo 89) and HST+GHRS (NGC 7714). Some of the most relevant photospheric (full line), wind (dotted) and interstellar lines (dashed) are labeled. The spectra correspond to the main cluster only (see Fig. 1).

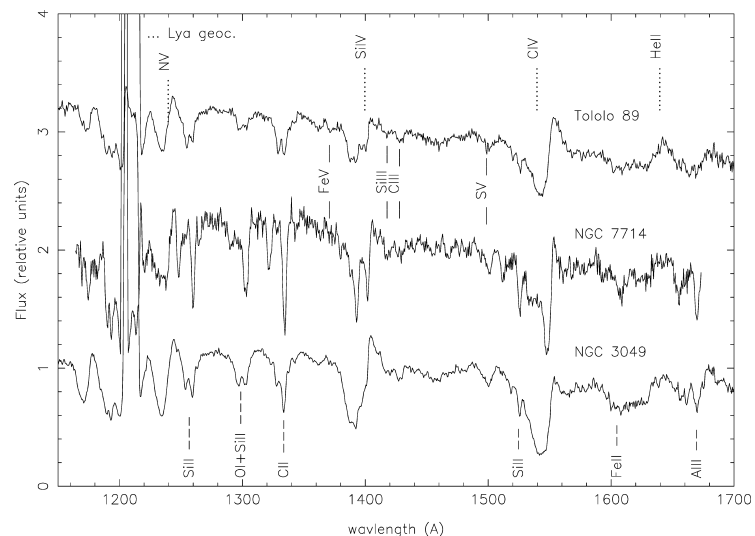
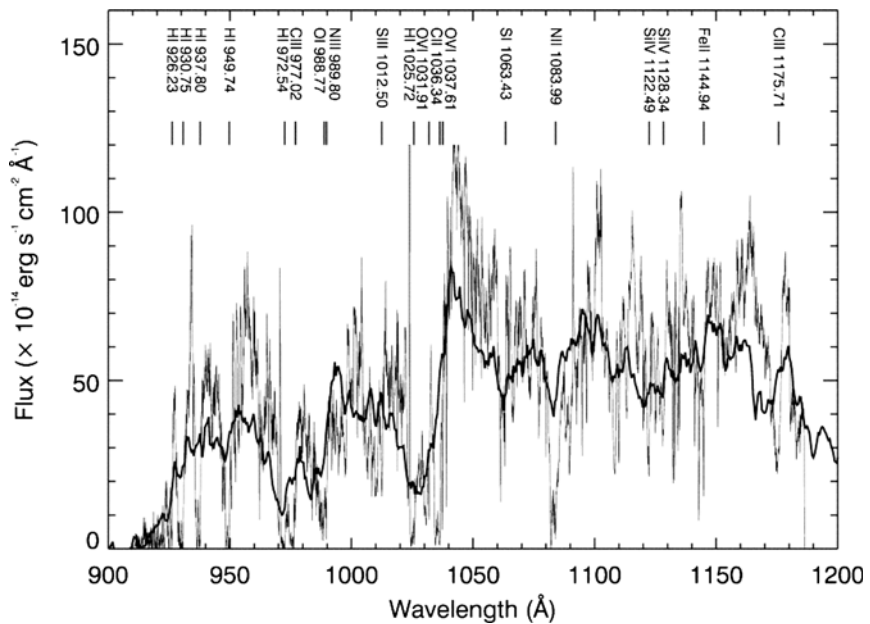


Fig. 3 FUV spectra of M83 taken with FUSE (thin line) and HUT (thick line). The main lines are labeled. (Figure adapted from Leitherer et al., 2002)



et al., 2000; Robert et al., 2003). In particular, blends of these lines in the ranges 1360–1380 Å and 1415–1435 Å show a strong dependence with metallicity (Leitherer et al., 2001). Rix et al. (2004) find also that the FeIII (1935–2020) index is a strong metallicity indicator. Some of the most relevant of these lines in starburst are: SV λ 1502, CIII λ 1426–1428 and CIII λ 1176.

– *Wind*: Hot stars develop strong wind stellar lines due to the radiation pressure in ultraviolet resonance lines. As a result, all the strong ultraviolet lines show a blueshifted absorption (about 2000–3000 km s $^{-1}$) or a P Cygni profile. The shape of the profile reflects the stellar mass-loss rate, which is related to the stellar luminosity, and thus to the stellar mass. Therefore, the shape of the line profiles in the UV integrated light of a stellar population is related to its content in massive stars. Thus, these features can be used to constrain the properties (such as age, and the slope and upper mass limit of the IMF) of the starburst. But due to the dependence of the mass-loss rate with the metallicity (Maeder & Conti 1994), wind lines are also strongly affected by metallicity. The most relevant wind lines in starburst are: NV λ 1240, SiIV λ 1400, CIV λ 1550, and HeII λ 1640.

– *Interstellar*: Low ionization lines are very useful to study the kinematics of the ionized gas because the interstellar component usually dominates over the stellar contribution in starbursts (González Delgado et al., 1998a). They are also useful to derive the metallicity of the gas (e.g. Pettini et al., 2000; Savaglio et al., 2004). The high ionization interstellar lines are blended with the wind lines, and a careful separation between both components is necessary. However, when the starburst is young (2–8 Myr), wind lines dominate over the interstellar ones.

In addition, the UV spectra of starbursts may show the Lyman series in emission or absorption. In particular the two strongest lines, Ly α and Ly β are very useful to study the interaction of the starburst with the interstellar medium. These lines may be in emission, if they are from the starburst HII region; but they may be in absorption due to the interstellar medium within the starburst. Photospheric components may also contribute to these lines. Ly α and Ly β are weak in very hot stars but they increase with decreasing effective temperature (Valls-Gabaud, 1993; González Delgado et al., 1997). Section 6 below is devoted to explain the relevance of Ly α in starburst galaxies.

4. Dust opacity in starbursts

The most direct way to measure the star formation rate in starbursts is through the UV luminosity. Unfortunately, starbursts are often dusty, and the presence of dust affects significantly the UV emission. The UV is more affected by extinction than any other wavelength. So, objects that are optically thin at visible wavelengths may be optically thick in the UV. Dust absorbs a fraction of the UV photons and reradiates in the far-infrared. Analyzing a sample of UV selected local galaxies observed with GALEX, Buat et al. (2005) have found that only 33% of the UV emission escapes from the galaxies and the remaining 66% is absorbed by dust and reradiated in the far-infrared.

Using IUE spectra of a variety of starburst galaxies (blue compact, starburst nuclei, also some luminous infrared galaxies, etc.), Calzetti et al. (1996) found that the UV spectral energy distribution is well parametrized by a power-law, $F \propto \lambda^\beta$, and the spectral slope of the continuum, β , correlates

with the nebular optical extinction derived using the Balmer decrement. On the other hand, from population synthesis models, Leitherer and Heckman (1995a) found that starbursts have an intrinsic spectral slope that changes very little with the initial mass function (IMF) or the age of the starburst, taking values around -2.3 . Then, according with these results, any deviation of the spectral slope from the intrinsic value can be interpreted as a reddening effect. This provides a nice recipe to correct the UV observed emission for extinction, and to find an effective attenuation law to perform the extinction correction (Calzetti 1997).

Gordon et al. (1997) built a model of the stars and dust distribution in a starburst, and concluded that the grey starburst extinction law is compatible with a clumpy shell geometry, with the UV radiation from the starburst viewed filtered through the dusty gas clouds (see also Charlot and Fall 2000). This distribution explains why the ionized gas extinction (derived using the Balmer decrement) is a factor of two higher than the stellar extinction (derived from the UV slope) in starbursts, because the emission lines are seen through a larger column of dust than the UV continuum (Fanelli et al., 1988).

Meurer et al. (1997) show that β correlates with the ratio of the far-infrared to UV fluxes, $L_{\text{IR}}/L_{\text{UV}}$. The straightforward interpretation of these results is that dusty starbursts absorb a large fraction of the UV radiation, that is subsequently reradiated in the far-infrared. This is an energy balance relationship, that allows us to recover the UV radiation without a detailed understanding of the dust grain properties or the extinction law. Following in the same line, Heckman et al. (1998) found that at low-metallicity, starbursts have blue colors and a significant fraction of the UV radiation escapes from the starburst. But at solar metallicity starbursts have redder UV colors. They have $L_{\text{IR}}/L_{\text{UV}} \geq 10$, indicating that only less than 10% of the intrinsic UV luminosity escapes from the starburst. These results imply that dustier starbursts are more frequent in more metal-rich galaxies. Note also, that the galaxies with higher star formation rate are, by the simple principle of causality, the most massive ones. Due to the mass-metallicity relation, they are the dustiest ones (Heckman, 2005). So, the most massive galaxies host more powerful, more metal-rich and dustier starbursts.

Is the $L_{\text{IR}}/L_{\text{UV}} - \beta$ correlation found for UV selected starbursts applicable to other objects? Goldader et al. (2002) obtained FUV and NUV STIS images for 9 ultraluminous infrared galaxies (ULIRGs). They found that, after correcting for dust reddening using the $L_{\text{IR}}/L_{\text{UV}} - \beta$ correlation, the UV luminosity is insufficient to account for the far-infrared luminosity. On the contrary, GALEX data of several samples of normal galaxies with star formation show that the observed UV luminosity overestimates the far-ultraviolet attenuation of these galaxies predicted from the relationship (Buat et al., 2005; Seibert et al., 2005).

Several attenuation laws have been proposed in the 1200–3000 Å spectral range (Rosa and Benvenuti 1994; Mas-Hesse and Kunth 1999; Calzetti 1997) to be applied to star forming regions, but all of them are coincident in showing a 2175 Å bump weaker than in the galactic extinction law. Recently, Leitherer et al. (2002) and Buat et al. (2002) have used HUT and FUSE data to extend the starburst attenuation law to the FUV.

5. Stellar content

Most starbursts are far enough that the stellar population is unresolved in individual stars even with the high spatial resolution of HST. Thus, the stellar content of starbursts has to be estimated through their integrated light. The first deep integrated spectra of galaxies were taken by IUE with apertures of 10×20 arcsec (see the spectral atlas by Kinney et al. (1993). Sekiguchi and Anderson (1987) were the first to build a stellar library of galactic O and B stars that could be used to predict the equivalent width of CIV $\lambda 1550$ and SiIV $\lambda 1400$ of a non-evolving stellar population of massive stars. Later, Mas-Hesse and Kunth (1991) extended this work using evolutionary models to predict the starburst properties as a function of age. The stellar content of starburst galaxies (e.g. Mas-Hesse and Kunth (1999) and giant extragalactic HII regions (e.g. Vacca et al., 1995; González Delgado and Perez, 2000; Jamet et al., 2004) have been estimated using these IUE spectra. High spatial resolution (sub-arcsec) HST spectra have been obtained (Leitherer et al., 1996; Conti et al., 1996; González Delgado et al., 1999, 2002; Johnson et al., 2000; Chandar et al., 2003a) and the results attained are discussed in Section 5.2.

Starbursts have a strongly absorbing interstellar medium, and a significant fraction of the equivalent width of the CIV $\lambda 1550$ and SiIV $\lambda 1400$ may be due to the interstellar component. This is particularly true if very massive stars do not form or if the starburst is not very young (10 Myr or older). In fact, the low spectral resolution of IUE (about 1000 km s^{-1}) did not allow us to separate the stellar from the interstellar components in most of the starbursts observed. The analysis of these spectra has provided an uncertain determination of the age and stellar content of some starbursts. IUE had also the capability of taking spectra at higher resolution; however, no starburst was bright enough to be observed in this mode. It has been later, in the HST era with higher spatial and spectral resolution observations, that some galaxies previously classified as very young starbursts have been recognized as evolved starbursts with a strong interstellar medium; NGC 1705 is a good example (Heckman and Leitherer, 1997a).

FOS, GHRS and STIS on board HST were used to obtain deep spectra at a resolution ($\sim 200 \text{ km s}^{-1}$) sufficient to resolve the interstellar from the stellar wind components. These

observations allow detailed profile analysis of the wind lines of nearby starbursts to investigate their stellar content. Evolutionary synthesis models that predict the UV wind profiles of a stellar population are used to estimate the age and the initial mass function (IMF) of the starburst. These models have been developed mainly in two spectral ranges, 1200–2000 Å and at the FUV, 1000–1200 Å. We first describe the models and then comment on the general properties of starbursts from the UV line synthesis.

5.1. UV line synthesis

Stellar wind lines contain information on the stellar mass; this is the basis of the UV line synthesis. Stellar winds are driven by radiation pressure. In O stars, a fraction of the radiative momentum (L/c) is converted to kinetic momentum (Mv_∞); so

$$\dot{M} v_\infty \propto (L/c)$$

where \dot{M} , v_∞ , L and c are the mass-loss rate, the wind terminal velocity, the radiant luminosity of the star and the speed of light. The profile of the wind line contains information about the terminal velocity and, via the previous relationship, about the stellar luminosity. So, the wind line profiles of the integrated spectra carry information about the massive stellar population of the starburst, hence about its IMF.

5.1.1. Range 1200–2000 Å

Robert et al. (1993) and Leitherer et al. (1995c) have computed an atlas of evolutionary synthesis models that predict the line profile of NV $\lambda 1240$, SiIV $\lambda 1400$, CIV $\lambda 1550$, HeII $\lambda 1640$ and NIV $\lambda 1720$ as a function of age and IMF, for an instantaneous burst and for continuous star formation.

Fig. 4 UV synthetic spectra generated with Starburst99 for an instantaneous burst at different ages that follows a Salpeter IMF in a mass range of 1 to $100 M_\odot$. Note the change of the SiIV and CIV profile with the age of the burst

Figures 4 and 5 show these lines for several ages and different IMF. The results indicate: (a) CIV always shows a P Cygni profile when O stars with $M \geq 50 M_\odot$ are in the zero-age main sequence; it is a good age diagnostic of the stellar population. (b) SiIV shows a conspicuous wind profile when O blue supergiants are present. A strong P Cygni profile appears between 3 to 5 Myr for a burst stellar population. It is also strong, when there is a large fraction of blue supergiants with respect to O main sequence stars, i.e., when the stellar population forms with a top-heavy IMF. (c) NV has a similar behavior to SiIV. (d) Hell and NIV appear as a strong broad emission feature when a large fraction of Wolf-Rayet stars are present, in the age range $\sim 3\text{--}4$ Myr.

Photospheric lines, such as CIII $\lambda 1426, 1428$, SV $\lambda 1502$, are also strong when the burst is only a few Myr old and the UV light is dominated by O stars. The contribution of B stars to the UV light has been predicted by de Mello et al., (2000). Si lines, such as SiIII $\lambda 1295, 1297, 1299$, SiIII $\lambda 1417$, SiII $\lambda 1485$, are good age diagnostics for evolved starbursts (age ≥ 10 Myr).

Initially, the spectral library used as input to the models was built with hot stars of solar or slightly subsolar metallicity. However, photospheric lines are much weaker at lower metallicity; and the stellar-wind properties are affected by line-blanketing, since the mass-loss rate scales with $(Z/Z_\odot)^{0.5}$ (Kudritzki et al., 1999). Leitherer et al. (2001) built a new stellar library with O and B stars in the LMC and SMC observed with HST. They implemented it in Starburst99 (Leitherer et al., 1999), providing new evolutionary synthesis models at $1/4 Z_\odot$. However, the behavior of the stellar wind lines is complex; while NV $\lambda 1240$ and SiIV $\lambda 1400$ do not scale monotonically with metallicity, CIV $\lambda 1550$ is significantly affected, showing a weaker P Cygni profile. Thus, while the wind NV and SiIV may be equally well predicted using the solar stellar library, CIV and the photospheric lines

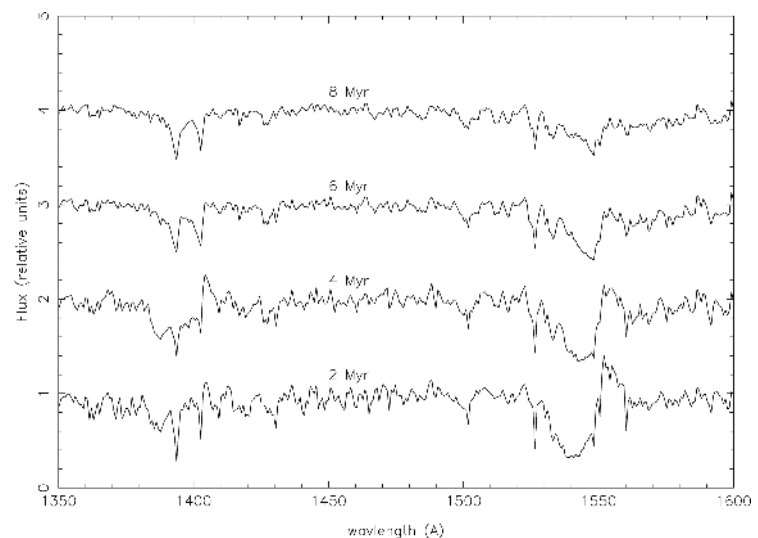
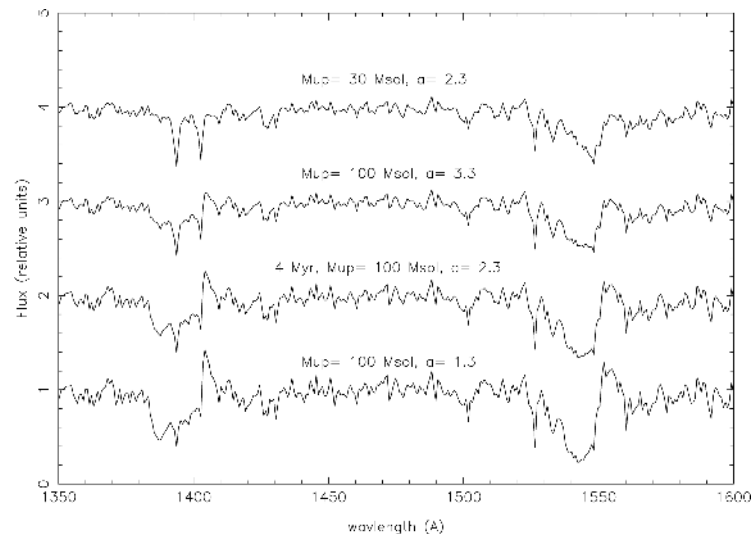


Fig. 5 As in Fig. 4 for an instantaneous burst 4 Myr old with different assumptions of the IMF. Note how weak become SiIV and CIV when very few massive stars form in the starburst



are overpredicted in low metallicity starbursts, inducing a wrong estimation of the age and of the IMF parameters.

5.1.2. Range 1000–1200 Å

The first evolutionary synthesis models at intermediate spectral resolution in the FUV were computed by González Delgado et al. (1997). Using a stellar library built with hot O and early B stars observed with Copernicus and HUT, they predicted the wind line OVI $\lambda 1032, 1038$ and the photospheric component of Ly β . OVI develops a P Cygni profile when formed in stellar winds of the most massive stars. When these stars are absent, no OVI is formed. In contrast, Ly β is a very sensitive indicator of B stars. If these stars dominate, as is the case in evolved starbursts (age ≥ 10 Myr), Ly β is present as a strong absorption feature. Because of the constant strength of OVI in O stars, OVI is not a good discriminator between instantaneous versus continuous star formation for ages when the starburst is in the nebular phase, but the absence of OVI and the presence of stellar Ly β is a good indicator of a short burst duration and of the galaxy being in an evolved starburst phase (age ≥ 10 Myr). However, careful attention to interstellar absorption of Ly β is needed before estimating the ages and stellar content in starbursts using these lines. Robert et al. (2003) have made an extension of these models predicting also the photospheric lines in the 1000–1200 Å range using O, B and Wolf-Rayet stars in the Galaxy and in the LMC and SMC observed by FUSE. Other wind lines observed in starbursts are NIV $\lambda 955$, CIII $\lambda 977$, NIII $\lambda 991$ and NII $\lambda 1083$ (Keel et al., 2004).

In contrast to wavelengths above 1200 Å, the FUV continuum suffers from an age-reddening degeneracy. Because at $\lambda \leq 1200$ Å hot stars are outside the Rayleigh-Jeans regime, the age effects are no longer negligible in the continuum slope for starbursts in an instantaneous burst (Leitherer, 2005).

For starbursts in the continuous star formation regime, the FUV continuum is less sensitive to the age than the near-UV, because the rate of death and birth of stars is reached earlier.

5.2. Results: Ages and IMF

5.2.1. Stellar Clusters

Intermediate (~ 1 arcsec) and high (~ 0.1 arcsec) spatial resolution spectra with HST have been obtained to constrain the IMF and age in stellar knots detected in starbursts. The main results derived from the UV light provided by stellar clusters can be summarized as follows: the spectral range 1200–2000 Å can be characterized by an instantaneous burst a few Myr old, populated by a Salpeter IMF with stars more massive than $50 M_\odot$ (e.g. Conti et al., 1996; Leitherer et al., 1996; González Delgado et al., 1999; Chandar et al., 2003b). When the integrated light is emitted by extended areas (~ 100 pc), the UV spectra are equally well fitted by continuous star formation lasting for a few Myr. These results indicate that clusters form with a very small age spread. In fact, this is the case for the starburst He2–10 (Johnson et al., 2000; Chandar et al., 2003a) in which the clusters are chained along ~ 100 pc with a mean separation ≤ 10 pc, and they are all 4–5 Myr old. These clusters have masses of several 10^4 to several $10^5 M_\odot$, that are typical of proto-globular clusters (Ho and Filippenko, 1996).

There are indications that the IMF and the global star formation processes are the same in metal rich clusters as they are in metal poor ones. A good example is the metal-rich, barred starburst NGC 3049. HST observations done with STIS/MAMA (FUV) indicate that most of the UV light is emitted within the central arcsecond. The wind lines detected in the spectrum indicate that the cluster(s) in the inner

50 pc formed 3–4 Myr ago in an instantaneous burst. Even though the metallicity of the stars is supersolar, stars more massive than $50 M_{\odot}$ form in the cluster(s) (González Delgado et al., 2002). This result has been confirmed by Chandar et al. (2003b) for other metal-rich starbursts. HeII $\lambda 1640$ has been detected in these objects, indicating the presence Wolf-Rayet stars in these starbursts. This finding provides an additional evidence of the population of the upper part of the IMF in high metallicity starbursts.

5.2.2. Diffuse UV Light

The main results in this topic come from high spatial observations taken with HST+STIS. The narrow slit (~ 0.1 – 0.2 arcsec) capability of STIS is needed to isolate the stellar clusters light from the diffuse component. Tremonti et al. (2001) have obtained long slit spectra of several stellar clusters plus the inter-cluster regions of diffuse light in the low-metallicity galaxy NGC 5253. They find that the UV light of clusters and that of the diffuse component have different spectral properties. The clusters are well fitted by an instantaneous burst with ages of several Myr that follow a Salpeter IMF extending up to $100 M_{\odot}$. However, the field spectrum is better fitted by continuous star formation models with either $M_{\text{up}} = 30 M_{\odot}$ or an IMF slope steeper than Salpeter's. Alternatively, the field stellar population could be formed following a Salpeter IMF but older than the clusters. Similar results have been obtained by Chandar et al. (2005) for a sample of starbursts. They propose that if the field is composed of older, dissolving clusters, they have to dissolve on timescales 7–10 Myr to create the field. If the field is composed of young clusters that are unresolved in the STIS observations, they would consist only of a few $100 M_{\odot}$ in order to be deficient in O stars. However, sampling effects in the IMF (Cerviño et al., 2002) must be taken into account before obtaining any realistic conclusion.

5.2.3. Lyman Break Galaxies

The UV-rest frame spectra of LBGs have been obtained from the ground with ~ 10 m class telescopes. These spectra are quite similar to local starburst galaxies in the sense that they are dominated by absorption lines (e.g. Shapley et al., 2003; Noll et al., 2004). They have strong high-and low-ionization interstellar lines that are thick in their cores. Photospheric and wind lines are also present. But, most of the high-ionization lines are dominated by the interstellar contribution. Probably due to the large spatial extension covered by these observations (1 arcsec = 8 kpc at $z = 2.5$, assuming a standard cosmology), the wind profiles of the integrated light look weaker than in many nearby starbursts, suggesting that star formation proceeds continuously, they have older ages, and/or the metallicity is lower.

Because of its gravitationally lensed nature, cB58 has the highest signal-noise rest-frame UV spectrum obtained to date for LBG (e.g. Pettini et al., 2002). Even so, the wind lines can not constrain well the age. The PCygni profiles of CIV and NV are compatible with csf during the last several 10 Myr, and a Salpeter IMF extended beyond $50 M_{\odot}$. No evidence exists for a flatter IMF or an IMF deficient in massive stars (Pettini et al., 2000; de Mello et al., 2000). Photospheric lines were detected and they are compatible with a metallicity below solar, $1/4 Z_{\odot}$. Spectra for other LBGs have been obtained with much lower signal-noise, and only a few of the individual objects can be analyzed. Composite spectra with the average of more than several dozen objects are more suitable to be studied. The results obtained in this way for LBGs at the ‘redshift desert’ ($1.4 \leq z \leq 2.5$) indicate that these galaxies have stellar properties similar to cB58 (Steidel et al., 2004). But the metallicity can be higher, closer to solar. Mehrt et al., (2005) have found an increase of the average metallicity of bright starbursts with cosmic time (decreasing redshift). A metallicity higher than solar has also been estimated using the photospheric 1425 Å index in the K20 survey (Daddi et al., 2004).

6. Starbursts in AGN

HST ultraviolet observations of Seyferts 2 and LINERs have contributed significantly to establish the role that starbursts play in the active galactic nuclei (AGNs) phenomena. The high spatial resolution provided by HST has been crucial to detect starbursts formed by stellar clusters in the center of galaxies with an AGN. This result implies a significant advance to establish a connection between violent star formation processes and nuclear activity, because in the IUE era, it was assumed that all the UV light obtained in the Seyfert spectra was produced by the AGN. An extended review of the role of UV observations in establishing the nature of AGNs is given elsewhere else in this book by Kollatschny and Ting-Gui.

6.1. Starbursts in Seyfert 2 nuclei

According to the unified scheme of AGNs, the main components of a Seyfert nucleus are: (1) A super-massive black hole and its associated accretion disk. (2) A circumnuclear dusty torus that collimate the AGN radiation through its polar axis. So, a Seyfert 2 nucleus should be a Seyfert 1 that is viewed close to the equatorial plane. This torus will facilitate the detection of starbursts in the circumnuclear region, blocking away the continuum radiation from the AGN. (3) A mirror of dust and warm electrons located along the polar axis of the torus, that reflects and polarizes the AGN radiation. Seyfert 2 nuclei exhibit a featureless continuum (FC) that comprises

much of the near-UV. It was long-thought that this FC was light from the hidden Seyfert 1 nucleus. However, optical spectropolarimetry (Tran, 1995) showed that this is not the case. Cid Fernandes and Terlevich (1995) proposed that a heavily-reddened starburst provides this FC.

Because of the high sensitivity of UV wavelengths to the presence of massive stars, HST UV observations were done to prove the role of starbursts in Seyfert 2 nuclei (Heckman et al., 1997b; González Delgado et al., 1998b). HST high spatial resolution (0.014 arcsec/pixel sampling) imaging shows that the UV continuum source is spatially extended (~ 100 pc) and it is resolved in knots with sizes of a few parsecs and properties similar to the stellar clusters detected in starburst galaxies (Fig. 6). GHRS spectra for four galaxies, corresponding to the central ~ 100 pc, were obtained. These galaxies were selected to have high UV surface brightness. The data provided direct evidence of the existence of a nuclear starburst. Absorption features formed in the photospheres and in the stellar winds of massive stars are detected (Fig. 6). Interstellar lines blueshifted by a few hundred km s $^{-1}$ with respect to the systemic velocity are also detected, indicating an outflow driven by the nuclear starburst (see Section 7). Their UV colors indicate that the starburst is quite reddened. Their bolometric luminosities are similar to the estimated luminosities of the hidden Seyfert 1 nuclei.

Subsequently, near-UV and optical spectra of a large sample of Seyfert 2 were obtained proving the unambiguous identification of circumnuclear starbursts in $\sim 40\%$ of nearby Seyfert 2 galaxies as well as their energetic significance (González Delgado et al., 2001; Cid Fernandes et al., 2001).

6.2. Starbursts in LLAGNs

Low-luminosity active galactic nuclei (LLAGNs) constitute a significant fraction of the nearby AGN population. These include LINERs, and transition-type objects (TOs, also called

weak-[OI] LINERs) whose properties are in between classical LINERs and HII nuclei. LLAGNs comprise $\sim 30\%$ of all bright galaxies and are the most common type of AGN (Ho et al., 1997). What powers them and how they fit in the global picture of AGN has been at the forefront of AGN research for over two decades. Are they all truly “dwarf Seyfert galaxies” powered by accretion onto a nearly dormant super-massive black hole, or can some of them be explained at least partly in terms of stellar processes?

HST observations at UV wavelengths of a few LLAGNs have also proven that at least weak-[OI] LINERs could be powered by young massive stars (Maoz et al., 1998; Colina et al., 2002; Gabel and Bruhweiler, 2002). Nuclear stellar clusters are detected in these objects through high spatial resolution UV imaging and spectra. NGC 4303 is probably the best example of the few objects observed (Colina et al., 2002). STIS imaging (0.027 arcsec/pixel sampling) shows that the nuclear knot has a size of only a few parsecs and its spectrum (taken with a slit width of 0.2 arcsec) shows characteristic broad P Cygni lines produced by the winds of massive young stars. These features are quite similar to those detected in the spectra of stellar clusters located in the starburst ring (Fig. 7). The line profile analysis suggests that the nuclear cluster formed in an instantaneous burst 4 Myr ago with a mass of $10^5 M_\odot$.

HST UV monitoring observations of 17 LLAGNs have detected variability with amplitudes from a few percent to 50% (Maoz et al., 2005). The variability is more frequently detected in those LINERs that have a compact radio core, as expected from bona fide AGNs.

Subsequent optical studies of a large sample of LLAGNs have shown that the contribution of an intermediate age stellar population is significant in TOs (González Delgado et al., 2004). Unfortunately, the premature death of STIS has not allowed us to find out the fraction of LLAGNs that have a young nuclear stellar cluster like NGC 4303 and which are “dwarf Seyfert galaxies” like those that show UV variability.

Fig. 6 UV image and nuclear spectrum of the Seyfert 2 galaxy NGC 7130 taken with HST+GHRS and 1.74×1.74 arcsec aperture. The UV light is dominated by the nuclear starburst that has an effective radius of ~ 80 pc. See González Delgado et al. (1998b) for further explanations

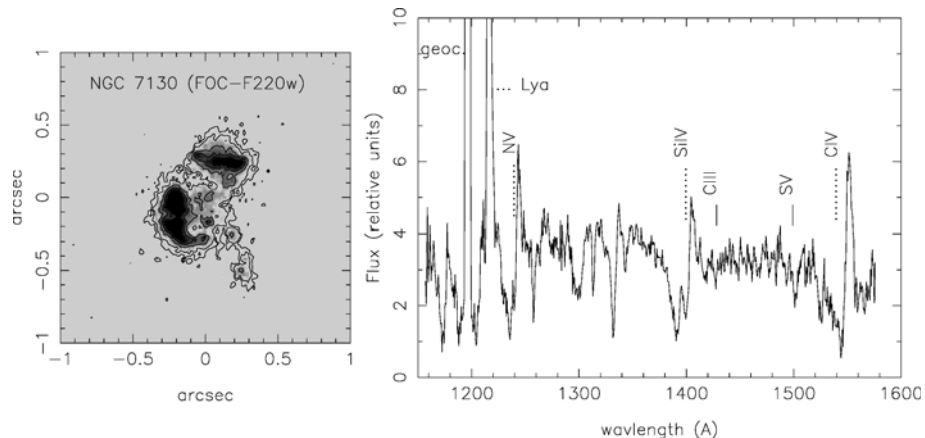
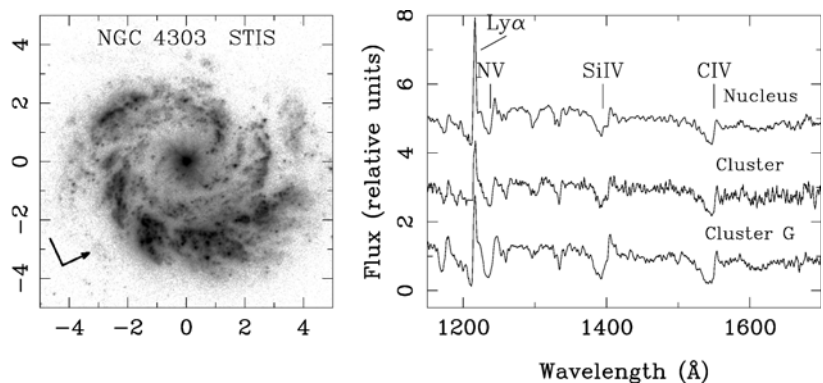


Fig. 7 UV image and spectra of the LLAGN NGC 4303 taken with HST + STIS/MAMA. The nucleus has a compact cluster of 3 pc size. The spectrum of the nuclear cluster is quite similar to the stellar clusters in the ring. See Colina et al. (1998b) for further explanations.



7. Interstellar lines: Starburst outflows

The large-scale outflow of interstellar material is a generic property of starbursts, since it is a consequence of the high star formation activity in these galaxies. Outflows are driven by the mechanical energy provided by the combined effect of stellar winds and supernovae in the starburst. Only a few Myr after the onset of the star formation in the starburst, the massive stars start to explode as supernovae. Hot gas bubbles (superbubbles) form inside the starbursts due to the deposition of mechanical energy. The hot gas expands, preferably along the direction perpendicular to the galaxy disk, sweeping up ambient material. When the superbubble reaches several vertical scale heights of the galaxy, Rayleigh-Taylor instabilities develop, and the wall of the bubble can dissipate. This allows the interior of the hot gas to blow out into the galactic halo in the form of a collimated bipolar outflow, called superwind (e.g. MacLow et al., 1989; Tenorio-Tagle and Muñoz-Tuñon, 1996). These outflows can accelerate the ambient halo gas, producing the bipolar regions of emission lines detected in the spectra of many starbursts at optical wavelengths, as well as the blueshifted interstellar absorption lines at UV.

Thus, outflows are ubiquitous phenomena not only in nearby starbursts, but also in LBGs. Note that, at some evolutionary phases of the starburst (ages older than 10 Myr if the starburst formed in a burst), the mechanical luminosity injected into the interstellar medium can dominate over the ionizing luminosity (Leitherer et al., 1992), becoming almost the only heating source of the interstellar medium. Outflows might also be the main source of chemical enrichment of the intergalactic medium, because they can blow out and escape from the gravitational potential of the galaxy, venting the metals produced by massive stars into the intergalactic medium. Outflows constitute an important energy source for the evolution of galaxies through the heating and enrichment of the interstellar and the intergalactic media.

UV is the perfect wavelength range to study the neutral, cold and warm phases of outflows. FUV is also useful to study the coronal phases, being the observations in this spectral range complementary to the X-ray data. Ly α emitting

gas traces the neutral HI outflows (cf. Section 8 below); low (e.g. CII, SiII) and high-ionization (CIV, SiIV, NV) interstellar lines trace the cold and warm phases, respectively, while interstellar OVI traces the coronal phase. GHRS+HST, HUT and FUSE spectra of nearby starbursts have contributed significantly to our understanding of the different outflow phases.

Dusty outflows have been detected through near and FUV images of the halo of the nearby starburst galaxies M82 and NGC 253 taken with GALEX (Hoopes et al., 2005). The UV luminosity in the halo is too high to be provided by continuum and line emission from shockheated or photoionized gas. They find that the UV halo light may be stellar continuum of the starburst scattered into our line of sight by dust in the outflow.

One critical point related with the outflows is to know which fraction of the kinetic energy supplied by supernovae is radiatively lost and which fraction is carried out into the outflow. If radiative cooling is not negligible, outflows can break out and are able to escape from the gravitational potential of the galaxy injecting metals into the intergalactic medium. This process is relevant for the evolution of starbursts and the intergalactic medium. A study of the different phases of the outflows is needed to settle its relevance.

7.1. Cold phase

Most starbursts have low-ionization absorption lines with equivalent widths of several Å. These lines are optically thick, and they are in the flat part of the curve of growth. This means that the equivalent width of these lines is not proportional to the column density of the gas, as would be the case if they were in the linear part of the curve of growth. In fact, these lines are saturated because the ratio of the equivalent widths of two transitions of the same ion is not proportional to the ratio of the $f\lambda^2$ of each transition, where λ is the rest-frame wavelength of the transition and f the oscillator strength. Instead, the equivalent width is determined by the velocity dispersion of the gas, and therefore an equivalent width of 2–3 Å implies a velocity dispersion larger than

200–300 km s⁻¹. This may indicate that several unresolved velocities are observed. This is the first evidence suggesting that the interstellar lines are not virialized but rather they are related with large-scale motions.

Other evidence of the large-scale motions of the interstellar gas in starbursts comes from the broadening of the low-ionization interstellar lines. The line profiles are asymmetric, and when observed at high spectral resolution, they are resolved into several interstellar components (González Delgado et al., 1998a).

An additional and the strongest evidence for outflows comes from the radial velocity of the lines. Many starbursts show the low-ionization lines, such as SIII $\lambda 1526$, CII $\lambda 1335$, SiII $\lambda 1260$, blueshifted by several hundred km s⁻¹ with respect to the systemic velocity of the starburst determined with the photospheric lines, or with respect to the HI systemic velocity of the galaxy (e.g. González Delgado et al., 1998a). Because these interstellar lines cover more than 50% of the UV light, they cannot be produced by isolated clouds, and they must be associated with a galactic-scale outflow. The shift to blue wavelengths detected in these lines is an unequivocal prove of the outflows in these galaxies.

7.2. Warm and coronal phases

High-ionization interstellar lines, such as NV $\lambda 1240$, SiIV $\lambda 1400$, and CIV $\lambda 1550$, can trace warm ionized gas outflows which are at $T \geq 10^4$ K. This gas is ionized by radiation from the massive stars in the starburst as well as by collisional processes associated with the outflow. However, measuring the blueshift of these lines is more difficult than in the low-ionization lines. This is due to the difficulty in isolating the wind and the interstellar components of these lines in intermediate spectral resolution observations. But when the starburst is not in a wind phase, and/or the spectral resolution is better than 100 km s⁻¹, the blueshift of the line is also a measure of the outflow speed.

The hot phase gas is traced by the OVI $\lambda 1032$, 1038 interstellar component. OVI could arise from collisionally ionized gas with $T \geq 10^5$ K. OVI has been detected in a sample of nearby starbursts observed by FUSE. The center of the lines is blueshifted by several 100 km s⁻¹. The lines are also very broad, with maximum outflow speeds of ~ 1000 km s⁻¹ (Heckman, 2004).

These two outflow phases have been measured in the nearby dwarf starburst galaxy NGC 1705. This galaxy hosts a 12 Myr old super star cluster (Vázquez et al., 2004). Outflows in the warm phase were detected in the SiIV high-ionization lines by Heckman and Leitherer (1997a). More recently, FUSE observations have shown that the warm gas outflow has a lower velocity (~ 50 km s⁻¹) than the coronal interstellar gas (~ 80 km s⁻¹, Heckman et al., 2001a). The kinematics

of the warm gas is compatible with a model of an adiabatic expansion of the superbubble driven by the kinetic energy supplied by the supernova. However, the expansion speed of the superbubble is too small to produce OVI behind its shock front. Instead, the column density and velocity of the OVI is compatible with a model in which the superbubble has begun to blow out of the interstellar medium of NGC 1705. OVI absorption is produced during the blowout phase, in which the superbubble shell is accelerated and fragmented. The interaction between the outflowing gas and the shell fragments create a high temperature coronal gas that produces the OVI absorption. Heckman et al. (2001a) found that the cooling rate in this phase is much less than the supernova heating rate; thus, they concluded that probably the outflow in NGC 1705 is able to blow out and to vent the metals into the intergalactic medium.

8. The Ly α line: Outflows of neutral H gas

Ly α in emission can in principle be produced by recombination of hydrogen photoionized by the O and B stars. Massive stars in the starbursts provide enough ionizing photons to produce a large Ly α flux. In fact, evolutionary stellar population models predict Ly α to be the strongest emission feature in the spectra of young starbursts. This is particularly true for primordial galaxies because in the absence of metals the cooling is produced by Ly α and He recombination lines (Schaerer, 2002). Ly α has been used to spectroscopically confirm galaxies at high- z . However, many observational programs in the past have failed to find a significant population of primordial galaxies based on the detection of Ly α . The reasons have to be found in the complex structure of the Ly α line.

The complexity of the line was noted more than 20 years ago with IUE. Ly α observations of nearby starbursts show that the line is weaker than the value expected from recombination, and there was a tendency to smaller Ly α /H β ratios with metallicity (Meier and Terlevich, 1981; Hartmann et al., 1988; Terlevich et al., 1993). Several arguments were proposed:

- Resonance scattering by neutral hydrogen: Ly α photons are attenuated by dust as a result of multiple resonant scatterings by hydrogen atoms that increase the path length of the Ly α photons and thus the probability that they will be absorbed by dust.
- Extinction: The Ly α light is affected by dust more than any other Balmer recombination line since extinction curves peak in the FUV. In fact, some starbursts have Ly α /H β ratio consistent with simple recombination theory if the ratio is corrected for reddening using the appropriate extinction law for the metallicity of the galaxy and the age

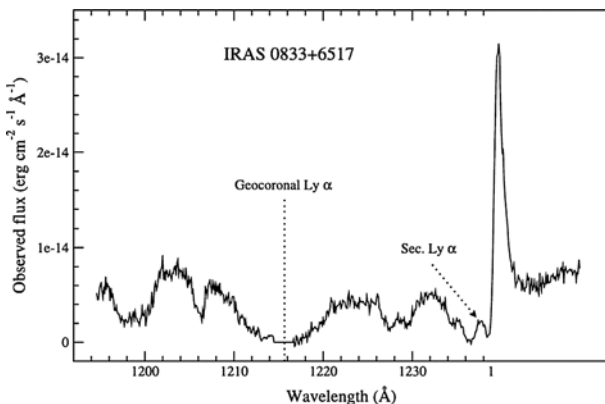


Fig. 8 Ly α profile of the starburst galaxy IRAS 0833 + 6517 taken with HST+STIS/MAMA. Note the PCygni profile of Ly α and a second blueshifted Ly α emission that forms in the expanding shell. (Figure adapted from Mas-Hesse et al., 2003.)

of the burst is taken into account (Calzetti and Kinney, 1992; Valls-Gabaud, 1993).

However, these arguments contrast with observations of low metallicity starbursts that are very little extinguished. No Ly α emission was detected in galaxies like IZw18 (Kunth et al., 1994), even though the metallicity and dust content are very low. HUT and HST observations of nearby galaxies have brought new insight into the nature of Ly α (Lequeux et al., 1995; González Delgado et al., 1998a; Kunth et al., 1998, 2003; Mas-Hesse et al., 2003). GHRS and STIS spectral resolution has been crucial to understand the role played by outflows in the structure of the Ly α emission.

– Neutral HI outflows: Many nearby starburst galaxies in which Ly α is detected in emission show an asymmetric profile, with the peak emission redshifted with respect to the systemic velocity, and a deep Ly α absorption is detected blueshifted by several 100 km s $^{-1}$ with respect to the emission (see Fig. 8). This shift is in agreement with the blueshift observed in the interstellar lines of the same galaxy. The natural explanation is that the neutral HI gas producing the absorption is outflowing from the starburst.

Tenorio-Tagle et al. (1999) have developed a detailed model to explain the different Ly α profiles, that requires the time evolution of an expanding shell created by the supernova explosions in the starburst. Some of the most relevant phases are:

- An expanding supershell forms by the SN action. Ly α photons will be absorbed by the HI galaxy disk. If the HI column density is very high, Ly α will show an absorption profile centered at the systemic velocity of the galaxy. The starburst in IZw18 is in this phase.
- Rayleigh-Taylor instabilities produce the shell fragmentation, and the shell will blow out. Ionizing radiation es-

capes into the halo and the IGM, producing an extended biconical emission line region. Ly α will be detected in emission at the systemic velocity of the galaxy. Recombination in the shell will produce an additional Ly α emission blueshifted at the shell expanding velocity. Tol1214 could be in this phase (Mas-Hesse et al., 2003).

- An HI trapped ionization front is formed at the external side of the expanding shell. Ly α photons are absorbed there. Ly α will show a PCygni profile. Backscattering and emission from the receding part of the shell will produce an extended red wing in the Ly α emission. IRAS 0833 + 6517 is in this phase (see Fig. 8).
- Finally the shell is slowed down in its expansion, and it will be completely recombined. A damped Ly α core profile will be observed with only a small blueshift.

Thus, Ly α emission, like the interstellar lines, is driven by the dynamical effects of the violent star formation processes ongoing in the starburst, rather than by the gravitational potential well of the galaxy.

9. Lyman continuum: The escape of ionizing radiation

The origin of the diffuse ultraviolet background that reionized the early universe is still unknown. Quasi-stellar objects (QSOs) are considered one of the main sources. However, QSOs alone cannot account for all the background radiation that maintains the diffuse intergalactic medium and the Ly α forest clouds highly ionized. Two other possible sources are: highly obscured QSOs that cannot be observed because of dust, and a large fraction of high-mass stars formed in primordial galaxies (Miralda-Escudé and Ostriker, 1990).

Observations of the Lyman continuum of starbursts have been done to estimate the contribution of massive stars to the reionization of the universe. However, this estimation depends critically on the determination of the fraction of ionizing photons (f_{esc}) that escape from the galaxies and reach the intergalactic medium.

Evidence exists that the HI disks surrounding galaxies may not be totally opaque to the ionizing photons. Bland-Hawthorn and Putman (2001) estimate that 5–10% of the ionizing photons escape from the Milky Way halo. Others (e.g. Castellanos et al., 2002) have found that a significant fraction of ionizing photons may locally escape from the H $_{\text{II}}$ regions in nearby galaxies, but it is unknown whether these photons will escape from the galaxies. Starbursts outflows may be an efficient mechanism to open channels in the HI halo disks of the galaxies through which the ionizing photons can escape and reach the intergalactic medium.

HUT and FUSE have contributed significantly in determining the value of f_{esc} in local starbursts. Leitherer et al., (1995b) find, in a small sample of four starburst galaxies, that $f_{\text{esc}} \leq 3\%$. Later, Hurwitz et al., (1997) reevaluate f_{esc} applying a detailed model of the absorption by interstellar gas in our Galaxy. They are not able to detect the Lyman continuum flux, but they derive an upper limit $f_{\text{esc}} \sim 10\%$. Deharveng et al. (2001) obtained FUSE observations of Mrk54 and found that the Lyman continuum radiation is not detected above the HI absorption edge in our Galaxy. Comparing with the number of ionizing photons derived from the H α flux, they estimate that $\sim 6\%$ of Lyman continuum photons escape the galaxy without being absorbed by interstellar material. Heckman et al. (2001b) also obtained FUSE data of five of the UV-brightest local starburst galaxies. They found that the interstellar line CII $\lambda 1036$ is essentially black. Because the opacity of the neutral ISM below the Lyman edge is larger than in the CII line, the residual UV intensity of the line can be used to put a constraint on f_{esc} . They found an upper limit of 6%. Thus, local starburst galaxies seem to be very opaque and they leak out only a few percent of their ionizing radiation.

Observations of the Lyman continuum flux in LBGs have provided more discrepant f_{esc} results. Steidel et al., (2001) built a composite spectrum of 29 LBGs at $z = 3.4$. These galaxies belong to the group of strong Ly α emitters found by Shapley et al. (2003). They estimate $f_{\text{esc}} \geq 50\%$. The implication of this result is that LBGs contribute at least as many ionizing photons as QSOs at $z \sim 3$. However, these results have not been confirmed by others. Giallongo et al. (2002) obtained VLT spectra of two of the LBGs from the sample of Steidel and collaborators. They set an upper limit of 16% to f_{esc} . Lyman continuum has been estimated also from deep HST images of the HDF (Fernández-Soto et al., 2003) and LBGs at $1.1 \leq z \leq 1.4$. Both works also found f_{esc} of a few % ($\leq 4\%$). High spectral resolution data are required to better constrain the Lyman continuum flux in LBGs, and to determine whether LBGs are opaque like local starburst galaxies or they are leaking out most of their photons as Steidel et al., estimate.

However, in most of the LBGs the absorption part of the Ly α PCygni profile is completely black. Therefore, the star-forming regions seem to be completely covered by neutral gas, and f_{esc} should be close to zero, unless the covering is not isotropic and the escape is produced along other directions.

Note, however, that many of the nearby starbursts for which f_{esc} has been estimated in a few % also have high-velocity outflows of neutral gas. But these outflows are also an ubiquitous phenomenon in LBGs. Thus, as it was pointed out by Heckman et al. (2001a) these outflows could be a necessary but not sufficient mechanism to open paths within the interstellar medium through which the ionizing radiation can escape.

10. Interstellar lines: Abundances

The large number of line transitions of many different ions that occur at UV wavelengths, makes this spectral range quite suitable to determine the chemical abundances and to study the chemical evolution of galaxies. Because metal transitions that form in the neutral gas phase are common in the UV, this range is quite suitable to determine the chemical abundances of the HI phase. Note, however, that most of our knowledge about the chemical abundances in starbursts comes from the collisional emission lines formed in the ionized gas associated to the HII regions that are observed at optical and infrared wavelengths. Thus, these abundances correspond to the gas ionized phase. This difference between the abundances determined using optical or UV transitions (collisional vs. recombination lines, HII vs. HI) is especially important for the study of the chemical evolution of galaxies and, in particular, for starburst galaxies.

As we pointed out earlier, many of the strongest interstellar lines in the spectra of starburst galaxies observed with an intermediate spectral resolution are saturated. Thus, the strength of these lines is related more with the kinematics of the gas than with the metallicity. But, unsaturated absorption interstellar lines have a suitable information of the gas metallicity. So, when a line is in the linear part of the curve-of-growth, its equivalent width is proportional to the column density of the corresponding species, and the metallicity of the element can be estimated. On the contrary, when the line is in the flat part of the curve-of-growth, the profile is quite insensitive to the abundances. For example, as shown in Pettini and Lipman (1995), the range of possible values of (O/H) admitted by the profile of the saturated OI $\lambda 1302$ absorption line is very large, spanning a factor of ~ 1000 . Then, only unsaturated, and presumably weak lines with a moderate or low transition-strength, $f\lambda$, are useful to estimate the column density of the ions. Therefore, only with good signal-to-noise and high spectral resolution spectra is it possible to determine the gas abundances.

Different approaches can be followed to determine the column densities of the different ions in starbursts. They are: (1) The curve-of-growth method, which relates the equivalent widths of the lines with $Nf\lambda^2$, where N is the column density. (2) The direct method, based on the fit of the absorption profiles to all the lines in the spectrum arising from transitions of the same ion. (3) The optical depth method. The optical depth is deduced from the observed intensity in the line at velocity v , and then, the column density that best fits the line profile is inferred (Savage and Sembach, 1991). Metal abundances are then determined through the column densities and assuming some ionization correction fraction. A hypothesis about the dust depletion has to be made to obtain the final values of the abundances.

Abundances for starbursting dwarf galaxies are easier to obtain than for nuclear starbursts since the former have lower metallicities. Starbursting dwarf galaxies are very interesting systems from the cosmological point of view. According to the hierarchical galaxy formation scenario, dwarf galaxies could be the building blocks of larger and massive galaxies that formed by merging. Thus, local starbursting dwarf galaxies could be considered the closest analogue to primeval galaxies. Local starbursting dwarf galaxies are gas rich and chemically relatively unevolved objects, as their low abundances indicate. They have HII region abundances between $\sim 1/50$ to $1/3 Z_{\odot}$, which are certainly not primordial. But Kunth and Sargent (1986) suggested that the ionized gas could be enriched with metals ejected by supernovae in a very short time-scale, the time-scale of a burst of star formation. Then, the HII abundances would not necessarily reflect the actual abundance of the HI phase, being the former lower if self-pollution is important. However, this hypothesis is not supported by Tenorio-Tagle (1996) that predicts a larger time-scale for the mixing of supernova ejected metals with the interstellar medium. This time-scale would be of the order of several 10^8 yr.

FUV observations of nearby starbursting dwarf galaxies taken with FUSE have contributed significantly to test if these galaxies are primeval, experiencing their first burst of star formation (Thuan et al., 2002; Lecavelier des Etangs et al., 2004; Aloisi et al., 2003; Lebouteiller et al., 2004; Aloisi et al., 2005; Cannon et al., 2005). These works agree in finding lower α element abundances in the neutral HI gas phase than in the HII regions. However, because these abundances are not really primordial, starbursting dwarf galaxies are not experiencing their first burst of star formation, and they are not primeval galaxies.

UV interstellar lines have also been used to estimate how chemically evolved are high- z star forming galaxies. In contrast to local starburst galaxies, HII region abundances are not known for LBGs, since collisional lines at the rest-frame optical wavelengths have not been observed yet for a significant population of high- z star forming galaxies. Neutral gas phase abundances have been determined for cB58 (Pettini et al., 2002). They found that the interstellar medium of this galaxy is highly enriched in elements released by type II supernovae, with abundances of O, Mg, Si, P and S $\sim 2/5 Z_{\odot}$. But, N and Mn, Ni and Fe are underabundant by a factor ~ 3 . Because these elements are produced by intermediate-mass stars, the enrichment in cB58 has probably taken place within the last 300 Myr, which is the lifetime of these stars and the release time scale for N.

Savaglio et al., (2004) have estimated column densities of Fe, Mg and Mn for a sample of 13 galaxies at redshifts $1.3 \leq z \leq 2$. These column densities are similar to those derived for cB58. But they are considerably larger than typical values in

damped Ly α systems. Making a rough estimation of the HI column density and assuming a moderate Fe dust depletion, they estimate an abundance of $1-0.2 Z_{\odot}$. Then, these galaxies are also metal-rich.

11. Summary and future prospects

IUE has made an important initial contribution to our knowledge of starbursts providing the first high quality UV spectra; however, most of our actual knowledge about UV in nearby starbursts comes from HST and FUSE observations. Along this paper, we have emphasized the contributions of high spatial (≤ 0.025 arcsec/pixel) resolution imaging and intermediate (~ 100 km s $^{-1}$) dispersion spectra taken with FOC, GHRS and STIS in the UV, and the high-resolution spectra with FUSE in the FUV (1200 Å down to the Lyman break). A significant progress has been made in the determination of the stellar content of starburst galaxies and the physical, chemical and dynamical properties of the interstellar medium in these galaxies. In particular, it has been possible to advance in our understanding of the role that stellar clusters play in starbursts and AGNs only thanks to the high spatial resolution of the imaging and spectral observations taken with the instruments on board HST. Stellar clusters have sizes of a few pc, so they can be isolated from the background radiation in very nearby starbursts if they are observed with resolution better than 0.1 arcsec.

During the next few years, the GALEX mission will certainly provide the means for an important progress in the study of the cosmic evolution of starburst properties, as well as providing a larger sample of local starbursts. But the limited capabilities of its spectroscopic mode (low spatial and spectral resolution and sensitivity) will not help to progress in understanding most of the physics that regulates the violent star formation processes in galaxies. Spatial resolution below 0.1 arcsec is needed to isolate the UV light of the center from the disk in the UV bright galaxies discovered by GALEX at $z = 0.1-30.3$. This resolution can provide in these galaxies a spatial sampling better than 500 pc which is the typical size of nuclear starbursts.

Thus, the lack of any actual (or scheduled) UV mission with a high spatial (better than 0.1 arcsec) and intermediate (better than 100 km s $^{-1}$) spectral resolution long slit spectrograph and a high spatial resolution imager with high sensitivity will slow down the progress in our knowledge of starbursts, and of their impact on the origin and evolution of galaxies.

There are still many open questions in starburst galaxies that need to be answered through space UV observations. Some of them, listed below, have been proposed by experts in the field.

11.1. Dr. Veronique Buat

- GALEX will observe thousands (and even millions) of galaxies in its imaging mode and new classes of objects will certainly be discovered, an example are the local ($0.1 \leq z \leq 0.3$) UV luminous galaxies (Heckman et al., 2005). The UV spectroscopic follow-up of these GALEX sources detected in the broad NUV and FUV bands is of prime importance. Indeed, the FUV-NUV color only gives a very crude estimate of the shape of the UV continuum, especially at high redshift (Burgarella et al., 2005). The GALEX capabilities in the spectroscopic mode are only limited to the brightest objects. The combined effects of the star formation history, the IMF and the interstellar dust will only be quantified with intermediate resolution spectra to model the SED between 1000 and 3000 Å.
- Our knowledge of the UV spectral distribution of starburst galaxies relies almost entirely on the IUE observations of bright nearby starbursting objects. But the IUE aperture can cover only the central starburst of many of the most nearby galaxies. The recent photometric observations of GALEX not only confirm that the UV characteristics of the central starbursts are not valid for normal star forming galaxies (cf. Section 4) but also show that these central properties may well not be representative of the entire starbursting galaxies: the interplay of the star formation history and the dust attenuation are likely to modify the UV spectrum in a rather complex way varying from place to place even in starburst galaxies. Unfortunately, the spectral capabilities of GALEX (slitless mode) will not allow us to carry out a detailed analysis of the UV spectral energy distributions in various media. The ideal mode for such studies is integral field spectroscopy on a large field with medium resolution (or at least slit spectroscopy) in order to be also sensitive to the diffuse emission.

11.2. Dr. Rosa M. González Delgado and Dr. Luis Colina

- There are still many open questions related with the starburst-AGN connection. In particular, the role that young stellar clusters play in the energetics of AGNs; the frequency of nuclear young stellar clusters in AGNs; their properties (luminosities, masses, ages, IMF, metallicities, etc.). High spatial resolution spectroscopy is needed to isolate stellar clusters (of a few pc size) in the region where the dynamical influence of the black hole is significant, within 10 pc of the Seyfert nuclei (Ferrarese et al., 2001). Intermediate spectral resolution (better than 100 km s^{-1}) is needed to isolate the interstellar from the stellar component of the high ionization UV lines.

11.3. Dr. Claus Leitherer and Prof. Timothy Heckman

- Is there direct evidence for macroscopic turbulence in the ISM? Interstellar absorption lines are thought not to indicate gravity but rather stirring by winds and supernovae. Testing this hypothesis requires spectrographs with resolving power of tens of thousand and higher sensitivity than, e.g., STIS. Such data would allow us to probe the kinematic structure and morphology of the ISM and construct a kinematic model for all its phases, including the outflow.
- Do starburst galaxies enrich the IGM in metals? There is paramount evidence for the existence of large-scale galactic superwinds transporting the nucleosynthetic products out of the star-forming regions into the galaxy halos. The question of material actually escaping from starburst galaxies is still unanswered. The next generation of spectrographs will need higher sensitivity to probe starburst galaxy environments out to tens of kpc using background quasars. This could be a decisive test of the metal escape likelihood and IGM enrichment.

11.4. Dr. J. Miguel Mas-Hesse

- The emission of Ly α photons is of paramount importance to study star formation episodes at redshifts $z \geq 2$, when the line becomes visible in the optical range, and H α is already shifted to the NIR. As discussed in Section 8 the visibility of the line depends on several factors, including the distribution and kinematics of the neutral gas, the covering by dust,... Understanding the process of emission and absorption of Lyman alpha photons requires not only spectroscopy, but also imaging, especially if combined with H α imaging of the same region. Kunth et al. (2003) and Hayes et al. (2005, A&A, in press [astro-ph/0503320]) have shown that it is possible to obtain Ly α emission maps of starburst galaxies, though the instrumental setup of HST/ACS was not optimized for it.

The process of Ly α emission and absorption could be better understood by performing imaging observations of starburst galaxies at redshifts $z = 0$ to 1, looking for correlations between the visibility of the line and the morphology, evolutionary state, size or metallicity of the different galaxies. This could be achieved with an UV imaging camera with the adequate set of narrow/broad band filters covering the 1200–2400 Å range. Complementary H α observations at this redshift range could be obtained from ground.

Acknowledgements We are very grateful to Veronique Buat, Luis Colina, Timothy Heckman, Claus Leitherer, and Miguel Mas-Hesse for discussing the main open questions that need to be answered with UV instrumentations. We also thank Enrique Pérez, Miguel Cerviño,

Valentina Luridiana, Jorge Iglesias, Jesús Maiz, Guillermo Tenorio-Tagle and an anonymous referee for very useful comments that improved the presentation of the paper. This work has been supported by the Spanish Ministerio de Educación y Ciencia through the grant AYA-2004-02703.

References

- Aloisi, A., Savaglio, S., Heckman, T.M., Hoopes, C.G., Leitherer, C., Sembach, K.R.: *Astrophysical Journal* **595**, 760 (2003)
- Aloisi, A., Heckman, T.M., Hoopes, C.G., Leitherer, C., Savaglio, S., Sembach, K.R.: Starbursts near and far: from 30 Dor to Lyman Break Galaxies. *Astrophysics & Space Science Library* **329**, P2 (2005)
- Balzano, V.A.: *Astrophysical Journal* **268**, 602 (1983)
- Bianchi, L., Thilker, D., Burgarella, D. et al.: *Astrophysical Journal* **619**, L71 (2005)
- Bland-Hawthorn, J., Putman, M.E.: in Hibbard, J.E., Rupen, M.P., van Gorkom, J.H.: (eds), *ASP Conf. Series* **240**, p. 369 (2005)
- Buat, V., Burgarella, D., Deharveng, J.M., Kunth, D.: *A&A* **393**, 33 (2002)
- Buat, V., Iglesias-Páramo, J., Seibert, M. et al.: *Astrophysical Journal* **619**, L51 (2005)
- Burgarella, D., Buat, V., Small, T. et al.: *Astrophysical Journal* **619**, L63 (2005)
- Calzetti, D., Kinney, A.L.: *Astrophysical Journal* **399**, 39 (1992)
- Calzetti, D., Kinney, A.L., Storchi-Bergmann, T.: *Astrophysical Journal* **467**, 38 (1996)
- Calzetti, D.: *Astronomical Journal* **113**, 162 (1997)
- Cannon, J.M., Skillman, E.D., Sembach, K.R., Bomans, D.J.: *Astrophysical Journal* **618**, 247 (2005)
- Castellanos, M., Díaz, A.I., Tenorio-Tagle, G.: *Astrophysical Journal* **565**, L79 (2002)
- Cerviño, M., Mas-Hesse, J.M.: *A&A* **284**, 749 (1994)
- Chandar, R., Leitherer, C., Tremonti, C.A., Calzetti, D.: *Astrophysical Journal* **586**, 939 (2003a)
- Chandar, R., Leitherer, C., Tremonti, C.A.: *Astrophysical Journal* **604**, 153 (2003b)
- Chandar, R., Leitherer, C., Tremonti, C.A., Calzetti, D., Aloisi, A., Meurer, G.R., de Mello, D.: *Astrophysical Journal* **628**, in press, astro-ph/0505024 (2005)
- Charlot, S., Fall, M.: *Astrophysical Journal* **539**, 718 (2000)
- Cid Fernandes, R., Terlevich, R.: *272*, 423 (1995)
- Cid Fernandes, R., Heckman, T., Schmitt, H., González Delgado, R.M., Storchi-Bergmann, T.: *Astrophysical Journal* **558**, 81 (2001)
- Colina, L., González Delgado, R., Mas-Hesse, J.M., Leitherer, C., Jiménez-Bailón, E.: *Astrophysical Journal* **579**, 545 (2002)
- Conti, P., Leitherer, C., Vacca, W.: *Astrophysical Journal* **461**, L87 (1996)
- Daddi, E., Cimatti, A., Renzini, A., Fontana, A., Mignoli, M., Pozzetti, L., Tozzi, P., Zamorani, G.: *Astrophysical Journal* **617**, 746 (2004)
- Deharveng, J.-M., Buat, V., Le Brun, V., Milliard, B., Kunth, D., Shull, J.M., Gry, C.: *A&A* **375**, 805 (2001)
- de Grijs, R., González Delgado, R.M.: *Astrophysics & Space Science Library* **329** (2005)
- de Mello, D.F., Leitherer, C., Heckman, T.M.: *Astrophysical Journal* **530**, 251 (2000)
- Fanelli, M., M.N., O'Connal, R.W., Thuan, T.X.: *Astrophysical Journal* **334**, 665 (1988)
- Fernández-Soto, A., Lanzetta, K.M., Chen, H.-W.: *MNRAS* **342**, 1215 (2003)
- Ferrarese, L., Pogge, R.W., Peterson, B.M., Merritt, D., Wandel, A., Joseph, C.L.: *ApJ* **555**, 79 (2001)
- Gabel, J.R., Bruhweiler, F.C.: *Astronomical Journal* **124**, 737 (2002)
- Giallongo, E., Cristiani, S., D'Odorico, S., Fontana, A.: *Astrophysical Journal* **568**, L9 (2002)
- Goldader, J.D., Meurer, G., Heckman, T.M., Seibert, M., Sanders, D.B., Calzetti, D., Steidel, C.C.: *Astrophysical Journal* **568**, 651 (2002)
- González Delgado, R.M., Leitherer, C., Heckman, T.: *Astrophysical Journal* **489**, 601 (1997)
- González Delgado, R.M., Leitherer, C., Heckman, T., Lowenthal, J.D., Ferguson, H.C., Robert, C.: *Astrophysical Journal* **495**, 698 (1998a)
- González Delgado, R.M., Heckman, T., Leitherer, C., Meurer, G., Krolik, J., Wilson, A.S., Kinney, A., Koratkar, A.: *Astrophysical Journal* **505**, 174 (1998b)
- González Delgado, R.M., García-Vargas, M.L., Goldader, J., Leitherer, C., Pasquali, A.: *Astrophysical Journal* **513**, 707 (1999)
- González Delgado, R.M., Pérez, E.: *MNRAS* **317**, 64 (2000)
- González Delgado, R.M., Heckman, T., Leitherer, C.: *Astrophysical Journal* **546**, 845 (2001)
- González Delgado, R.M., Leitherer, C., Stasinska, G., Heckman, T.M.: *Astrophysical Journal* **580**, 824 (2002)
- González Delgado, R.M., Cid Fernandes, R., Pérez, E., Martins, L.P., Storchi-Bergmann, T., Schmitt, H., Heckman, T., Leitherer, C.: *Astrophysical Journal* **605**, 127 (2004)
- Gordon, K.D., Calzetti, D., Witt, A.N.: *Astrophysical Journal* **487**, 625 (1997)
- Hartmann, L.W., Huchra, J.P., Geller, M.J., O'Brien, P., Wilson, R.: *Astrophysical Journal* **326**, 101 (1988)
- Heckman, T.M., Leitherer, C.: *Astronomical Journal* **114**, 69 (1997a)
- Heckman, T.M., González-Delgado, R., Leitherer, C., Meurer, G.R., Krolik, J., Wilson, A.S., Koratkar, A., Kinney, A.: *Astrophysical Journal* **482**, 114 (1997b)
- Heckman, T.M., Robert, C., Leitherer, C., Garnett, D.R., van der Rydt, F.: *Astrophysical Journal* **503**, 646 (1998)
- Heckman, T.M.: *ASPC* **148**, 127 (1998)
- Heckman, T., Sembach, K.R., Meurer, G., Strickland, D.K., Martin, C.L., Calzetti, D., Leitherer, C.: *Astrophysical Journal* **554**, 1021 (2001a)
- Heckman, T., Sembach, K.R., Meurer, G., Leitherer, C., Calzetti, D., Martin, C.L.: *Astrophysical Journal* **558**, 56 (2001b)
- Heckman, T.M.: *Astrophysic in the Far-Ultraviolet*, *ASP Conf. Series*. astro-ph/0410383 (2004)
- Heckman, T.M.: Starbursts: From 30 doradus to lyman break galaxies. *Astrophysics & Space Science Library* **329**, 3 (2005)
- Heckman, T., Hoopes, C.G., Seibert, M. et al.: *Astrophysical Journal* **619**, 35 (2005)
- Ho, L., Filippenko, A.: *Astrophysical Journal* **472**, 600 (1996)
- Ho, L., Filippenko, A., Sargent, W.: *Astrophysical Journal Supplement* **112**, 315 (1997)
- Hoopes, C.G., Heckman, T.M., Strickland, D.K. et al.: *Astrophysical Journal* **619**, L99 (2005)
- Hurwitz, M., Jelinsky, P., Van Dyke Dixon, W.: *Astrophysical Journal* **481**, L31 (1997)
- Jamet, L., Pérez, E., Cerviño, M., Stasinska, G., González Delgado, R.M., Vilchez, J.M.: *A&A* **426**, 399 (2005)
- Johnson, K.E., Leitherer, C., Vacca, W., Conti, P.S.: *Astrophysical Journal* **120**, 1273 (2000)
- Keel, W., Holberg, J.B., Treuthardt, P.M.: *Astronomical Journal* **128**, 211 (2004)
- Kinney, A.L., Bohlin, R.C., Calzetti, D., Panagia, N., Wyse, R.F.G.: *Astrophysical Journal Supplement Series* **86**, 5 (1993)
- Kudritzki, R.-P., Puls, J., Lennon, D.J., Venn, K.A., Reetz, J., Najarro, F., McCarthy, J.K., Herrero, A.: *A&A* **350**, 970 (1999)
- Kunth, D., Sargent, W.L.W.: *Astrophysical Journal* **300**, 496 (1986)
- Kunth, D., Lequeux, J., Sargent, W.L.W., Viallefond, F.: *A&A* **282**, 709 (1994)

- Kunth, D., Mas-Hesse, J.M., Terlevich, E., Terlevich, R., Lequeux, J., Fall, S.M.: *A&A* **334**, 11 (1998)
- Kunth, D., Leitherer, C., Mas-Hesse, J.M., Ostlin, G., Petrosian, A.: *Astrophysical Journal* **597**, 263 (2003)
- Lebouteiller, V., Kunth, D., Lequeux, J., Lecavelier des Etangs, A., Désert, J.-M., Hébrard, G., Vidal-Madjar, A.: *A&A* **415**, 55 (2004)
- Lecavelier des Etangs, A., Désert, J.-M., Kunth, D., Callejo, G., Ferlet, R., Hébrard, G., Lebouteiller, V.: *A&A* **413**, 131 (2004)
- Leitherer, C.: Starbursts near and far: From 30 Dor to Lyman break galaxies. *Astrophysics & Space Science Library* **329**, 89 (2005)
- Leitherer, C., Robert, C., Drissen, L.: *Astrophysical Journal* **401**, 596 (1992)
- Leitherer, C., Heckman, T.M.: *Astrophysical Journal Supplement Series* **96**, 9 (1995a)
- Leitherer, C., Ferguson, H.C., Heckman, T.M., Lowenthal, J.D.: *Astrophysical Journal* **454**, 19 (1995b)
- Leitherer, C., Robert, C., Heckman, T.M.: *Astrophysical Journal Supplement Series* **99**, 173 (1995c)
- Leitherer, C., Vacca, W.D., Conti, P.S., Filippenko, A.V., Robert, C.: *Astrophysical Journal* **465**, 717 (1996)
- Leitherer, C. et al.: *Astrophysical Journal Supplement Series* **123**, 3 (1999)
- Leitherer, C., Leao, J.R.S., Heckman, T.M., Pettini, M., Robert, C.: *Astrophysical Journal Supplement Series* **550**, 724 (2001)
- Leitherer, C., Li, I.-H., Calzetti, D., Heckman, T.M.: *Astrophysical Journal* **140**, 303 (2002)
- Lequeux, J., Kunth, D., Mas-Hesse, J.M., Sargent, W.L.W.: *A&A* **301**, 18 (1995)
- MacLow, M.-M., McCray, R., Norman, M.: *Astrophysical Journal* **337**, 141 (1989)
- Madau, P., Ferguson, H.C., Dickinson, M.E., Giavalisco, M., Steidel, C.C., Fruchter, A.: *MNRAS* **283**, 1388 (1996)
- Maeder, A., Conti, P.: *ARA&A* **32**, 227 (1994)
- Malkan, M., Webb, W., Konopacky, Q.: *Astrophysical Journal* **598**, 878 (2003)
- Maoz, D., Koratkar, A., Shields, J.C., Ho, L.C., Filippenko, A.V., Sternberg, A.: *Astronomical Journal* **116**, 55 (1998)
- Maoz, D., Nagar, N.M., Falcke, H., Wilson, A.S.: *Astrophysical Journal* **625**, 699 (2005)
- Martin, D. et al.: *Astrophysical Journal* **619**, L1 (2005)
- Mas-Hesse, J.M., Kunth, D.: *A&AS* **88**, 399 (1991)
- Mas-Hesse, J.M., Kunth, D.: *A&A* **349**, 765 (1999)
- Mas-Hesse, J.M., Kunth, D., Tenorio-Tagle, G., Leitherer, C., Terlevich, R.J., Terlevich, E.: *Astrophysical Journal* **598**, 858 (2003)
- Mehlert, D., Tapken, C., Appenzeller, I., Noll, S., de Mello, D., Heckman, T.M.: Starbursts: From 30 Doradus to Lyman Break Galaxies. *Astrophysics & Space Science Library* **329**, 299 (2005)
- Meier, D., Terlevich, R.: *Astrophysical Journal* **246**, L109 (1981)
- Meurer, G.: *Nature* **375**, 742 (1995)
- Meurer, G.R., Heckman, T.M., Leitherer, C., Kinney, A., Robert, C., Garnett, D.R.: *Astronomical Journal* **110**, 2665 (1995)
- Meurer, G.R., Heckman, T.M., Lehnert, M.D., Leitherer, C., Lowenthal, J.: *Astronomical Journal* **114**, 54 (1997)
- Meurer, G.R., Heckman, T.M., Calzetti, D.: *Astrophysical Journal* **521**, 64 (1999)
- Miralda-Escudé, J., Ostriker, J.P.: *Astrophysical Journal* **350**, 1 (1990)
- Noll, S., Mehlert, D., Appenzeller, I. et al.: *A&A* **418**, 885 (2004)
- Pettini, M., Lipman, K.: *A&A* **297**, L63 (1995)
- Pettini, M., Steidel, C.C., Adelberger, K.L., Dickinson, M., Giavalisco, M.: *Astrophysical Journal* **528**, 96 (2000)
- Pettini, M., Shapley, A.E., Steidel, C.C. et al.: *Astrophysical Journal* **554**, 981 (2001)
- Pettini, M., Rix, S.A., Steidel, C.C., Adelberger, K.L., Hunt, M.P., Shapley, A.E.: *Astrophysical Journal* **569**, 742 (2002)
- Rosa, M.R., Benvenuti, P.: *A&A* **291**, 1 (1994)
- Rix, S.A., Pettini, M., Leitherer, C., Bresolin, F., Kudritzki, R.-P., Steidel, C.C.: *Astrophysical Journal* **615**, 98 (2004)
- Robert, C., Leitherer, C., Heckman, T.M.: *Astrophysical Journal* **418**, 749 (1993)
- Robert, C., Pellerin, A., Aloisi, A., Leitherer, C., Hoopes, C., Heckman, T.M.: *Astrophysical Journal Supplement Series* **144**, 21 (2003)
- Savage, B.D., Sembach, K.R.: *Astrophysical Journal* **379**, 245 (1991)
- Savaglio, S., Glazebrook, K., Abraham, R.G. et al.: *Astrophysical Journal* **602**, 51 (2004)
- Schaerer, D.: *A&A* **382**, 28 (2002)
- Seibert, M., Martin, C.D., Heckman, T.M. et al.: *Astrophysical Journal* **619**, L55 (2005)
- Sekiguchi, K., Andersson, K.S.: *A&A* **94**, 644 (1987)
- Shapley, A.E., Steidel, C.C., Pettini, M., Adelberger, K.L.: *Astrophysical Journal* **588**, 65 (2003)
- Steidel, C., Giavalisco, M., Pettini, M., Dickinson, M., Adelberger, K.L.: *Astrophysical Journal* **462**, L17 (1996)
- Steidel, C., Pettini, M., Adelberger, K.L.: *Astrophysical Journal* **546**, 665 (2001)
- Steidel, C.C., Shapley, A.E., Pettini, M., Adelberger, K.L., Erb, D.K., Reddy, N.A., Hunt, M.P.: *Astrophysical Journal* **604**, 534 (2004)
- Tenorio-Tagle, G.: *Astronomical Journal* **111**, 1641 (1996)
- Tenorio-Tagle, G., Muñoz-Tuñon, C.: *Astrophysical Journal* **478**, 134 (1996)
- Tenorio-Tagle, G., Silich, S.A., Kunth, D., Terlevich, E., Terlevich, R.J.: *309*, 332 (1999)
- Terlevich, R.: *RM×AC* **6**, 1 (1997)
- Terlevich, R., Melnick, J., Masegosa, J., Moles, M., Copetti, M.V.F.: *A&A* **91**, 285 (1991)
- Terlevich, E., Díaz, A.I., Terlevich, R., García Vargas, M.L.: *MNRAS* **260**, 3 (1993)
- Thuan, T.X., Lecavelier des Etangs, A., Izotov, Y.I.: *Astrophysical Journal* **565**, 941 (2002)
- Tran, H.: *Astrophysical Journal* **440**, 565 (1995)
- Tremonti, C.A., Calzetti, D., Leitherer, C., Heckman, T.M.: *Astrophysical Journal* **555**, 322 (2001)
- Vacca, W., Robert, C., Leitherer, C., Conti, P.S.: *Astrophysical Journal* **444**, 647 (1995)
- Valls-Gabaud, D.: *Astrophysical Journal* **419**, 7 (1993)
- Vázquez, G.A., Leitherer, C., Heckman, T.M., Lennon, D.J., de Mello, D.F., Meurer, G.R., Martin, C.: *Astrophysical Journal* **1600**, 162 (2004)
- Walborn, N.R.: International Astronomical Union. Symposium The stellar content of 30 doradus derived from spatially integrated ultraviolet spectra: A test of spectral synthesis models **148**, 145 (1991)
- Weedman, et al.: *Astrophysical Journal* **248**, 105 (1981)
- Whitmore, B.C., Schweizer, F., Leitherer, C., Borne, K., Robert, C.: *Astronomical Journal* **106**, 1354 (1993)
- Williams, R.E. et al.: *Astronomical Journal* **112**, 1335 (1996)

A View to the Future: Ultraviolet Studies of the Solar System

Noah Brosch · John Davies · Michel C. Festou[†] ·
Jean-Claude Gérard

Received: 9 August 2005 / Accepted: 21 November 2005
© Springer Science + Business Media B.V. 2006

Abstract We discuss the status of ultraviolet knowledge of Solar System objects. We begin with a short historical survey, followed by a review of knowledge gathered so far and of existing observational assets. The survey indicates that UV observations, along with data collected in other spectral bands, are necessary and in some cases essential to understand the nature of our neighbors in the Solar System. By extension, similar observations are needed to explore the nature of extrasolar planets, to support or reject astro-biology arguments, and to compose and test scenarios for the formation and evolution of planetary systems.

We propose a set of observations, describing first the necessary instrumental capabilities to collect these and outlining what would be the expected scientific return. We identify two immediate programmatic requirements: the establishment of

a mineralogic database in the ultraviolet for the characterization of planetary, ring, satellite, and minor planet surfaces, and the development and deployment of small orbital solar radiation monitors. The first would extend the methods of characterizing surfaces of atmosphere-less bodies by adding the UV segment. The latter are needed to establish a baseline against which contemporaneous UV observations of Solar System objects must be compared.

We identify two types of UV missions, one appropriate for a two-meter-class telescope using almost off-the-shelf technology that could be launched in the next few years, and another for a much larger (5–20 meter class) instrument that would provide the logical follow-up after a decade of utilizing the smaller facility.

Keywords Planets · Comets · Solar system · Ultraviolet

[†]Deceased 11 May 2005

Dedication: Michel Festou, our co-author and a very important contributor to this paper, passed away while this paper was being completed. We dedicate it to his memory

N. Brosch
The School of Physics and Astronomy, Beverly and Raymond Sackler Faculty of Exact Sciences, Tel Aviv University, Tel Aviv 69978, Israel

J. Davies
UKATC, Royal Observatory, Blackford Hill, Edinburgh EH9 3HJ, UK

M. C. Festou
Observatoire Midi-Pyrénées 14, avenue E. Belin 31400 Toulouse, France

J.-C. Gérard
Laboratoire de Physique Atmosphérique et Planétaire, Université de Liège, allée du 7 aout, 4000 Liège, 94720 Belgium

Introduction

The UV window extends from 20 to 400 nm. It covers the spectral domain where atoms have most of their resonance lines and where simple ions and molecules have their fluorescence transitions. This is also the region where most molecules and atoms are photodissociated and photoionized. Below 100 nm is the spectral segment where most rare gases have their resonance lines. Solar system objects can be observed in this spectral region either because they harbour hot or violent environments or because the solar light that is being absorbed and then scattered by them contains thousands of lines below 200 nm.

One of the basic questions in modern astrophysics is how planets “work,” how planetary systems originated, and how life emerged on Earth. By studying our Solar System we are linking ‘local’ studies to the issue of the existence of

Earth-like extrasolar planets and the conditions expected on their surfaces. The discovery of biomarkers on Earth analogs is the essence of the search for extra-terrestrial life addresses the question “are we alone in the Universe?” These are the basic questions being asked by NASA and ESA: “How did our Earth and our Solar System evolve, where are we in the Universe, where are we going, and where did life come from?”

Planets and other minor bodies represent the end stage of the Solar System’s formation and their present state is the result of numerous accretion, coalescence, and evolution processes. The various components are inter-related: planets were formed through planetesimal accretion, evidence of which remains in the form of asteroids and other bodies such as Trans-Neptunian Objects (TNOs). Some comets are fragments of TNOs; others come from the Oort cloud, both in very cold and protective environments of the Solar System. Thus the minor bodies of the Solar System have retained information that allows us to study the primordial cloud that formed our Solar System some 4.5 Gyrs ago. The traditional rocky asteroids are intermediate objects, between planetesimals and fully-grown planets, and thus contain information on the stage of nebular matter condensation prior to the planet accretion. The collisional history of the Solar System can be investigated by studying the internal structures and size distributions of asteroids, TNOs and Near Earth Objects (NEOs). Finally, the interplanetary dust is mostly the result of the “grinding down” of Main Belt asteroids, probably TNO debris, and ejecta from cometary nuclei.

While many objectives of solar system research can be achieved by optical and near-IR (nIR) imaging, surface mineralogic characterization requires a wide spectral range including the UV. Observations of planetary aurorae from the Earth are impossible, owing to the brightness of the sunlit planetary disks and the lack of contrast at visible and nIR wavelengths. Planetary missions with UV capabilities (such as the Mercury Atmospheric and Surface Composition Spectrometer (MASCS) on the Mercury probe MESSENGER, and the ALICE instrument on the Pluto/Kuiper Belt New Horizons mission) are rare and far apart; so it is necessary to consider Solar System studies in the context of general-purpose astronomical payloads. Even though a UV space telescope might not be fully dedicated to planetary astronomy, a complement of valuable targets exists and Solar System observations can be made without compromising the astrophysical goals of such a mission.

Planetary studies require synoptic observations over periods of time ranging from a single revolution (hours to days), to the length of a comet passage through the inner planetary region and the seasons of telluric planets (months), to orbital revolutions about the Sun and to seasons on giant planets and their satellites (months to years). Since some planetary phenomena, such as aurorae, are directly linked to the solar

activity, studies should span one or more 11-year solar cycles. The variability of Solar System objects, sometimes on short time scales, underlines the need for long-term studies to separate intrinsic from evolution-driven properties of planetary bodies and comets.

For a given aperture size, UV astronomy from space can achieve much higher spatial resolution than from the ground because of the absence of the smearing effect of the Earth’s atmosphere (“seeing”) and because of the smaller diffraction limit of UV telescopes. Present-day 8-m and larger ground-based optical telescopes, equipped with adaptive optics (AO) and with fields of view restricted to the “coplanarity patch,” offer the same angular resolution as a two-meter space UV telescope but are restricted to the optical-near IR bands and are hampered by the natural sky brightness. The sky background at UV wavelengths is darker by about five magnitudes than at the best ground-based observatories (O’Connell 1987) and allows observations of very faint objects, in particular those with extended very low surface brightness features.

Why argue now for UV astronomy? Few instruments that allow UV planetary observations are presently available and none will be available in the near future as the few existing missions reach their design and even extended lifetimes. The heritage of past missions, and the expertise of scientists in designing, performing, and analyzing UV planetary observations are dwindling as individuals reach the end of their active careers. New scientists refrain from entering a field devoid of a promise to access cutting-edge research instrumentation. There is need to continue synoptic observations of variable sources even after specific planetary probes complete their missions, and it is necessary to maintain the know-how of observing and working with specific data sets.

Review of achievements

The study of the UV emission from Solar System bodies, which started as an exploratory task in the middle of the last century, proved useful for the understanding of planetary atmospheres and of plasma phenomena. Results obtained about distant bodies were applied to the understanding of our Earth. Spectroscopy of comets in the UV revealed the presence of new compounds and clarified the mechanisms accounting for their presence.

Key missions of solar system UV exploration

Rocket flights of (very) short durations provided the first exploratory data and flights of that nature still remain useful for developmental and testing purposes. As late as 2004 a Black Brant rocket lofted a telescope and spectrometer to record the UV emission from Mercury. Modern payloads

Table 1 Past space missions that performed UV observations of Solar System bodies

Dates	Mission	Agency	Instrument	Resolution	Range (nm)	Comment
1968	OAO-2	NASA	Photometer + spectrometer	~100	100–400	H coma of Comet Tago-Sato-Kosaka
1970	OGO-5	NASA	Lyman alpha photometer	Low	121.6	Interplanetary H. Comets Bennett and P/Encke
1972	TD-1A	ESRO	S-59 + S2/68 Spectrometers	~70	133–280	UV sky survey
1975	ASTP	NASA	EUV Telescope	Imager	5–150	Manned space flight
1977–1989	Voyager 1/2	NASA	UV Spectrometer	~40	40–180	Planetary Mission
1972–1981	OAO-3 Copernicus	NASA	UV Telescope	~200	75–300	Giant Planets and Comets
1983	Astron	USSR/CNES	Spectrometer	~200	150–350	P/Halley
1993&96	ASTRO-SPAS	NASA/DARA	ORPHEUS	~5000 Spectrometer	39–91	Shuttle Free Flyer
1993&96	ASTRO-SPAS	NASA/DARA	IMAPS	~200,000 Spectrometer	95–115	Shuttle Free Flyer
1990&95	ASTRO 1/2	NASA	HUT	~100	45–185	Venus, Mars-Polarimetry
1990&95	ASTRO 1/2	NASA	WUPPE	~100	140–320	Moon, Mars, Io, Halley
1990&95	ASTRO 1/2	NASA	UIT	Imager	120–300	
1978–96	IUE	NASA/ESA	UV Spectrometer	~50 and ~5000	115–320	Giant Planets, Aurora, 50+ Comets
1992–2000	EUVE	NASA	EUV Spectrometer and Imager	~400	8–75	Sky Survey & follow-up, comets, Venus, Jupiter
1989–2003	HST	NASA/ESA	WFPC, GHRS	Imaging, 2000–80000	>115	Superb images
1998–2004	HST	NASA/ESA	STIS	100–100000	115–310	All planetary objects
2000–	FUSE	NASA	High Resolution Spectrometer	~27,000	90–120	H ₂ on Mars, comets

Not included in this list are several small experiments carried on various missions such as Cosmos 51, 215, 262, Apollo 16, ANS, D2B-Aura, Skylab and Soyuz/Salyut, as well as short-duration rocket flights.

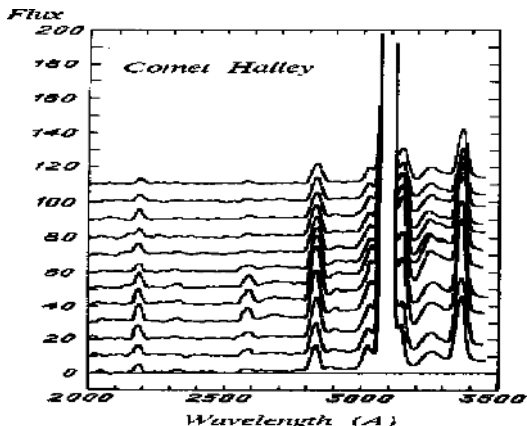


Fig. 1 Time series observation of the UV spectrum of P/Halley obtained by the ASTRON orbital observatory (see Table 1) showing the strong OH feature at 308 nm.

[<http://www.crao.crimea.ua/astron/astron.html>]

can achieve more than a simple exploration but still lack the temporal coverage characteristics of Solar System object phenomena.

The Voyager spectrometers were non-imaging, with mechanical collimators defining their fields of view. Their spectral coverage was from 40 to 180 nm, the throughput was rather low and no spatial information was available. Even so, their results regarding the properties of giant planet

atmospheres, obtained by occultation techniques or in direct “airglow” mode, were unique because of the proximity of the instruments to their targets.

NASA’s Copernicus satellite (Orbiting Astronomical Observatory-3, launched in 1972 and operated till February 1981) performed Far-UV (FUV) investigations and allowed the detection of important atomic and molecular species of the local interstellar medium, among which molecular hydrogen and deuterium. OAO-3 offered a unique way to study the upper atmospheres of planets and key components of cometary atmospheres.

Copernicus was followed by ORFEUS (Orbiting and Retrievable Far and Extreme Ultraviolet Spectrometer) and by HUT (Hopkins Ultraviolet Telescope), both Shuttle-launched and retrievable payloads. HUT flew twice on the ASTRO platform for missions of order 12 days, along with WUPPE (Wisconsin Ultraviolet Photo-Polarimeter Experiment), the only instrument that has provided polarization measurements in the UV. WUPPE was used to study the Moon, Mars, Io, and comet Halley. HUT observed Jupiter, Venus and Mars. IMAPS (Interstellar Medium Absorption Profile Spectrometer) operated, as ORFEUS did, on board the AstroSPAS space shuttle-borne platform (1993).

Most missions mentioned above were limited in duration or in the observing time allocated for Solar System studies.

Their role was, by necessity, mainly exploratory. The exciting results indicated the need for missions of much longer duration.

The spectroscopic results obtained by the International Ultraviolet Explorer (IUE) spacecraft with its 45-cm telescope surpass by far those obtained by any other spacecraft, perhaps with the exception of the Hubble Space Telescope (HST). IUE was launched in January 1978 and its three-year mission was extended year after year until it was deliberately terminated in September 1996. These mission extensions provided much of the most valuable science return. IUE performed comparative studies of auroral activity at Jupiter, Saturn, and Uranus and demonstrated the impact of solar wind variations on the brightness of the Jovian aurora. The amount of hydrocarbon absorption in auroral spectra was used to determine the FUV color ratio, from which the energy of the primary auroral electrons could be inferred. The spectra revealed the existence of new sulphur-bearing compounds in cometary spectra (S_2 in comet IRAS-Araki-Alcock; CS_2 in numerous comets) and investigated the abundance of water and carbon compounds such as CO and CO_2 , providing a database on gas production rates in over 50 comets that is only surpassed in size by OH 18 cm radio surveys and by the ground-based survey of the UMD-Lowell group (A'Hearn 1995).

The field of Extreme UV (EUV) observations was covered by the Extreme Ultra Violet Explorer (EUVE) satellite, launched in 1992 and operated until 2000. EUVE detected emission from comets resulting from charge-exchange reactions with highly charged Solar wind particles, observed the dayglow of the atmosphere of Venus, showed the existence of EUV emission from the Full Moon that indicated differences on the local albedo, and detected helium emission from the atmosphere of Jupiter following the impact of km-sized disruption fragments from D/Shoemaker-Levy-9 (SL9).

The workhorse of solar system studies in the field of high-resolution imaging, or observations in spectral domains not visible from the Earth's atmosphere, has been the Hubble Space Telescope (HST), a 2.4-meter telescope for the UV-to-NIR domain launched in 1990. The HST has produced the best imaging database of other celestial bodies obtained from the Earth's vicinity. The HST results range wide, from atmospheric studies of the giant and the terrestrial-like planets, to imaging the dynamics of Jupiter's and Saturn's aurora down to 10-s variations and monitoring the energy of the impinging auroral electrons in regions connected to different magnetospheric plasma sources, to single-pixel imaging of Sedna and the coarse mapping of the surfaces of Pluto, 1 Ceres and 4 Vesta. HST tracked the disintegration of comets (SL9 and C/1999 S4 (LINEAR)) and found ozone on Ganymede and molecular oxygen in the atmosphere of Europa. With the demise in 2004 of the Space Telescope Imaging Spectrometer (STIS) and with a refurbishing mission that could repair

or replace STIS doubtful, the lack of a general-purpose UV spectroscopic facility is becoming acute.

The Far Ultraviolet Spectroscopic Explorer (FUSE) satellite was launched in 2000; it covers the spectral range from 90.5 to 119.5 nm with reasonably high resolution ($R = 24,000$ – $30,000$) and is still operating when these lines are written. FUSE has a 352 by 387 mm² aperture and a PSF of 1.5 arcsec. The FUSE spectral range was chosen to contain the most important interstellar and hot environment lines of deuterium, H_2 , and lines arising from high level ionization states of the most abundant atoms in the universe (O, C, N, . . .). FUSE has a relatively low sensitivity, with effective areas of 20 cm² at 90 nm and 80 cm² at 120 nm, although this is 10,000 times the sensitivity of Copernicus and the resolution is much better than any of the space FUV instrumentation built before. Among the achievements of FUSE in the field of Solar system studies we count the discovery of H_2 on Mars (Krasnopolsky and Feldman 2001), presumably the result of photo-dissociation of water and subsequent molecular formation at mid-altitudes of the Martian atmosphere, the measurement of the D-to-H ratio from which the existence of an old global ocean on Mars can be inferred, the detection of numerous new lines in comet spectra and an unprecedented coverage of the auroral phenomena in the giant planets. The measured intensity distribution amongst H_2 lines affected by self-absorption was used to infer the pressure level of the Jovian aurora, which was shown to be quite different from Saturn's case.

The FUSE spectra of comet C/2001 A2 LINEAR provided the first high resolution EUV spectrum of a comet. In addition to the H_2 lines, many new lines have been discovered. Quite a few of these features are still unidentified and require more work to be understood, and some of them likely are due to electron impact excitation.

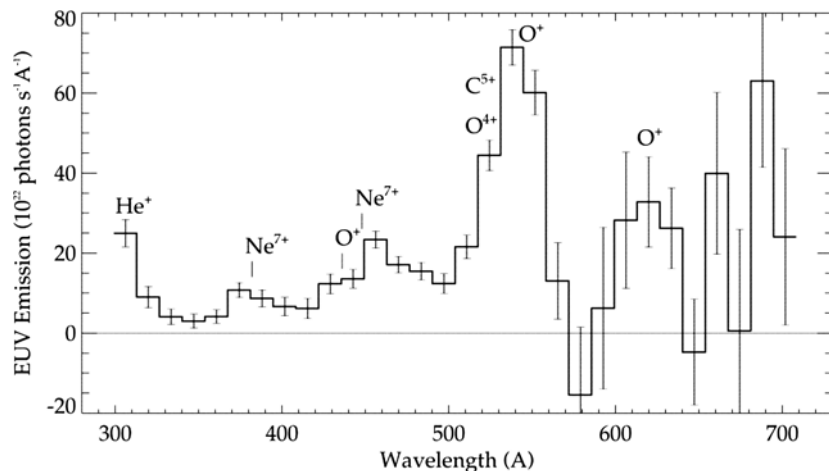
Key results from past UV astronomy missions

Planetary atmospheres and magnetospheres

Results from comparative studies of planetary atmospheres indicate that the Solar System family can be separated into four groups:

1. Bodies with Nitrogen dominated atmospheres (Earth, Titan, Triton, Pluto)
2. Bodies with carbon dioxide dominated atmospheres (Venus and Mars)
3. Hydrogen & Helium dominated giant planets (Jupiter, Saturn, Uranus, and Neptune)
4. Bodies with thin atmospheres, separable further into three subgroups:
 - a. Rocky surfaces (Mercury, the Moon)
 - b. Volcanic bodies (Io)
 - c. Icy surfaces (Europa, Ganymede, Callisto, Charon)

Fig. 2 The EUV long wave spectrum of comet Hyakutake barely shows the emission lines originating from charge-exchange reactions with solar wind particles (source Krasnopolksy and Mumma 2001). The need for better spectral resolution is evident



Studies of the atmospheres of Venus and Mars have helped our understanding of the greenhouse effect and the impact of the continuous release of anthropogenic gases such as CO₂ into the Earth's atmosphere. The CO₂-dominated planets can only be studied in the UV, as telluric CO and CO₂ features severely limit what can be observed from the ground. The cycle of water and water-dissociation products, in particular the deuterated species, allows one to investigate the exchange of water between the surface and the atmosphere and, ultimately, the escape of atmospheric constituents. Recent FUSE observations of the H₂ and D lines showed that in the past Mars was probably covered by a thick water ocean (Yung 1998; Krasnopolksy 2003).

The NO ultraviolet night airglow on Venus was discovered in 1978 by the Pioneer-Venus UV spectrometer; it was followed in 1989 by the detection of the UV day glow. The existence of a suitable orbital platform could have allowed synoptic observations of these phenomena. On 24 June 1999 the Cassini spacecraft flew by Venus. Prominent features detected by the UVIS instrument include the HI 121.6 nm (Ly α) line, the OI 130.4 and 135.6 nm, the CI 156.1 and 165.7 nm multiplets, and the CO Fourth Positive bands. Weaker features of NI, CI, CII, OI and CO were also present. The EUV spectrum contained well-defined features at 58.4 nm (HeI), 83.3 nm (OII), 98.9 nm (OI), and 102.6 nm (HI Ly β). Weaker emissions included OI 104.1 nm, CO (C-X) 108.8 nm, NI 113.5 nm, and a blend of CO (B-X) and OI near 115 nm.

The composition of the upper atmosphere of the giant planets indicates how these planets and their atmospheres originated and evolved. Studies of giant planets in our Solar System provide the knowledge base against which such observations must be interpreted. As an example, let us mention the spectacular Ly α absorption produced by the exoplanet HD209458b during its transits in front of its star disc (Vidal-Madjar et al. 2003).

Images of Jupiter and Saturn auroral emissions with the constantly improving sensitivity of the HST cameras have

opened a new era in the understanding of the interaction of giant planets with their magnetic environment. They have revealed the general morphology of the precipitation patterns and their dynamical behaviour. Our knowledge of the complex interaction between the solar wind, the giant planets' magnetospheres, the current systems flowing through these magnetised environments and their signature in the planet ionospheres has thus dramatically improved. In particular, Jupiter's main auroral oval probably results from breakdown of outward corotating and drifting plasma from Io, which drives currents between Jupiter's magnetosphere and ionosphere (Bunce and Cowley, 2001; Grodent et al., 2003). In the region of upward current (downward-moving electrons), field-aligned potentials accelerate electrons to auroral energies, producing the main auroral oval emissions.

Based on HST FUV images, a similar concept has recently been proposed in the case of Saturn. It is now believed that the auroral oval at Saturn corresponds to a ring of upward current bounding the region of open and closed field lines. Following extensive study of Earth's aurora, we now have three cases of magnetosphere-ionosphere coupling whose most dramatic aspect is the aurora. The discovery of the FUV magnetic footprints of Io, Ganymede and Europa, and of Io's trailing tail (Clarke et al., 2002) generated new theories on the acceleration of electrons in the flux tubes and their time stability. Spectral observations of the FUV-EUV H₂ line intensity distribution have indicated that the global thermal structure of the giant planet upper atmospheres is strongly controlled by the redistribution of the energy flux occurring after the precipitation of magnetospheric plasma (Grodent et al., 2002).

Cometary physics

The major result of the early years of exploration in the newly opened UV window was the detection of water dissociation products. The HI Lyman alpha (Ly α) emission was studied

in detail by Bertaux et al. (1973) and Keller (1973a, 1973b) who revealed the existence of hot hydrogen components in the coma resulting from the photodissociation of water molecules. This naturally led to the proposal by Blamont and Festou (1974) and Keller and Lillie (1974), who measured the scalelength and the production of OH in comet Kohoutek (1973 XII) and Bennett (1970 II), respectively, that in comets the water molecule was the parent of most observed hydrogen atoms and OH radicals.

The use of UV and EUV space telescopes allowed the detection of important secondary parent molecule emissions such as those of CO, S₂ and CS₂ and the CO Cameron bands, a proxy for the CO₂ molecule. Feldman et al. (2002) used FUSE on C/2000 A2 (LINEAR) to detect new bands of CO at 98.9 and 198.8 nm and also the H₂ emission, as this molecule is a natural breakdown product of water. The overall picture of a comet that emerged around 1980 was that water was indeed the most abundant nuclear species, as first speculated by Whipple (1950).

The measurement of the elemental composition of the UV coma, containing all the most abundant atoms, numerous ions and simple molecules that are dissociation products of nuclear species, yields the elemental composition of the nucleus. As a consequence, as shown by Huebner and Benkhoff (1999), it is possible to investigate the water/CO mixing ratio variation with heliocentric distance. The measurement of the major compound production rates, and their evolution with time, delivers fundamental information on how parent molecules are stored in the comet nuclei and released into the comae upon heating by sunlight.

The observation of species evaporated from the dust in Sun-grazing comets and the discovery of over 700 such comets by SOHO, particularly by the visible-light coronagraphs (e.g., Biesecker et al., 2002), demonstrates the value of observations at low solar elongations. In the UV domain, the results obtained by the SOHO/SWAN instrument (Mäkinen et al., 2001) show the power of an all-sky Ly α instrument to discover and study comets with low water production rates. The lack of complementary follow-ups, which would have required the use of other instruments capable of low-elongation observations, is obvious. In such cases, spectroscopic observations would likely reveal the presence of many new lines that are usually unseen because of the weakness of the exciting flux.

Asteroids and planetary surfaces

The reflectivities of planet, asteroid and satellite surfaces are important ingredients in modeling their thermal evolution (solar heating vs. cooling to space), in understanding the weather in these planets, in devising scenarios for the ‘chemical’ weathering of their surfaces, etc.

Stern et al. (1991) obtained some interesting results regarding the UV reflectivity of Triton and of the binary Pluto/Charon from HST observations, following the optical band surface “mapping” of the two bodies through observations of the mutual events’ series in 1985–1990 (Young et al., 2001). Triton’s reddish color in the optical does not continue into the UV. Instead, a blue upturn appears shortward of 275 nm. Charon, on the other hand, is grey in the UV as well as in the optical. The differences among these bodies, which are at similar heliocentric distances and probably evolved together, are not currently understood and require more observations.

The UV spectra of Pluto and Charon obtained with the HST (e.g., Krasnopolsky 2001) emphasize the difficulty of obtaining observations of these distant bodies in the UV: these observations demanded 24 and 16 orbits respectively yet yielded only ambiguous results. The availability of an instrument with a larger collecting area, and of a space platform with higher observing efficiency than the HST, is obvious.

The interplanetary medium

Cosmic dust covers the surfaces of atmosphereless bodies and is an important component that rains down on Earth as visible meteors. In principle, these could originate from the grinding down of TNOs and Main Belt asteroids, or from the disintegration of comets, but the relative ratios are unknown. Each possible source could produce grains with different chemical compositions, porosity, and complexity and this would result in different optical properties that would be exhibited also in the UV.

The grains show evolution under the gravitational influence of the planets, solar radiation pressure, the Yarkovsky and Poynting-Robertson effects, and solar wind drag. Recent observations with the Wisconsin H α mapper (Reynolds et al., 2004) show that the zodiacal cloud has a definite prograde signature. The broadened widths of the H α profiles, together with the large amplitude variations in the centroid velocity with elongation angles, indicate that a significant population of the dust grains is in elliptical orbits. These grains could be part of the debris trails of comets seen in IRAS and ISO maps (by Davies et al., 1984; Davies et al., 1997; Sykes et al., 1986; Sykes and Walker, 1992).

The reason to study the ZodiacaL Light in detail in the UV is that an accurate measurement of the diffuse UV light in the Solar System is still lacking. Scattering off small dust particles in the zodiacal cloud, at heliocentric distances up to 5–10 a.u., provides the UV light (Leinert et al., 1998). The UV maps of the zodiacal light are much less complete than in other spectral bands. Information about the UV emission from zodiacal dust is necessary for the computation of the thermal equilibrium of dust grains.

Table 2 Science issues and instrument requirements

Scientific focus	Instrumentation and mission
<ul style="list-style-type: none"> • Time-variable solar system phenomena • Interaction of the solar wind with planets, their satellites and rings • Size distribution and chemical composition of comets and TNOs and diversity among comets • Circulation and dynamics of planetary atmospheres • Geochemical provinces on planetary surfaces, volatile transport processes • Comparative planetology: Mercury to the TNOs and beyond, Solar System evolution • Other planetary systems 	<ul style="list-style-type: none"> • Large collecting aperture ($>2\text{m}$) • Diffraction limited high angular resolution (better than $0.02''$) • Pointing accuracy and guidance stability • Ability to observe moving targets at full performance • Imaging and high resolution spectroscopy • Minimum solar elongation $< 20^\circ$ • Mission lifetime $>15\text{--}20$ years, real-time operations • Data from solar photon and particle monitors • High operational efficiency

One of the basic parameters in understanding cosmology lies in the measurement of the background light. While this background light component has been well mapped in the IR by COBE/DIRBE, in the optical the still-quoted measurements date back to Pioneer 10 (Toller and Weinberg, 1985). Worse still, in the UV, where the Local Universe is observed, the background emission by the zodiacal light is not well defined at all. The brightness distribution over the sky varies much less than in the optical, where a factor of three between the ecliptic poles and ecliptic equator has been measured. This would imply that while the dust grains that scatter the visible light are somewhat confined to the ecliptic, those that produce the UV zodiacal light are more spherically distributed. The different spatial distribution may reflect a difference in particle size, with the UV scatterers being smaller, on average, than the particles responsible for the optical emission, as well as a possible different origin. Henry and Murthy (1998) also claim the appearance of a spectral feature at ~ 280 nm that has no readily available explanation.

A future UV observatory for solar system studies

In this section we derive observational requirements for future UV instruments. We start by listing scientific goals that will drive the instrumental requirements. Note that Solar System phenomena are time-variable. The atmospheres of many planets reveal structures and variation with longitude, latitude, and season and everything changes with the solar cycle phase. Such studies require the performance of synoptic observation for all types of objects.

The primary scientific objectives of a UV observatory are a complete characterization of the properties of all types of solar system bodies, from object sizes, internal structure, and rotational properties, to surface properties and atmospheric composition. From these observations, comparisons can be

made to determine how solar system objects form and evolve. Table 2 lists a number of science questions in the left column and instrumental requirements in the right column. These requirements are derived from a number of concurrent considerations; for example, large apertures are required not only to compensate for the low solar flux in the UV, but also to counterbalance the low albedos in this spectral region.

Future scientific results

We mentioned above that a particular advantage of observing in the UV is the possibility of achieving a high angular resolution by designing diffraction-limited telescopes used at as short as possible a wavelength. Because of basic optics, the resolving power of the JWST at its main operational band ($4\text{-}\mu\text{m}$) can be achieved by a half-meter aperture UV telescope. The WSO/UV telescope, which is one option for a next generation UV telescope facility, will have in imaging mode at 100 nm a spatial resolution one order of magnitude better than that of the JWST.

Note that the ELT (Extremely Large Telescope) as was discussed in 2005 for possible realization in about two decades, with a filled 100-m aperture, will offer a field of view of three arcmin that, with the adaptive optics option, will have a 1.4 mili-arcsec (mas) resolution with pixels that are less than one mas in size. This angular resolution is now only the province of VLBI, but could be achieved in the UV without the AO option with a $\sim 20\text{-m}$ spaceborne telescope. In the sub-mm domain, when the Atacama Large Millimetre Array (ALMA) will be operational, its highest angular resolution will be only 5.8 mas (at 720 GHz).

It is possible to translate this angular resolution into spatial resolution by considering a few examples where we give the linear and angular size of bodies at their typical distances. We ask the reader to consider the amount of information

retrievable for a nominal angular resolution of one mas (\sim one km at one a.u.); note that this is the diffraction limit at 100 nm for a 20-m telescope while the same limit is $0''.01$ for a 2-m telescope.

Planetary atmospheres and magnetospheres

Some key research areas in the field of atmospheric chemical composition and dynamics are:

- Mars: CO₂ and ozone absorptions, transport of water and CO₂. Loss of ancient oceans. Dust storms. CO₂ recycling.
- The role of cold traps and the transport of condensable species on planets (Mercury, Moon, Mars, Jovian satellites, Triton, Pluto, Charon and TNOs).
- Global circulation of the giant planets, especially the poorly studied planets Uranus and Neptune. The longitudinal distribution of aerosols and UV absorbers can be determined and studied over many successive planet rotations. The comparison of the properties of Uranus (“rolling” along the ecliptic) and of Neptune will be particularly enlightening.
- Study of the evolution of local atmospheric phenomena in giant planets by imaging the different kinds of spots and measuring the evolution of their shape and their transport.
- Distribution of SO₂ on Venus and on Io, and its relation to the internal and volcanic activity.
- The solar Ly α line nearly coincides with a line of the fourth positive (14,0) band of CO; fluorescent scattering in the (14,v) band is therefore observable and can be used to monitor this species’ abundance in the upper atmosphere of Mars and Venus.
- The emission lines of atomic oxygen at 130.2 and 135.6 nm in the dayglow spectra of Mars and Venus are very strong and are tracers of the thermospheres of those planets. These observations, coupled with those of CO, O₃ and CO₂ (via their absorptions) are essential to understand the aeronomy of the telluric planets, in particular atmospheric species’ transport and production/destruction mechanism as a function of solar cycle activity and input of energetic solar wind particles.
- Searches for Ar, Ne and N in all atmospheres of solar system objects to constrain the temperature distribution in models of the presolar nebula.
- Use of emissions from H, C, O, S and N and their ions to investigate the physics of the planetary ionospheres.
- Investigate on a long term basis the role and sources of neutrals in Saturn’s magnetosphere.
- Search for activity on low-gravity bodies, in particular TNOs, by detecting traces of cryovolcanism through ejection of dust particles.

Sunlight at long UV wavelengths is reflected from stratospheres of planets by a combination of Rayleigh (atomic and

molecular) and aerosol scattering. Signature absorptions at specific wavelengths can be used to identify trace organic species (e.g., hydrocarbons, nitriles, etc.), many of which are produced by non-equilibrium processes such as auroral chemistry and photochemistry. A global latitudinal study of the abundance of the atmospheric constituents allows one to separate these two sources of compounds. These tracers can also be used to study the dynamics of the atmospheres. A spatial resolution of order 100 km at Jupiter would permit unprecedented synoptic observations of the atmosphere of this planet.

The atmosphere–surface interactions at Mars, Io, Ganymede, Mercury, and the Moon could be studied with unprecedented details. The surface of these bodies feeds the atmosphere with volatiles and solid particles and the surface is more or less covered with condensable materials during the planet/satellite seasons. The solid particles play a key role in the thermal balance of some atmospheres (Mars, Titan and possibly Pluto, if the presence of a haze layer in this planet’s atmosphere is confirmed).

UV observations allow the characterization and monitoring of the transport of condensable species on planetary surfaces such as those of Mercury, the Moon, Mars, Triton, Io, Pluto and TNOs. The study of volatile escape from low-gravity bodies, in particular TNOs, is greatly facilitated. The transient atmosphere of most low-gravity bodies such as the Moon, Mercury, asteroids, and giant-planet satellites is due to impact of highly energetic particles. The mid-UV region offers the possibility to study most of these atmospheric compounds.

Observations of stellar occultations can be used to obtain atmospheric density profiles. The high time resolution of large instruments allows a very good resolution of the atmosphere height where the occultation takes place. The occultation signature is stronger in the UV because of the higher refraction coefficient. The atmospheric absorptions that could possibly be studied are those of H₂, CO₂, and hydrocarbons. Note though that the occultation rate will mostly be determined by the population of occulted stars, which must be rather strong UV emitters, rather than by the spatial resolution of the telescope.

Characterization of the Jovian magnetized environment, and observations of auroral phenomena at Jupiter and Saturn, which is traditionally done with probes in the vicinity of these planets, can be routinely performed with a spaceborne UV telescope. Combining the two options, an orbital spacecraft and a telescope near the Earth as done by e.g., Mauk et al. (2002), would show the similarity of auroral processes on Jupiter and on our Earth. Under this heading we could include also charge-transfer reactions with exospheric gases on low-magnetic field objects (Moon, Mercury, and Mars) and comets.

Table 3 Physical and Angular size of solar system bodies

Object	D (km)	D (arcsec)	Type of observation
Mercury	4,878	4.6–12.5	Map of specific regions
Venus	12,102	10–60	Map of specific regions
Moon	3,476	1.865	Map of specific regions
Mars	6,787	14–24	Map of specific regions
Largest asteroids	Up to 960	Up to 0.8	Complete maps
Asteroids D > 50 km	50	>0.05	From coarse to detailed maps
Jupiter	143,000	47	Maps of regions of interest
Io	3,640	1.2	Complete map
Ganymede	5,280	1.7	Complete map
Saturn + rings	121,000	19.5	Maps of regions of interest
Titan	5,150	0.8	Complete map
Tethys & Rhea	1,500–1060	0.17–0.25	Complete map
Uranus	52,400	4.0	Complete map
Oberon & Titania	1,575	0.12	Complete map
Neptune	50,000	2.4	Complete map
Triton	3,200	0.15	Complete map
Pluto	2,200	0.1	Complete map
Charon	1,200	0.055	Coarse map
Sedna	1,600	0.037	Coarse map
P/Encke	5	0.007	A few points
P/Halley	10	0.015	A few points
Hale-Bopp	50	0.075	Coarse map

Charged particles moving along magnetic field lines produce auroral phenomena (Jupiter, Saturn). The diagnostic H₂ emissions (self-absorbed below 110 nm) can be used to monitor this interaction all over the giant planets with special emphasis on auroral regions. The H₂ emission is very sensitive to the height of the emissions, and thus may be used to determine the mean energy of the precipitated electrons, as was illustrated with FUSE spectra (Gustin et al., 2004). However, future instruments should have improved spatial resolution so that specific areas of the aurora may be selected.

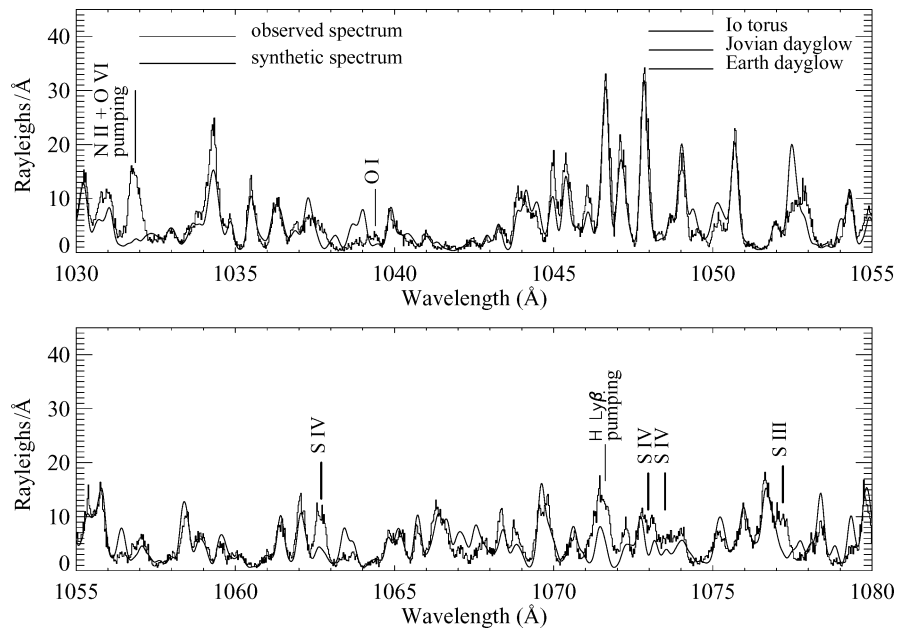
Equally interesting would be a detailed study of the flux tube footprints in the auroral regions of Jupiter, first identified in HST STIS spectra. The study of the multiple heads observed at the Io magnetic footprint, in particular their relative intensities and inter-separations, and relationship with the location of Io in its plasma torus, requires systematic FUV surveys of Io and its environment at all orbital phases.

Io provides a unique opportunity to study how volcanism is related to the ionosphere of the satellite and to its accompanying torus, while the ensemble is also dependent on the highly dynamic and variable Jovian magnetosphere. The environment of Io and of the Io torus is very hot and many of its emissions (in particular those of the multiply-ionized O, S and C ions) are in the EUV and FUV regions. A detailed study of such an intricate system requires synoptic observations over large times scales made at spatial resolutions commensurate with the size of the sources and sinks of the neutral and ionized species. In particular, measurements of FUV emissions from the major ionic species in the torus can provide images of the warm plasma in the main torus region with sufficient spatial resolution to detect detailed structures, yielding a map of plasma conditions dependent on radius, longitude, latitude, and local time. Several unsolved questions concerning the stability and variability of the torus with longitude, local time and intrinsic temporal variability

Fig. 3 The three pictures show the evolution of spatial resolution in observing the Jupiter aurora. The STIS MAMA image (at the right) is the only one showing the trail of the Io magnetic footprint below the auroral oval. Source: Gerard et al. (2003)
<http://lpap.astro.ulg.ac.be/jupiter>



Fig. 4 FUV spectrum of Jupiter's aurora obtained with the FUSE large aperture. The observed intensity distribution of the H₂ lines is very well reproduced by the synthetic spectrum for a foreground H₂ column of $7 \times 10^{20} \text{ cm}^{-2}$, corresponding to a pressure level of 1 microbar at 800 K (from Gustin et al., 2004)



(possibly linked to volcanic activity) can be addressed with multispectral FUV imaging.

While auroral and airglow emissions have been detected by a few UV instruments in the past, none studied in detail the variation of these phenomena as a function of local time, magnetic longitude and solar activity. How these effects control the observed emissions is not yet understood. The magnetospheric activity seems to correlate with the solar activity. A dramatic example of UV imaging capability, emphasizing the need for narrow-band filters and excellent time resolution by using STIS on HST, was given by Waite et al. (2001). The auroral oval light is comprised of the Lyman and Werner bands of molecular hydrogen and the Ly α line of atomic hydrogen. UV observations of the aurora offer a much stronger contrast of the emission against the disk of the planet than does the optical imaging.

It was long assumed that Saturn's magnetosphere and aurora are intermediate between the case of the Earth, where the dominant processes are solar wind driven, and the case of Jupiter, where processes are driven by a large source of internal plasma, the Io torus. Recent HST UV images show instead that Saturn's auroras differ notably from those of the Earth and of Jupiter. Saturn's auroral emissions are only in partial corotation, the auroral oval quickly moves toward higher latitudes in response to solar wind enhancements, and it often exhibits an unexpected "spiral" structure.

The study of the production and evolution of neutrals in the highly variable and neutrals-dominated magnetosphere of Saturn is imperative. Saturn's magnetosphere presents a unique feature: it contains an abnormally large abundance of neutrals, in particular H and OH, both dissociation products of water vapour (O has recently been detected by the Cassini

spectrometer). The source of OH is poorly known, although it is probably from the sputtering of icy satellite surfaces by energetic ions and interplanetary particles. Saturn will be studied by the UV spectrometer of the Cassini mission, although not on a regular basis because of mission constraints. Paradoxically, one constraint is that the viewing direction is not easily directed towards this large object; remote sensing techniques are actually better suited for such observations

The magnetospheres of Uranus and Neptune are poorly known; the role of their icy and rocky planetary cores on the planet dynamos has not yet been investigated. Why Uranus does not emit as much energy as Neptune is still mysterious. The two planets have very similar interiors but very different rotation axis orientations, hence very different interactions with the solar wind particles. Auroral phenomena are essential to unravel the properties of the magnetic fields of these two distant planets. Neptune and Uranus change their magnetic configuration on time scales shorter than 24 hours because of the relative inclinations of their magnetic and spin axes. Uranus also shows secular changes, because of the high spin-to-orbit inclination. Thus, frequent observations of their auroral activity, achievable only by planetary probes or by a space UV facility, are necessary to investigate these interactions.

Studying the influence of satellites on planetary plasmas and magnetic fields, such as the relation between Io and Jupiter, Triton and Neptune, or between Saturn's satellites and its rings, requires the availability of UV imagers. Although quite spectacular, the results that the UVIS spectrometer on board Cassini (Esposito et al., 2003) will deliver would span only a short time period, in comparison to the time constant of the phenomena to be investigated. Moreover,

since this instrument resides constantly within the magnetosphere of Saturn, its data would be complementary to what an Earth-based instrument would deliver.

Planetary surfaces and rings

The repartition of ices and condensable materials due to seasonal effects on Mars, Ganymede, Io, Triton, Pluto, Charon, and the larger TNOs can be studied through albedo maps. The transport of condensable gases on the surface of planetary bodies is controlled by seasonal effects. We are currently witnessing the displacement of the nitrogen frost from the surface of Pluto, and the surface of Triton may possibly be a template for an unchanged Pluto surface since its heliocentric distance hardly varies. In 10–20 years from now, the surface of Pluto should be very different from what it is today and could reveal underlying layers of yet unknown composition. In addition, the UV is an excellent location to look for organic absorptions on these surfaces.

The global characterization and long-term variation of the properties of the rings of Jupiter, Saturn, Uranus and Neptune has not been done (Cassini will do this only during its four-year mission). A space UV facility could monitor the evolution of ring structures coupled to satellite motions by seeing these almost continuously. These observations could determine the lifetime of ring systems and derive the formation times of the existing rings. In low resolution mode, images of Saturn's rings could reveal the amount of absorption by water ice. Note that one may also image the rings in reflection and in absorption at Ly α to attempt a detection of H, a water dissociation product. As the majority of the absorption features lie below 150 nm, and in order to acquire a significant signal-to-noise result, it would be necessary to observe the ring absorption during occultations of O, B and A stars.

The rings can be imaged in the visible or in the NIR (e.g., the 2- μ m absorption band) but this will not be done at 0.02" resolution. Also, UV observations will help the search for minor species that are diagnostics of the chemical composition

Fig. 5 Polar projections of individual FUV STIS images. The South pole is at the center, noon is downward, dawn to the left and dusk to the right. The left image shows a clear “spiral structure,” while the image to the right exhibits a bright spot, tentatively identified as a cusp signature observed at higher latitude, probably due to high-latitude reconnection. (Gérard et al., 2004)

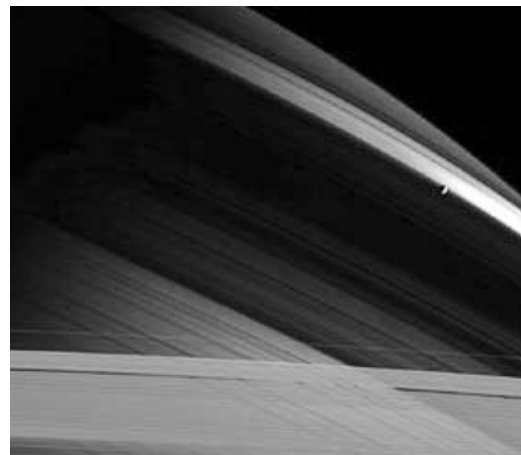
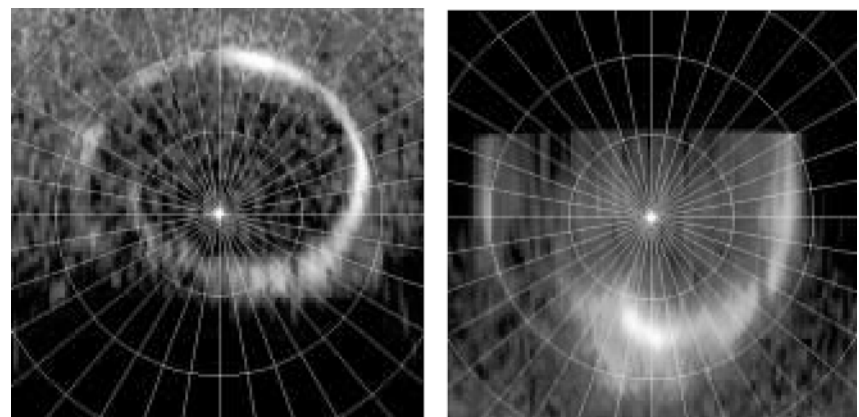


Fig. 6 Saturn's rings imaged by the Cassini probe from 3.7 million km with a resolution of 22 km per pixel. Such images could be routinely obtained by a large orbital UV telescope. [Source: JPL PR at <http://saturn.jpl.nasa.gov/cgi-bin/gs2.cgi?path=../multimedia/images/large-moons/images/PIA06142.jpg&type=image>]

of the ring particles. The ring properties can be fairly well represented by assuming that their constituent particles are mostly water ice. However, the red color of the rings is an indication that ice contaminants, probably refractory organics, are present. Since the ring particles are leftovers of the disruption of what was once an icy satellite (or a number of such satellites), a major objective for ring particle studies is the determination of the nature and abundance of these organics. Photometric studies could also shed some light on the abundance of small inorganic particles, as well as on their production and destruction timescales.

Comets

One of the key goals of cometary studies is to reveal the composition of the solid nucleus, the source of gases and dust particles that scatter sunlight in the coma and tails. Comets have spent most of their life at vast distances from the Sun,

essentially preserved in “deep freeze” in either the TN belt or the Oort cloud until they enter the inner Solar System. If the composition of a cometary nucleus can be determined, then the temperature and density of the material from which these remnants of the primordial solar nebula formed, would be probed. Nuclei cannot be directly studied by telescopic observation except at large heliocentric distances where they are only little shielded or fully unshielded by the gas and dust coma, yet at such distances they are very faint. It is through spectroscopic observations of the coma and tail that key information on the nuclei is obtained. In situ observations concern only a few individual objects and need to be complemented by observations of representatives of the entire population.

Molecules are expelled from the nucleus as this latter is heated by the Sun. The ejected molecules are dissociated by solar photons into molecular fragments and may become ionized. The main nuclear component of comets, water, appears in the coma as atomic H and O, and as the OH radical. All three species have very strong transitions in the UV region. The UV is the only domain where the three emissions can simultaneously be detected and imaged at high spatial resolution. Some of the primary molecules, such as CO and CO₂, can also be studied in the UV.

The abundant CO₂ molecule can be probed using its ion and dissociation products, all with their strongest transitions in the UV region. The CO 4th positive bands and the CO Cameron bands are used for this purpose. The first emission is due to fluorescence of the CO molecule, while the second is produced by prompt emission upon dissociation of the CO₂ molecule or by electron impact onto a CO molecule. UV observations allow one to separate the production mechanisms and distinguish between the emission parent species. Since observations of the strong CO₂ band at 4.7 μm are difficult, thus rare, observing the CO Cameron bands is the only way to probe the elusive but cosmogonically important CO₂ molecule. The statistical basis for a comparison of the abundances of CO and CO₂ is currently insufficient to derive any firm conclusion, but the existing evidence leans towards a fairly large and stable abundance of the latter molecule in cometary nuclei. Aging processes could be less efficient for CO₂ because of the way the molecule is stored in nuclear cometary ices.

Spatial information is crucial to disentangle the various production and excitation mechanisms at play in the coma. The best example is that of CO, which can be produced either directly from the nucleus, from the dissociation of large molecules ejected into the coma, or indirectly by desorption from ejected grains from the surface of the nucleus. The nature of the extended gas sources in the coma needs further investigation, and requires simultaneous UV observations of the CO and C I lines, as well as of the dust grains. High sensitivity observations of the reflectivity of grains near 220 nm will indicate whether the interstellar absorption bump,

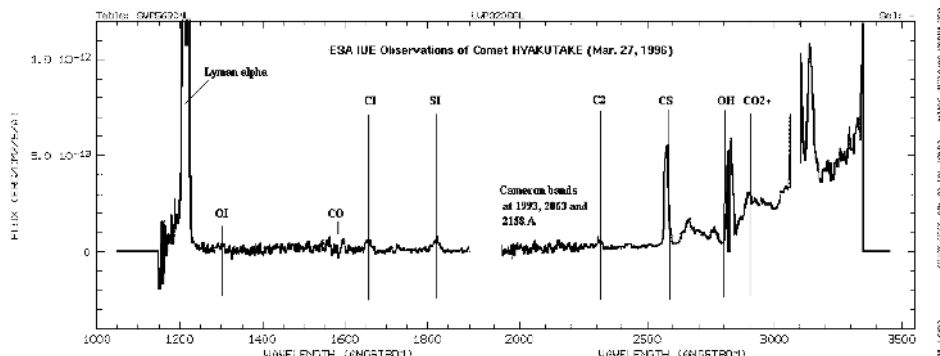
observed in the ISM at 217.5 nm, is present in Solar System grains, and if some interstellar grains have survived the collapse of the pre-solar nebula indicating a possible role of these grains as a source of the observed carbon. Radio and NIR observations of CO do not have the sensitivity, or the spatial and temporal resolution of UV observations, leading to coarser results.

The UV region contains emissions of other short-lived nuclear species, namely S₂ and CS₂ (via the CS emission). These molecules have abundances relative to water that vary greatly from comet to comet, especially S₂. The storage of these species in the nucleus, and the relation of their outgassing to that of the water and other ices, is unknown. High spatial resolution UV observations are required to reveal their onsets of production and their spatial distributions, hence their production and storage mechanisms. Radio and NIR observations complement the UV in the detection and monitoring of the global production of most parent species, but the spatial resolution achievable in the UV is still unsurpassed in comparison with that in other wavelength domains. The short lifetime of CS₂ makes CS an interesting probe for the eventual anisotropic distribution of gas sources on the surface of the nucleus.

The sensitivity of the instrumentation must allow one to completely map the key atomic species H, O, C, N and S emissions. Production processes and coma production rates could then be investigated and the global atomic budget of the volatiles in the nucleus obtained. The sensitivity must be sufficient to detect these emissions beyond the Solar System “snow line” at ~5 a.u. This would allow the detection of yet unseen species, in particular N or N₂ and rare gases. The presence of an H emission beyond the snow line would directly give the contribution of the non-water H-atom carriers. Since they have low sublimation temperatures, Ar and Ne with transitions at 104.8 and 106.6 nm and at 63 nm respectively can only be trapped in amorphous ice cages, from which they should have escaped rather rapidly if the thermal history of the comets is characterized by high temperature episodes. EUVE and FUSE observations indicate strong depletions of these species by factors of 10–25 but very deep searches still remain to be conducted. Given the fact that CO has about the same volatility as Ar, one may speculate that the polarity of CO could explain its high abundance in some comets by providing an electrostatic force to retain it in low-temperature ices.

The EUV region contains numerous ion emissions that allow the detailed study of the solar wind interaction with the comet ionosphere. Observations with FUSE revealed the presence of the important H₂ molecule, a direct tracer of water. The Lyman series of atomic hydrogen lines can also be observed. In addition, the H₂ (6,v") bands can be seen because of the coincidence of the P₁ line of the (6,0) H₂ Lyman system with Lyα (Bowen fluorescence mechanism).

Fig. 7 IUE UV spectrum of comet Hyakutake



A similar phenomenon explains the strength of the O I 130.2 nm triplet: the solar Ly β line at 102.572 nm resonates with the O I 3D -3P transition at 102.576 nm. The Ne line at 63 nm could also be detected, thanks to a coincidence with a strong O V line.

The FUV region contains the important deuterium line at 121.53 nm, very close to Ly α , that was first detected in 2004 in comet NEAT (Weaver et al., 2004). Such observations can be used to determine the D/H ratio in comets as a function of dynamical type, thus allowing an investigation of the source regions of comets in the solar nebula. Based on our knowledge of the D/H ratio in the giant planets, and if comets formed mostly by nebular gas recondensation, one does not expect those formed in the Jupiter region to be as deuterium-rich as those formed at greater heliocentric distances. So far, four comets have yielded a very similar value that could indicate that the D/H ratio in comets is mostly fixed by the solid component of the presolar nebula that has probably not been fully evaporated. This hypothesis requires a larger observation sample than presently available to be confirmed.

The interaction of the solar wind with the coma will be studied in detail through:

- (1) Observations of the O $^+$ (83.4 nm), N $^+$ (108.5 nm), S $^+$ (125.0 – 125.9 nm), C $^+$ (133.5 nm), CO $^+$ (200 – 230 nm), and CO $_2^+$ (289.0 – 289.6 nm) emissions,
- (2) Emissions produced ahead of the comet by charge-exchange reactions with highly charged solar wind ions. These emissions are spread all over the EUV and FUV regions (some are likely to be present in the FUSE spectra of comets).

The O $^+$ and CO $^+$ emissions may be the best tracers of the solar wind interaction with the comet. O $^+$ will fill out a larger coma volume than CO $^+$ and will oppose a weaker force to the solar wind than CO $^+$, a mostly nuclear species with large densities near the nucleus. The slowing down of the solar wind particles will be completely revealed by imaging in these lines. The coma response to a solar wind disturbance will also be documented for the first time, and at high spatial

resolution. Note that the CO $^+$ lines are hard to separate in the optical from weak C $_2$ and C $_3$ lines, and they appear on top of a sometimes strong continuum. The continuum contribution does not exist, or is extremely weak, in the UV domain and this offers very clean data.

The continuum spectrum of comets below 300 nm has rarely been studied. The spectrum seems to be solar, with a slope of order 10% per 100 nm near 290 nm. Since the albedo of solar system surfaces exhibits large changes in the 280–400 nm range, which are caused by the physical as well as the chemical nature of the surface materials, this part of the spectrum should be observed with great care in the hope of measuring a size/chemical nature-dependent change of the albedo curve of the targets with wavelength.

Detailed observations of the UV spectrum of a periodic comet are still to be made. One expects, due to a very different thermal history, that the spectrum of periodic comets would be severely depleted in some highly volatile species, e.g., CO. This can be tested by detecting and monitoring the emissions of CO and CO $_2^+$, or those of C and O when the former are not detected.

Other small bodies in the solar system

Objectives of a UV observational program for small Solar System bodies would be the imaging of the surface, the production of albedo maps, and the characterization of the regolith properties for all objects larger than 50 km (0.04 arc sec at 2 a.u.). The determination of shapes and rotational properties could be inferred, from which the collisional history for these objects would result automatically.

The characterization of the surfaces of asteroids and satellites is traditionally done with optical and NIR information. The UV could add a new dimension to planetary mineralogy, but this would require a baseline laboratory program to characterize the likely minerals in this spectral region. Lunar UV mapping was done for the first time using UIT on the Astro platform (Henry et al., 1995). The Astro results indicate a lunar albedo of 0.038($\pm 10\%$) at 170 nm and no opposition

effect was found. The reflectivity of the lunar material below 400 nm was also discussed by Zou et al. (2004).

The requirement for surface characterization is adequate surface resolution: 0.01 arcsec is 25 km at 3 a.u., necessary to resolve approximately 1,000 Main Belt asteroids or coarsely map TNOs at 60 a.u. with 500 km resolution. Such angular resolution capabilities, or better, are also necessary in order to resolve binary asteroids to derive their densities, in particular for TNOs. Typical asteroid rotation periods are a few hours; in order to avoid smearing the data, the necessary information must be obtained within ~10 minutes (surface brightness constraint).

Using the UV to search for comet-like activity in small bodies is beneficial, because in many cases activity manifests itself as grain ejections and these will only scatter sunlight. This diffuse scattered light would be seen in the UV better than in the visible, because of better contrast against the darker sky. The detection of activity from very distant bodies would confirm the predictions of models of thermal evolution at large heliocentric distances, mainly caused by the transport of gases at low temperatures.

The study of transitional objects, dormant and/or extinct comets, is particularly fascinating. The asteroid 3200 Phaeton, the source of the Geminid meteors, is presumably an extinct comet despite the failure to detect a coma (Hsieh and Jewitt, 2005). A claim that asteroid 2001 YB₅ is the source of a new meteor shower visible on January 7.5 was recently published by Meng et al. (2004). As this object is a Potentially Hazardous Asteroid (PHA), and such objects have been linked theoretically to extinct comets, it is possible that this is another case of a transitional object. Note however a dissenting opinion by Lupishko and Lupishko (2001). The use of UV is beneficial because of the ability to image low surface brightness features; therefore even low levels of activity that would result in a very faint tail or a dusty coma ejection could produce measurable signals.

A search and study of Trojans of all giant planets will help determine whether it is possible that the Trojans were accreted to their present locations at the early stages of solar system formation. Peale (1993) showed that the Lagrangian locations could be stable at the planet accretion phase; the planetesimals could have been captured there by drag in the primeval nebula. The question whether the Trojans are comet-like bodies or not could be solved, as in the case of extinct comets among the NEOs, by searching for comet-like outgassing activity.

A search for multiple asteroid systems in order to determine their density, from which their interior structure could be inferred, can be conducted better with a UV space telescope than with an optical one because of the superior angular resolution that can be achieved. Note that even ESO's Very Large Telescope Interferometer (VLTI) will not achieve a resolution of one mas. With high angular resolution, from

a space platform that is not affected by seeing, it would be possible to perform companion searches at much closer distances from the main body of a binary system than if using visible light.

Outer solar system objects

After the discovery of 90377 Sedna (2003 VB₁₂), it appears that bodies in the inner part of the Oort cloud or scattered out of the TNO belt are observable. Sedna never approaches the Sun closer than ~76 a.u., it was at about 90 a.u. at discovery, and will become slightly better located for observations in the next decades as it approaches perihelion. This is an opportunity to characterize the nature of a body which has resided in the far outskirts of the Solar System since its formation and can show best the influence of eons of cosmic ray irradiation. Other similar bodies, some possibly larger than Pluto (e.g., 2003 UB₃₁₃), exist at tens of a.u. heliocentric distances and should also be included in such studies.

Observations of Sedna and its cousins imply that not only ground-based optical observations from the largest telescopes are required, but also the use of adequate space assets. In particular, the use of low-resolution spectroscopy may be preferable to photometry through a few filters to obtain a global reflectivity profile. Sedna is a 20.5 mag object in the R-band; assuming its UV albedo is only 10% of its visible one, it would look like a 23rd mag UV star. Broadband photometry in the UV, or very low resolution spectroscopy, is possible for such sources using a 2-m class spaceborne telescope. There are tens of other bright TNOs that could be characterized in the FUV region and a new taxonomy for these objects will emerge when all wavelength ranges will have been observed.

Recent models predict cometary activity of TNOs at rather large (tens of a.u.) heliocentric distances. This arises from the influx of heat input at perihelion passage building up the CO release from within the icy body, combined with transport and recondensation of volatiles within the TNO. The thermal evolution model by Choi et al. (2005) for the scattered TNO 1999 TD₁₀ showed an outburst at ~60 a.u. after 75 orbits! Cometary-like activity has been reported for a number of TNOs, with candidates for activity including the above-mentioned scattered TNO (Choi et al., 2003) although this claim was rejected by Mueller et al. (2004) and by Rousset et al. (2003), as well as the earlier observation of 1996 TO₆₆ (Hainaut et al., 2000). It is possible that cryovolcanism activity could take place, whereby the ejection of a dust/ice grains plume is observed due to pressure build-up in the icy body. Imaging in the UV could facilitate the detection of such cometary activity through the detection of faint dust features because of the low sky background in the UV.

The size distribution of TNOs should be determined to establish to what extent the TN belt is the source of short-period

comets. Even though faint objects like TNOs will probably not yield a strong signal below ~ 180 – 190 nm, and the ice absorption at 175 nm may not be seen, the advantage in angular resolution of UV observations could allow the estimation of size for some of the objects. The UV segment is necessary also to investigate a possible signature near 220 nm from possible traces of interstellar compounds that would serve for surface characterization.

Interplanetary material

A long-term goal could be the complete characterization of the properties of the interplanetary H and He, and the detection of temporal variations in the emissions/gas temperatures. This, like zodiacal light studies, could be done if a large FOV is available. Apart from a better characterization of the zodiacal light, a large FOV integral field spectrometer would also allow the measurement of the UV spectrum of interplanetary particles and its comparison to that of comet dust and asteroidal surfaces in order to determine the relative contributions of the sources.

The influx of interstellar material into the Solar System may be an elemental ingredient of planetary evolution as the influx of interstellar material could modify the reflection properties of outer Solar System bodies. The Solar System moves through the local ISM at ~ 20 km/sec with the strongest contribution from ~ 5 a.u. upstream and with a local cavity extending to ~ 20 a.u. downstream. The solar wind interacts with the ISM and reaches equilibrium at ~ 200 a.u., at the heliosphere boundary. Dust particles, detected by the Ulysses spacecraft, have increased by a factor of three from 1997 to 2000. Landgraf et al. (2003) argue that this could increase by another such factor by the end of the next solar cycle, in 2012–3. It is possible to detect very nearby (to the solar system) gas by studying at high resolution the absorption lines of very nearby stars. Frisch (2004) discusses the interaction of the heliosphere with the very nearby ISM. The incoming ISM, detected as gas by Frisch and others, is probably also related to the particulate influx detected by probes in the vicinity of the giant planets.

The Tools

The proposed Solar System research in the UV relies on several observational techniques. We list these below, before describing the necessary facilities. The techniques, together with the scientific goals of the different projects, set the instrumental constraints of any proposed space facility.

Photometric imaging

This technique yields the position, location and structure of sources. We assume that any instrument designed for imaging will have a photometric capability, good calibration, and long-term stability. In order to be efficient in this task, it should be done in narrow spectral bands centered on strong emission or absorption features. However, as a database for planetary mineralogy in the ultraviolet range is not yet established, this requires preliminary laboratory work.

Few UV images of solar systems objects not acquired by specific planetary missions exist, mostly obtained during rocket flights or by HST for target acquisition. This is quite surprising, since such data are very powerful and offer a global view of extended objects that helps characterize global variations of the object appearance on a scale of order 1/100 the size of the object and on timescales that vary from minutes to days. Each specific filter requires at least one adjacent “continuum” filter for background subtraction.

Table 4 lists examples of spectral features that could be observed during a program of high-resolution UV imaging. The list is limited to the stronger features shortward of 315 nm, is by no means exhaustive, and no attempt was made to prioritize the spectral bands.

Spectroscopy

In high resolution mode, $R \sim 100,000$ (0.001 nm resolution at 100 nm) is required to resolve plasma velocities in a number of environments such as cometary comae. This has to be achieved at a spatial resolution of 0.05 arcsec or better. In low-resolution mode the emphasis is on detecting and characterizing faint objects, and these figures become 2000 to 3,000 and 0.1 arc sec. An integral field spectrograph is highly desirable as this would reduce the total exposure time. Another solution is a spectrograph like STIS with scanning possibilities.

The efficiency of classical spectrometers is notoriously low, partly, because of the low efficiency of reflection gratings. This has been mitigated by the use of high-efficiency transmission gratings and grisms but it is possible that Volume-Phase Holographic Gratings (VPHG) would offer an additional 50% gain in efficiency. However, it will be necessary to extend to the UV the present effort, which concentrates on visible and near-IR light.

(Photo)Polarimetry

Light scattered by dust and magnetized media is often polarized so studies of comet comae and auroral regions could benefit from polarization measurements. For comets, and if the instrument sensitivity is sufficiently high, one could expect to detect the continuum emission down to about 200 nm

Table 4 UV Spectral features observable in Solar System targets

Wavelength (nm)	Species	Targets (non-comprehensive list)	Note
58.4	HeI	Interplanetary material, comets	Can be observed in 2 nd order
63	Ne	Comets, Saturn rings	Resonates with OV
83.4	OII	Comets, Saturn rings	
98.9	OI	Comets, Saturn rings	
102.6	H I Ly β	Interplanetary material, comets	
102.576	OI	Comets, Saturn rings	Resonates with Ly β
104.1	OI	Comets, Saturn rings	
108.5	NII	Comets	
108.8	CO (C-X)	Comets	
112–115	H ₂ Lyman & Werner bands	Giant planets, comets	Aurora phenomena, satellite footprints
113.5	NI	Comets, Triton, Pluto	
115	CO (B-X)+OI	Comets	Blend of features
121.53	DI Ly α	Comets, IPM, giant planets	
121.6	H I Ly α	Interplanetary material, comets, Mars	The interplanetary H I signal can be absorbed by various H ₂ O clouds
125.0–125.9	SII	Comets	
130.2	OI	Comets, Saturn rings	
133.5	CII	Comets	
135.6	OI	Comets	
156.1	CI	Comets	
165	H ₂ O 1 st continuum band	Comets, Saturn rings, icy satellites	Absorption feature
165.7	C I	Comets	
175	Water ice	TNOs	Absorption feature
198.8	CO	Comets	
198–220	SO ₂ absorptions	Venus	Surface/atmosphere interaction
200–230	CO ⁺	Comets	
217.5 (wide)	ISM absorption	Comets, TNOs, zodiacal dust	
250	Continuum	Comets, zodiacal dust	Dust size distribution
255.4	O ₃ Hartley	Mars, Venus, Callisto?	
257.6	CS	Comets	
289.0–289.6	CO ₂ ⁺	Comets, Venus, Mars	
300.4	O ₃ Hartley	Mars, Venus, Callisto?	
302	Continuum	Comets	Differential dust size distribution
308	OH	Comets, Saturn rings	H ₂ O dissociation product

and thus collect information on the very small and irregular particles that should polarize these wavelengths more than larger particles.

Asteroid and other atmosphere-less bodies' surfaces will polarize the light they scatter. The polarization properties of asteroid and comets should differ if they are due to particles of different nature and shape. This would also be useful in establishing whether the bodies have been heavily fractured ("rubble piles") or are solid.

Astrometry

This is the accurate measurement of the position and motion of the source. We assume that any imaging device will have

the required electronic and mechanical stability to ensure astrometric capability.

Occultations

Occultations offer a unique and efficient way of probing the atmosphere of faint bodies such as Pluto, Charon, TNOs, and comets. To be of use the telescope must offer (a) a large collecting area to reach faint targets of occultations, and (b) high observing efficiency to allow the utilization of rare observing opportunities.

Absorptions in comets will mostly be due to water vapour in the first continuum band centered at 165 nm. The IPM Ly α emission could also be absorbed by the water vapour cloud

surrounding the nucleus once the structure of the H I comet emission has been subtracted. This can be used to map of the water cloud, hence to provide information on its emission pattern at the nucleus.

In spectrographic mode, the absorption of a hot star spectrum must be easily seen in the second continuum absorption of water vapor in bright comets within about 100 km from the nucleus, if opacities of order 1/100 could be measured. Note that absorptions by coma species other than water are probably much harder to detect, because their column densities times the absorption cross section are significantly smaller. In imaging mode, the opacity of the dust comae can be probed through the observation of O-B-A stars occulted by a comet, from which a column density profile independent of any model assumptions can be derived.

The atmosphere of Pluto, discovered in 1985 by Brosch (1985, 1995) when observing a stellar occultation by Pluto and confirmed by other occultations observed from the ground (e.g., Elliot et al., 2003), and the possible existence of an atmosphere around Charon, could be probed during stellar occultations observed in the UV from a space platform. Mink (1993) found 26 possible occultations of stars brighter than 16th mag by Pluto and 25 by Charon from 1993 to 2010 as seen from Earth. The observations of stellar occultations by Pluto during the years following the first atmosphere detection revealed the expansion of the atmosphere while the planet is receding from perihelion (Elliot et al., 2003). A series of occultation measurements over the years will reveal further secular changes.

The presence of atmospheres around TNOs can be tested for in a similar manner once the number of TNOs with adequate orbits increases and a search is conducted for occultation opportunities. The use of the UV allows the tailoring of the observations to specific absorption bands for definite gases and, for thin atmospheres, allows a higher sensitivity due to the higher refraction index of gases in the UV. On the other hand and as already mentioned above, this requires the identification of an UV-bright star that becomes occulted by the target; the rareness of suitable candidates emphasizes the need for large collecting optics. The large number of TNOs compensates partly for the low occultation rate.

What is currently available?

At present and in the near future UV capabilities are very limited. With the demise of STIS on HST there is now no capability for UV spectroscopy, but some UV imaging is still viable through WFPC2 and, for small angular extent targets, also with the ACS. Note that UV imaging using CCD detectors is fraught with red leaks of UV filters which prevent the derivation of proper photometry. If an HST refurbishing mission is performed, and if that includes COS, some form of UV spectroscopic capability will return. Similarly, “wide-field”

imaging would return with WFC3. Note that long uninterrupted HST observations will always be hampered by the availability of a suitable target in the Continuous Visibility Zone; otherwise typical 30 min observations are the rule for this and other missions in Low Earth Orbits. With FUSE, the capability exists for FUV spectroscopy from 90 to 119 nm but for most planetary targets, is very limited by the brightness of the objects.

GALEX offers the capability of low-resolution (~ 7 arc-sec) UV imaging and photometry in two UV bands from 135 to 300 nm, and of low-resolution $R \sim 200$ “objective prism” mode spectroscopy in the same spectral region. The latter is useful for obtaining the spectral energy distribution in the UV for relatively bright objects, in cases when the objects are at high galactic latitudes (to avoid confusion). Given the use of non-integrating, time-tagged photon detectors in GALEX, this mission has the possibility of electronically “tracking” and following a target for as long as it stays in the field of view, in order to build up the S/N or to provide a time-resolved photometric light curve. Similar imaging capabilities, with slightly different collecting apertures, plate scales, and spectral stretch as defined by the filter sets and detector response, will be offered by TAUVEK on GSAT-4 (launch planned for 2006), and by ISRO’s ASTROSAT (launch planned for 2007-8), though in both cases the effective photon-collecting efficiency will be similar to that of GALEX. This implies sensitivity sufficient to observe a 12th mag (monochromatic) object in a few seconds with $S/N \sim 5$.

UV instruments on planetary probes produce science only when they encounter the planet. Although the information collected by these probes is invaluable, the results are not useful for synoptic studies because of the spotty coverage. The same is true of various small instruments for the Shuttle or the ISS. Similarly, the small imagers on major satellite platforms (e.g., the XMM Optical/UV Monitor) provide a certain very restricted UV capability. The restrictions, in these cases, come from pointing limitations that are dictated by the main satellite instrument, from the low throughput due to the relatively small aperture, and from the tailoring of the filter complement. In most cases, these auxiliary instruments have no spectroscopic capability.

Mission requirements

In this section we derive the requirements for two future UV telescopes that could satisfy the planetary community’s needs until the mid-21st century. The view is guided through the perspective of the HST achievements and aims to provide significant advantages over that mission.

The objectives, which need not be realized by a single mission, would be to:

- Explore the EUV region simultaneously with the FUV region.
- Operate with a smaller Sun-avoidance angle than HST.
- Have an optical system much faster than the HST, even for a similar size instrument.
- Provide off-axis or Gregorian optics for efficient scattered photon rejection.
- Have solar-blind detectors with high quantum efficiency.
- Have higher observational efficiency (90% or more of each orbital revolution).
- Avoid contamination by the Earth geocoronal emissions and from the interplanetary H I Ly α background.
- Have near real-time response capability for targets of opportunity.
- Provide higher angular resolution than HST.
- Offer a large number of imaging filters.
- Allow simultaneous use of a number of filters.
- Regain UV capabilities lost with the HST and provide a superior future facility.
- Protect detectors from bright FUV or UV targets.

Spatial resolution

Aside from the Moon, Venus, Jupiter and Saturn and comets, most Solar System objects have small spatial extensions and require very high spatial resolutions. One hundredth of an arcsec is required to adequately resolve of order 1,000 asteroids and a few hundred TNOs, or to map planetary surfaces and atmospheric phenomena, and can be achieved with a modest-sized telescope (see table above). A second generation telescope could benefit from the lessons of HST and of the first generation instrument, as well as from techniques developed for telescopes operating in other spectral bands, to yield the milli-arcsec resolution argued for above.

Because of detector limitations, there must be a trade off between spatial resolution and FOV. Large solar system objects such as cometary comae, the zodiacal light, etc., require large FOVs, although key scientific programs need not generally cover the targets entirely. A medium (10 by 10 arcsec at sub-arcsec resolution) and a high-resolution mode (1–2 by 1–2 arcsec at 0.01 arcsec resolution) should be available.

Apart from the planetary probes, the Earth orbiters are also generally limited by their ability to point accurately at details of the planetary surfaces (or atmospheres) and by the capability for tracking features on planets and satellite. To track the Great Red Spot of Jupiter and keep it (or part of it) in the spectrometer slit, for example, requires a tracking accuracy of ~1 mas/sec (1 km/sec at 5 a.u., assuming zonal winds of ~one km/sec). Any jitter in the tracking would smear the spectral resolution, which will dilute the feature

response by that of its neighborhood, or will require closing the tracking loop using imaging in the telescope itself (this task is deemed to be very difficult).

Spectral resolution

This refers to the capabilities of an instrument operating with any of the two telescopes considered here. The spectral resolution must be matched to the detector's capabilities and to the spectral stretch considered, unless one wishes to consider an echelle configuration.

Pointing range, accuracy and stability

Targets near the Sun must be observable which imposes a requirement for strong rejection of sunlight. Mercury and comets close to perihelion must be accessible. The minimum elongation angle is of order 15°. If technically not feasible, the elongation limit would be set by Venus (about 40°) and by low-q comets, in which case the limit must be as low as possible since comets inside the orbit of Venus are usually extremely bright (this requires protection against damage from bright targets).

Moving target capabilities should allow observations of targets at a rate of at least one arcsec per second of time. Note that the reflex motion of a body at the distance of Neptune is ~four arcsec/hour.

Spacecraft and spacecraft orbit

A high apogee orbit is required to allow nearly continuous operations and minimum obscuration by the Earth disc. To avoid penetrating for too long deep into the Earth geocorona, a highly elliptical or at least a geosynchronous orbit is preferable. It should be possible to use the Earth's shadow to perform observations that require special protection from sunlight. The second Lagrangian point L₂ location would be a bonus, but solar panel constraints would restrict the availability of any Solar System target, unless fully orientable solar panels and good stray light suppression are implemented. The radiation background at L₂ would be similar to that encountered in any high Earth orbit.

The above-mentioned requirements cannot be realized in a single payload. To achieve an angular resolution of one mas that would be diffraction limited at 100 nm requires a 20-m aperture. It makes sense to combine this with other cutting-edge technologies that are in design stages now but are likely to mature within one or two decades. Such technologies might include in-space coating of the mirrors with aluminum for best-possible throughput. Such a mission is our long term objective. However, to achieve the goals of quick realization and continuity of UV astronomical efforts, we must also have a mission that would provide a limited

Table 5 UV missions for Solar System exploration

Property	Two-meter aperture	Twenty-meter aperture
Straylight rejection	10^{-11}	10^{-13}
Minimal elongation for observation	60°	20°
Angular resolution@ 100 nm	10 mas	1 mas
5σ imaging detection@ 100 nm in one sec [$\text{ergs}^{-1}\text{cm}^{-2}\text{A}^{-1}$]	10^{-16}	10^{-18}
Orbit	Geosynchronous or L ₂	L ₂ or deep space
Number of imaging filters	5?	50?
FOV for imaging	Few arcsec	Few arcsec
Spectrometer	Single-object, R~50000 Long slit, R~1000	Single-object, R~200000 Imaging spectrometer, R~1000
Stability	0''.1/sec	1 mas/sec
Moving target capability	1''/sec	1''/sec

enhancement with respect to the HST capabilities in the very near future. A longer term goal might include a larger instrument with enhanced capabilities. Therefore, we conclude with a proposal for two UV space observatories, as detailed in Table 5.

A solar monitor

Phenomena observed in Solar System objects are either triggered by sunlight and impinging solar particles (resonance fluorescence, excitation of line emissions) or are the consequence of the input of solar energy on them (thermal spectrum, evaporation or sublimation processes). In order to properly interpret the observations of various Solar System bodies, one requires a good knowledge of the solar flux impinging onto these bodies.

The solar spectrum produced in the EUV/FUV regions is due to physical phenomena occurring mostly in the chromosphere and corona of the sun, while the photospheric part dominates beyond 200 nm. Below 150 nm, the solar spectrum is mostly composed of individual lines. The variability of the solar flux is wavelength-dependent and variabilities of order 10% are observed in the 150–200 nm regions and may reach 50% or so near 120 nm. In the EUV region, flux variations can reach one order of magnitude. These line flux variations translate into highly variable excitation rates of comet transitions on timescales of hours to years. The 27-day and 11-year cycles are particularly important. The knowledge of the solar spectrum at a resolution of order 0.1 nm is required to correctly interpret observations of Solar System objects. Because of the slow rotation of the Sun about its axis and, often, significant differences in the ecliptic longitudes of the Earth and the target, observations from the Earth are often not sufficient. Latitudinal solar flux variations and solar line shapes have to be modelled, as they are not easily measurable without complex instrumentation.

In principle, it would be possible to achieve this by observing with a low-resolution spectrometer a point-like constant object that reflects solar radiation, but the requirements for a long duration mission, excellent instrumental stability, and high sampling frequency would make this approach extremely difficult. It is possible to design such an instrument around a small-aperture payload locked onto the Sun. The Solar Radiation Monitor will be a basic tool for planetary research. Because of possible azimuthal differences in the solar emission that may influence the results obtained for other planets and bodies in the system, it is necessary to deploy 2–3 such instruments in orbit around the Sun. As most Solar System objects are confined close to the ecliptic, it is probably not necessary for monitoring purposes to have such instruments in solar polar orbits.

Conclusion

We argued above the necessity of a two-stage approach in assuring the continued access to the space ultraviolet for the planetary science community. A first stage should be an instrument that would provide the community with better UV capabilities than HST but would be fully dedicated to observations in this spectral segment. Because of this conservative approach, we estimate that this goal could be achieved relatively cheaply and could be implemented almost immediately. If this first step were to be adopted, a suitable instrument could be functioning within five years.

A second stage must represent a breakthrough in all the characteristics of a space telescope and should provide a UV capability commensurate in angular resolution with that of the cutting-edge instruments of the mid-21st century: ELT and ALMA. By adopting a 20-m aperture, the throughput with respect to the HST or with the first generation instrument would be increased by two or

ders of magnitude. With proper optical construction and platform design, such an instrument could observe Mercury in the ultraviolet and follow Sun-grazing comets relatively soon after their perihelion passage. The angular resolution and sensitivity limit will allow the mapping of Sedna and of other inner Oort cloud objects when these are discovered.

We identified the need for the construction and deployment of solar monitors, to establish the baseline signal that activates atmospheric phenomena in planets, satellites, and comets. We also identified the need for laboratory mineralogic studies to provide the baseline information for UV planetology.

Acknowledgements NB is grateful for continued support of the UV astronomy efforts from the Ministry of Science and Technology of the Israel Government, the Israel Space Agency, and the Austrian Friends of Tel Aviv University. JCG is supported by the Belgian Fund for Scientific Research (FNRS).

NUVA is supported by OPTICON, a project funded by the European Commission under contract RI3-CT-2004-001566

References

- A'Hearn, M.: *Icarus* **118**, 223 (1995)
- Bertaux, J.L., Blamont, J.E., Festou, M.: *A&A* **25**, 415 (1973)
- Biesecker, D.A., Lamy, P., St. Cyr, O.C., Llebaria, A., Howard, R.A.: *Icarus* **157**, 323 (2002)
- Blamont, J.E., Festou, M.: *Icarus* **23**, 538 (1974)
- Brosch, N.: IAUC 4117 (1985)
- Brosch, N.: *MNRAS* **276**, 571 (1995)
- Bunce, E.J., Cowley, S.W.H.: *P&SS* **49**, 261 (2001)
- Choi, Y.-J., Brosch, N., Prialnik, D.: *Icarus* **165**, 101 (2003)
- Choi, Y.-J., Prialnik, D., Brosch, N.: DPS **37**, 56.04 (2005)
- Clarke, J.T. et al.: *Nature* **415**, 997 (2003)
- Davies, J.K. et al.: *Nature* **309**, 315 (1984)
- Davies, J.K. et al.: *Icarus* **127**, 251 (1997)
- Elliot, J.L. et al.: *Nature* **424**, 165 (2003)
- Esposito, L. et al.: Space Science Reviews, in press (2004)
- Feldman, P.D., Weaver, H.A., Burgh, E.B.: *ApJ* **576**, 91 (2002)
- Frisch, P.C. *Adv. Space Res.* **34**(1), 20 (2004)
- Gérard, J.-C. et al.: (<http://lpap.astro.ulg.ac.be/jupiter>) (2003)
- Gérard, J.-C. et al.: *J. Geophys. Res.* **109**(A9), 207 (2004)
- Grodent, D. et al.: *J. Geophys. Res.* **106**(A7) (2001)
- Grodent, D. et al.: *J. Geophys. Res.* **108**(A7), 1366 (2003)
- Gustin, J. et al.: *Icarus* **171**, 330 (2004)
- Hahn, J.M. et al.: *Icarus* **158**, 360 (2002)
- Hainaut, O.R. et al.: *A&A* **356**, 1076 (2000)
- Henry, R., Murthy, J.: AFRL report from MSX (1998)
- Henry, R. et al.: *ApJL* **454**, L69 (1995)
- Huebner, W.F., Benkhoff, J.: *Space Sci. Rev.* **90**, 117 (1999)
- Hsieh, H., Jewitt, D.: *ApJ* **624**, 1093 (2005)
- Keller, H.U.: *A&A* **23**, 269 (1973a)
- Keller, H.U.: *A&A* **27**, 51 (1973b)
- Keller, H.U., Lillie, C.F.: *A&A* **34**, 187 (1974)
- Krasnopolsky, V.A.: *Icarus* **153**, 277 (2001)
- Krasnopolsky, V.A., Feldman, W.C.: *Science* **294**, 1914 (2001)
- Krasnopolsky, V.A., Mumma, M.J.: *ApJ* **549**, 629 (2001)
- Krasnopolsky, V.A. et al.: *Science* **280**, 1576 (1998)
- Krasnopolsky, V.A.: Sixth International Conference on Mars (2003)
- Landgraf, M. et al.: *J. Geophys. Res.* **108**(A10), LIS5 (2003)
- Leinert, Ch. et al.: *A&AS* **127**, 1 (1998)
- Lupishko, D.F., Lupishko, T.A.: *Solar System Res.* **35**, 227 (2001)
- Makinen, J.T.T. et al.: *A&A* **368**, 292 (2001)
- Mauk, B.H. et al.: *Nature* **415**, 1003 (2002)
- Meng, H. et al.: *Icarus* **169**, 385 (2004)
- Mink, D.J.: At the Pluto/Charon conference in Flagstaff (1993)
- Mueller, B.T.A. et al.: *Icarus* **171**, 506 (2004)
- O'Connell, R.C.: *AJ* **94**, 876 (1987)
- Peale, S.J.: *Icarus* **106**, 308 (1993)
- Reynolds, R.O., Madsen, G.J., Moseley, S.H. et al.: *ApJ* **612**, 1206 (2004)
- Rousselot, P. et al.: *A&A* **407**, 1139 (2003)
- Stern, A. et al.: *Icarus* **92**, 332 (1991)
- Sykes, M.V. et al.: *Science* **232**, 115 (1986)
- Sykes, M.V., Walker, R.G.: *Icarus* **95**, 180 (1992)
- Toller, G.N., Weinberg, J.L.: In: Giese and Lamy (eds.), *Properties and Interactions of Interplanetary Dust*, Reidel, p. 21 (1985)
- Vidal-Madjar, A. et al.: *Nature* **422**, 143; (2003); *ApJ* **604**, L69 (2004)
- Young, E.F. et al.: *AJ* **121**, 552 (2001)
- Yung, C.: *Science* **280**, 1545 (1998)
- Zou, Y.-L. et al.: *Chin. J. Astron. Astrophys.* **4**(1), 97 (2004)
- Waite, J.H. et al.: *Nature* **410**, 987 (2001)
- Weaver, H.A., A'Hearn, M.F., Arpigny, C., Combi, M.R., Feldman, P.D., Festou, M.C., Tozzi, G.-P.: 36th DPS, paper 23.01, November (2004)
- Whipple, F.L.: *ApJ* **111**, 375 (1950)

Active Galaxies in the UV

Wolfram Kollatschny · Wang Ting-Gui

Received: 4 October 2005 / Accepted: 10 October 2005
© Springer Science + Business Media B.V. 2006

Abstract In this article we present different aspects of AGN studies demonstrating the importance of the UV spectral range. Most important diagnostic lines for studying the general physical conditions as well as the metallicities in the central broad line region in AGN are emitted in the UV. The UV/FUV continuum in AGN excites not only the emission lines in the immediate surrounding but it is responsible for the ionization of the intergalactic medium in the early stages of the universe. Variability studies of the emission line profiles of AGN in the UV give us information on the structure and kinematics of the immediate surrounding of the central supermassive black hole as well as on its mass itself.

Keywords Ultraviolet: galaxies · Galaxies: active · Galaxies: seyfert · Quasars · Emission lines · Quasars · Absorption lines

1. Introduction

Active Galactic Nuclei (AGN) are the most luminous objects in the universe. Their luminosities, their spectral energy distribution from the radio to the γ -ray range, as well as their emission line ratios cannot be generated by normal stars. Galaxies containing an active nucleus are called active galaxies. We divide the AGN in different subclasses such as Quasars, Seyfert galaxies and Liners.

W. Kollatschny (✉)
Institut für Astrophysik, Universität Göttingen,
Friedrich-Hund-Platz 1, D-37077 Göttingen, Germany
e-mail: wkollat@astro.physik.uni-goettingen.de

W. Ting-Gui
Center for Astrophysics, University of Science and Technology of China, Hefei, 230026, China

Many aspects of the generation of the energy in AGN are still unknown. Accretion of gas onto a central supermassive black hole (SMBH) is generally accepted to be the dominant physical process generating the enormous energies we are observing (Rees, 1984). The accretion flow is the source of the non-thermal continuum emission in the UV, X-ray and optical. The spectral energy distribution (SED) of the non-thermal continuum emission in typical AGN has its maximum in the UV.

The central continuum source ionizes the circumnuclear gas in the so called broad line region (BLR) and narrow line region (NLR). The majority of the most important emission lines are emitted in the UV spectral range. The overall continuum distribution as well as the UV spectral lines (narrow emission lines, broad emission lines, absorption lines) are tracers of the physical conditions of those regions where these emission lines originate. The emission line region of the narrow lines is spatially resolved in some nearby objects. They originate at distances of pc to kpc from the central ionizing source. However, the broad emission lines originate at distances of light days to light months only from the central ionizing source. This BLR is unresolved by orders of magnitudes even for the nearest AGN.

Various excellent reviews about AGN have been published over the past years. Different aspects of AGN spectra were highlighted in those papers as (e.g., Netzer, 1990; Urry and Padovani, 1995; Koratkar and Blaes, 1999; Hamann and Ferland, 1999; Veron and Veron, 2000; Ho, 2004; Heckman, 2004; Peterson et al., 2004).

This article is devoted to the UV spectral range of AGN. The UV spectral range is important for our understanding of active galaxies because:

- The maximum flux of AGN is emitted in the UV.

- The rest frame EUV continuum in highly redshifted AGN is important for our understanding of the early universe.
- The UV spectra of the class of low luminous AGN can only be observed in the local universe because of their faintness.
- The most important diagnostic emission and absorption lines are emitted in the UV: they give information on the physical conditions in the emission line region next to the central ionizing source.
- For the study of the cosmological and chemical evolution of AGN the UV spectra of ‘nearby’ objects ($Z = 0\text{--}2$) have to be known.
- Important far UV diagnostic lines can only be observed in the UV – even for high redshift objects.
- Variations of the emission lines give us information on the structure and kinematics of the innermost AGN regions. The most important lines next to the central black hole are emitted in the UV/FUV.

2. The AGN Family

2.1. Seyfert galaxies and quasars

Quasars are the most luminous subclass of the AGN family having nuclear magnitudes of $M_B < -21.5$. Seyfert galaxies are by definition those AGN with $M_B > -21.5$. Besides a strong non-thermal continuum their spectra are dominated by broad permitted emission lines in the UV and optical. Typical observed line widths (full width at half maximum (FWHM)) are $3000\text{--}6000 \text{ km s}^{-1}$ with maxima of up to $30,000 \text{ km s}^{-1}$. The line widths are interpreted as Doppler motion of the BLR clouds where these lines are emitted. The non-thermal ionizing source in AGN is surrounded by the central BLR clouds at distances of less than 1 pc (10^{15} to about 10^{17} cm). Typical electron densities in these emission line regions are $n_e = 10^9\text{--}10^{11} \text{ cm}^{-3}$ for temperatures of about $T \sim 20,000 \text{ K}$. Most of the important diagnostic lines of this BLR are emitted in the UV spectral range – except for the optical Balmer and a few Helium lines.

In the spectra of Seyfert 2 galaxies only narrow (permitted and forbidden) emission lines with typical line widths (FWHM) of $300\text{--}500 \text{ km s}^{-1}$ are present in contrast to those of Seyfert 1 galaxies and quasars. These narrow emission lines originate at distances of about 100 to 1000 pc from the center. Electron densities in the range from 10^2 to 10^4 cm^{-3} are derived for typical electron temperatures of $10,000\text{--}25,000 \text{ K}$. Even if many of the narrow emission lines are emitted in the optical wavelength range too – the most important ones are emitted in the UV.

2.2. Low luminosity AGN

Low Luminosity AGN (LLAGN) refers to those objects with $\text{H}\alpha$ luminosities less than $10^{39} \text{ erg s}^{-1}$. They are the most abundant type of AGN and reside in 40% of bright galaxies in the local universe (Heckman, 1980; Ho et al., 1997). There are evidence that LLAGN may consist of two different subclasses. The first subclass is accretion onto small black holes, i.e., a scaled version of Seyfert galaxies (Filippenko and Ho, 2003; Barth et al., 2004). In the second subclass, it is the very low accretion rate that leads to low nuclear luminosity but otherwise with black holes of similar masses to those in quasars and Seyfert galaxies (e.g., Di Matteo et al., 2003). Both classes of objects have attracted much attentions in the past decade because of their role in the history of black hole growth in the universe and the accretion physics. The black hole-host galaxy connection in the low mass end of black hole, which is likely in their infants, is crucial to the origin of such relations in the massive quiescent and active galaxies, which were found in the last five years (e.g., Magorrian et al., 1998; Gebhardt et al., 2000; Ferrarese et al., 2001), and clues to the formation of seeded BH in the early universe. The state of very lower accretion rate is the end point of the AGN evolution and provides the test-bed for accretion process at very low rate, which is in a very different form from those seen in Seyfert galaxies and quasars. Very low radiative efficiency and the lack of big blue bump is the major prediction of theoretical models for the latter type (e.g., Narayan et al., 1998). Thus the ultraviolet observation is critical to discriminate the two possibilities.

Owing to the weakness of the active nuclei, stellar light usually dominates the continuum emission in the optical band even at the resolution of Hubble Space Telescope. As stellar spectrum drops rapidly towards ultraviolet in most of LLAGN, UV observation is one of the most important spectral regimes for exploring the continuum properties of those objects. Reverberation mapping of broad line region described in the next section can only be carried out in ultraviolet for this type of AGN since one has to measure precisely small variations in the continuum flux. In addition, these AGN are so faint, only nearby objects can be studied in detail. However, they are much less studied in the UV than other type of AGN due to their intrinsic faintness (Maoz et al., 1999).

The majority of these sources show characteristics of Low Ionization Nuclear Emission Line Region (LINER), which can be produced either through photo-ionization of the AGN/young stellar clusters or shock process (Heckman, 1980). Some key issues that might be solved with future UV observations include: (1) How much fraction of LINERS are powered by nuclear activity, how much by star forming process and what is the role of shocks? Measuring high excitation lines (such as CIII/CII) in UV is critical

to distinguish photo-ionization process by the central continuum from opaque shock ionization models (Dopita and Sutherland, 1996). The measurement of UV absorption lines of young stellar component or the featureless AGN continuum will allow to determine the contribution of the ionizing source, directly. (2) What is the UV continuum spectrum of these active nuclei, which is closely related to the truncate radius of the geometrically thin and optically thick part of the disk and coupling between electron and proton in the case of low rate accretion onto large mass BH (Quataert et al., 1999), or to the global energy output in the accretion onto low mass AGN. (3) How does the BLR structure of LLAGN fit into the whole picture of AGN? There is indirect evidence that the size of BLR in LLAGN deviates systematically from the relation extrapolated from the known one for Quasars and Seyfert galaxies (Wang and Zhang 2003). But a direct measurement of the size of BLR by reverberation mapping is required.

3. Spectral Energy Distribution and Rest Frame EUV Continuum in AGN

The mean broadband continuum spectral energy distribution (SED) for radio-quiet and radio-loud AGN is shown in Fig. 1. The flux scale has been normalized at $1 \mu\text{m}$. The AGN continuum flux is relatively flat from the radio to the X-ray range. The bulk of this flux is thought to arise from synchrotron emission. Besides a bump in the infrared due to thermal dust reemission the overall continuum flux peaks additionally in-between the optical and soft X-ray spectral range in the UV. This spectral feature is sometimes called the big blue bump. More than half of the bolometric luminosity of an (un-obscured) AGN is emitted in this big blue bump. The big blue bump is thought to arise from an accretion disk surrounding the central black hole. Gravitational

energy from the central accretion flow is converted into the observed UV radiation of the disk. The thermal emission in the UV corresponds to typical temperatures of 10^5 K (e.g., Koratkar and Blaes, 1999).

The study of the UV/EUV spectral range is very difficult because of the absorption caused by our own galaxy, the intrinsic absorption in distant galaxies, as well as the absorption in the intergalactic medium. Figure 2a shows the UV composite spectrum derived from more than 2000 AGN spectra. Before combining the spectra (Telfer et al., 2002) corrected them for internal and external extinction as good as possible. The dotted line shows accretion disk models of (Mathews and Ferland, 1987). The dashed line corresponds to simple power law models with a thermal cutoff corresponding to a temperature of $5.4 \times 10^5 \text{ K}$. Figure 2b again shows a composite optical–soft X-ray spectrum for radio-loud and radio-quiet quasars. One can see the flux is peaking not as extreme as model calculations of accretion disk models predict (e.g., Laor et al., 1997). The accretion disk models cannot reproduce in a simple way the observed spectral shape. There are indications in the observed composite AGN spectra that the spectral index brakes at $\sim 1000 \text{ \AA}$. Observational difficulties are caused by dust obscuration and the contamination of the host galaxy. Furthermore, the composite spectrum has been derived from different classes of AGN. Far more observations in the UV of all classes of AGN are needed to understand the details of accretion disks surrounding the central black hole in AGN.

The knowledge of the UV/FUV spectral shape of quasars is of outmost importance for our understanding of the evolution of the early universe. The UV continuum of quasars ionizes the intergalactic medium at the end of the dark ages. At $z \geq 6$ the neutral hydrogen has been re-ionized by the ionizing radiation of quasars at very early stages of the universe. The epoch of the ionization of HeI and HeII is even less clear. Figure 3 shows a spectrum of the high redshift

Fig. 1 Schematic representation of the mean spectral energy distributions (SED) for a sample of radio-quiet (solid lines) and radio-loud (dashed lines) QSOs (from Elvis et al., 1994)

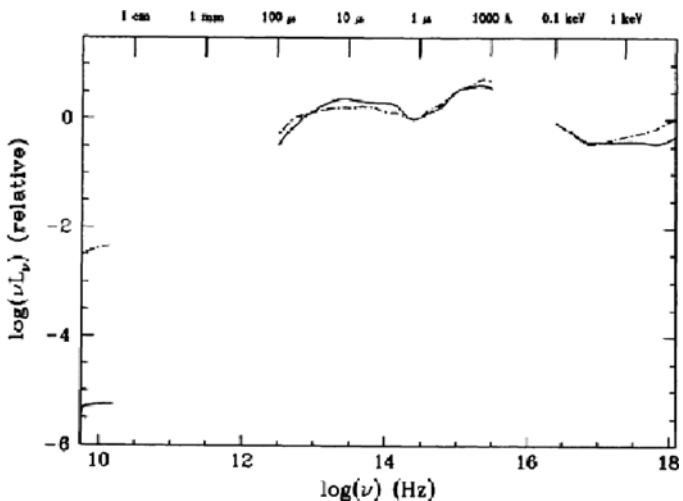


Fig. 2 Left: Composite optical–soft X-ray spectrum for the RQQs and RLQs in our sample (thick solid line). Three X-ray–weak quasars, and PG 1114+445, which is affected by a warm absorber, were excluded from the composite. Right: Observed energy distribution of some quasars vs. two accretion disk model spectra (Laor et al., 1997)

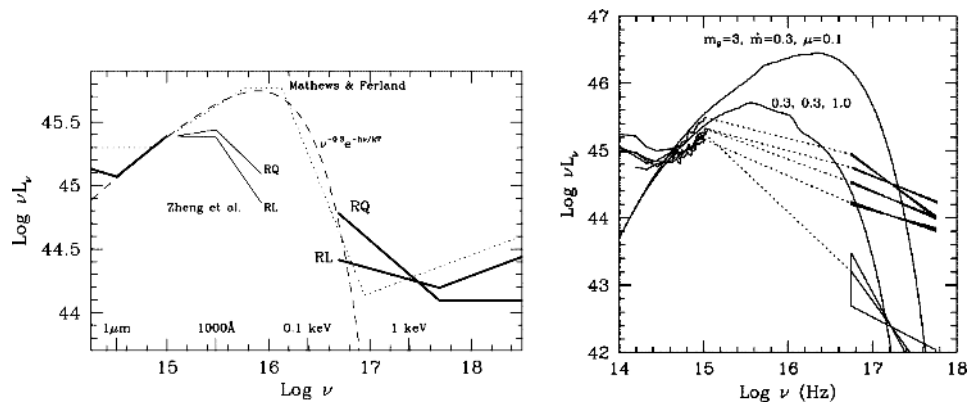
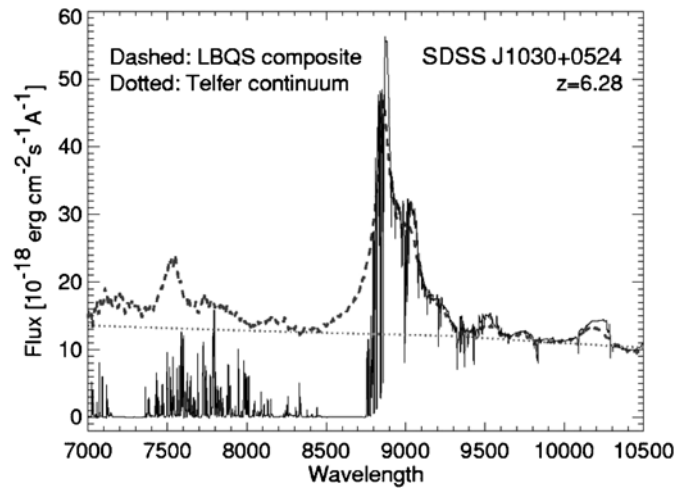


Fig. 3 De-noised, full-resolution spectrum of SDSS J1030+0524 with matched templates from the LBQS and Telfer et al. (2002). The template is a very good match to the quasar redward of the Ly α IGM absorption (White et al., 2003)



quasar SDSSJ1030 + 0524 ($z = 6.28$) with the UV spectral template of Telfer et al. (2002). The Gunn-Peterson absorption troughs show no emission over a redshift interval of 0.2 starting at $z = 6$.

4. UV Emission Line Diagnostics

A UV spectrum of the Seyfert 1 galaxy NGC 4151 is shown in Fig. 4. Some emission lines as well as some absorption features are indicated in Fig. 4. The spectrum has been taken with the Hopkins Ultraviolet Telescope (HUT) (Kriss et al., 1992). The most important AGN diagnostic lines between 950 and 2000 Å are: CIII 977, NIII 991, Ly β +OVI 1034, Ly α , NV 1240, OI 1303, CII 1335, SiIV+OIV] 1394, 1402, NIV] 1486, CIV 1549, HeII 1640, OIII] 1663, NIII] 1750, and CIII] 1909. These emission lines show a wide range of ionization states. They originate at different distances from the central ionizing source in clouds with densities from $n_e = 10^8$ – 10^{12} cm^{-3} .

Photoionization calculations predict line flux ratios we can compare with the observations. Figure 5 shows a series of calculations of emission line ratios for different slopes

of the ionizing continuum flux (from Hamann and Ferland (1999)).

4.1. Metallicities

The determination of the heavy element abundances in AGN is one further aspect of quasar emission line studies. This is connected with the investigation of the chemical evolution of the universe as quasars can be observed at extreme distances and therefore at very large look-back times. Surprisingly, the broad line spectra of nearby AGN resemble those of the most distant quasars. Furthermore, there are indications in the spectra of some distant luminous quasars that their metallicity abundances are very high even at $z \geq 5$ (e.g., Ferland et al., 1996).

In early investigations of AGN spectra the collisionally excited inter-combination lines NIII] λ 1750, NIV] λ 1486, OIII] λ 16664, CIII] λ 1909 have been used to derive the abundance ratios of the elements nitrogen, oxygen and calcium (e.g., Shields, 1976; Davidson, 1977; Baldwin and Netzer, 1978). But these diagnostic lines are weak in most spectra. Furthermore, the densities in the BLR ($n_e = 10^9$ – 10^{11} cm^{-3}) are near the critical densities of these lines. Therefore these lines have different degrees of collisional suppression.

Fig. 4 The ultraviolet spectrum of the Seyfert galaxy NGC 4151 obtained by the Hopkins Ultraviolet Telescope (HUT). Emission line features and absorption features are marked. They are due to various ionization states of different elements in the hot gas present in the nucleus of this active galaxy (from Kriss et al., 1992)

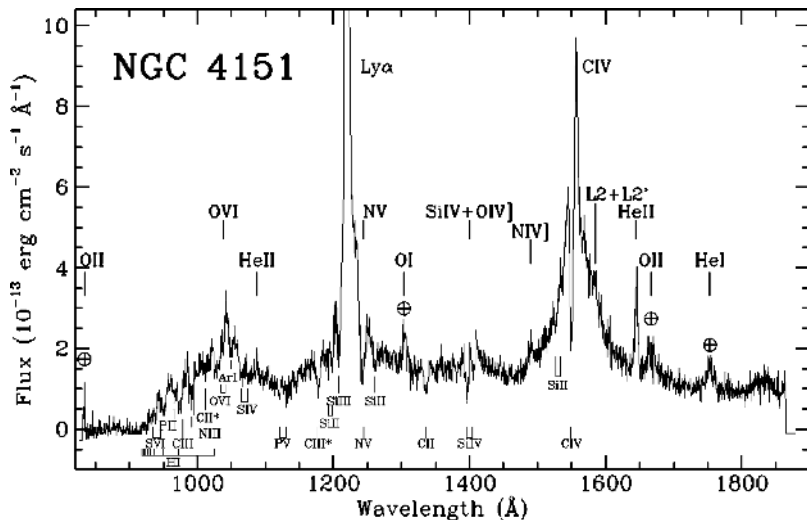
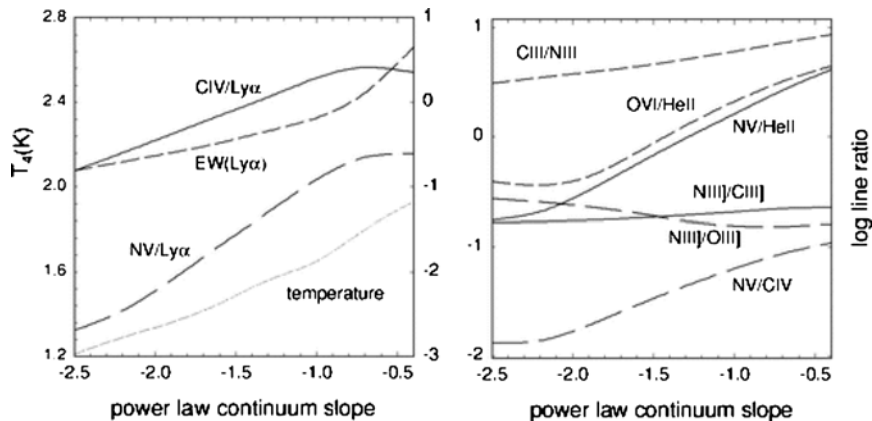


Fig. 5 Predicted line flux ratios, gas temperatures and dimensionless equivalent widths in Ly α plotted for clouds photo-ionized by different power-law spectra. (from Hamann and Ferland, 1999)



Permitted lines might be better candidates for deriving the element abundances in AGN. Detailed calculations have been carried out (e.g., Hamann et al., 2002) proving the sensitivity of the UV broad emission lines with respect to the metalicity in AGN spectra. The most important diagnostic lines are NIII λ 991, NV λ 1240, CIII λ 977, CV λ 1550, CIV+OIV λ 1034, HeII λ 1640.

All these diagnostic lines are emitted in the UV. It is possible to derive the metalicities only for distant ($z \geq 2$) as well as luminous quasars when the diagnostic lines are shifted into the optical range. Very few is known about nearby and/or low luminous AGN. But it is necessary to have this information for deriving the chemical evolution of the universe.

A few very interesting AGN show clear indications of abundance anomalies as e.g. Q0353-383 (Osmer and Smith, 1980). But they are rare and nothing is known about their evolution and their number in the present day universe. Very recently (Bentz et al., 2004) checked the Sloan Digital Sky Survey for all nitrogen-rich quasars. They investigated more than 6000 quasars with appropriate redshifts that the important UV diagnostic lines were shifted into the optical range. Only four candidates show very strong nitrogen emission

lines comparable to those in the spectrum of Q0353-383 (see Fig. 6). This means that only about one in 1700 distant quasars ($z \geq 2$) has extreme nitrogen over-abundances. Further spectra of nearby and distant, as well as of bright and low luminous AGN are needed to understand these galaxies within the overall AGN population. There is the basic question whether the nitrogen enrichment is a short phase in an AGN lifetime only or whether only a certain percentage of quasars reaches extremely high metalicities. We need UV spectra to detect high or even very high metalicities in present day AGN to answer this question.

4.2. Far UV diagnostic lines

Very few is known about line strengths of diagnostic emission lines in the extreme ultraviolet spectral range between 300 and 900 Å. Composite far UV spectra have been constructed from the spectra of highly redshifted QSOs taken with the Hubble Space Telescope (HST) and the Far Ultraviolet Spectroscopic Explorer (FUSE). They show the HeII λ 304 and HeI λ 584 lines as well as the high ionization NeVIII + OIV lines at 772 Å and OIII at 831 Å (Telfer et al., 2002,

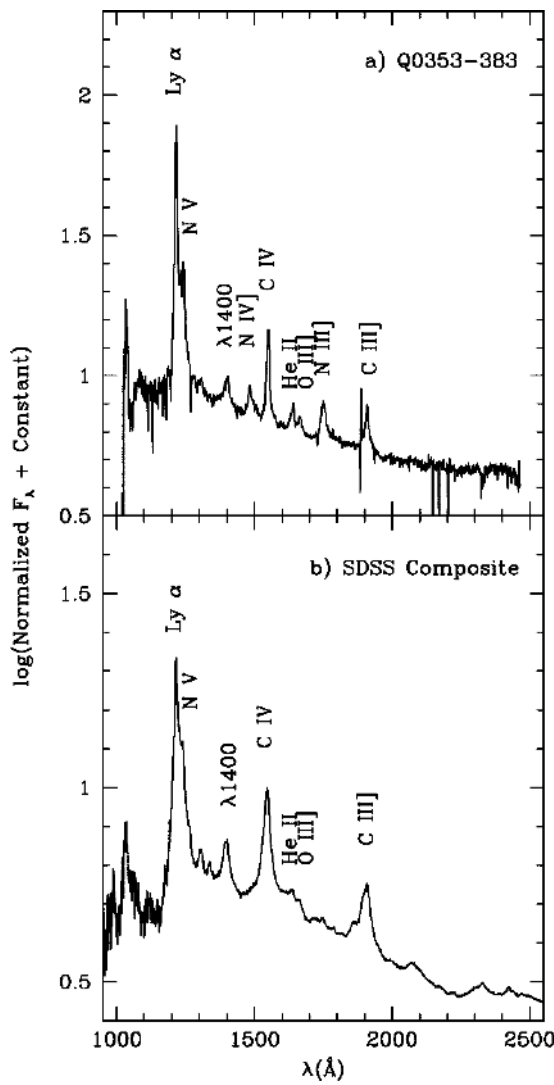


Fig. 6 Rest-frame spectra of (a) Q0353-383 and (b) the SDSS composite, composed of 2204 quasar spectra. Both spectra are plotted in semi-log format to enhance fine details (Bentz et al., 2004)

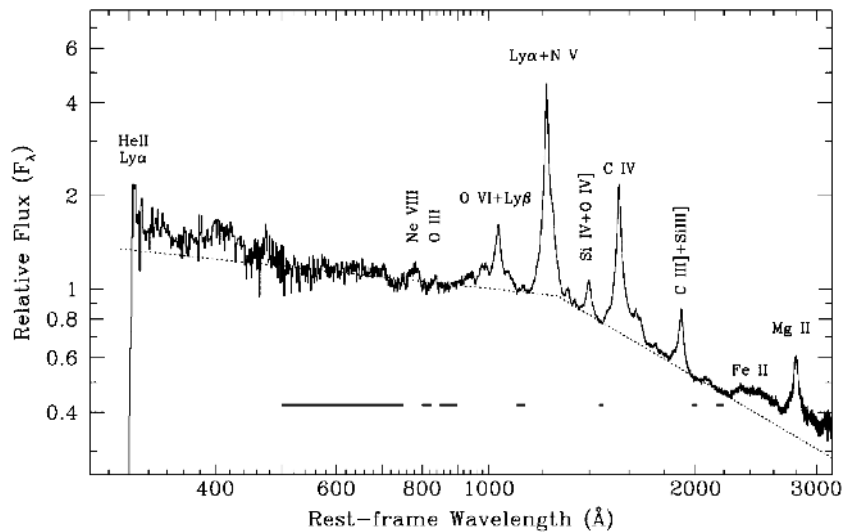
Fig. 7 Overall mean composite QSO spectrum in 1 Å bins with some prominent emission lines marked. The dotted line shows the best-fit broken power-law continuum, excluding the region below 500 Å. The lines at the bottom indicate the continuum windows used in the fit (Telfer et al., 2002)

Scott et al., 2004) (see Fig. 7, Telfer et al., 2002). Considerably more UV spectra of intermediate and high redshift AGN are needed to compile far UV spectra with better S/N ratio and to investigate the spectral details of different classes of AGN.

The UV and EUV diagnostic lines are of outmost importance to understand the AGN phenomenon. Their properties reflect the highest energetic areas next to the central black holes in AGN.

4.3. UV absorption lines

Broad blue shifted resonant absorption lines in the ultraviolet have been detected in 10–20% optically selected quasars (Weymann et al., 1991), while narrow intrinsic absorption lines are much more common (~40% of Seyfert galaxies and ~20–30% in quasars (Hamann and Sabra, 2004, and references therein)). The predominance of blue-shift among absorption lines suggests that partially ionized gas outflows from the active nucleus. Recent X-ray observations with moderate spectral resolution have found similar blue-shifted absorption lines in the X-ray bands (e.g., Collinge et al., 2001). There are suggestion that the mass loss rate and kinetic energy associated with the outflow may be large and can have significant impact on the structure of disk itself if it is disk-wind and on the ISM of the host galaxies. But evidence for this is still ambiguous for following reasons. Because strong UV absorption lines may be severely saturated and partially covering, the column density and ionization state of major UV absorbing ions are poorly determined (e.g., Arav et al., 2001). Although the total absorption column density can be better determined from photo-electronic absorption in X-rays, very little information about velocity structure of X-ray absorption line/edge can be obtained from the current data. Resonant line absorptions in X-ray can be a very



powerful diagnostics of properties of ions at different level of ionizations, but spectral resolution comparable to those in optical and UV band will not be available within next decade. Therefore, it is necessary to observe the weak absorption lines of the same elements that produce strong absorption lines in order to derive both the covering factor and column density as a function of velocity. Most these lines fall in the spectral domain of far to extreme ultraviolet. Figures 8 and 9 shows absorption lines in the UV spectral range of 3C191 taken with Keck (Hamann et al., 2001) and of Mrk509 taken with FUSE (Kriss et al., 2003). UV observations, simultaneously in soft X-rays with future more sensitive X-ray missions, may improve our understanding of the problem in several aspects: (1) Simultaneous observations of UV and soft X-ray absorption

of low red-shift AGN would allow to determine the total column densities of material, especially those at the ionization level similar to that of UV absorbing material, and ionization states of the X-ray absorbing material (Wang et al., 2000). At the same time we get velocity structure information from UV absorption lines. This will permit a detailed modeling of the physical state of outflows. (2) By studying absorption lines in UV bright $z \sim 2$ BAL QSOs, we will obtain the kinematical properties of absorption lines of highly ionized species at far UV. Comparison of those with low ionization species will allow to study the changes in the kinematics with ionization state, thus to bridge the gap between that with X-ray absorbing material in these objects. Observing bright $z = 2$ BAL QSOs will also allow to better determine

Fig. 8 High resolution Keck spectrum of 3C191 showing the strong associated absorption lines in the UV (Hamann et al., 2001)

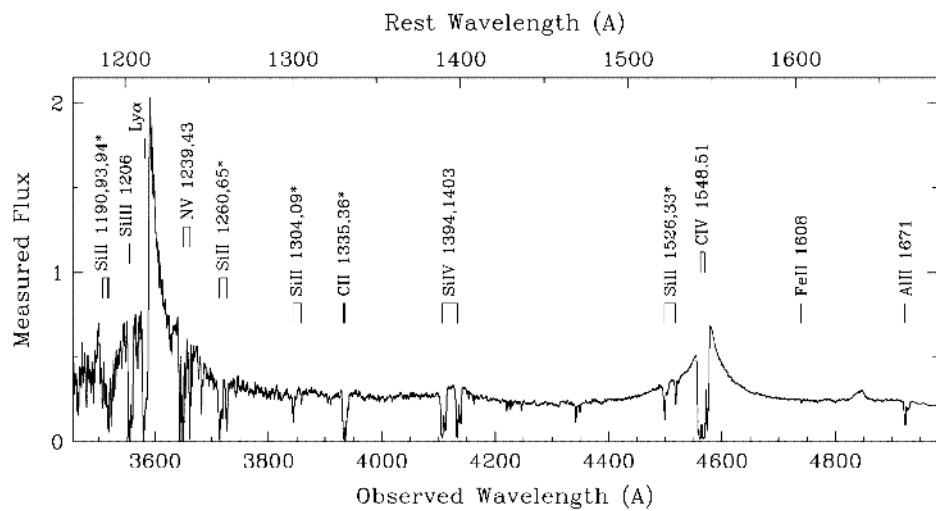
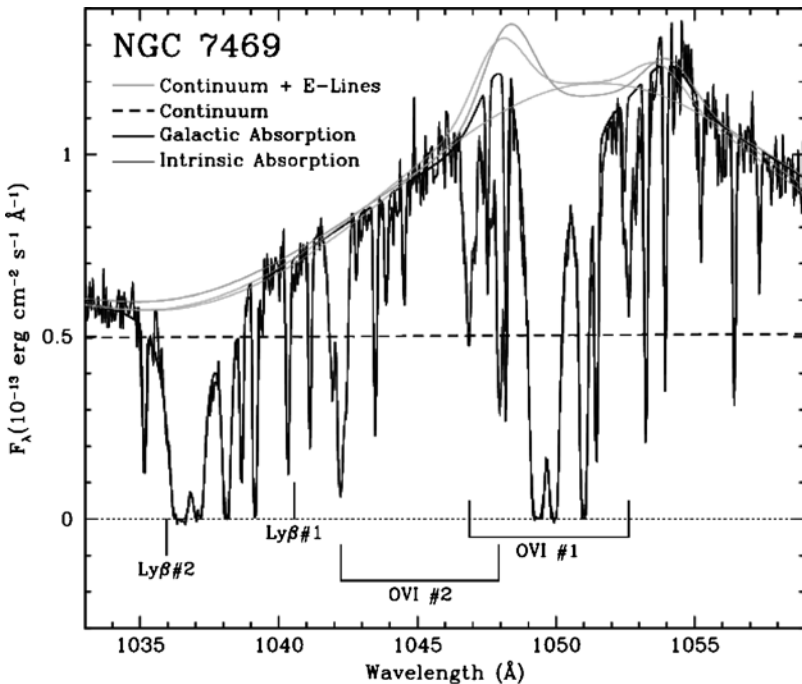


Fig. 9 FUSE spectrum of NGC 7469 in the Ly β /O VI region (thin black line) (Kriss et al., 2003)



the shape of the ionizing continuum, one uncertainty in the modeling of the ionization structure of absorbing gas. (3) Variations of intrinsic UV absorption lines can put strong constraints on the density of the absorbing material, and thus give an upper limit on the distance to the continuum source. If these observations are carried out simultaneously in soft X-rays for low- z AGN, one might distinguish the variations caused by changes in the flow and ionization effect (e.g., Gebel et al., 2002). (4) Comparison of abundances derived from absorption lines with those from emission lines will give an independent check of those derived from emission lines.

5. Structure and Kinematics of the Central Region in AGN

The innermost line emitting region in AGN – the broad emission line region (BLR) – surrounds the central supermassive black hole at distances of about 10^{15} to 10^{17} cm. This corresponds to radii of light days to light months. The motions of the line emitting clouds give us information on the mass of the central black hole (e.g., Kaspi et al., 2000; Peterson et al., 2004). The broad-line region is spatially unresolved even in the nearest AGN. But we can derive the structure and kinematics with indirect methods by studying their line and continuum variability (e.g., Kollatschny, 2003; Horne et al., 2004).

5.1. Reverberation mapping

In a first step one has to correlate observed light-curves of integrated broad emission line intensities with the ionizing continuum light curve. It is of great advantage to observe the ionizing flux in the UV since the optical continuum flux is far more contaminated by the stellar continuum flux of the host galaxy. Figure 10 shows the results of an optical/UV variability campaign (including HST observations) of the prototype Seyfert galaxy NGC5548 (Peterson and Wandel, 1999). Plotted is the time lag of the emission lines with respect to continuum variations as a function of their linewidth (FWHM) in the rms profiles. The time lag corresponds to the mean distance of the line emitting region from the central ionizing source. One can see a clear trend: the higher ionized lines originate closer to the central source. UV lines originate about ten times closer to the center than optical emission lines. The most successful monitoring campaign of the integrated UV lines of an AGN has been carried out for NGC5548 so far (Clavel et al., 1991; Korista et al., 1995). Variability campaigns of e.g. 3C390.3 (O'Brien et al., 1998) and Akn 564 (Collier et al., 2001) demonstrated the power of UV reverberation studies but the S/N ratio and/or the fractional variability am-

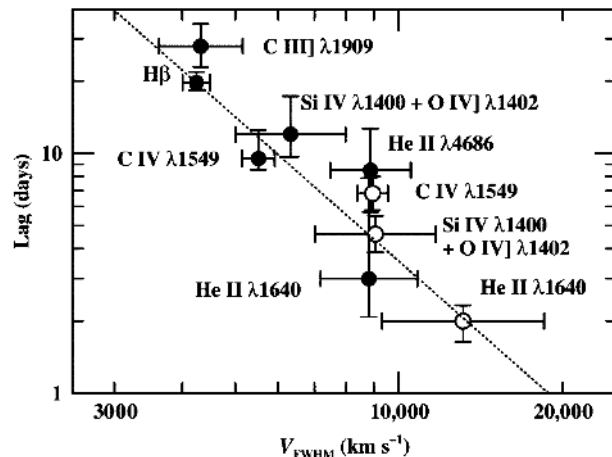


Fig. 10 Time lags (cross-correlation function centroids τ_{cent}) in days ($1 \text{ lt-day} = 2.6 \times 10^{15} \text{ cm}$) for various lines in NGC 5548 are plotted as a function of the FWHM of the feature (in the rest frame of NGC 5548) in the rms spectrum. The filled circles refer to data from 1989, and the open circles refer to data from 1993. The dotted line indicates a fixed virial mass $M = 6.8 \times 10^7 M_\odot$ (Peterson and Wandel, 1999)

plitudes of the continuum variations were not strong enough for detailed line profile studies.

Future monitoring campaigns of many galaxies including the UV spectral range of the highly ionized OVI lines ($\lambda\lambda 1032, 1038$) e.g. will uncover the innermost broad line region in AGN. The clear trend that higher ionized emission lines originate closer to the center has been seen in optical variability campaigns of e.g. Mrk 110 too (see Fig. 11) (Kollatschny, 2003). But the most important lines for reverberation studies are: CVλ1550, SiIV+OIV]λ1400, HeIIλ1640, NVλ1240, CIV+OIVλ1034 (see Fig. 10). These lines give us information about the immediate surrounding

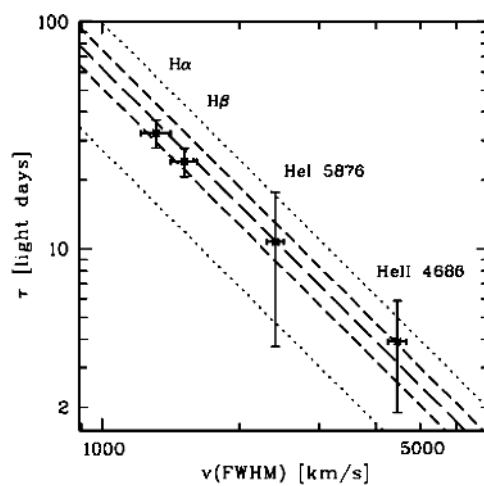


Fig. 11 The distance of the Balmer and Helium emitting line regions from the central ionizing source in Mrk 110 as a function of the FWHM in their rms line profiles. The dotted and dashed lines are the results from model calculations for central masses of 0.8, 1.5, 1.8, 2.2, and $2.9 \cdot 10^7 M_\odot$ (from bottom to top) (Kollatschny, 2003)

of the central black hole one order of magnitude closer than we can do it with optical lines.

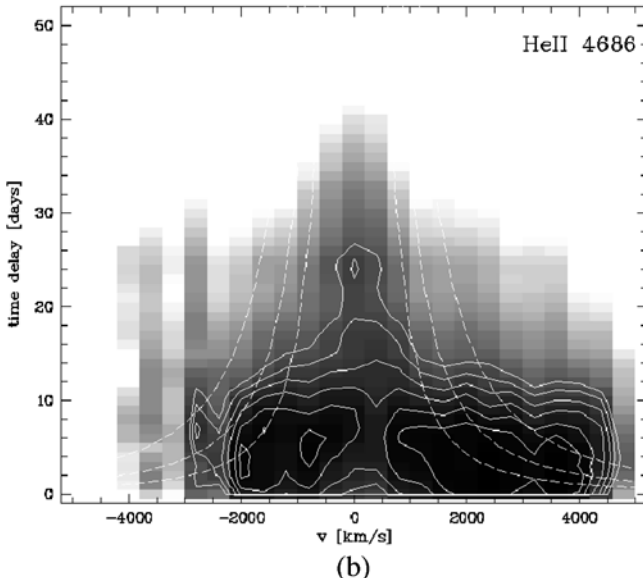
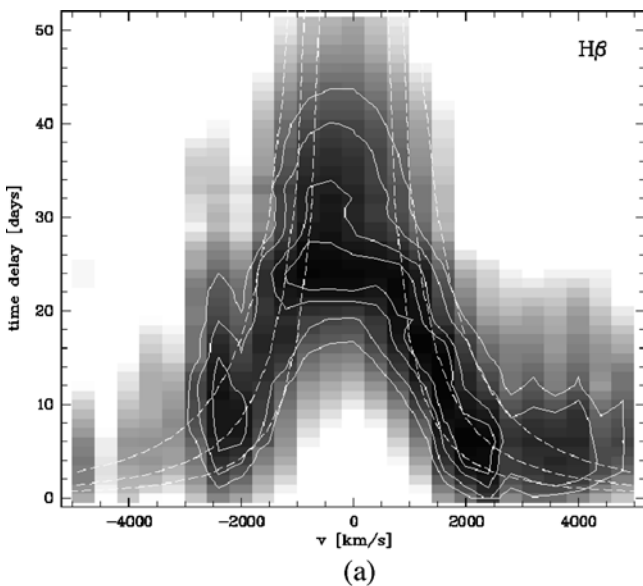
The line profile variations of UV lines should be studied in a second step. They give us information on the kinematics in the broad line region. Detailed profile variations have been studied in the optical lines of Mrk 110 (Kollatschny and Bischoff, 2002; Kollatschny, 2003) only so far. Different delays of emission line segments (the velocity-delay maps) measure the geometry and flow of the line emitting gas when we compare observed two-dimensional velocity-delay maps with model calculations (e.g., Welsh and Horne, 1991). Figure 12 shows the correlation of H β and HeII $\lambda 4686$ line profile segments with continuum variations. The data are from the variability campaign of Mrk 110 taken with the 10 m Hobby Eberly Telescope at McDonald Observatory. Only

Keplerian disk BLR models can reproduce the observed fast and symmetric response of the outer line wings. The H β line center originates at distances of 25 light-days while the HeII line center originates at distances of 4 light-days only.

5.2. Central black hole mass in AGN

It is possible to calculate the central black hole mass in AGN. One has to know the distances of the line emitting clouds as well as the velocity dispersion of these clouds (e.g., Peterson et al., 2004). We derived a central black hole mass of $1.4 * 10^8 M_\odot$ in Mrk110. In that case we used additional information about the projected angle of the accretion disk where the broad emission lines originate (Kollatschny, 2003). A Schwarzschild radius r_s of 4×10^{13} cm corresponds to this

Fig. 12 The 2-D CCFs(τ, v) show the correlation of the Balmer and Helium line segment light curves with the continuum light curve as a function of velocity and time delay (grey scale) in Mrk110. Contours of the correlation coefficient are over-plotted at levels between .800 and .925 (solid lines). The dashed curves show computed escape velocities for central masses of $0.5, 1, 2 \times 10^7 M_\odot$ (from bottom to top) (Kollatschny and Bischoff, 2002; Kollatschny, 2003)



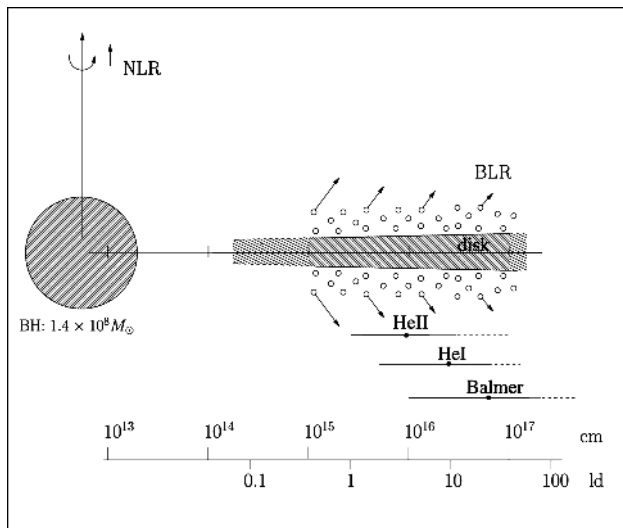


Fig. 13 Schematic model of the innermost region in the Seyfert galaxy Mrk110 derived from 2D-reverberation mapping (Kollatschny, 2003)

black hole mass. Figure 13 shows the inner broad line region structure of Mrk 110 derived from 2D-reverberation mapping. The HeII line originates at a distance of 230 Schwarzschild radii only from the central black hole. The monitoring of highly ionized UV lines in AGN enables us to study the physics of the immediate environment of black holes even more closer to the center. This helps us to derive the central black hole mass more precisely. Finally, we will achieve a clear progress in our knowledge of black hole physics by monitoring different types of AGN in the UV.

References

- Arav, N., et al.: ApJ **561**, 118 (2001)
 Baldwin, J.A., Netzer, H.: ApJ **226**, 1 (1978)
 Barth, A.J., Ho, L.C., Rutledge, R.S., Sargent, W.L.C.: ApJ **607**, 90 (2004)
 Bentz, M.C., Hall, P.B., Osmer, P.S.: AJ **128**, 561 (2004)
 Clavel, J. et al.: ApJ **366**, 64 (1991)
 Collinge, M.J., et al.: ApJ **557**, 2 (2001)
 Collier, S., Crenshaw, D.M., Peterson, B.M., Brandt W.N., et al.: ApJ **561**, 146 (2001)
 Davidson, K.: ApJ **218**, 20 (1977)
 Di Matteo, T., Allen, S.W., Fabian, A.C., Wilson, A., Young, A.J.: ApJ **582**, 133 (2003)
 Dopita, M.A., Sutherland, R.S.: ApJS **102**, 16 (1996)
 Elvis, M., Wilkes, B.J., McDowell, J.C., Green, R.F. et al.: ApJS **95**, 1 (1994)
 Ferland, G.J., Baldwin, J.A., Korista, K.T., Hamann, F., Carswell, R.F., Phillips, M., Wilkes, B., Williams, R.E.: ApJ **461**, 683 (1996)
 Ferrarese, L., Pogge, R.W., Peterson, B.M., Merritt, D., Wandel, A., Joseph, C.L.: ApJ **555**, L79 (2001)
 Filippenko, A.V., Ho, L.C.: ApJ **588**, L13 (2003)
 Gebhardt, K., et al.: ApJ **539** (2000)
 Gebel, J.R., et al.: ApJ **595**, 120 (2003)
 Hamann, F., Ferland, G.J.: ARAA **37**, 487 (1999)
 Hamann, F., Barlow, T.A., Chaffee, F.C., Foltz, C.B., Weymann, R.J.: ApJ **550**, 142 (2001)
 Hamann, F., Korista, K.T., Ferland, G.J., Warner, C., Baldwin, J.: ApJ **564**, 592 (2002)
 Hamann, F., Sabra, B.: In: Richards, G.T., Hall, P.B. (eds.), ASP Conf Series 311, San Francisco ASP, p. 203 (2004)
 Heckman, T.M.: A & A, **87**, 142 (1980)
 Heckman, T.M.: In: L.C. Ho (ed.), Coevolution of Black Holes and Galaxies, from the Carnegie Observatories Centennial Symposia. Published by Cambridge University Press, p. 359 (2004)
 Ho, L.C., Filippenko, A.V., Sargent, W.L.W.: ApJ **487**, 568 (1997)
 Ho, L.: In L.C. Ho (ed.), Coevolution of Black Holes and Galaxies, from the Carnegie Observatories Centennial Symposia. Published by Cambridge University Press, p. 292 (2004)
 Horne, K., Peterson, B.M., Collier, S.M., Netzer, H.: PASP, **116**, 465 (2004)
 Kaspi, S., Smith, P.S., Netzer, H., Maoz, D., Jannuzi, B.T., Giveon, U.: ApJ **533**, 631 (2000)
 Kollatschny, W., Bischoff, K.: A & A, **386**, L19 (2002)
 Kollatschny, W.: A & A, **407**, 461 (2003)
 Koratkar, A., Blaes, O.: PASP, **111**, 1 (1999)
 Korista, K.T., et al.: ApJS **97**, 285 (1995)
 Kriss, G.A., Davidsen, A.F., Blair, W.P. et al.: A & A, **392**, 485 (1992)
 Kriss, G.A., Blustin, A., Branduardi-Raymont, G., Green, R.F., Hutchings, J., Kaiser, M.E.: A & A **403**, 473 (2003)
 Laor, A., Fiore, F., Elvis, M., Wilkes, B.J., McDowell, J.C.: ApJ **477**, 93 (1997)
 Magorrian, J., et al.: AJ, **115**, 2285 L13 (1998)
 Mathews, W.G., Ferland, G.J.: ApJ **323**, 456 (1987)
 Maoz, D., et al.: AJ, **116**, 55 (1999)
 Narayan, R., Mahadevan, R., Grindlay, J.E., Popham, R.G., Gammie, C.: ApJ **492**, 554 (1998)
 Netzer, H.: In: T.J.-L., Courvoisier et al. (eds), Active galactic nuclei, Saas-Fee advanced course 20, p. 57 (1990)
 O'Brien, P.T. et al.: ApJ, **509**, 1630 (1998)
 Osmer, P.S., Smith, M.G.: ApJS, **42**, 333 (1980)
 Peterson, B.M., Ferrarese, L., Gilbert, K.M., Kaspi, S. et al.: ApJ **613**, 682 (2004)
 Peterson, B.M., Wandel, A.: ApJ **521**, L95 (1999)
 Quataert, E., di Matteo, T., Narayan, R., Ho, L.C.: ApJ **525**, L89 (1999)
 Rees M.: ARA & A **22**, 471 (1984)
 Scott, J.E., Kriss, G.A., Brotherton, M., Green, R.F., Hutchings, J., Shull, J.M., Zheng, W.: ApJ **615**, 135 (2004)
 Shields, G.A.: ApJ **204**, 330 (1976)
 Telfer, R.C., Zheng, W., Kriss, G.A., Davidsen, A.F.: ApJ **565**, 773 (2002)
 Urry, C.M., Padovani, P.: PASP **107**, 803 (1995)
 Veron, M.P., Veron, P.: Astron. Astrophys Rev. **10**, 81 (2000)
 Wang, T.G., Brinkmann, W., Yuan, W., Wang, J.X., Zhou, Y.Y.: ApJ **545**, 77 (2000)
 Wang, T.G., Zhang, X.G.: MNRAS **340**, 793 (2003)
 Welsh, W.F., Horne, K.: ApJ **379**, 586 (1991)
 Weymann, R.J., Morris, S.L., Foltz, C.B., Hewett, P.C.: ApJ **373**, 23 (1991)
 White, R.L., Helfand, D.J., Becker, R.H., Gregg, M.D., Postman, M., Lauer, T.R., Oegerle, W.: AJ **126**, 706 (2003)

Fundamental Problems in Astrophysics

Ana I. Gómez de Castro · Willem Wamsteker ·
Martin Barstow · Noah Brosch · Norbert Kappelmann ·
Wolfram Kollatschny · Domitilla de Martino ·
Isabella Pagano · Alain Lecavelier des Étangs ·
David Ehenreich · Dieter Reimers ·
Rosa González Delgado · Francisco Najarro ·
Jeff Linsky

Received: 21 February 2006 / Accepted: 14 March 2006
© Springer Science + Business Media B.V. 2006

Abstract Progress of modern astrophysics requires the access to the electromagnetic spectrum in the broadest energy range. The Ultraviolet is a fundamental energy domain since it is one of the most powerful tool to study plasmas at temperatures in the 3,000–300,000 K range as well as electronic transitions of the most abundant molecules in the Universe. Moreover, the UV radiation field is a powerful astrochemical and photoionizing agent.

The objective of this review is to describe the crucial issues that require access to the UV range. A summary has been added to the end with a more classic view of UV needs by astronomical object type; this approach is followed at length in the rest of the contributions of this issue.

A. I. G. de Castro (✉)
Instituto de Astronomía y Geodesia (CSIC-UCM), Universidad
Complutense de Madrid, Madrid, E-28040, Spain

W. Wamsteker (†)
INTA-LAEFF, Apartado 50.727, E-28080 Madrid, Spain

M. Barstow
Dept of Physics and Astronomy, University of Leicester
University Road, Leicester LE1 7RH UK

N. Brosch
The Wise Observatory, Tel Aviv University, Tel Aviv 69978, Israel

N. Kappelmann
Institut für Astronomie und Astrophysik Tübingen (IAAT),
Universität Tübingen, Germany

W. Kollatschny
Institut für Astrophysik, Universität Göttingen,
Friedrich-Hund-Platz 1, D-37077 Göttingen, Germany

D. de Martino
INAF-Osservatorio Astronomico di Capodimonte Napoli, Via
Maiariello 16, I-80131, Italy

Keywords UV astronomy

1. Introduction

Access to the UV range is fundamental for the progress of astrophysics since UV spectroscopy is the most powerful tool to study plasmas at temperatures in the 3,000–300,000 K range. Also, the electronic transitions of the most abundant molecules in the Universe (H_2 , CO, OH, CS, CO_2^+ , C_2^+ ...) are in this range. Moreover, the UV radiation field is a powerful astrochemical and photoionizing agent.

The impact of UV instruments in modern astronomy can be clearly traced through the considerable success of the

I. Pagano
INAF-Catania Astrophysical Observatory, via Santa Sofia 78,
95125 Catania, Italy

A. L. des Étangs · D. Ehenreich
Hamburger Sternwarte, Universität Hamburg, Gojenbergsweg 112,
D-21029 Hamburg, Germany

D. Reimers
Institut d' Astrophysique de Paris, UMR7095 CNRS, Université
Pierre & Marie Curie, 98^{bis} boulevard Arago, F-75014 Paris,
France

R. G. Delgado
Instituto de Astrofísica de Andalucía (CSIC), Apdo. 3004, 18080
Granada, Spain

F. Najarro
Instituto de Astrofísica Molecular e Infrarroja, Instituto de
Estructura de la Materia, CSIC, Serrano 121, E-28006 Madrid

J. Linsky
JILA/University of Colorado and NIST/Boulder, CO 80309-0440
USA

International Ultraviolet Explorer (IUE) observatory and successor instruments such as the GHRS and STIS spectrographs on-board the Hubble Space Telescope (HST), or the FUSE satellite operating in the far UV (90–120 nm range). Of particular importance has been access to high resolution $R \simeq 40,000\text{--}100,000$ spectra providing an ability to study the dynamics of hot plasma and separate multiple galactic, stellar or interstellar spectral lines. Furthermore, the GALEX satellite is providing new exciting views of UV sources. As a result, UV facilities are in high demand; observing time on HST remains heavily oversubscribed (a factor ~ 6 in 2004), but its UV spectroscopic capabilities were hampered by STIS closure. Far-UV observations with FUSE also take a large share. This success has an interesting consequence: while astrophysicists world-wide are used to have a observatory-like access to the space telescopes working in this range, the BIG funding required to create/maintain large space facilities is driven by key scientific projects. The objective of this review is to describe briefly the crucial problems of modern astrophysics that require access to the UV range. A summary has been added to the end with a more classic view of UV needs by astronomical object type; this approach is followed at length in the rest of the contributions of this issue.

2. Crucial problems in modern astrophysics that require access to the UV range

Modern astrophysics is a mature science that has evolved from its early phase of discovery and classification to a physics-oriented discipline focussed in finding answers to fundamental problems ranging from cosmology to the origin and diversity of life-sustainable systems in the Universe. This evolution is not uniform; research in fields like compact objects or cosmology is clearly at this stage but the detection of extrasolar planets or the identification of the sources of γ -rays bursts are still at early stages. This diversity can be nicely traced in several recent collections of articles devoted to the identification of “unsolved problems in astrophysics” or to the “fundamental problems in astrophysics” (see, for instance, Bahcall and Ostriker, 1997). Though a much wider science case can be drawn, we have identified three key fields in astrophysics that cannot progress without easy and widespread access to modern UV instrumentation; these are:

1. Extrasolar planetary atmospheres and astrochemistry in the presence of strong UV radiation fields.
2. Chemical evolution of the Universe and the diffuse baryonic content.
3. The physics of accretion and outflow: the astronomical engines.

This list is by no means complete, but it certainly includes the most exciting and active problems that the majority of the

astrophysical community would like to see solved. We detail each of these below.

2.1. Extrasolar planetary atmospheres and astrochemistry in young planetary disks

Since the mid 1990’s, more than one hundred extrasolar planets (hereafter called “exoplanets”) have been discovered. Since the unexpected discovery of the first hot-Jupiter extrasolar planet by Mayor and Queloz (1995), it is clear that exoplanets are an extremely diverse group. With the discovery of more than one hundred exoplanets, this diversity is clearly demonstrated by their orbital properties. We have “hot-Jupiters” with orbital periods as short as 3 days, and several “very hot-Jupiters” with orbital periods even shorter than 2 days but also exoplanets with periods of months to years. Less massive exoplanets have also recently been discovered (Santos et al., 2004; McArthur et al. 2004; Butler et al., 2004, Rivera et al., 2005), and the discussions on the true exoplanet nature show that a large variety is certainly possible.

The same variety is also expected for the atmospheres of these exoplanets. A quick look at the atmospheric content and history of the solar system’s inner planets shows that with four terrestrial planets, we find four very different possibilities: Mercury has almost no atmosphere, Mars’ atmosphere is tenuous with atmospheric pressure at ground level about one-hundredth that of the Earth, and Venus is the extreme opposite with more than ninety times the atmospheric pressure of the Earth with the same physical size of the planet. Note that Titan, although much smaller than the Earth, also has an atmosphere of 1.5 Bar and is very different from other giant planet satellites lacking atmospheres.

This diversity shows how difficult it is to predict what should be the content of an exoplanet’s atmosphere. In the solar system, the terrestrial atmosphere is unique with abundant O₂ and O₃ produced by biological activity though traces of O₃ have also been detected on the Jupiter’s satellite Europa. Another important characteristic of the terrestrial atmosphere is the significant amount of water. The Earth and Titan have both much N₂ in their atmospheres, but Titan contains more methane and no O₂. Mars and Venus have similar atmospheric composition, but they differ in total amount by a ratio of more than 10⁴.

Thus, there is no simple answer to the question of the expected characteristics of planets and their atmospheres. The solar system planets provide a first hint of the expected diversity of the exoplanets and their atmospheres. Observations of exoplanets and the detailed characterization of their atmospheres will help us understand better the physical processes at work in the building of a planet and its atmosphere, and in the further evolution of such a system.

It is clear that the detailed processes that created the solar system planets are still a matter of debate and the impact of many processes must still be clarified. In short, we do not yet know the key physical parameters that govern the formation, evolution and fate of a given planet and its atmosphere.

How do properties such as effective temperature, stellar type, high-energy particle environment, and metallicity of the central star alter the evolution of its planetary system? What effects do a planet's orbital parameters (orbital distance and eccentricity) have on its size, mass and potential migration during the formation process? Are there volatile-rich planets like the proposed “Ocean-planets”? (Kuchner, 2003; Léger et al., 2004) How do interactions with other planets and planetesimals in their environment influence the evolution of a planet? This last question is undoubtedly related to the origin of water on the Earth. Are water-rich planets in the “habitable zone” common, rare, or exceptions?

Several processes believed to play key roles in building a planet can now be identified. To begin with, we can look at the best known planet, our Earth. Although still controversial, it is generally accepted that the Earth's original atmosphere was accumulated simultaneously with the planet's formation. However, the heating of the atmosphere by the young Sun's UV and X-ray flux, and the pressure of the strong solar wind at this period, led to the hydrodynamical escape of this primary atmosphere (as observed on HD 209458b in Ly α λ 1216Å, OI λ 1305Å and CII λ 1330Å, Vidal-Madjar et al., 2003, 2004). Tectonic activity, volcanism and planet out-gassing then formed the secondary atmosphere in which we now live. Late bombardment by planetesimals in the young planetary system contributed a large fraction of the terrestrial water but the fraction of water originating from the Earth itself vs. the external contribution is still a matter of debate. Finally, photosynthetic plants enriched the atmosphere in O₂ and ozone, which are poisons to the first proto-life and are therefore considered as atmospheric bio-markers for advanced life forms. The observation of O₂ and ozone in the atmosphere of the Earth or of any exoplanet can lead to the conclusion that something very particular is happening there. This something could suggest the presence of life.

In the coming decade, several ground and space-based observing programs will lead to the discovery of an extremely large number of exoplanets, in particular, near-future space missions including Corot, Kepler or GAIA will discover large numbers of exoplanets transiting their parent stars. To acquire a revealing picture of these new worlds, we need to characterize the planetary atmospheres of a large sample of these exoplanets. The observation of UV and optical absorptions occurring when an exoplanet transits its parent star are a very powerful diagnostic technique; in fact, the most powerful technique for detecting Earth-like life-bearing planets because of the strong absorption of stellar UV photons by the ozone molecule in the planetary atmosphere (see Gómez

de Castro et al., in this book). We cannot predict what will be discovered, but this will be an unprecedented opportunity to better understand the key processes at work in the shaping of planets and, in particular, to better understand the origin of our own Earth.

In addition, ultraviolet radiation plays a very important role in the evolution of the primary atmospheres of planetary embryos through photoionization and photochemical reactions (Watson et al., 1981; Lecavelier des Etangs et al., 2004). Thus, UV spectroscopy will allow the study of the interactions between the stellar UV field with the atmospheres and, as important, with the young planetary disks. Very recent chemical models are showing that the penetration of UV photons coming from the central engine in a dusty disk could produce an important change in the chemical composition of the gas allowing the growth of large organic molecules. In this context, UV photons at $\lambda > 1500 \text{ \AA}$ photodissociating organic molecules could play a key role in the chemistry of the inner regions of the proto-planetary disk, while those photodissociating H₂ and CO would control the chemistry of the external layers of the disk directly exposed to the radiation from the star. The radiation field can produce a rich photochemistry on timescales shorter than the dynamical evolution time scales, leading to the formation of large carbon-rich molecules such as C_nH₂, HC_(2n+1)N, and C_n. Reactions between these species and H and H₂ may maintain their high abundances in spite of the strong radiation field emerging from the central star (see e.g., Cernicharo, 2004).

2.2. Chemical evolution of the Universe

The gas and stars are the dominant baryonic components of the Universe which can be understood in terms of a two-fluids system interacting through gravitation, starbirth and death; the massive stars life cycle controls the chemical enrichment of the Universe. Key parameters in the evolution of this system are the relative contributions to the energy and chemical input from the various possible sources to the gas phase (SNe, massive star winds and radiation fields, mass infall from the halo, galactic fountains and gas ejection in the intergalactic medium (IGM), galactic dynamics, cosmic rays and magnetic fields); also the roles of magnetohydrodynamical (MHD) turbulence and shocks in the energy cascade and structure formation need to be determined. During the last few years, a very efficient feed-back loop has been operating between radio observations and numerical simulations to study the role of MHD turbulence in the energy cascade within the densest regions of the galactic ISM (H I and molecular clouds). A similar feed-back loop needs to be established with UV observations to understand the heating/cooling processes and the overall thermal and dynamical evolution of the two-fluids system, including the formation

of molecular clouds and massive stars clusters (starbursts). This loops needs to be established at two scales:

At galactic scale where the details of the physics of the process can be tested. The dynamical evolution of the ISM concentrates cold matter in dense shells and filaments in the disk, while the halo acts as a pressure-release valve for the hot ($T > 10^{5.5}$ K) phase, thereby controlling its volume-filling factor. Here a large-scale fountain is set up by hot ionized gas injected from either the gas streaming out of the thick disk or directly from superbubbles inflated in the disk underneath. The gas then escapes in a turbulent convective flow enriching the halo with warm-hot gas. The detection of O VI, C IV and Si IV absorption in many High Velocity Clouds (HVCs) of our Galaxy indicates that they have hot, collisionally-ionized envelopes (Danly et al., 1992, Tripp et al., 2003). Understanding the ionization of such envelopes will constrain the properties of the Galactic corona and the Local Group medium. UV absorption lines are also the most sensitive probes for determining the abundances (and hence their Galactic or extragalactic origin) of the HVCs (see e.g., Richter et al., 2001). Note that the most robust species for constraining the metallicity of HVCs is O I, since oxygen is only slightly depleted by dust grains (Moos et al., 2002) and the ionization potential of O I is very similar to that of H I. Thus, oxygen abundances based on the O I/H I ratio, depend only slightly on the ionization of the gas in substantially ionized plasmas.

At low redshifts ($z \sim 0.1\text{--}0.2$) where it is feasible to resolve the starbursts and thus understand the violent star formation processes in galaxies and the variation of the Initial Mass Function (IMF) across the Universe. Because most of the massive stars form in starburst sites, starburst galaxies play a significant impact on the cosmic evolution of galaxies. Starbursts are responsible for the thermal and kinetic heating of the interstellar medium, and they are the factory where most of the heavy elements form. These elements are dispersed throughout the interstellar medium when massive stars explode as supernovae, and they can escape from the galaxy to the intergalactic medium through high velocity outflows generated by the violent star formation events occurring in these galaxies.

UV observations are relevant not only because this range is very sensitive to the star formation history of galaxies, but also because it contains valuable tracers of the cold and warm phases of the ionized interstellar medium in starbursts that allow us to investigate the physics of the feedback and its consequences. Thus, high-spatial resolution UV spectra and imaging of nearby starbursts are crucial to further progress in understanding the violent star formation processes in galaxies, the interaction be-

tween the stellar clusters and the interstellar medium, and the variation of the IMF. High-spatial resolution spectra are also needed to isolate the light from the center to the disk in the UV luminous galaxies found by GALEX at $z = 0.1\text{--}0.3$. Observations at high spectral resolution ($R \geq 10000$) are required to isolate the galactic, the stellar and the interstellar components of several ions to perform a quantitative characterization of the outflows. A significant increase in spectral sensitivity ($\geq 10\text{--}100$) with respect to HST + STIS is required to characterize superstellar stellar clusters of $10^5\text{--}10^6 M_{\odot}$ beyond Virgo, nuclear starbursts at $z = 0.1\text{--}0.2$, and to probe the starburst galaxy environments out to tens of kpc using background quasars.

In addition, it is fundamental to map *the distribution and metallicity of diffuse baryonic matter and radiation in the Universe*. Independent of the different proposed models of the early Universe, the major baryonic component at $z < 3$ must be associated with the InterGalactic Medium (IGM). Recent studies suggest that the Warm-Hot Intergalactic Medium (WHIM) at low z contains more baryonic mass than stars and galaxies (Richter, 2005). These observations have been done in the UV with FUSE (the OVI triplet) and HST/STIS (broad Ly α absorption (BLA)) and imply cosmological mass densities of $\Omega_b(\text{OVI}) \simeq 0.0021 h_{70}^{-1}$ and $\Omega_b(\text{BLA}) \simeq 0.0027 h_{70}^{-1}$ (Sembach et al., 2004; Richter et al., 2004). These results have tremendous implications for our understanding of the intergalactic medium and galaxy formation.

Further out, looking into the past, the HeII $\lambda 304\text{\AA}$ effect provides the most sensitive tool to detect and analyze the properties of the intergalactic medium. From theoretical modeling of the IGM we know that after the HI reionization, the IGM cools by expansion, is reheated by the delayed HeII reionization at $z = 3$, and continues to cool with decreasing redshift. Observations of the HeII $\lambda 304\text{\AA}$ forest over the redshift range $2.1 < z < 2.9$ will test this model in the most direct way. Besides observing the evolution of the mean IGM temperature, the characteristic scale of the density fluctuations of the IGM and its relation to the fluctuating ionizing radiation field at a spatial resolution of less than 1 Mpc (co-moving distance) will be observed (see Wamsteker et al., this book).

Spectroscopic observations of the HeII $\lambda 304\text{\AA}$ forest with HST and FUSE in two bright QSOs have shown that the HeII reionization phase of the universe ends at roughly $z = 2.9$ (Reimers et al., 1997), i.e., we observe a transition from optically-thick HeII $\lambda 304\text{\AA}$ absorption (the Gunn-Peterson trough) to a resolved HeII $\lambda 304\text{\AA}$ forest below $z = 2.8$. While FUSE was able to resolve the HeII $\lambda 304\text{\AA}$ forest in only two of the brightest high redshift QSOs in the sky (HE2347-4342, Kriss et al., 2001; HS1700 + 6416, Reimers et al., 2004), the

true potential of these fundamental observations could not be exploited due to the very low S/N of the HeII FUSE spectra. Future observations of the HeII λ 304Å forest at high spectral resolution and better S/N have the potential to map both the intergalactic matter and radiation field in much detail.

Due to the possibility of observing HI and HeII simultaneously, the redshift range $2.1 < z < 2.9$ is the only cosmic epoch where the evolution of the fluctuating IGM can be compared in detail with predictions of theoretical models of large-scale structure formation. Knowledge of the shape of the ionizing UV background is also necessary for the determination of heavy element abundances in more than 90% of the baryonic component. The reason is that from the few ions observable from the ground (CIV, SiIV, OVI,...) the state of ionization and therefore, the element abundances cannot be determined quantitatively. Most of the relevant lines formed in the highly ionized component are in the intrinsic EUV at rest wavelengths between 300 and 900Å (OIII-OV, NeIII-NeVII, SIII-SVI,...). The combination of HeII λ 304Å forest observations with high resolution EUV metal-line spectra and optical spectra of laboratory quality from 10m-class ground-based telescopes in a few strategic objects, such as HS 1700 + 6416 with its rich metal line spectrum (Reimers et al., 1992), will lead to a more quantitative understanding of the evolution of matter composition, radiation field and structure formation in the strategic redshift regime between 2 and 3.

No further progress is feasible without high spectral resolution/high sensitivity UV spectroscopy.

2.3. Astronomical engines

Astronomical engines (stars, black holes, etc...) can accelerate large masses to velocities close to the speed of light or generate sudden ejections of mass as observed in Supernova explosions. They are also able to produce significantly milder winds, as seen in the Sun, or to eject gas shells induced by pressure pulsations in the stellar atmosphere. All of these phenomena transform energy of various forms (gravitational, thermal, radiative, magnetic) into mechanical energy to produce outflows in conditions very different than those tested in Earth laboratories. Mass ejections are hot, since a fraction of the mechanical energy involved in the acceleration heats the gas. The ejected matter is also diffuse, since it emerges from rarefied environments and the plasma confinement there is weak. Thus, the study of the thermal and kinetical properties of the ejected matter most astronomical engines need to be studied in the UV, with the only possible exception being very dense and slow outflows where molecules and dust can form.

The least conventional engines are those generating highly collimated bipolar outflows and jets. These are thought to be driven by a combination of gravitational energy, differential

rotation and magnetic fields. They are among the most exciting objects in nature; however, their underlying physics is poorly known. This physical regime affects all of the many scales of Astrophysics; it determines the luminosity of the AGNs and the re-ionization of the Universe at $z \simeq 3$. It also determines the properties of planetary systems, which are just angular momentum reservoirs left over when the engine is turned off in pre-main sequence stars.

The physics of accretion-based engines, i.e., the way by which gravitational energy is transformed into radiation and mechanical energy (outflow) within accretion disks, is poorly known. Recently, linear instability analyses have demonstrated that keplerian hydrodynamical disks are stable; however, magnetohydrodynamic (MHD) disks are quite generally turbulent, and transport angular momentum outwards quite effectively. Thus, accretion disks ought to be magnetized in order to be turbulent and thus be able to dump gravitational energy into heat, as predicated in the standard α -disk model. After the recognition of this fact, accretion physics research is now focused on the study of the implications of magnetic fields both for the physics of the disks and for the disk interaction with the gravitational source. Today, this process is identified in many astrophysical objects spanning a range of 10^{10} in mass (from protostars, to white dwarfs, neutron stars, black holes and supermassive black holes). There are three common properties to all of these phenomena:

1. At very high energies, there is excess energy compared with the expected radiation from the central object and the thin accretion disk model.
2. When jets are generated, their velocity is similar to the keplerian velocity at the inner disk radius; e.g., ranging from a few hundred kilometers per second in protostars to velocities comparable to the speed of light in QSOs and micro-QSOs.
3. Violent ejections, eruptions, and rapid flux variations are detected. Knots are detected in the outflows, indicating that these contain a significant non-stationary component.

This physical behaviour applies to phenomena ranging from the formation of the Solar System, to interacting binaries, microquasars, Seyfert galaxies and quasars.

Gravity is the driving force in this process thus, the key to understand the underlying physics lies deep inside the gravitational potential well, in the interaction region between the dominant source of gravity (star, white dwarf, neutron star or black hole) and the inner disk. The radiative output from this region is produced in the UV-range for the vast majority of sources:

1. In AGN's and microquasars far UV radiation ($\lambda \sim 1500\text{\AA}$) is produced by the accretion disk, however UV

photons are energized to the X-rays range by inverse Compton scattering with the ambient highly relativistic electrons and the observed UV radiation is dominated by the reprocessing of the inner UV and X-ray photoionizing spectrum in the circum-nuclear matter: the gas clouds of the Broad Lines Region (BLR). As accretion is not stationary, the reverberation of the variations is observed in the UV range providing a powerful method to study the gas distribution around such sources allowing the determination of the characteristic scales and masses (e.g., Wandel, Peterson and Malkan, 1999; Kaspi et al., 2000).

2. *In accreting white dwarfs (WD)*, UV radiation is produced in the atmosphere of the accretion disk (and in the WD itself providing a useful tool to identify its characteristics). The propagation of the heating fronts generated in disk instabilities through the inner disk is tracked in the UV providing detailed information on the inner disk structure: disks seem to be strongly depleted during quiescence. The UV spectral energy distribution (SED) is crucial to assess temperature profiles and extension of the disk down to the magnetospheric radius in magnetized cataclysmic variables (CVs). Moreover, in magnetized CVs, the accretion flow is channelled by the field to the poles where the gravitational energy is released in a shock that heats the flow to 10^6 – 10^7 K. These X-ray photons are reprocessed into the UV in the infalling gas column; thus UV monitorings allow tracking the shape and properties of the funnel.
3. *In T Tauri Stars (TTSs)*, UV radiation is produced in an extended magnetosphere, in accretion shocks alike the observed in accreting WD and in the outflow. Though many properties of the TTSs systems are alike the observed in WD, there are two fundamental differences: the central object is not compact and the accretion rate is controlled by the evolution of the accretion disk itself (instead of mass transfer from a companion star). It also adds an important extra motivation: understanding how dynamos are set in cool stars.

In TTSs, the magnetic interaction between the star and the keplerian disk transforms angular momentum into magnetic field. Differential rotation in the disk, generates toroidal flux and the corresponding pressure push the field lines outwards and inflate them. The dissipation of magnetic energy through reconnection heats up the plasma to very high temperatures (see e.g. von Rekowski and Branderberg, 2005) producing a magnetosphere that extends up to $4\text{--}5R_*$ becoming a major contributor to the UV radiation flux. In a sense, the mediation of the magnetic field heats up the accretion process. This also have important implications for the radiative environment in protostellar disks and young planetary systems (see Gómez de Castro et al., 2006).

The most general physics controlling accretion-based engines is non-stationary and highly non-linear, since magnetic fields and relativity are involved. This implies an enormous mathematical complexity that can only be addressed in two manners: either by working with simplified models, or by designing good numerical experiments (which, in turn, require the simplified models to be properly understood). Thus, from the physics point of view, non-relativistic objects represent the very best laboratory to test our understanding of accretion.

Key questions that remain open concern:

1. What controls the efficiency of accreting objects as gravitational engines?, is the magnetic field needed to guarantee that outflows are fast?, what are the relevant timescales for mass ejection?
2. How does the accretion flow proceed from the disk to the source of the gravitational field in the presence of moderate magnetic fields?, which fraction of the gravitational energy lost in this process is deposited on the stellar surface?, which fraction is lost in amplification/dissipation of magnetic flux?
3. Which is the role played by radiation pressure in this whole process?
4. What role do disk instabilities play in the whole accretion/outflow process?, which are the key mechanisms driving these instabilities?

Though interacting binaries and AGNs have been studied by the main UV missions for many years there are still many problems to be studied because as our understanding of the underlying physics improves, new observations are required to test the improved theory (see Gaensicke et al., 2006; Kolлатсhny and Ting-Gui, 2006). A major breakthrough in our understanding of these objects will come from UV spectroscopic observations of the pre-main sequence systems because:

TTSs represent an intermediate class of objects, where the field plays a significant role but it is not as strong as observed in magnetic cataclysmic binaries or in neutron stars. Yet TTSs produce strong bipolar outflows and jets lasting a long fraction of their pre-main sequence evolution (from some 1000 years to 10^7 years) with velocities comparable to the keplerian velocity at 0.01 AU (or $2.1 R_\odot$). Thus, TTSs are the most efficient, accretion-based engines, in the non-relativistic regime.

As accretion progress, the configuration of the TTSs field evolves and the stellar dynamo sets-in. This evolution also provides fundamental information on how the solar dynamo was formed and evolved in the early phases. A significant fraction of the radiation that keeps the gas ionized (and the field coupled to it) is produced by magnetic

reconnection associated with the performance of the engine.

In addition, TTSs are unique to study the environment (radiation, high energy particles, dynamical processes) in which planetary systems, like ours, grow. Notice that recent theories proposed that the inner, Earth-like, planets begin to build-up some 10^6 after the star begin to form and, at this stage, the accretion-based engine is still operating. The radiation produced by the engine ought to have an important effect on the inner disk evolution and the evaporation of the primary atmospheres of the planets-embryos.

As shown in Gómez de Castro et al. (2006), UV spectroscopy carried out with HST/STIS has shown that this work is feasible from observations of the brightest TTSs. The emission from the accretion flow in CIV, SiIII, CIII has been detected as the contribution of the wind to the CIII, SiIII, CII lines. High resolution spectroscopy with an instrument 20 times more efficient than HST/STIS will allow to reach the major factories of stars in the nearby Lupus or Taurus-Auriga complexes. An additional advantage of this improved sensitivity is that it will allow the carrying out of short-term variability studies; these are essential for studying properly the non-stationary components. This type of study has proven to be very valuable to distinguish the different sources of non-stationary phenomena such as flares or shocks (Gómez de Castro, 2002).

3. The ultraviolet Universe

In the following, a brief summary is presented on the major issues raised by the astronomical community when asked about whether and why access to the UV range is important for the progress of the various research fields in astrophysics. All these points are discussed at length in the subsequent articles of this special volume:

3.1. The solar system

Our Solar System serves as the nearest laboratory for planet formation and evolution and the detailed studies of its members are applied to the understanding of other, distant planetary systems. One of the basic questions in modern astrophysics is how planets “work”, how planetary systems originated, and how life emerged on Earth. By studying the large and the small bodies in our system, we link “local” studies to the issue of the existence and properties of Earth-like extra-solar planets. UV observations, along with data collected in other spectral bands, are necessary and in some cases essential to understand the nature of our neighbours in the Solar System.

While many objectives of solar system research can be achieved by optical and near-IR (nIR) imaging, topics from surface mineralogic characterization to auroral activity require the combination of information spanning a wide spectral range including the UV.

Planetary studies require synoptic observations over periods of time ranging from a single revolution (hours to days) to many years (to span at least a full solar cycle). For a given aperture size, UV Astronomy from space can achieve much higher spatial resolution than from the ground because of the absence of the smearing effect of the Earth’s atmosphere and because of the smaller diffraction limit of UV telescopes.

We identify two immediate programmatic requirements: the establishment of a mineralogic database in the ultraviolet for the characterization of planetary, ring, satellite, and minor planet surfaces, and the development and deployment of small orbital solar radiation monitors. The former would extend the methods of characterizing surfaces of atmosphereless bodies by adding the UV segment and permit the study of volatile transport on bodies with atmospheres. The latter are needed to establish a baseline against which contemporaneous UV observations of Solar System objects must be compared.

We identify two types of UV missions that would be two stages in a single process: one requires a two-meter-class telescope using almost off-the-shelf technology and could be launched in the next few years. The other requires a much larger (5–20 meter class) instrument that would provide the logical follow-up after a decade of utilizing the smaller facility. The very large UV telescope will offer angular resolution at par with that of the 100-m OWL telescope allowing coarse mapping much beyond the Kuiper-Edgeworth belt.

3.2. Cool stars

Emission in the UV is an essential probe for studying important physical processes related to the production and transport of magnetic energy in plasmas. Our understanding of such processes is closely related to our ability to predict the evolution of the solar magnetic activity and, therefore, to simulate the conditions in which life has evolved on Earth and how the solar emission of radiation will change due to the evolution of its magnetic dynamo. Future UV missions will advance the study of the consequences of stellar magnetic activity on planets orbiting around them.

Cool star atmospheres represent, undoubtedly, a laboratory in which magnetic activity phenomena can be studied under a large variety of conditions, placing strong constraints on our knowledge of the fundamental processes involved. The consequences of both large and small magnetic activity can these be studied extensively. The UV range is unique as it permits the study of cool star atmospheres from the chromosphere to the corona using powerful diagnostics. Recent techniques

have used the hydrogen Ly α line profile to study, for the first time, the wind from cool stars through its interaction with the interstellar gas (Wood, et al.,).

A 2m class UV telescope with high-resolution spectroscopy and monitoring capabilities would allow important discoveries in this field. A larger aperture telescope (from 4 to 6m) would permit the study of the plasma dynamics and the chromospheric – transition region structures of fainter magnetic active stars, like brown dwarfs and stars in clusters. This is required to characterize the outer atmospheres of parent stars of extrasolar planets that will be discovered by future space missions like *COROT*, *Kepler*, and *Darwin*.

3.3. Massive stars

Massive stars and their descendants are important constituents of galaxies. Because of their high luminosities (up to $10^6 L_\odot$) and their massive winds ($\dot{M} = 10^{-8}$ to $10^{-4} M_\odot \text{yr}^{-1}$, $v_\infty = 100$ to 2000 km s^{-1}) they have an extremely important influence on the dynamics and energetics of the interstellar medium. They also enrich the interstellar medium in nuclear processed material. This enrichment occurs via mass loss (a massive star can lose 2/3 or more of its mass via a stellar wind) or during the SN explosion. They directly influence star formation by disrupting molecular clouds via SN explosions, or conversely they can initiate star formation through massive wind-blown bubbles and Sn shells compressing nearby molecular clouds. Massive stars are also thought to be responsible for the reionization of the early Universe. More recently, it has been proposed that the most massive stars are the progenitors of gamma-ray bursts.

The UV constitutes an optimum spectral window as the spectra energy distributions of massive stars reach their maxima within this wavelength range. Apart from this efficient coincidence established by nature, massive stars decorate the UV spectral region with a number of key diagnostics to our understanding of the nature of these objects and their interaction with the surrounding media.

High spectral resolution spectroscopy provides unique information about massive stars winds (P-Cygni profiles produced by the resonance transitions of CIV, NV, SiIV, OVI, etc). In addition, the unsaturated line profiles from ionized species trace very efficiently the mass-loss rate characterizing the stellar wind. Further, when combined with ρ^2 sensitive diagnostics at other wavelengths they may be used to calibrate the presence of inhomogeneities (“clumping”) in the wind.

The next step is to extend this work to external galaxies. The optimized spatial/spectral resolution achieved at UV wavelengths is fundamental for this purpose.

3.4. Star formation: From the ISM to planets

Planetary systems are angular momentum reservoirs generated during *star formation*. Solutions to three of the most important problems in contemporary astrophysics are needed to understand the entire process of planetary system formation:

The physics of the ISM. Stars form from dense molecular clouds that contain $\sim 30\%$ of the total interstellar medium (ISM) mass. The structure, properties and lifetimes of molecular clouds are determined by the overall dynamics and evolution of a very complex system – the ISM. Understanding the physics of the ISM is of prime importance not only for Galactic but also for extragalactic and cosmological studies. Most of the ISM volume ($\sim 65\%$) is filled with diffuse gas at temperatures between 3000 K and 300,000 K, best observed in the UV, representing about 50% of the ISM mass.

The physics of accretion and outflow. Powerful outflows are known to regulate angular momentum transport during star formation, the so-called accretion-outflow engine. Elementary physical considerations show that, to be efficient, the acceleration region for the outflows must be located close to the star (within 1 AU) where the gravitational field is strong. According to recent numerical simulations, this is also the region where terrestrial planets could form after 1 Myr. One should keep in mind that today the only evidence for life in the Universe comes from a planet located in this inner disk region (at 1 AU) from its parent star. The temperature of the accretion-outflow engine is between 3000 K and 10^7 K. After 1 Myr, during the classical T Tauri stage, extinction is small and the engine becomes naked and can be observed at ultraviolet wavelengths.

The physics of planet formation. Observations of volatiles released by dust, planetesimals and comets provide an extremely powerful tool for determining the relative abundances of the vaporizing species and for studying the photochemical and physical processes acting in the inner parts of the protoplanetary disks. This region is illuminated by the strong UV radiation field produced by the star and the accretion-outflow engine. Absorption spectroscopy provides the most sensitive tool for determining the properties of the circumstellar gas as well as the characteristics of the atmospheres of the inner planets transiting the stellar disk. UV radiation also pumps the electronic transitions of the most abundant molecules (H_2 , CO,...) that are observed in the UV. See, for instance, the HST and FUSE observations of the Beta Pictoris disk which led to conclusion that CO is produced by an extremely large number of comets orbiting in this young planetary system (Jolly et al., 1998; Lecavelier des Etangs et al., 2001)

A rather modest UV telescope (2-m telescope with state-of-the-art optics, instruments and detectors) would produce an extraordinary scientific return as outlined above. A large, 50-m, UV-optical instrument would provide an efficient mean for measuring the abundance of ozone in the atmosphere of the thousands of transiting planets expected to be detected by the next space missions (GAIA, Corot, Kepler...). Thus a follow-up UV mission would be optimal for identifying Earth-like candidates.

3.5. Structure and evolution of white dwarfs and their interaction with the ISM

The development of far-UV astronomy has been particularly important for the study of hot white dwarf stars. A significant fraction of their emergent flux appears in the far-UV and traces of elements heavier than hydrogen or helium are, in general, only detected in this waveband or at shorter wavelengths that are also only accessible from space. Therefore, high-resolution far-UV spectroscopy has been essential for measuring white dwarf composition, to delineate the evolution of their atmospheres and to examine the relationship between the various physical processes that determine the appearance of these stars. In addition to highlighting photospheric material, the strong blue continua of hot white dwarfs also act as a backdrop to absorption lines from the interstellar medium. Consequently, observations of white dwarfs also provide an important probe of the interstellar space with which they interact, their progenitors supplying material and possibly accreting from interstellar clouds as they age. High-resolution spectra can also provide dynamical information on white dwarfs in binaries from which stellar masses can be estimated. UV imaging yields complementary information by resolving these systems, allowing direct detection of hot white dwarfs that might otherwise be hidden in the glare of much brighter companions at visible wavelengths.

Although white dwarfs have been studied in the far-UV throughout the past 25 years, since the launch of IUE, only a few tens of objects have been studied in great detail and a much larger sample is required to gain a detailed understanding of the evolution of hot white dwarfs and the physical processes that determine their appearance. Many outstanding problems remain, including the origin and relationships of the H and He-rich groups, the initial-final mass relation for white dwarfs and their progenitors and the 3D structure of the ISM. All white dwarfs that have ever been studied in the UV reside within our own galaxy and must have emerged from stellar populations with different ages and environments. To solve the outstanding problems and make significant further progress in the study of white dwarfs requires a substantial enlargement of the sample, to properly examine the full range of temperatures, gravities and possible environmental conditions by probing deeper into our own galaxy and extending

studies to co-eval populations in globular clusters, the Magellanic clouds and nearby galaxies.

To achieve these goals there is a need for dramatically enhanced instrument sensitivity, providing high (R 50,000–100,000) and low resolution spectroscopy, with diffraction limited imaging. Coupled with advances in instrument and detector design, a 2-m class telescope would be able to address many of the science goals relating to observation of white dwarfs in our own galaxy, but in the time frame beyond 2015, it is absolutely essential that a large UV facility is constructed to reach outside the galaxy.

3.6. Interacting binaries

Interacting binaries (IBs) are among the most intriguing and exotic stellar systems, since the stellar components interact each other affecting their physical status and evolution. IBs consist of a variety of stellar objects in different stages of evolution and those containing accreting compact objects still represent a major challenge to our understanding of not only close binary star evolution but also of the chemical evolution of the Galaxy. These end-points of binary star evolution are showcases of wide variety of processes including mass accretion and outflow, stellar wind interaction with plasma conditions spanning a wide range of physical conditions including relativistic environments and extreme magnetic field strengths. Consequently, IBs are also extremely versatile plasma physic laboratories.

Despite their great importance for a vast range of astrophysical questions, our understanding of close binary stars and their evolution is still very fragmentary. The ultraviolet is of outmost importance in the study of IBs, as a large part of their luminosity is radiated in this wavelength range, and, more importantly, as the UV hosts a multitude of low and high excitation lines of a large variety of chemical species. These transitions can be used both as probes of the plasma conditions, as well as tracers of individual components within the binary through time-resolved spectroscopy. Moreover, the physical status of the binary components and in particular the accreting white dwarf primaries in cataclysmic variables (CVs), symbiotic stars, and double-degenerate binaries can be easily isolated and studied in the UV range.

Even though substantial scientific progress has been achieved throughout the last three decades, primarily using the International Ultraviolet Explorer (IUE), the Hubble Space Telescope (HST), and the Far Ultraviolet Spectroscopic Explorer (FUSE), there are still many open problems. Among them, key issues are: (i) the nature of SNIa progenitors exploring both single and double-degenerate channels, (ii) the physics of accretion discs, in particular the role of viscosity and its time-dependence, and the development of winds, (iii) the fundamental properties of white dwarfs in CVs, as these are strongly affected by accretion and its

associated angular momentum and (iv) the nature of the IB population in globular clusters. These can be efficiently achieved by means of UV observations surveying much larger samples than done so far. In particular the first three goals require medium ($R \simeq 2000$) to high ($R \simeq 20000$) FUV (possibly down to 912 Å) resolution spectroscopy with high temporal resolution capabilities (time-tag) to allow phase-resolved studies along the binary orbit as well as with a high duty cycle to monitor outburst evolution. The latter goal instead requires a large (10 arcmin) field-of-view imager with diffraction-limited spatial resolution using broad band FUV and NUV filters with accurate timing capabilities.

A large collecting area is relevant to deeply investigate fast UV variability which is an ubiquitous feature in IBs. Fast non-periodic and quasi-periodic variations on timescales from seconds to tens of minutes are commonly observed in CVs. Quasi-periodic-oscillations (QPOs) of a few seconds were discovered in the optical in the eighties and in the UV range in the early nineties in a few bright strongly magnetized CVs. They are believed to arise from shock oscillations though the driving mechanism is still unclear. A proper knowledge of their energy distribution and of the variations of amplitudes and phases is of great potential to diagnose the magnetic field and cooling process in the radiative shocks. Furthermore, oscillations during dwarf novae outbursts (DNOs) and QPOs from a few seconds to thousands of seconds were detected for the first time in the UV and now have been recently recognized as parallel to the high- and low-frequency QPOs observed in X-ray binaries (Warner, 2004) with an origin likely residing in the magnetic nature of the accreting white dwarf. Also, flickering on timescales of minutes are believed to be associated to fluctuations in the mass accretion.

3.7. Active Galaxies

Active Galaxies emit their maximum flux in the UV/FUV. The overall continuum flux peaks in-between the optical and soft X-ray spectral range. More than half of the bolometric luminosity of an (un-obscured) AGN is emitted in this big blue bump. Models of hot accretion disks – surrounding the central super-massive black hole in AGN – cannot reproduce in a simple way the observed spectral shape.

This rest frame EUV continuum of highly redshifted AGN is important for our understanding of the evolution of the early universe. The UV continuum of quasars ionizes the intergalactic medium at the end of the dark ages.

Furthermore, the central continuum source in AGN ionizes the circumnuclear gas in the so called broad line region (BLR) and narrow line region (NLR). The overall continuum distribution as well as the UV spectral lines (narrow emission lines, broad emission lines, absorption lines) are tracers of the physical conditions of those regions where these emission lines originate. Most important diagnostic lines for studying

the physical conditions and metallicities in the central regions of AGN are emitted in the UV. It is possible to derive some information for distant ($z \geq 2$) as well as luminous quasars when the diagnostic lines are shifted into the optical range with ground-based telescopes. But it is necessary to observe the UV-spectra of 'nearby and present-day' AGN for studying their cosmological evolution as well as the evolution of the universe. The UV spectra of the class of low luminous AGN can be observed only in the local universe because of their faintness.

The emission line region of the narrow lines is spatially resolved in some nearby objects. They originate at distances of pc to kpc from the central ionizing source. However, the broad emission lines originate at distances of light days to light months only from the central ionizing source. This BLR is unresolved by orders of magnitudes even for the nearest AGN. But variability studies of the ionizing continuum flux and the emission line intensities/profiles give us information on the structure and kinematics of the surrounding of the central supermassive black hole in AGN as well as on their mass itself. The monitoring of highly ionized UV lines in AGN enables us to study the physics of the immediate environment of black holes nearest to the center.

3.8. Starbursts

Starbursts are systems with very high star formation rates per unit area. They are the preferred places where massive stars form, the main source of thermal and mechanical heating in the interstellar medium, and the factory where the heavy elements form. Thus, starbursts play an important role in the origin and evolution of galaxies. The similarities between the physical properties of local starbursts and high- z star-forming galaxies highlight the cosmological relevance of starbursts. On the other hand, nearby starbursts are laboratories for studying violent star formation processes and their interaction with the interstellar and intergalactic media, in detail and deeply. Starbursts are bright at ultraviolet (UV) wavelengths, as they are in the far-infrared, due to the 'picket-fence' interstellar dust distribution. After the pioneering IUE program, high spatial and spectral resolution UV observations of local starburst galaxies, mainly taken with HST and FUSE, have made relevant contributions to the following issues:

- *The determination of the initial mass function (IMF)* in violent star forming systems in both, low and high metallicity environments, and in dense (e.g. in stellar clusters) and diffuse environments: A Salpeter IMF with high-mass stars constrains well the UV properties.
- *The modes of star formation:* Starburst clusters are an important mode of star formation. Super-stellar clusters have properties similar to globular clusters.

- *The role of starbursts in AGN:* Nuclear starbursts can dominate the UV light in Seyfert 2 galaxies, having bolometric luminosities similar to the estimated bolometric luminosities of the obscured AGN.
- *The interaction between massive stars and the interstellar and intergalactic media:* Outflows in cold, warm and coronal phases leave their imprints on the UV interstellar lines. Outflows of a few hundred km s⁻¹ are ubiquitous phenomena in starbursts. These metal-rich outflows and the ionizing radiation can travel to the halo of galaxies and reach the intergalactic medium.
- *The contribution of starbursts to the reionization of the universe:* In the local universe, the fraction of ionizing photons that escape from galaxies and reach the intergalactic medium is of a few percent. However, in high- z star-forming galaxies, the results are more controversial.

Despite the very significant progress over the past two decades in our understanding of the starburst phenomenon through the study of the physical processes revealed at satellite UV wavelengths, there are important problems that still need to be solved. High-spatial resolution UV observations of nearby starbursts are crucial to further progress in understanding the violent star formation processes in galaxies, the interaction between the stellar clusters and the interstellar medium, and the variation of the IMF. High-spatial resolution spectra are also needed to isolate the light from the center to the disk in UV luminous galaxies at $z = 0.1\text{--}0.3$ found by GALEX. Thus, a new UV mission containing an intermediate spectral resolution long-slit spectrograph with high spatial resolution and high UV sensitivity is required to further progress in the study of starburst galaxies and their impact on the interstellar and intergalactic media.

3.9. Supernovae (SNe)

UV observations of SNe are required not only for understanding of the SN phenomenon itself, such as the kinematics and the metallicity of the ejecta, but also for providing exciting new findings in Cosmology, such as the tantalizing evidence for “dark energy” that seems to pervade the Universe and to dominate its energetics. SNe are bright events that can be detected and studied even at very large distances. Ultraviolet spectroscopy is crucial in order to:

Study the metallicity of individual SNe

Study the metallicity of the intervening ISM/IGM

Study the kinematics of the fast moving (i.e. the outermost layers) of the ejecta through the analysis of strong UV lines with P-Cygni profiles.

Study the overall energetics of SNe explosion at early phases (from shock breakout to optical maximum for types of SNe, but most importantly for all Type II SNe)

Study of the strong emission lines produced in the interaction of the ejecta with pre-SN circumstellar material, e.g. NV 1240 Å and collisionally excited CIV 1550 Å, NIV] 1470 Å, OIII] 1665 Å, NIII] 1750 Å, CIII] 1908 Å.

SNIa are very good standard candles (e.g. Macchetto and Panagia, 1999) to measure distances to distant galaxies, currently up to redshift $z \simeq 1$ and, considerably more in the foreseeable future. This is a challenging proposition, both for technical reasons (observations in the near IR of increasingly faint objects) and for more subtle reasons, i.e. one must verify that the discovered SNe are indeed SNIa and that these SNe share the same properties of their local Universe relatives. One can only discern Type I from Type II SNe on the basis of the overall properties of their UV spectral energy distributions (Panagia, 2003, 2005).

4. Summary

This review outlines the scientific reasons behind the need for an ultraviolet observatory. Most of science described here could be carried out with two basic instruments:

1. A high-resolution (50,000–100,000) spectrograph covering the whole 90–320 nm spectral range.
2. A low-spectral resolution (1000–5000) high-sensitivity spectrograph allowing integral field spectroscopy (long-slit in its simplest version) with spatial resolution (50 mas) and wavelength coverage from 110–450 nm.

These instruments should provide an improvement by a factor of ~ 20 in effective area over the HST/STIS capabilities. This improvement is rather conservative from the technological point-of-view since it could be achieved by improving optical designs and coatings and make use of MCP detectors with enhanced sensitivity, bigger size and improved dynamic range related to new fast read-out electronics. It is amazing the large progress that could be achieved with a relatively modest investment; a good example of this is the proposed *World Space Observatory* project.

Looking into the far future, it is clear that the frontier is building larger facilities that increase the effective collecting surface by, at least, 2 orders of magnitude. A properly instrumented 4–6 m telescope in space would be very useful for future UV observations.

A larger, 20 m size, telescope in space represents a huge technological leap. Coordinated constellations of 1-m size telescopes seem to be the most realistic manner to get large collecting surfaces. In turn, this would allow carrying out UV interferometry. The potential of high spatial resolution (milliarcsecond scale) instruments is enormous. One promising concept to get micro-arcsecond resolution imaging is the Stellar Imager mission under study at NASA GSFC, a

kilometer scale interferometer composed of around 30 small telescopes formation, flying in space (Carpenter et al., 2004).

Another possibility would be building large ground-based telescopes in ozone depleted areas. The discussion of the ‘ozone hole’ due to human activity on the one hand, and the realization that photon absorption by ozone in the UV is one of the important sources of opacity in the atmosphere, would argue that the location of a ground-based telescope underneath an ozone hole may extend the spectral range accessible from the ground into the UV. Assuming this effect to be present and significant, the best place for such a ground-based UV telescope would be in the Antarctic, possibly at the Concordia station at Dome C. This location shows the best seeing for any Earth based observatory, but as far as we are aware no long-term study of the atmospheric transparency at short wavelengths has been conducted there. The study should also consider the atmospheric emissions at a location relatively close to the South Magnetic Pole, and the influence of sunlight scattered into the telescope when the Sun is below the horizon.

A detailed accounting on the scientific requirements to UV observatories can be found in Kappelmann et al. contribution to these proceedings.

Acknowledgements During the editing of the present volume, our dear colleagues Willem Wamsteker, Michael Festou and Marcello Rodonó suddenly passed away. We dedicate this work to them with the hope that their worldwide contribution to UV science will be kept recognized in the future of UV astronomy.

References

- Avillez, M., Breitschwerdt, D.: Volume filling factors of the ISM phases in star forming Galaxies. I. The role of the disk-halo interaction. *Astronomy and Astrophysics*, in press (2005)
- Avillez, M., Breitschwerdt, D.: Global dynamical evolution of the ISM in star forming Galaxies – I. high resolution 3D HD and MHD simulations: effect of the magnetic field. *Astronomy and Astrophysics* **425**, 899 (2004)
- Bahcall, J.N., Ostriker, J.P.: Unsolved problems in astrophysics princeton university press (1997)
- Carpenter, K.G., Schrijver, C.J., Allen, R.J., et al.: SI- The stellar imager SPIE astronomical telescopes and instrumentation. SPIE paper # 5491, V28
- Cernicharo, J.: The polymerization of acetylene, hydrogen cyanide, and carbon chains in the neutral layers of carbon-rich proto-planetary nebulae. *Astrophysical Journal* **608**, L41 (2004)
- Ehenreich D., Tinetti G., Lecavelier des Etangs A., Vidal-Madjar A., Selsis F.: The transmission spectrum of earth-size transiting planets. *A&A*, in press (2005)
- Gómez de Castro, A.I.: On the source of the flaring activity in AB Doradus: the UV spectral signatures. *Monthly Notices of the R.A.S* **332**, 409 (2002)
- Gómez de Castro, A.I.: Magnetic activity and the interaction between the stellar magnetosphere and the accretion disk. *Astrophysics and Space Science* **292**, 561 (2004)
- Jolly, A., McPhate, J.B., Lecavelier, A., Lagrange, A.M., Lemaire, J.L., Feldman, P.D., Vidal Madjar, A., Ferlet, R., Malmasson, D., Rostas, F.: HST – GHRS observations of CO and CI fill in the beta – Pictoris circumstellar disk. *Astronomy and Astrophysics* **329**, 1028–1034 (1998)
- Kriss, G.A., Shull, J.M., Oegerle, W., Zheng, W., Davidsen, A.F., Songaila, A., Tumlinson, J., Cowie, L.L., Deharveng, J.-M., Friedman, S.D., et al.: Resolving the structure of ionized helium in the intergalactic medium with the far ultraviolet spectroscopic explorer. *Science* **293**, 1112 (2001)
- Kaspi, S., Smith, P.S., Netzer, H.M.D., Jannuzzi, B. T. Giveon, U.: Reverberation measurements for 17 quasars and the size-mass-luminosity relations in active galactic nuclei. *Astrophysical Journal* **533**, 631 (2000)
- Kutchner, M.J.: Volatile-rich earth-mass planets in the habitable zone. *Astrophysical Journal* **596**, L105–L108 (2003)
- Léger, A., et al.: A new family of planets? “Ocean-Planets”. *Icarus* **169**, 499–504 (2004)
- Lebouteiller, V., Kunth, D., Lequeux, J., Lecavelier des Etangs, A., Désert, J.-M., Hébrard, G., Vidal-Madjar, A.: Abundance differences between the neutral and the ionized gas of the dwarf galaxy IZw 36. *Astronomy and Astrophysics* **415**, 55–61 (2004)
- Lecavelier des Etangs, A., et al.: Deficiency of molecular hydrogen in the disk of β pictoris. *Nature* **412**, 706–708 (2001)
- Lecavelier des Etangs, A., Vidal-Madjar, A., McConnell, J.C., Hébrard, G.: Atmospheric escape from hot Jupiters. *Astronomy and Astrophysics* **418**, L1 (2004a)
- Lecavelier des Etangs, A., Désert, J.-M., Kunth, D., Vidal-Madjar, A., Callejo, G., Ferlet, R., Hébrard, G., Lebouteiller, V.: FUSE observations of the H I interstellar gas of I Zw 18. *Astronomy and Astrophysics* **413**, 131–137 (2004b)
- Mayor, M., Queloz, D.: A Jupiter-mass companion to a solar-type star. *Nature* **378**, 6555–355 (1995)
- Moos, H.W., Sembach, K.R., Vidal-Madjar, A., York, D.G., Friedman, S. D. et al.: Abundances of deuterium, nitrogen, and oxygen in the local interstellar medium: overview of first results from the FUSE mission. *Astrophysical Journal, Suppl. Series* **140**, 3 (2002)
- Reimers, D., Vogel, S., Hagen, H.-J., Engels, D., Groote, D., Wamsteker, W., Clavel, J., Rosa, M.R.: The O/C abundance ratio in absorbing gas clouds at high redshift. *Nature* **350**, 561 (1992)
- Reimers, D., Koehler, S., Wisotzki, L., Groote, D., Rodriguez-Pascual, P., Wamsteker, W.: Patchy intergalactic He II absorption in HE 2347–4342. II. The possible discovery of the epoch of he-reionization. *Astronomy and Astrophysics* **327**, 890 (1997)
- Richter, P., Savage, B.D., Wakker, B.P., Sembach, K.R., Kalberla, P.M.W.: The FUSE spectrum of PG 0804 + 761: a study of atomic and molecular gas in the lower galactic halo and beyond. *Astrophysical Journal* **549**, 281 (2001)
- Richter, P., Savage, B.D., Tripp, T.M., Sembach, K.R.: FUSE and STIS observations of the wram-hot intergalactic medium toward PG 1259 + 593. *Astrophysical Journal Suppl* **153**, 165 (2004)
- Richter, P.: Perspectives for hunting the missing baryons in the local universe. Proc. 39th ESLAB Symp, Noordwijk 19–21 (2005), F. Favata, J. Sanz-Forcada, A. Giménez (eds.), p. 157, (2005)
- Rivera, E.J., Lissauer, J.J., Butler, R.P., Marcy, G.W., Vogt, S.S., Fischer, D.A., Brown, T.M., Laughlin, G., Henry, G.W.: A 7.5 M_⊕; Planet Orbiting the Nearby Star, GJ 876. *Astrophysical Journal* **634**, 625–640 (2005)
- Sembach, K.R., Tripp, T.M., Savage, B.D., Richter, P.: Physical properties and baryonic content of low-redshift intergalactic Ly α and OVI absorption line systems: the PG 1116 + 215 sight line. *The Astrophysical Journal Suppl* **155**, 351 (2004)
- Tripp, T.M., Wakker, B.P., Jenkins, E.B., Bowers, C.W., et al.: Complex C: A low-metallicity, high-velocity cloud plunging into the milky way. *Astronomical Journal* **125**, 3122 (2003)
- Vidal-Madjar, A., Lecavelier des Etangs, A., Désert, J.-M., Ballester, G.E. et al.: An extended upper atmosphere around the extrasolar planet HD209458b. *Nature* **422**, 143 (2003)

- Vidal-Madjar, A., Désert, J.-M.: Lecavelier des Etangs, A., Hébrard, G. et al.: Detection of oxygen and carbon in the hydrodynamically escaping atmosphere of the extrasolar planet HD 209458b. *The Astrophysical Journal* **604**, L69 (2004)
- Wandel, A., Peterson, B.M., Malkan, M.A.: Central masses and broad-line region sizes of active galactic nuclei. I. comparing the photoionization and reverberation techniques. *The Astrophysical Journal* **526**, 579 (1999)
- Warner, B.: Rapid oscillations in cataclysmic variables. *PASP* **116**, 115 (2004)
- Watson, A.J., Donahue, T.M., Walker, J.C.G.: The dynamics of a rapidly escaping atmosphere – applications to the evolution of earth and Venus. *Icarus* **48**, 150 (1981)

Guidelines for Future UV Observatories

Norbert Kappelmann · Jürgen Barnstedt

Received: 13 March 2006 / Accepted: 14 March 2006
© Springer Science + Business Media B.V. 2006

Abstract Ultra-violet image sensors and UV optics have been developed for a variety of space borne UV astronomy missions. Technology progress has to be made to improve the performance of future UV space missions. Throughput is the most important technology driver for the future. Required developments for different UV detector types – detectors are one of the most problematic and critical parts of a space born mission – and for optical components of the instruments are given in these guidelines. For near future missions we need high throughput optics with UV sensors of large formats, which show simultaneously high quantum efficiency and low noise performance.

Keywords UV astronomy

1. Introduction

Within the last years a lot of workshops have taken place in which the need for new instruments for future space-borne UV astronomy missions was discussed (e.g. “Report of UV/O Working Group to NASA”, 1999, “Hubble’s Science Legacy: Future Optical-Ultraviolet Astronomy from Space”, 2002, “Innovative Design for the next large aperture optical/UV Telescope”, STSI, 2003). In a large number of publications the characteristic parameters for new developments and associated technologies for future UV instrumentations are described (eg. Proc. SPIE, Volume 2999, 1997 “Photodetectors: Materials and Devices II”). Therefore this paper is not a comprehensive review of future UV technology developments, but focuses on the requirements for new UV

instruments which will give the astronomical UV community the possibility to meet the science goals, described in the papers of this book.

2. General remarks

An improvement on current UV capabilities of the HST in the order of magnitudes could be made by high quantum efficiency UV detectors, high efficiency optics and the use of 3–4 m telescopes. The technology needed for advanced UV-astronomy can benefit from advances being made in other wavelength regimes, in particular from developments in the visible, infrared and x-ray wavelength bands. In general throughput is the most important technology driver for future UV space astronomy missions, especially for UV spectroscopy. UV technology development has to be made in the areas of detectors, optical components and their coatings and large light weighted mirrors.

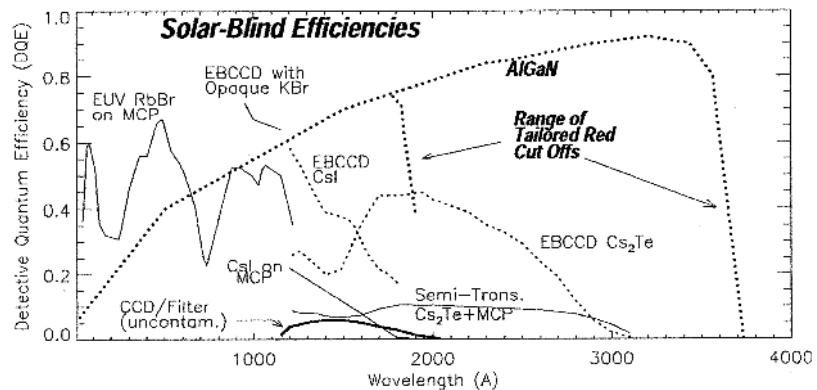
2.1. UV sensors

Many astronomical objects produce orders of magnitudes more photon fluxes at optical wavelengths than they do in the vacuum UV. In order to eliminate this huge background contribution and substantial source of noise solar-blind detector and imaging systems are required. A comprehensive overview about UV imaging detectors is given by Joseph (2000). Furthermore the reader is referred to Welsh and Kaplan (1992), Ulmer (2002) and references therein.

Several specific detector types can be used for vacuum UV astronomy in the future, multidimensional detectors, semi-conductive array (e.g. CCDs) and microchannel plate detectors (MCP). The further development of technologies for

N. Kappelmann (✉) · J. Barnstedt
Institut für Astronomie und Astrophysik, Abteilung Astronomie
(IAAT), Universität Tübingen, Tübingen, D-72076, Germany

Fig. 1 Solar-blind detective quantum efficiencies obtained by various UV detectors adopted from Joseph (2000)



these detectors is the basis to enhance the performance for UV applications. The current technology can be classified in two categories: Solid-state devices based on silicon or wide bandgap semiconductors and photoemissive devices, coupled with a gain component and an electron detector. The detective quantum efficiencies (DQE) for various UV detectors as MCPs, CCDs, Electron-Bombarded CCDs and for the expected DQEs for future AlGaN solid-state sensors are shown in Fig. 1.

“3D” energy-resolving detectors such as photon counting superconducting tunnel junction (STJ) or transition-edge detectors (TES) have the potential to replace the detectors which are now in use for UV mission in the far future. The development of these energy resolving detectors will improve efficiency and reduce the number of optical elements.

MCPs have a good potential to stay for the next years the default detectors in the UV regime especially below 200 nm, due to the fact that they have a very good flight history, they are solar blind, have a very low readout-noise and are radiation hard. A review about the actual image detector technology, including different readout anode types, like image readout anodes, delay line image readout anode, intensified CCD/CIDs (CCD devices couples to an MCP image intensifier), cross strip anodes and pixel array anodes, is given by Siegmund (2000). A review about the performance of larger format CCDs and future directions of the developments of CCDs suitable for wide field UV imaging is given by Clampin (2000). The primary technical problems of CCDs are the high QE in the visible, low QE in the UV and the radiation tolerance of these imaging sensors. Improvement of solarblind UV imaging CCDs with excellent radiation tolerances have been made by the production of CCDs made out of SiC (Sheppard, 1996) and GaN.

Dynamic range and linearity technology investments should be made to ensure that potential flight detectors have large dynamic range. It is very important that detectors are stable and provide a linear response to the signals. It is essential to reduce substantially the background rates: the detector background noise should not become the limiting factor and should not determine the sensitivity of the measurements.

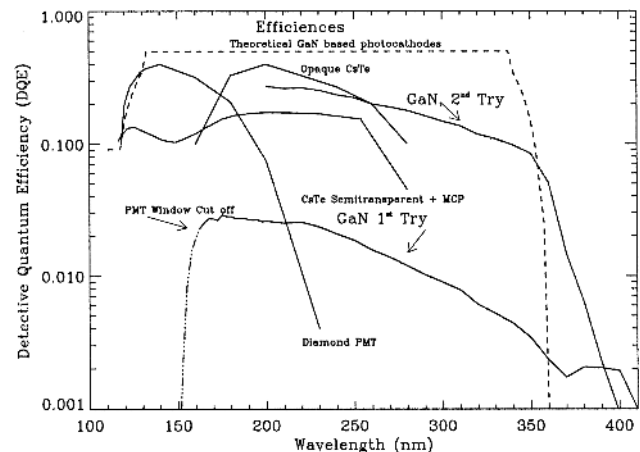


Fig. 2 GaN photocathodes compared with other photocathodes adopted from Ulmer (2002)

2.2. Photocathodes

The development of new photocathodes is the approach to lead to devices for UV space mission for the next decade. Significant impact on future capabilities can be made by advances in new materials for the photocathodes as GaN, diamond or GaAs (e.g. Ulmer, 2003). For example diamond photocathodes show efficiencies of 50% in the 200–1200 Å band. For MCP detectors based on silicon substrates diamond can be used as a direct opaque cathode (e.g Beetz, 2000). A comparison of GaN photocathodes with other photocathodes is shown in Fig. 2.

Walker (2000) has reported the fabrication and characterization of solar-blind $\text{Al}_x\text{Ga}_{1-x}\text{N}$ photodiodes ($x \sim 0.70$) grown on sapphire with an internal quantum efficiency which is greater than 90%. The device response drops four orders of magnitude at 275 nm and remains at low response for the entire near-ultraviolet and visible spectrum. Promising future technology is based on the production of high quality films made of wide bandgap semiconductors. For UV detectors it is absolutely necessary to suppress the sensitivity in the red, and wide-band gap semi-conductors fulfill this requirement very well. Coupling the resulting photocathode to a device

such as a micro-channel plate (MCP) is necessary to produce imaging (Ulmer, 2002). Because UV coatings are extremely sensitive to highly absorbing molecular contaminations careful attention must be paid to possible contamination sources and investments have to be made in the long term stability of the coatings.

2.3. Optical components: Gratings

Throughput can be maximized with intelligent optical system designs and by judicious use of optical materials and coatings. Effective coatings for the optical elements are needed to maximize throughput: high reflectivity particular below 200 nm is required. One part of the optical elements are gratings and therefore it is essential to develop gratings which have high efficiency, efficient groove shapes and produce very low scatter. Holographic gratings are today's standard gratings for most UV spectroscopic instruments. This is largely due to their scattering (typically around 10^{-5} \AA^{-1}) and to their large sizes. Interesting developments are made by direct-writing technologies. Today they are still in an early stage of development, but this technology is able to produce gratings with very low scatter, efficient groove shapes, and excellent aberration correction. Due to low ruling densities direct-write technologies cannot be used in the current stage of development in high-resolution UV spectroscopy but within the next years large, corrective gratings with high groove densities will be available (e.g. Wilkinson, 1999).

2.4. Optical components: Filters

Several designs of filters for use in vacuum UV imaging systems are discussed. These designs incorporate all reflective optics, and are characterized by comparatively high in-band throughout and very low out-of-band transmission. Filters which can be tuned over ranges useful for vacuum UV astronomical observations will be a very good tool for imaging. Adjustable broad band and small band imaging will give access to a bunch of diagnostic lines over the whole UV wavelength regime.

Acousto-optical-tunable-filters (AOTFs) have the potential of providing a bandwidth selectable across 1 octave. A tunable RF signal is applied across a birefringent crystal, resulting in a selectable output wavelength. AOTFs have been built and are in use at IR wavelengths on ground-based instruments. To use these filters at vacuum UV wavelengths in the future, considerable work must be done to characterize birefringent UV-transmitting crystals, followed by extensive prototype development (e.g. Voloshinov, 2004).

Preliminary research by Jelinski (2000) indicates that alkali halides, as CaF_2 , BaF_2 , LiF , MgF_2 , may be excellent candidates for FUV tunable transmission crystal filters.

The transmission curves of these halides shift to longer wavelengths as the temperature is increased and to shorter wavelengths if the halides are cooled down (Davis, 1966). This temperature dependent optical behavior can be utilized in the design of tunable filters in two different ways, with tunable bandwidth or tunable center wavelength.

2.5. Optical Components: Micro-mirrors, fibres

Very efficient spectroscopic observation can be done by observing multiple objects or positions simultaneously in the focal plane. In ground based instruments more than 1000 objects can be observed. Micro-mirror arrays can be used as programmable masks. In this arrangement, micro-mirrors are reflecting/blocking unwanted light and open a path for the desired rays. This concept shows great promise for UV applications although it is in an early phase of development. In another arrangement the incoming light is partly reflected into a spectrograph (from the desired objects) and the other part is reflected into a light baffle. To use micro-mirror arrays in the UV wavelength regime, UV coatings should be applicable to these arrays but it needs to be verified that the mirrors can be manufactured with the required surface quality.

In ground-based multiple objects instruments light-transmitting fibres feed light from selected targets into a spectrograph. However, development of new fibres with excellent transmission throughout the UV would greatly simplify this concept since the entire focal plane would be accessible to a single spectrograph with fibre reformatting. Unfortunately optical fibres are opaque in the UV. Progress is made for example with silica-core fibres (e.g. Wang, 2005) and one type of fused silica fibres will transmit light to wavelengths as short as 180 nm. Developments have to be made to create transmissive fibres for use at shorter wavelengths down to 91 nm. Considerable development work also needs to be done to couple these fibers into a powered optical system, to bundle them, and to understand their flexibility properties and their behavior under extreme thermal conditions.

3. Requirements for UV mission in the near future

The detailed needs for future UV space-born instruments and the justification for the required parameters are given for every science case described in the papers of this book. High throughput is a request from all science cases (e.g $\text{S/N} = 10$ within 10 minutes for a target with a flux of $10^{-16} \text{ ergs cm}^{-2} \text{ sec}^{-1}$) The specific requirements to the wavelength range and the spectral resolution for spectroscopic ($R = \lambda/\delta\lambda$) and imaging observations are summarized as follows:

1. Medium spectral resolution:

$R \leq 5000$ with a simultaneous wavelength coverage from 91 nm to 450 nm.

Additionally a spatial resolution in the order of ~ 0.01 arcsec is required.

2. High spectral resolution:

$R \geq 30.000$ with a simultaneous wavelength coverage from 91 nm to 350 nm.

High spectral resolution of $R \sim 50.000$ or even $R \geq 100.000$ is required for example for a galactic white dwarf spectroscopic survey (Barstow and Werner, this book), for resolving plasma velocities in a number of environments such as cometary comae (Brosh et al. this book), for measurements of thermal broadening of absorption lines in exospheres (Gomez et al., this book), for studies of cool winds and astrospheres (Pagano et al, this book) and for detailed ISM studies (Wamsteker et al., this book).

3. Efficient spectroscopic observation should be performed by integral-field spectroscopy, for example multiple object spectroscopy of white dwarfs in the 90–130 nm range with $R \sim 1.000$ and a limiting flux of around 10^{-20} ergs cm^{-2} sec^{-1} (Barstow and Werner, this book).

4. For imaging at least a spatial resolution of 0.01 arcsec and field of views with up to 2 arcmin is required (Brosh et al., this book). For a white dwarf survey of the LMC/SMC and of globular clusters a field of view of 10 arcmin is required (Barstow and Werner, this book). Additionally tunable filters will be a very good tool to select spectral lines of interest.

5. Furthermore some science cases need time-tagged observations with a time accuracy down to fractions of a second (e.g. Gänsicke et al., this book).

Similar science questions given in this book can be addressed with a planned 2 m – class UV mission, the WSO/UV project. The spectroscopic capabilities of this mission are a spectral resolution of $R \simeq 50.000$ and a coverage of the whole wavelength regime(102–310 nm) with two observations(102–178 nm and 275–310 nm). A detailed overview of this project is given by Barstow et al. (2003).

4. Summary

In summary it is shown, that with modest developments the scientific objectives outlined in this book can be achieved with 3–4 m class telescopes. Most of the described science in this book can be achieved basically by two spectrographs, which should have a simultaneous wavelength coverage from 90 nm to 450 nm and a high throughput.

1. A high spectral resolution spectrograph with $R \sim 50.000$ –100.000
2. A medium spectral resolution spectrograph with $R \sim 1.000$ –5.000 allowing integral field spectroscopy with a spatial resolution of ~ 0.01 arcsec

To fulfill these requirements for near future UV missions especially developments of microchannel-plate detectors and semiconductor arrays with high quantum efficiency, large dynamic range, low background noise and with large formats are necessary. This should be accompanied by improving the technology of optical components to provide high throughput and low scatter and by the development of large, precision, lightweight mirror surfaces with good micro-roughness properties.

References

- Hubble's Science Legacy: Future Optical/Ultraviolet Astronomy from Space ASP Conference Proceedings **291**, (2002)
- Barstow, M., et al.: Proc. SPIE **4854** 364–374 (2003)
- Beetz, C.P., Boerstler, R., Steinbeck, J., Lemieux, B., Winn, D.R.: Nucl. Instr. and Meth. in Phys. Res., A**442**, Issue 1–3, 443–451 (2000)
- Clampin, M.: UV-Optical CCDs, proceedings of the space astrophysics detectors and detector technologies conference held at the STScI. Baltimore, June 26–29 (2000)
- Davies, R.J.: J. Opt. Soc. Am. **56**, 837 (1966)
- Jelinski, P., Siegmund, O.H.W., Welsh, B.: Narrow-band tunable filters for use in the FUV region. Proceedings of the Space Astrophysics Detectors and Detector Technologies Conference held at the STScI. Baltimore, June 26–29
- Joseph, C.: UV Technology Overview, in proceedings of the space astrophysics detectors and detector technologies conference held at the STScI. Baltimore, June 26–29 (2000)
- Joseph, C.: Proceedings of the space astrophysics detectors and detector technologies. ASP Conf. Ser. **164**, 420 (1999)
- Ulmer, M.P., et al.: Proc SPIE **4650** (2002)
- Ulmer, M.P., Wessels, B.W., Han, B., Gregie, J., Tremsin, A., Siegmund, O.H.W.: Advances in wide-bandgap semiconductor base photocathode devices for low light level applications Proc. SPIE **5164**, 144–154 (2003)
- Ulmer, M.P.: Requirements and design considerations of UV and x-ray detectors for astronomical purposes, Proc. SPIE **2999**, p. 259 (1997)
- Ulmer, M.P., Razeghi, M., Wessels, B.W.: Development of GaN-based films for use in UV sensitive but visible blind detectors in Proceedings of the Space Astrophysics Detectors and Detector Technologies Conference held at the STScI, Baltimore, June 26–29 (2000)
- Siegmund, O.H.W.: MCP imaging detector technologies for UV instruments, in proceedings of the space astrophysics detectors and detector technologies conference held at the STScI. Baltimore, June 26–29 (2000)
- Sheppard, S.T., Melloch, M.R., Cooper, J.A.: IEEE Electron Device Letters **17**, 4 (1996)
- Voloshinov, V., Gupta, N.: Applied Optics IP, **43**(19), 3901–3909 (2004)
- Walker, D., Kumar, V., Mi, K., Sandvik, P., Kung, P., Zhang, X.H., Razeghi, M.: Solar-blind AlGaN photodiodes with very low cutoff wavelength. Appl. Phys. Lett. **76** 403 (2000)

Wang, T., Guo, X., Chen, Z.: Proc. SPIE **5623**, 145–150 (2005)
Welsh, B.Y., Kaplan, M.: NASA's ultraviolet Astrophysics Branch: the next decade, in EUV, X-Ray and Gamma-Ray instrumentation for astronomy III 452–463 (1992)

Wilkinson, E.: Maturing and developing technologies for the next generation of UV gratings ultraviolet-optical space astronomy beyond HST. Conference held at the STScI, ASP Conference Series 164, 420 (1999)

Massive stars in the UV

F. Najarro · A. Herrero · E. Verdugo

Received: 14 February 2006 / Accepted: 27 February 2006
© Springer Science + Business Media B.V. 2006

Abstract We emphasize in this paper the importance of the UV range for our knowledge of massive stars and the fundamental role played by past and present space-based UV capabilities (IUE, HST, FUSE and others). Based on a review of the work developed in the last years and the state of the art situation for quantitative spectroscopy of massive stars, we present crucial advances which could be addressed by hypothetical future space-based UV missions. Advantages and unique data that these missions could provide are explained in the context of our present knowledge and theories on massive stars in the Milky Way and nearby galaxies. It is argued that these studies are our key to a correct interpretation of observations of more distant objects.

Keywords UV astronomy · Massive stars · Winds · Abundances

1. Introduction

Massive stars and their descendants are important constituents of galaxies. Because of their high luminosities (up to $10^6 L_\odot$) and their massive winds ($M = 10^{-8}$ to 10^{-4}

$M_\odot \text{yr}^{-1}$, $v_\infty = 100$ to 2000 km s^{-1}) they have an extremely important influence on the dynamics and energetics of the interstellar medium. They also enrich the interstellar medium in nuclear processed material. This enrichment occurs via mass loss (a massive star can lose 2/3 or more of its mass via a stellar wind) or during a SN explosion. They directly influence star formation by disrupting molecular clouds via SN explosions, or conversely they can initiate star formation through massive wind-blown bubbles and SN shells compressing nearby molecular clouds. Massive stars are also thought to be responsible for the reionization of the early Universe. More recently it has been proposed that the most massive stars are the progenitors of gamma-ray bursts.

Being crucial in many relevant aspects of astrophysics, detailed knowledge of massive stars have been hampered by the presence of strong stellar winds which dominate the resemblance of the atmospheres, the yields of ionizing radiation (Gabler et al., 1989; Najarro et al., 1996) and the evolution of these objects, leading to significant modifications in their observable spectra. Thus, we find stellar wind signatures at all wavelength ranges, from the UV ionized resonance transitions through the optical (H_α) to the Infrared and Radio.

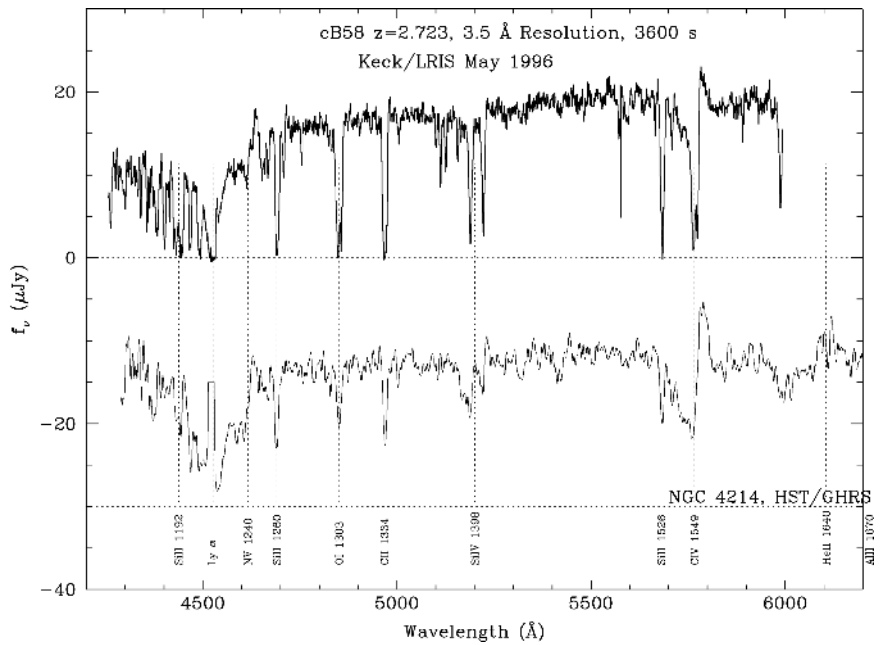
Nevertheless, the correct interpretation of their wind lines in terms of radiation driven wind theory has provided the spectroscopist with a wonderfull tool to investigate the physics of galaxies. As they can be observed in medium resolution spectra as individual objects in galaxies out of the Local Group or as integrated spectra of starburst regions in galaxies with significant redshifts (see Fig. 1), the correct knowledge of the physics of massive stars will yield information about the energy budget and chemical composition of galaxies along the cosmos history.

F. Najarro (✉)
Departamento de Astrofísica Molecular e Infrarroja, Instituto de
Estructura de la Materia, CSIC, Serrano 121, 28006, Madrid,
Spain
e-mail: najarro@damir.iem.csic.es

A. Herrero
Instituto de Astrofísica de Canarias, C/ Vía Láctea s/n,
E-38200 La Laguna, Tenerife, Spain ; Departamento de
Astrofísica, Avda, Astrofísico Francisco Sánchez 2, E-38271 La
Laguna

E. Verdugo
ESAC-ESA, P.O. Box 50727, 28080 Madrid, Spain

Fig. 1 UV astronomy as key to understand high redshift galaxies. Optical spectrum of a galaxy at very high redshift ($z=2.732$) compared to a local starburst (adapted from Kudritzki, 1998)



1.1. Importance of UV observations of massive stars

The UV constitutes an optimum spectral window as the spectral energy distributions of massive stars reach their maxima within this wavelength range. Apart from this efficient coincidence established by nature, massive stars decorate the UV spectral region with a number of key diagnostics to our understanding of the nature of these objects and their interaction with the surrounding media. The relevance of such diagnostics in the UV can be easily recognized since:

- The presence of P-Cygni profiles produced by the resonance transitions of C IV, N V, Si IV, O VI, etc, provides unique information about the stellar winds associated with massive stars.
- The bulk of blocking lines over several ionization stages from elements from the iron group enable to estimate metallicity and other stellar properties such as effective temperature.
- The unsaturated line profiles from ionized species trace very efficiently the mass-loss rate characterizing the stellar wind. Further, when combined with ρ^2 sensitive diagnostics at other wavelengths they may be used to calibrate the presence of inhomogeneities (“clumping”) in the wind.
- They encompass enough number of X-Ray sensitive diagnostic lines such as O VI, C IV and N V.
- The optimized spatial resolution achieved at UV wavelengths allows to resolve individual stars in starforming regions in external galaxies.

In this paper we review recent progress within the field of massive stars and discuss open problems which could be addressed by future UV missions.

2. Temperature scale for massive OB stars

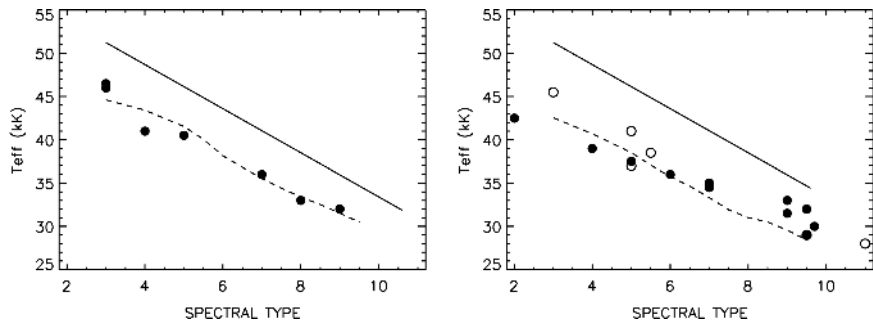
A calibration of the effective temperature of O supergiants is a key issue for the correct description of the radiation hardness in the EUV and UV spectral ranges and the corresponding ionizing photons released by the stars. This can have enormous consequences on the energy budget of their surroundings, as well as of starburst regions and galaxies whose UV spectra are characterized by these stars.

Since NLTE models are available, the temperature scale of massive OB stars has been determined using model atmospheres to fit a given ionization equilibrium. Helium, being the atom used to spectroscopically classify the earliest stars, has become the traditional temperature indicator for these objects, although other ionization balances are formally possible. Of course, the resulting temperature scale is model dependent.

Very recently a number of calculations from different authors have strongly changed the temperature scale of massive OB stars. These calculations have been based on new families of model atmospheres that include sphericity, mass-loss and line-blanketing, in addition to NLTE. The combination of all these factors results in temperatures that are much cooler than those hitherto assumed.

Vacca, Garmany and Shull (1996) presented a compilation of the spectroscopic determinations of effective temperatures of massive OB stars. They gave preference to the most recent calculations, that at that time were mostly based on plane parallel, hydrostatic, unblanketed model atmospheres. Their temperature scale for dwarfs and supergiants can be seen in Fig. 2.

Fig. 2 The temperature scale for Galactic O dwarfs (left) and supergiants (right). The solid lines are for the Vacca et al. (1996) scale, the dashed line for the scale defined by Martins et al. (2005) (the one the authors define as the theoretical scale), filled symbols are data from Repolust et al. (2004) and open symbols are data from Herrero et al. (2002)



The first calculations pointing to a cooler temperature scale were those from Martins et al. (2002), who used CMFGEN (Hillier and Miller, 1998), a code with all the improvements indicated above. These authors limited their calculations to OB dwarfs, so that the influence of mass-loss effects were negligible. Therefore, the main differences with Vacca, Garmann and Shull were clearly due to line-blanketing. These differences could reach up to 4000 K for early types, and decreased towards O9 and B0 types, as can be appreciated in Fig. 2.

The work from Martins et al. was followed by a series of papers with similar results. Herrero, Puls and Najarro (2002) gave a temperature scale for supergiants in Cyg OB2 using FASTWIND (Santolaya et al., 1997; Puls et al., 2005), another code with NLTE, sphericity, mass-loss and (in this case approximated) line-blanketing. They found differences up to 8000 K. In this case both mass-loss and line-blanketing, played a role. These authors also showed that two stars with the same spectral type and luminosity class may have different effective temperatures if their wind densities are different. While the results from Herrero, Puls and Najarro were based on analyses of only seven Cyg OB2 supergiants, Repolust, Puls and Herrero (2004) presented an analysis of 24 stars (17 giants and supergiants and 7 dwarfs), based on a slightly improved version of FASTWIND that confirmed the same trends. These same trends have also been confirmed by Martins, Schaefer and Hillier (2005) who have calculated models with CMFGEN and have given a new temperature scale for massive OB stars of different luminosity classes. These temperature scales agree quite well with those from Repolust, Puls and Herrero, and confirm that new models result in effective temperatures that are several thousands Kelvin cooler for early and intermediate spectral types, decreasing towards late spectral types. The different temperature scales can be seen in Fig. 2.

OB stars in the Magellanic Clouds have been analyzed by Massey et al. (2004, 2005) using FASTWIND. Their results confirm that supergiants are 3000–4000 K cooler than dwarfs of the same spectral type at any metallicity. However, a clear trend of temperature with metallicity at a given spectral type and luminosity class is not seen: authors obtain that SMC dwarfs and supergiants are hotter than Milky Way

counterparts, but while LMC dwarfs seem to extend the SMC scale, LMC supergiants seem to extend the Milky Way scale. In addition, SMC dwarfs of types O3–O4 do not fit into the relation indicated by the later O types in that galaxy, but have a temperature closer to their Milky Way analogues. When comparing to other authors we find further inconsistencies: O4–O5 SMC dwarfs analyzed by Massey et al. (2004, 2005) are hotter than Milky Way ones, but O4–O5 SMC dwarfs analyzed by Bouret et al. (2003) are cooler than similar objects in our Galaxy. While the analyses by Massey et al., 2004, 2005 constitute a major step forward to understand the metallicity dependence of the temperature scale of massive OB stars, the low number of objects and the large scatter in the relations indicate the necessity of further analyses, particularly because the scatter could be related to differences in wind density at a given spectral type.

We should finally mention the temperature scale obtained by Bianchi and García (2002) and García and Bianchi (2004). These authors analyse stars by means of UV spectra (FUSE and IUE) using WM-basic (Pauldrach, Hoffmann and Lennon, 2001). The temperatures they find are much cooler than those from other authors. Wind clumping (see Section 5) affecting their results is a plausible explanation still requiring investigation.

For types O9–B0 there is no clear difference between temperature scales from different authors or metallicities. It is then not strange that a comparison of temperatures scales for B supergiants results in no apparent difference between Galactic (from McErlean, Lennon and Dufton (1999)), LMC (Evans et al., 2004) and SMC analyses (Trundle et al., 2004; Trundle and Lennon, 2005) (see Fig. 3; the figure includes a few giants, but this does not change the conclusions that follow). We can see in Fig. 3 that the scatter at a given spectral type is very large. At spectral type B1, for example, we find a difference of 3500 K between the hottest and coolest B1 supergiants (both from the SMC), and the difference increases to 4500 K if we include the hottest object, a B1 III star. This large difference can be attributed to the different wind densities: the coolest B1 supergiant (AV78) has a mass-loss rate of $2.29 \pm 0.34 \times 10^{-6} M_{\odot} \text{ yr}^{-1}$, while the hottest one (AV242) has $0.84 \pm 0.13 \times 10^{-6} M_{\odot} \text{ yr}^{-1}$. The larger radius of the first star (79.0 versus $36.6 R_{\odot}$) also contributes to a cooler

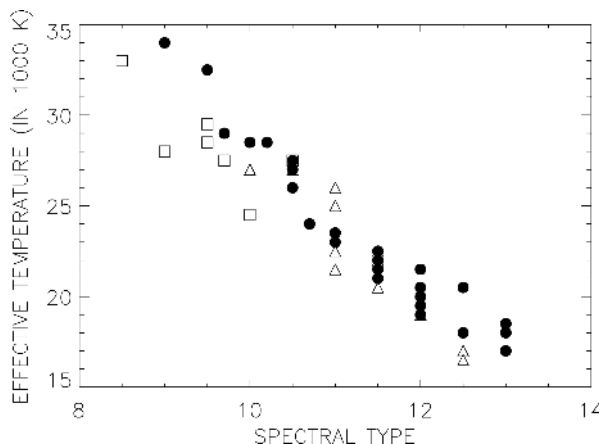


Fig. 3 The temperature scale for early B supergiants in the Milky Way and the Magellanic Clouds. Spectral types are coded so that 9 means O9, 10 means B0 and so on. Solid circles are data by McErlean et al. (1999) for the Galaxy; triangles are data from Trundle et al. (2004) and Trundle et al. (2005) for the SMC; and squares are data from Evans et al. (2004) for the LMC

temperature. For details of the analysis, see Trundle et al. (2004).

2.1. Potential of UV temperature diagnostics

We have seen above the impact of the new generation of atmospheric models on the temperature scale of massive OB stars. One of the immediate advantages of blanketed models is the simultaneous use of different ionization equilibria to determine the effective temperature of the star. Thus, apart from the “traditional” He I/He II ionization balance, we may utilize unsaturated C II–IV, N II–V, O II–V, Si III–IV, etc diagnostic lines from which we, ideally, should obtain consistent values with the helium ionization equilibrium. Besides, the UV range encompasses a whole forest of iron group lines and enables to use the strength ratios of combined features of different ionization stages of the same ion to constrain the effective temperature of the star. Recently, several studies have been performed identifying key diagnostic lines to trace effective temperature of OB stars in the UV (Heap et al., 2004, Bouret et al., 2005 and references therein). Fig. 4-left shows the sensitivity of the so called WFE54 index to temperature and gravity (Heap et al., 2004), where WFE54 represents a weighted ratio of the equivalent widths of the Fe V and Fe IV around $\lambda 1370$ and 1620\AA respectively. We note that, although this index displays a relatively high sensitivity to stellar temperature, it also depends strongly on gravity. Therefore, if gravity is determined from other diagnostics (optical spectrum), this index constitutes an excellent temperature indicator for $T_{\text{eff}} \geq 35,000\text{K}$. On the other hand, the ratio of the carbon C III1175–IV1169 line strengths (see Fig. 4-right) is essentially only dependent on the effective temperature (Heap et al., 2004). The reader is referred to

Heap et al. (2004) for a detailed identification of temperature UV diagnostics in O dwarfs.

For supergiants, the situation is very similar. However, the stellar wind may play a fundamental role. Thus, the sensitivity of some strategic UV lines to effective temperature will be shifted in the parameter domain compared to the O dwarfs case. Fig. 5 shows how the C III1175 and Si IV1400 lines react considerably to changes of barely 1000 K in a mid type O supergiant.

We may then conclude that the new generation of blanketed models for massive stars provide powerful diagnostics to obtain reliable effective temperatures for massive OB stars by means of ionization equilibria of metals other than H and He, allowing this way direct estimates of temperature from UV observations. This opens an important window to study massive stars in star forming regions in external galaxies using the unique spatial and spectral capabilities of future UV missions.

3. Abundances

With the advent of new blanketing codes, quantitative spectroscopic studies of the UV forest of metal lines has become reality. These codes allow to fit not only the outshining UV saturated and unsaturated profiles from metal ions but also the underlying blanket of lines from iron group elements. Therefore, the new generation of models provides, for the first time, direct estimates for abundances of elements such as C, N, O, Si or S by fitting individual unsaturated lines while robust estimates of abundances of iron group elements may be obtained fitting integrated features in strategical UV wavelength regions. Of course, the analysis has to provide as well stellar parameters such as T_{eff} , stellar mass, M , L_* and clumping.

Figure 6 displays the potential of new blanketed models to perform quantitative analyses of UV spectra for massive stars. It displays the excellent agreement for the Luminous Blue Variable (LBV) P Cygni between the model and the observed IUE SWP region (Najarro, 2001). Interestingly, we see from Fig. 6 that the main contributor to blanketing in this zone is Fe III. However, we can see as well that there are some regions (e.g. 1420 – 1500\AA , 1570 – 1730\AA) where the model clearly underestimates the blanketing. Before tentatively blaming it on the behavior of the extinction law, it is necessary to investigate the effects of other iron-group elements (Ni, Co, Cr) which are normally not included in many new models from computational saving reasons. Recomputing the same model but adding Ni and Co Najarro (2001) found that, indeed, Ni III provides most of the missing blanketing as shown in Fig. 6. Further, Co III also contributes significantly in the 1750 – 1800\AA region. When these two species are included, the agreement of the model with the observations is excellent throughout the whole IUE SWP range.

Fig. 4 Temperature diagnostics in the UV for O dwarfs. left Fe v/Fe IV index as function of temperature and gravity. Right C III/C VI line sensitivity as a function of effective temperature (adapted from Heap et al., 2004)

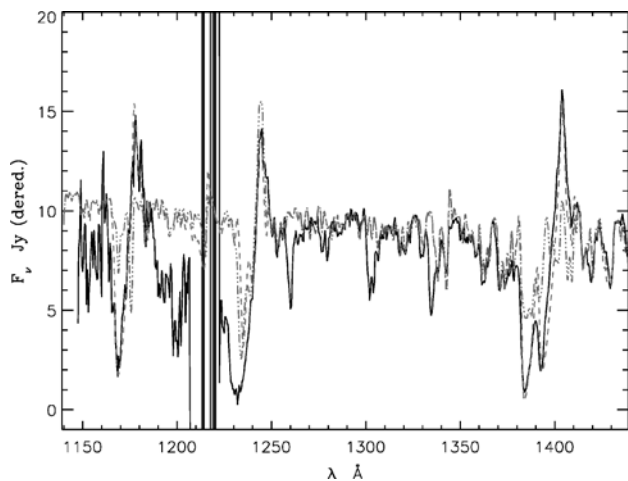
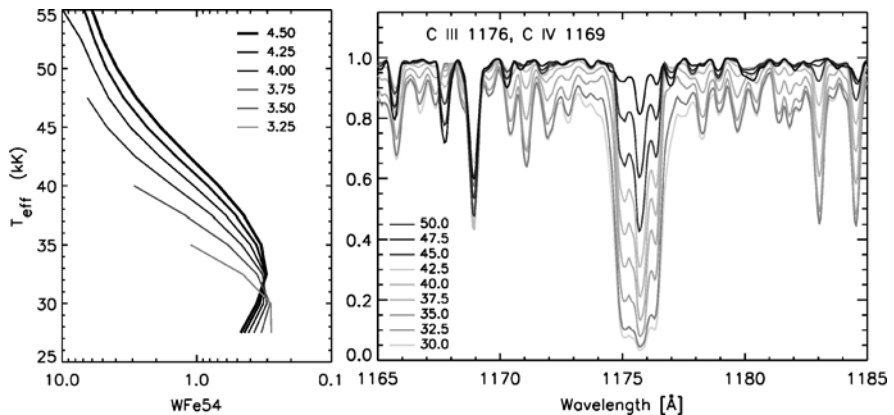


Fig. 5 Temperature sensitivity of C III and Si IV in mid-type supergiants. HST-spectra of CygOB2#11 and model fits with $\Delta T = 1000K$

In O stars, the need of UV spectra to determine metal abundances becomes a must as the optical spectra no longer show the strong metal features present in B and A stars and we run out direct diagnostics to constrain the abundance of iron group elements. Fig. 7 displays the potential of the UV to determine metal abundances in O type stars. We see from Fig. 7-top the strong dependence with metallicity and spectral type of the UV C IV line, while Fig. 7-bottom demonstrates the possibility to estimate the iron abundance in O stars.

We also see that as metallicity decreases (Fig. 7-bottom) the strengths of metal features in the UV become weaker, and enhanced S/N is required to perform reliable metal abundance determinations. Future missions with enhanced UV sensitivity will play a key role in our ability to derive accurate abundances in low-metallicity environments

4. X-rays

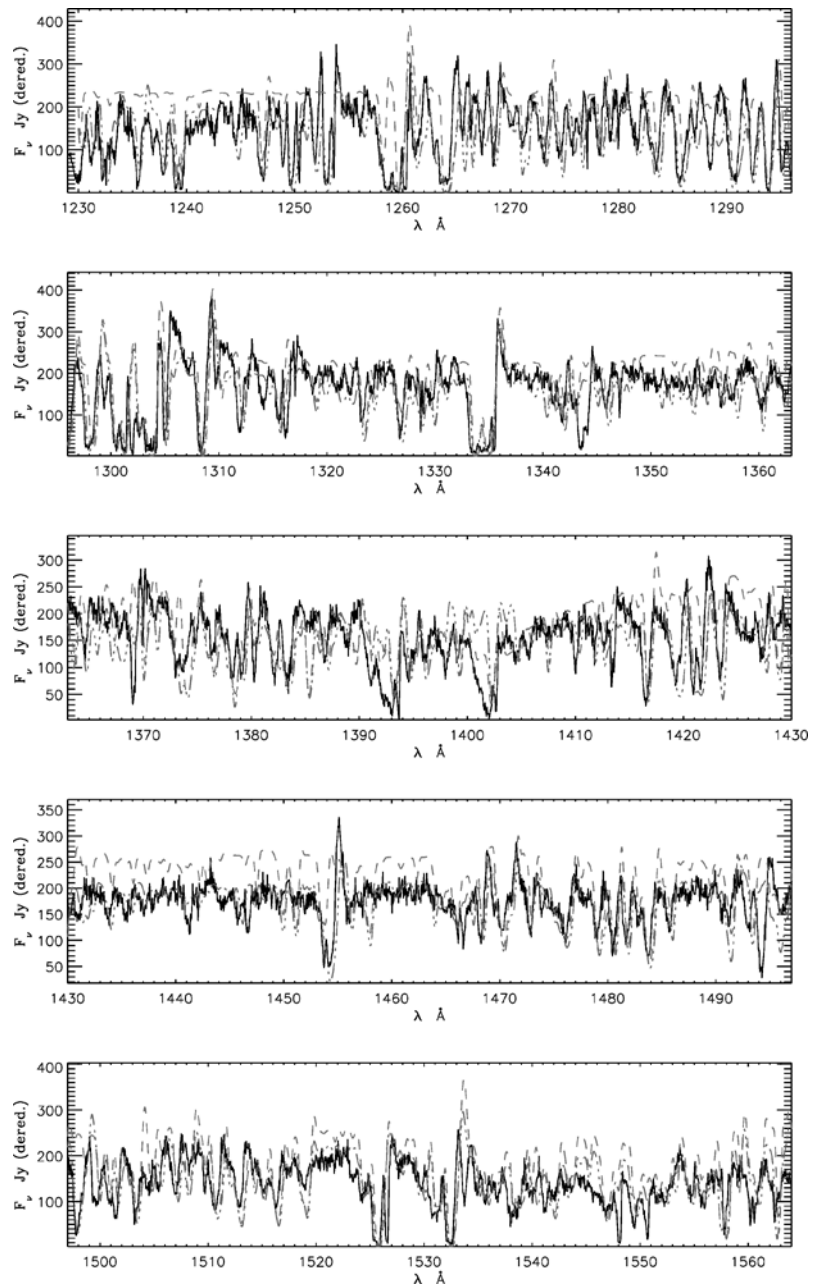
UV spectra of massive stars also trace the presence of X-rays in their stellar winds. X-ray emission in the wind alters

significantly the wind ionization structure, enhancing the populations of the so called “superions” such as N V and O VI. In fact, X-rays were utilized more than ten years ago to explain the observed strength of O VI λ 1036 in galactic and LMC O supergiants Pauldrach et al. (1994). For O and B dwarfs (low density winds) Macfarlane et al. (1994) showed that the effects of X-rays were enhanced when compared to supergiants (high density) as for lower wind densities we get significantly less recombinations to compensate the Auger ionization. They also found that these effects increased towards later spectral types. This effect is driven by the drop of the photospheric to X-ray flux ratio as the lower effective temperature for a later spectral type reduces drastically the bolometric stellar luminosity. Recent studies, confirming these findings have been carried out for a extended sample of O stars by Bouret et al. (2003, 2005) and Martins et al. (2005). Fig. 8 displays the crucial effects of including X-rays on key diagnostic features such as N V λ 1240 and several Fe IV lines around λ 1640 for α Cam, a late O supergiant (Najarro et al., in prep). Given the distance limited sample of massive stars from which current X-ray missions may provide direct measurements of X-rays, it is evident that future UV missions with enhanced sensitivity will constitute our ideal tools to probe the presence of X-rays in the winds of massive stars in external galaxies.

5. Clumping

Recent evidence indicates that currently accepted mass-loss rates may need to be revised downwards by as much as a factor of ten or more, because the most commonly used mass-loss diagnostics are severely affected by small-scale density inhomogeneities (“clumps”) in the wind, redistributing the matter into regions of enhanced and depleted, almost void density. The amount of clumping is quantified by the so-called clumping factor, f_{cl} . Diagnostics sensitive to the square of the density, ρ^2 , will tend to overestimate the mass-loss rate of a clumped wind by a factor $\sqrt{f_{\text{cl}}}$. Considering that numerous

Fig. 6 Comparison of the blanketed model (dashed) and the averaged observed (solid) UV IUE-SWP spectrum of P Cygni. A model including Nickel and Cobalt (dashed-dotted) is also displayed in the IUE-SWP region (adapted from Najarro, 2001)



stellar evolution calculations have found that changing the mass-loss rates of massive stars by even a factor of two has a dramatic effect on their evolution (Meynet et al., 1994), it is clear that such revisions would have enormous implications.

Indeed, strong clumping has been claimed to be present in stellar winds of early type stars (e.g., Eversberg et al., 1998; Lépine et al., 1999; Crowther et al., 2002; Hillier et al., 2003; Bouret et al., 2003). Herrero, Puls and Najarro (2002), Repolust, Puls and Herrero (2004) and Markova et al. (2004) report that clumping may cause mass-loss rates for O-stars with H_{α} in emission to be overestimated by factors of 2.5. Detailed modelling of the UV and optical spectra of selected O stars by Bouret et al. (2005) indicates that not only are the

winds strongly clumped, but that the clumping seems to begin very close to the wind base so that *all* mass-loss rates may need to be revised downwards, by factors of $\lesssim 7$. Prinja et al. (2005) analyzed unsaturated wind lines in lower luminosity B supergiants and showed that their mass-loss rates may be factors of 10 or more less than theoretical expectations.

A compelling, independent indication for clumping has come from analyses of the Far-UV wind lines due to the P $v\lambda\lambda 1118, 1128$ doublet (Crowther et al., 2002; Hillier et al., 2003; Bouret et al., 2005; Massa et al., 2003; Fullerton et al., 2006), which has only become widely accessible since the launch of FUSE. Because Phosphorus has a low cosmic abundance, this doublet never saturates, providing useful

Fig. 7 (Top) Metallicity dependence of metal ions UV lines. Compilation of UV C iv stellar wind profiles of O dwarfs and giants in the Galaxy, LMC and SMC (adapted from Kudritzki, 1998). (Bottom) Model fits with different metallicities of the observed UV Fe iv spectrum of an O star in the SMC (adapted from Haser et al., 1998)

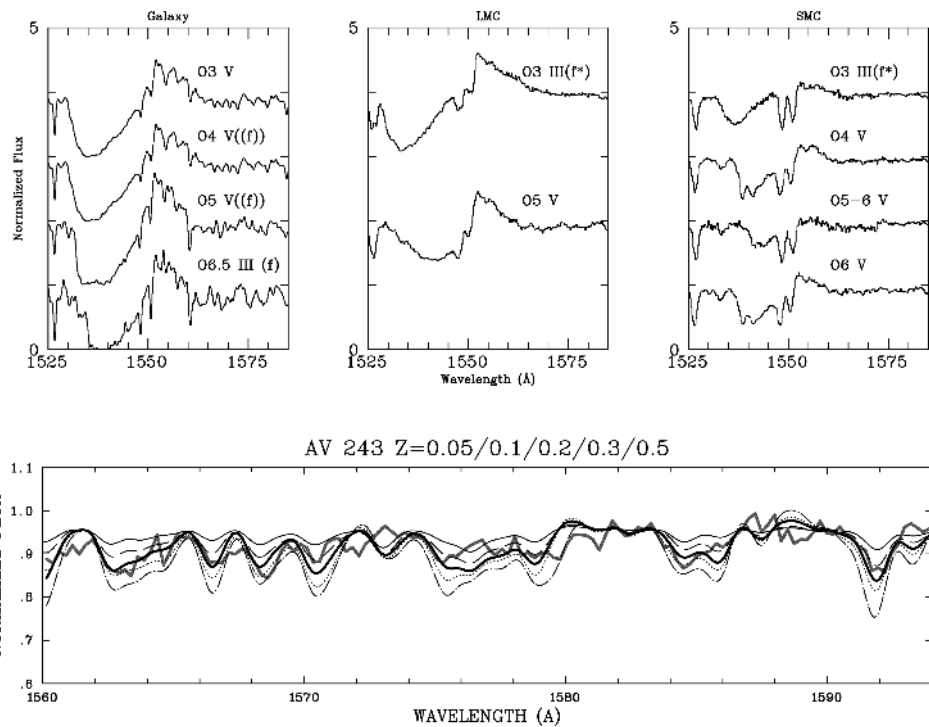
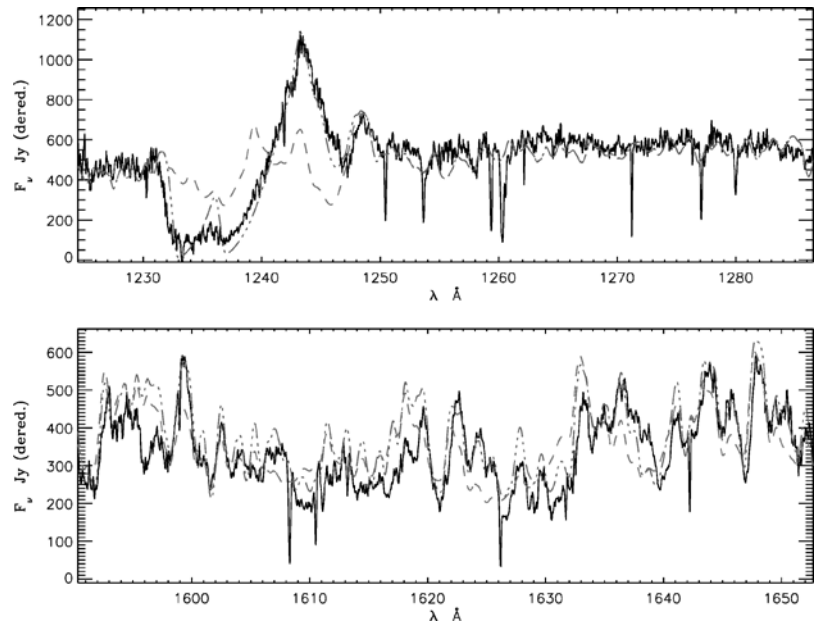


Fig. 8 Effects of X-Rays in α -Cam O9If. The strong changes induced by including X-rays (dashed-dotted line) in the ionization structure of N and Fe in the wind are reflected in the observed N v λ 1240 and Fe iv lines around λ 1640



estimates of M for those cases where the ionization fraction is computed consistently (Crowther et al., 2002; Hillier et al., 2003; Bouret et al., 2005) or to Mq , where q is the ionization fraction of P v. At least for mid-O stars Massa et al. (2003) and Fullerton et al. (2006) have shown that P⁴⁺ is a dominant ion. Therefore, for these stars the P v $\lambda\lambda$ 1118, 1128 doublet constitutes a useful constrain to determine M itself. This is demonstrated in Fig. 9 which displays model fits from Crowther et al. (2002) to a SMC O supergiant for different combinations of clumping, mass-loss rate and phosphorus

abundance. Interestingly, the mass-loss rates derived by all these authors turned out to lie considerably below those inferred from other diagnostics.

The most reasonable way to resolve this discordance, unless nature does not like phosphorus to participate in massive stars, is to invoke extreme clumping in the wind. In a clumped wind, the continuum and H $_{\alpha}$ measurements (both sensitive to ρ^2) overestimate the actual M , whereas the line strengths of PV, being $\propto \rho$, are not directly affected by clumping. If the winds of OB stars are indeed substantially clumped, then

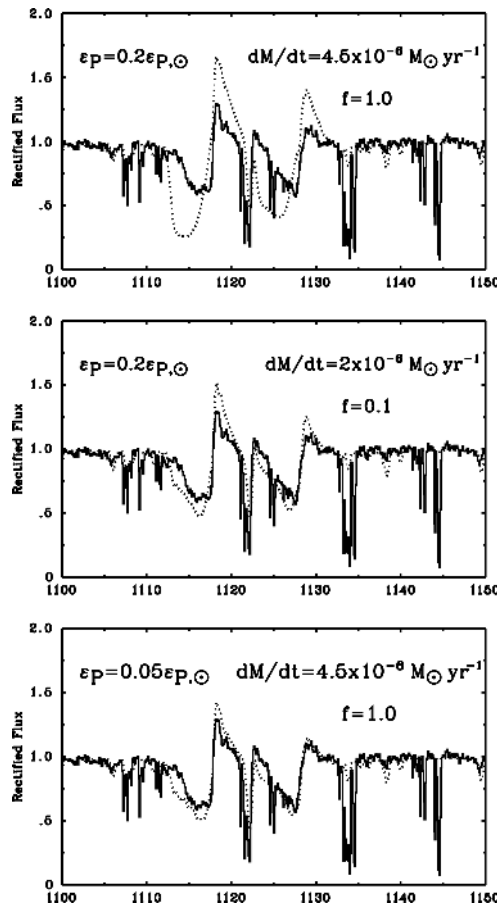


Fig. 9 Clumping diagnostics in O stars. The P $\nu\lambda\lambda 1118, 1128$ as tracer of low M (adapted from Crowther et al., 2002)

the actual mass-loss rates are *much* lower than previously thought, by a factor of 10 or even more. Further, in cases of strong clumping the ionization structure of relevant species may be altered as well affecting key diagnostic lines at all wavelength ranges.

The downward mass-loss rate revisions suggested above would have dramatic consequences for the evolution of and feed-back from massive stars. Therefore, it is important to have robust and precise determinations of the mass-loss rates. All clumping diagnostics are subject to some degree of uncertainty which can be reduced by combining suitable diagnostics, scanning different portions of the wind, from close to the base (H_α) and near IR lines (Najarro et al., 2004) over intermediate regions (Br_α , mid-/far-IR continua) to the outermost (radio) region. A *consistent* analysis will severely constrain the *radial stratification* of the clumping, expressed in terms of the clumping-factor, $f_{cl}(r)$. If used in combination with other diagnostics from (F)UV wind lines *and state-of-the-art model atmospheres* allowing for a decent description of the required ionization balance, the “true” mass-loss rates can be uniquely derived. Fig. 10 shows that, apart from the P $\nu\lambda\lambda 1118, 1128$ doublet there are other UV lines from

different metals which can trace very efficiently the presence of clumping, especially for those regions of the parameter domain where the lines are unsaturated. Therefore, future UV missions with enhanced sensitivity will provide enough number of observations of OB stars over different spectral types and allow this way, to constrain the presence of clumping in these objects.

6. The wind momentum luminosity relation (WLR)

The winds of massive OB stars are driven by the absorption of photons from the radiation field by thousands of spectral lines from many atomic elements. These photons accelerate the atoms towards the empty surrounding space in such a way that the atom velocity increases with the distance to the stellar surface, until the material no longer absorbs them.

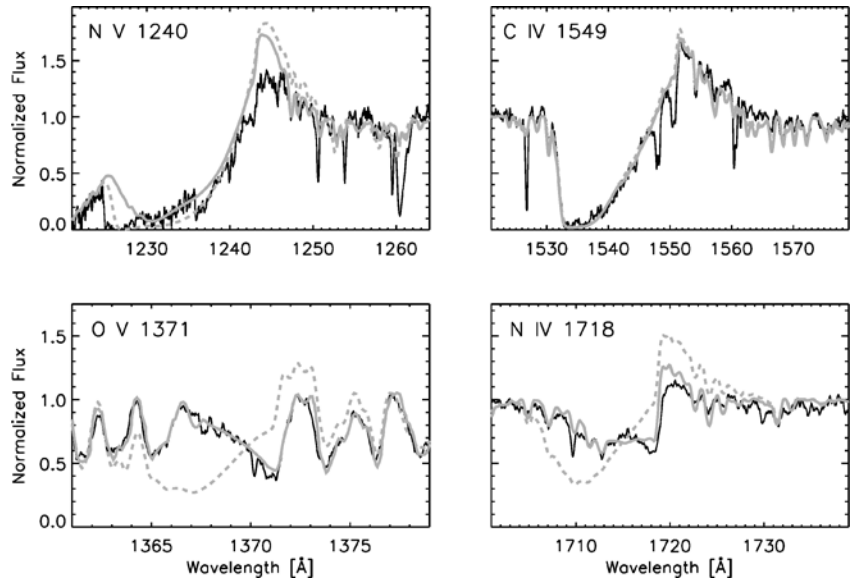
Since the winds of hot stars are driven by radiation, we expect a tight relationship between the mechanical momentum of the stellar wind and the photon momentum. Actually, the theory of radiative driven winds (Castor et al., 1975; Kudritzki et al., 1989) predicts that the “modified stellar wind momentum” depends directly on luminosity through the Wind Luminosity relation (WLR)

$$\begin{aligned} \log D_{\text{mom}} &= \log D_0 + x \log(L/L_\odot) D_{\text{mom}} \\ &= \dot{M} v_\infty (R_*/R_\odot)^{0.5} \end{aligned} \quad (1)$$

where the coefficients D_0 and x are a function of spectral type and luminosity class. Further, the coefficient controlling the dependence on luminosity, x , is determined by the statistics of the thousands of metal lines driving the wind, so a different WLR has to be established for each metallicity environment. The weak dependence on stellar radius arises from the competition of the accelerated stellar wind against the gravitational potential. We immediately see that, once calibrated on stars with known distance, the WLR may constitute a powerfull indicator of extragalactic distances (see Kudritzki and Puls, 2000, for a thoroughfull discussion). During the last decade an enormous effort has been made to calibrate the WLR as function both of spectral type and metallicity and compare the results with the predictions by theory (Puls et al., 2000; Vink et al., 2000, 2001).

Fig. 11 shows the different relationships obtained by Kudritzki et al. (1999) for different spectral types in the galaxy. Of concern is the shift by more than one decade in modified momentum between the relation of early and mid B-supergiants. Though not totally, blanketing may provide the key to partially reduce the discrepancy between the observed WLR for O and early B supergiants and that obtained for mid Bs. In fact, Urbaneja (2004) found a significant correction on the modified momenta of these stars with respect

Fig. 10 Unsaturated UV lines as tracers of clumping in O stars (adapted from Bouret et al., 2005)



to the values derived by Kudritzki et al. (1999) as shown in Fig. 12-right.

Results on the metallicity dependence of the WLR for O stars and B supergiants and their comparison with theoretical predictions are displayed in Fig. 12. From Fig. 12-right we see how the modified momenta of galactic B-supergiants obtained with blanketed models (Urbaneja, 2004) agree much better with theoretical predictions than those obtained with unblanketed models (Kudritzki et al., 1999), although a significantly different slope is obtained. The whole worsens in the case of the SMC, where the WLR obtained from blanketed models (Trundle and Lennon, 2005) differs severely from theoretical predictions (Vink et al., 2001). In the case of O stars, the situation is significantly improved. From Fig. 12-left (see Massey et al., 2005, and references therein) we see how the theoretically predicted WLRs for O stars in the Galaxy, LMC and SMC are reasonably well reproduced by spectroscopic studies.

The WLR provides a strong test for the theory of radiatively driven winds, and the UV provides the best region to test the WLR, as it allows derivations of the mass loss rate, the terminal velocity and the metallicity. Stellar parameters can also be derived from the UV (Bianchi and Garcia, 2002; Garcia and Bianchi, 2004), although further work is needed for some of them (mainly gravity and radius). What we need here are observations of high resolution and high S/N at different metallicities. Inspection of figures 11 and 12 tell us that the number of observed stars is too low to provide a really constraining test of the theory. The Magellanic Clouds, together with the Milky Way, provide a wide range in metallicity, and other galaxies in the Local Group offer additional opportunities. Thus, M31 may extend the observed metallicities towards supersolar values, Sex A or Leo A may extend them below SMC values and M33 offers a system

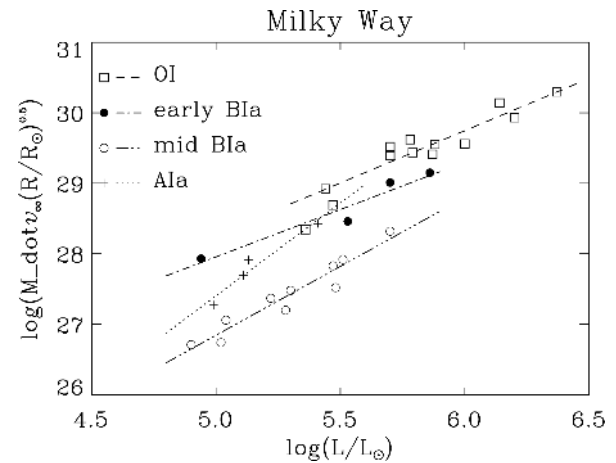


Fig. 11 The WLR as a function of spectral type. Galactic WLR for O, B and A supergiants (Kudritzki et al., 1999). Note the considerable offset between the WLR for early and mid B supergiants

with a strong metallicity gradient seen nearly face-on. The ability to get UV spectra for stars in all Local Group galaxies is the key to our correct understanding of the spectral type and metallicity dependence of the WLR. To that end, an UV telescope with more collecting power than HST is required.

6.1. The thin winds problem

Puls et al. (1996) showed that the observed WLR for O-type dwarfs exhibited a severe curvature toward very low wind momenta for luminosities lower than $\log L/L_\odot = 5.3$. Kudritzki and Puls (2000) reviewed three effects present in the physics of thin winds in dwarfs which may introduce deviations from the standard WLR. The first one is related to the decoupling of metal ions with the rest of the

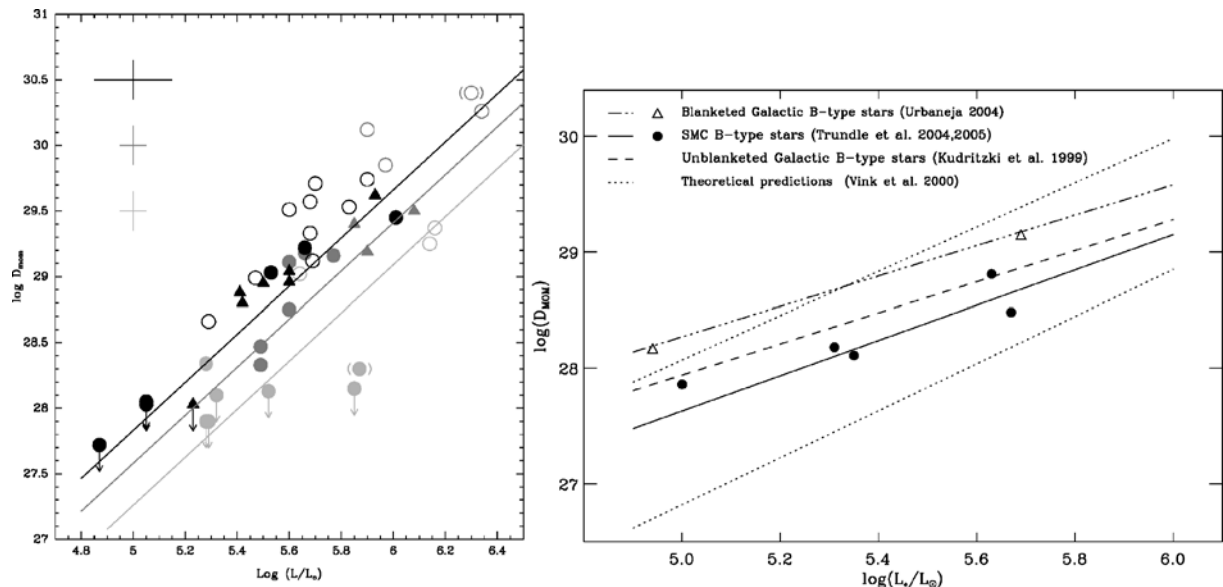


Fig. 12 Metallicity scaling of the WLR for O and B supergiants. (left) Z scaling for O supergiants (adapted from Massey05). (Right) Z scaling for B supergiants (Kudritzki et al., 1999; Urbaneja, 2004; Trundle and Lennon, 2005). (dash-dot): linear regression to galactic stars with blanketed models (Urbaneja, 2004); (dash-dot): unblanketed

galactic (Kudritzki et al., 1999); (solid): blanketed SMC (Trundle and Lennon, 2005); (upper dotted) theoretical galactic predictions (Vink et al., 2000); (lower dotted) theoretical SMC predictions (Vink et al., 2001). Note the considerable correction to the modified wind momenta for B-supergiants due to line blanketing

plasma. This will happen if the density falls below the range for which coulomb-collisions are able to redistribute the photon momentum absorbed by the metal ions to the bulk of wind plasma (Springmann and Pauldrach, 1992; Babel, 1995). The second one is caused by the shadowing of photospheric lines which considerably lower the line force, resulting on a net reduction of the mass-loss rate, especially in the case of B-dwarfs (Babel, 1996). Finally, for low mass-loss rates where the continuum is thin throughout the transonic region, curvature terms of the velocity field may lead to line-accelerations much smaller than in the standard computations, resulting again on reduced mass-loss rates (Puls et al., 1998; Owocki and Puls, 1999))

Recent spectroscopic analysis using unified models seem to confirm the presence of this turnover. Herrero, Puls and Najarro (2002) obtained a very low value for the mass-loss rate of the O9.5V star 10 Lac. Their result, displayed in Fig. 13 showed that in order to match the observed UV spectra of the star, the mass-loss rate had to be reduced more than one order of magnitude below the theoretical prediction. It must be stressed that, although the presence of X-rays could introduce a significant uncertainty in the absolute M value, the upper limit is still well below the predictions from radiatively wind theory (Vink et al., 2000). Recently Bouret et al. (2003) and Martins, Schaerer and Hillier 2004, 2005 have obtained similar results on analysis of O dwarfs in the SMC and the Galaxy (see Fig. 14). One important conclusion from the above studies is that the discrepancy in the mass loss rates obtained seems not to be related to

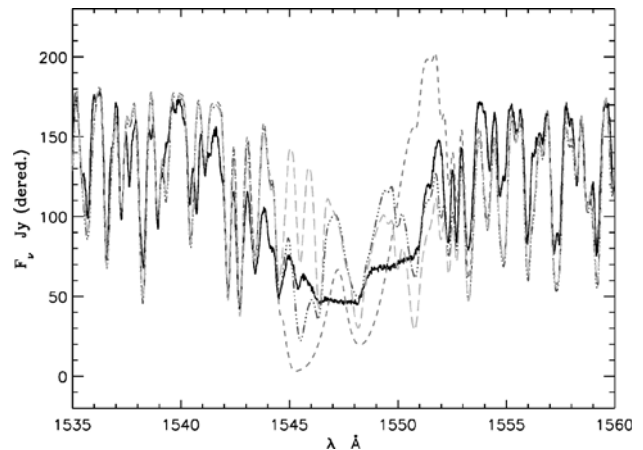


Fig. 13 The weak wind problem in O dwarfs. Model fits with different mass-loss rates of the UV C IV λ 1550 for the O9V star 10 Lac. \dot{M} values are $1, 2$ and $8 \times 10^{-10} M_\odot \text{ yr}^{-1}$

metallicity, as is present on both the Galactic and SMC stars.

Figure 14 clearly shows a breakdown of the WLR for low luminosity O dwarfs. Although present results based on UV studies may suffer from effects such as X-rays, advection or adiabatic cooling, results from other indicators like H_α are not appropriate because of insensitivity to very low mass-loss rates. Moreover, other indicators in the IR and radio may be affected by clumping. Detecting this clumping in thin winds may be extremely difficult, and therefore high resolution, high S/N in the UV becomes the best (if not the only) way to derive the correct mass loss rate.

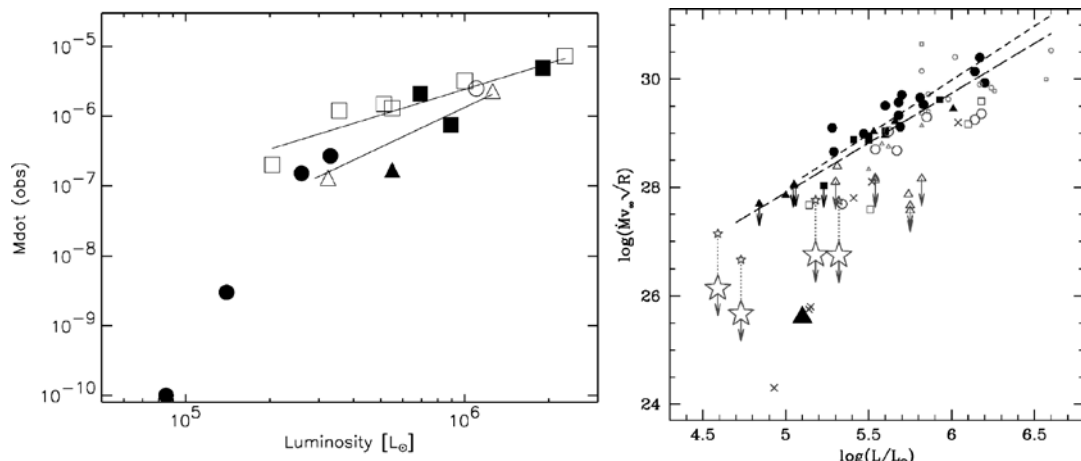


Fig. 14 The problem of thin winds. (Left) Mass loss rates derived for O dwarfs in NGC 346 (Bouret et al., 2003, LMC). (Right) Modified wind momenta as a function of stellar luminosity for O stars (from Martins et al., 2005). Filled (open) symbols are Galactic (LMC, SMC) stars.

Triangles and stars (squares, circles) correspond to luminosity class V (III, I). Note the low momenta of the SMC objects and the galactic star IOLac (large triangle)

7. Wind terminal velocity

In the previous section we have seen that winds in massive OB stars are driven by photon absorption by numerous metal spectral lines. Atoms are accelerated until they cannot absorb photons anymore. From that moment on, atoms move freely into space asymptotically approaching a maximum velocity, which is formally reached at infinity. This is the so-called *wind terminal velocity*, v_{∞} . While the structure of the velocity field resulting from this process is very difficult to determine, the terminal velocity can be derived in a comparatively easy way.

Determination of the terminal velocity is one of the key aspects in studying the stellar wind. As explained in the introduction to this chapter it enters the expression for the modified Wind momentum-Luminosity Relationship (WLR), the product of the wind momentum times the square root of the radius, which is proportional to a power of the stellar luminosity. Therefore, reproducing the correct terminal velocity with models is crucial to obtain the correct mass-loss rate for a given luminosity, and to use the modified WLR as distance indicator. Moreover, one of the strong predictions of the theory of radiatively driven winds is the metallicity dependence of the terminal velocity. Therefore, a determination of v_{∞} in regions of different metallicity constitutes a strong test for the theory.

Some of the spectral lines in the winds of OB stars are so optically thick, that they absorb photons even at large distances, when the terminal velocity has been reached and the wind density has fallen by orders of magnitude. We should note that these absorbed photons do not accelerate the wind significantly further, as their number and integrated momentum is very low compared to that of the whole wind. But

leave their signature in the stellar spectrum, an thus we can derive the terminal velocity.

Atoms moving at a given velocity in the wind will absorb photons shifted to the blue with respect to their laboratory wavelength (at which they have been emitted at the stellar surface). Atoms moving at the largest velocity reached by the wind will absorb photons with the largest blueshift. Therefore, determining the maximum blueshift in an optically thick line we will obtain the wind terminal velocity. Of course, the number of absorbing atoms has to be large enough to absorb photons at the low densities present in the layers moving at the terminal velocity. Blue saturated P-Cygni profiles are therefore ideal to determine the wind terminal velocity as they fulfill this requirement. In addition, a number of effects that we describe below have to be taken into account.

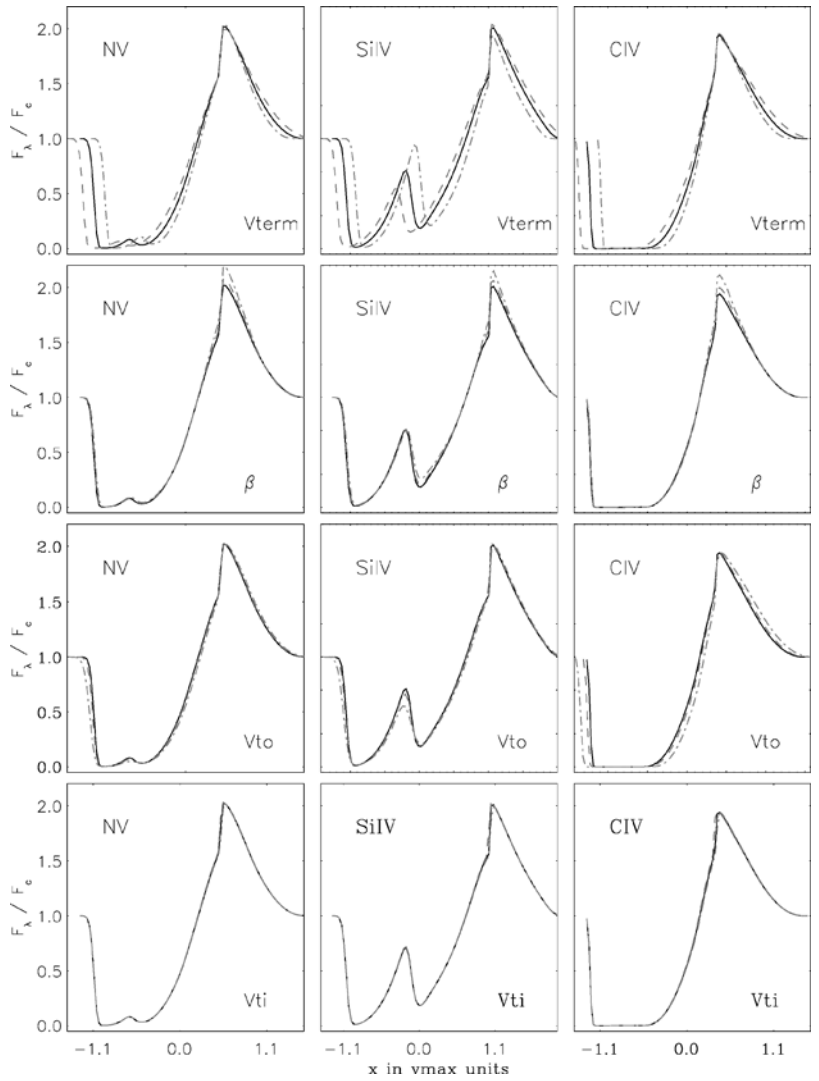
While we could directly try to derive the terminal velocity from this maximum blueshift, the fitting of the whole P-Cygni profile formed in the wind gives us much more information. Fortunately, there is a simple method that allows us to calculate this profile in an approximated way, but precise enough to derive a number of interesting physical magnitudes, like the terminal velocity or the number of absorbing atoms. It is the *Sobolev plus Exact Integration* (SEI) method. We use here the formulation as described by (Herrero et al., 2001) (see also Haser, 1995, Lamers et al. (1999)). The velocity stratification is usually parameterized with a β -law,

$$w(x) = (1 - b/x)^{\beta} \quad (2)$$

with

$$w(x) = \frac{v(x)}{v_{\infty}}, \quad x = r/R_{*}, \quad b = (1 - w_{\min}^{1/\beta})$$

Fig. 15 Effects of the global parameters on the SEI synthetic profiles of the strongest UV wind lines in OB stars. X-axis units expressed as velocities, in units of the wind terminal velocity, referred to the rest wavelength of the blue component of each doublet. In each plot, three synthetic profiles are shown, one that defines the central value (solid line) and two others with a variation of $\pm 10\%$ (dashed lines) of the central value. From Urbaneja (2004)



R_* being the stellar photospheric radius and w_{\min} the ratio of the velocity at $x = 1$ to the terminal velocity, fixed at a value of 0.01.

This is consistent with more exact hydrodynamical calculations. However, the indetermination in the exponent of the velocity field, β , produces an additional uncertainty in the terminal velocities.

When deriving wind terminal velocities, it is important to account for the velocity dispersion v_{turb} (usually termed as “turbulent velocity”) present in those winds, to correctly reproduce the position of the emission peak, the blue through and the slope of the blue absorption, as originally proposed by Hamann (1981). Following (Haser, 1995) we adopt a parameterization of the form

$$v_{\text{turb}} = a_t v(r) + b_t, \quad (3)$$

i.e., the turbulent velocity is assumed to be (roughly) proportional to the local wind-speed $v(r)$, and the coefficients are

defined by

$$a_t = \frac{v_{ta} - v_{ti}}{1 - v_{\min}}; \quad b_t = v_{ta} - a_t,$$

where $v_{ti} = v_{\text{turb}}(v = v_{\min})$ is the minimum turbulent velocity (chosen to be of order sound-speed) and $v_{ta} = v_{\text{turb}}(v = v_{\infty})$ the maximum one. These parameters affect the overall appearance of all synthetic lines. Fig. 15 shows their effects on the synthetic profiles for a saturated case.

We also have to correct for the underlying photospheric components, which we do in an approximate way, by using IUE spectra of hot stars with weak winds and low projected rotational velocities as templates. Selection of photospheric template and continuum rectification has a big impact when fitting emission peaks, but has little effect in the determined terminal velocities. For Galactic stars a sample of Milky Way dwarfs with appropriate spectral types is usually selected (i.e., from the INES database). Of course, when working with

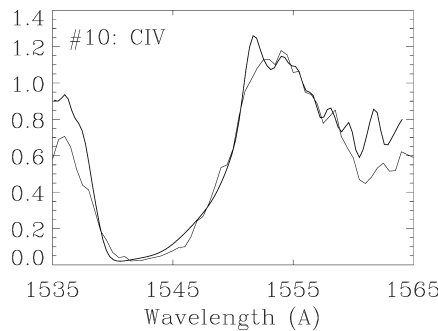


Fig. 16 Fit to the C IV profile in Cyg OB2#10. The terminal velocity v_∞ is 1650 km s^{-1} and the turbulent velocity has been set to 300 km s^{-1} . The exponent β in the velocity law is 0.8 (from Herrero et al., 2001)

extragalactic stars we have to use photospheric templates with the correct metallicity. Differences in metallicity may be a small source of error.

Because terminal velocities are derived from broad absorption features we can use modest resolution to obtain them. This allows us to look at relatively faint stars. These may be stars in other galaxies or Galactic stars that are optically bright but UV faint because of extinction in the Galactic plane. This extinction limits seriously our ability to observe massive stars in very young Galactic clusters.

Figures 16 and 17 give an example of profile fitting for Cyg OB2#10, an O9.5 I Galactic star, and M33-0900, a M33 B0.5-B1 Ia star. Both spectra have been observed with HST-STIS at an approximate resolution of 1200 during one and half hours, reaching the same S/N ratio (25). In both cases the wind terminal velocity was derived with an accuracy of 5%, although Cyg OB2#10 is a relatively bright star with $V=9.88$ and M33-0900 has $V=17.3$. This accuracy is of the order of that given by the radius term in the WLR expression (the total error is actually dominated by the mass-loss rate uncertainty).

These numbers therefore may be taken as a lower limit in terms of v_∞ observations, and indicate that most of the early OB stars in young Galactic star-forming (or recently star-formed) regions are hidden to us by dust obscuration in the UV. In Cyg OB2, for example, one of the richest Galactic OB associations, only six O stars have been observed in the UV with HST, and only another 3 might be observed under the same conditions.

The number of stars for which v_∞ has been determined is therefore small. For example, Howarth and Prinja (1989) list 203 Galactic O stars that were observed with IUE and for which they determined the wind terminal velocity. This work still constitutes the main source of data for Galactic v_∞ , but only a few stars belong to a given cluster. More recently, Prinja and Crowther (1998) list terminal velocity determinations for 31 stars between O3 and B1 in the LMC (including six O3 stars in R136) and 9 stars in the SMC. More scarce are data for M31 and M33 stars. Bresolin et al.

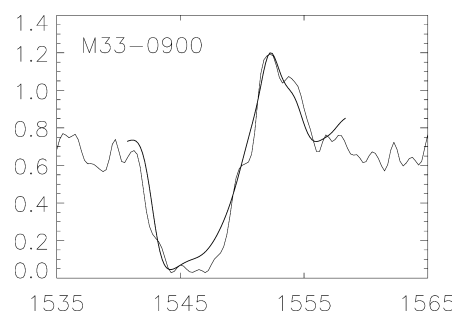


Fig. 17 Fit to the C IV profile in M33-0900. The terminal velocity v_∞ is 950 km s^{-1} and the turbulent velocity has been set to 170 km s^{-1} . The exponent β in the velocity law is 1.0 (from Urbaneja et al., 2002)

(2002) and Urbaneja et al. (2002) list six early B supergiants each, in M31 and M33 respectively.

While this allows us to study the behavior of the terminal velocity within our Galaxy, it is barely enough to study its behavior as a function of the spectral type and luminosity class for a given metallicity, or to study it within a single young cluster.

With a sensitivity 20 times larger, as expected for new UV missions we could see a qualitative change in the present situation. In our Galaxy we could gain a few magnitudes, depending on extinction conditions, reaching deeper in the dusty young clusters. However the real gain would be in the extragalactic stars. Even at the distance of M31 and M33 we could observe the O dwarfs and determine their terminal wind velocities. With modern ground-based optical telescopes we can secure their optical spectra and derive their stellar parameters. This would allow us to disentangle the v_∞ – spectral type – metallicity relation, providing us with a very tight test for the theory of radiatively driven winds.

8. A-type supergiants in the ultraviolet

A-type Supergiants are evolved massive objects ($\sim 9 - 25 M_\odot$) located in a region of the H-R diagram where evolution is very rapid. Therefore, they are few in number: only about one hundred galactic stars are classified as such. Among these supergiants there is a clear gap between spectral types A5 and F0, which could be related to the evolution of these objects. The evolutionary stage of A-supergiants is still unclear. Although the most extensive work on their abundances suggests that these stars have evolved directly from the main sequence (Venn, 1995a), the uncertainties in these studies are very high, due to the well recognized difficulty of modeling their atmospheres (Venn 1995b; Verdugo et al. 1999a). A recent work by Przybilla et al. (2005) analyses the various effects involved in the modelling of A-supergiants atmospheres (line blanketing, non-LTE, helium abundances, spherical extension, velocity fields, variability). In this work,

accurate stellar parameters are determined from a hybrid non-LTE spectrum synthesis technique for four BA supergiants. From the abundances analysis these authors found that three of the stars studied appear to have evolved directly from the main sequence but for the Alb star, η Leo, a blue-loop scenario is derived.

A-type Supergiants are intrinsically the brightest stars at visual wavelengths, and therefore the best potential extragalactic distance indicators using the wind momentum-luminosity relation (Kudritzki et al., 1999). This relation is derived from the radiation-driven wind theory and mainly based on Balmer line fits.

Radiation pressure is adopted as the dominant driving mechanism for the mass loss of A-supergiants. Unified wind models, which include a solution of the spherical transfer equation in the comoving frame and a non-LTE treatment of hydrogen and helium, were developed by Santolaya et al. (1997). These models succeed in fitting a number of profiles of the Balmer series for the brightest A-supergiants (Kudritzki et al., 1999), but cannot reproduce neither all the H_{α} profiles observed, nor their variability. An even more sophisticated model developed by Aufdenberg (2000), which includes non-LTE line blanketing for several metallic lines, failed to fit a typical H_{α} P-Cygni profile for the brightest A-supergiant Deneb (Aufdenberg et al., 2002).

Stellar winds in A-type supergiants can be studied using the optical spectrum or/and the ultraviolet (UV) spectral range. In the optical all lines seem to be photospheric except H_{α} which shows a variety of very different profiles: symmetric absorption, P-Cygni, double-peaked or pure emission profiles (Verdugo et al., 1999). It is in the UV range and particularly in the ultraviolet resonance lines where the presence of a stellar wind is cleanly traced. However, compared to the amount of work devoted to OB stars, the UV spectra of A-supergiants have scarcely been examined (e.g. Lamers et al., 1995, 1978; Praderie et al., 1980; Underhill and Doazan 1982; Hensberge et al., 1982). The most comprehensive studies of A supergiants in the ultraviolet range were performed by Talavera and Gómez de Castro (1987) and Verdugo, Talavera and Gómez de Castro (2006, 2003, 1997) from the observations taken by the International Ultraviolet Explorer (IUE) satellite.

The UV spectrum of A-supergiants is characterized by the presence of variable discrete absorption components (DACs; see some examples in Verdugo et al., 1999b) associated with the resonance lines of different ions, mainly Mg II, Al II, Si II, C II and Fe II. The appearance of these DACs is also related to the luminosity of the star. In Fig. 18 we show three typical observed Mg II[uv1] profiles: symmetric absorption profiles in Ib stars, profiles formed by several components, and a classical radiative-wind profile (without emission) in the Ia and Iab stars. The same behavior is observed in the

other lines cited above as is also shown in Fig. 18 for the Fe II[uv1] lines.

It may therefore seem that the less luminous A-supergiants do not show any perceptible trace of mass motion in their spectrum, but a variability analysis showed the presence of DACs in the ultraviolet Mg II[uv1] lines of two Ib stars, which indicates that mass outflow exists. DACs in the UV spectrum of A-supergiants were initially found only in the brightest A-supergiants. The time scales of variability of these components are of the order of several months. However, a monitoring programme performed with the IUE satellite in two Ib A-supergiants revealed the appearance and evolution of a single blueshifted component in a much shorter time scale (~ 1 month; see Fig. 19).

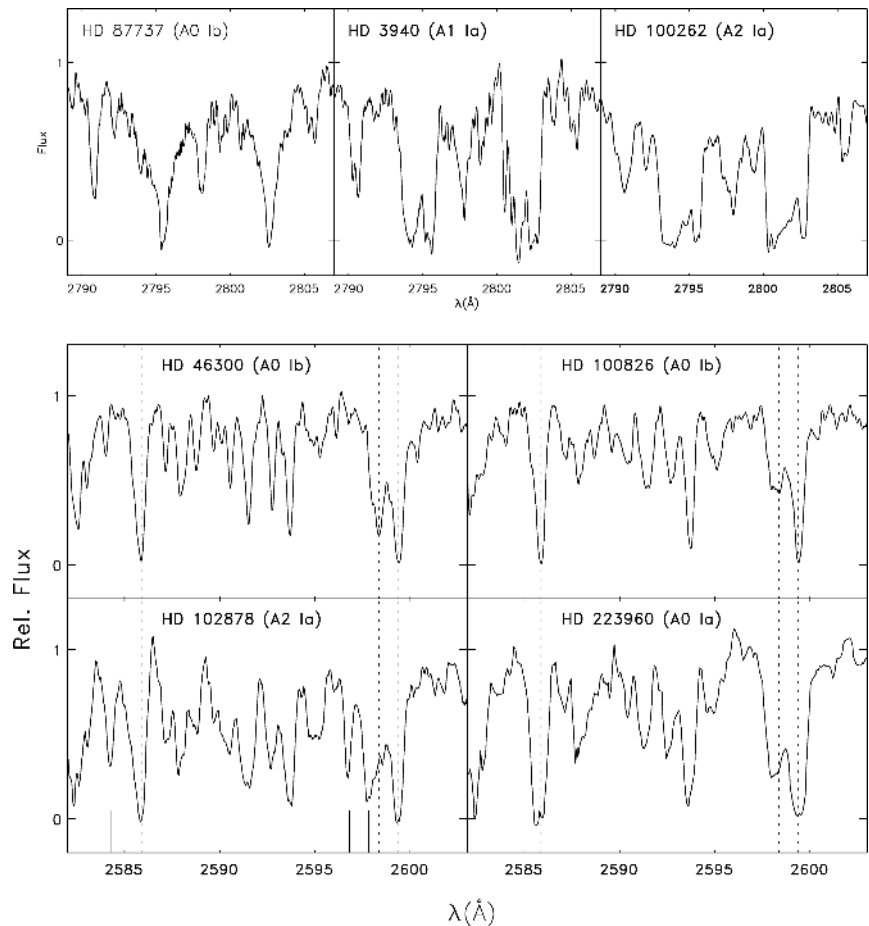
The DACs are stronger and more steady in luminous A-supergiants, whereas the Ib stars exhibit these features in a smoother but more variable way.

These two groups are also found from the analysis of the optical spectrum of A-supergiants (mainly from the H_{α} profile; Verdugo et al., 1999a, 2003). The existence of these two groups must lie in a different extension, density and properties, in general, between the envelope of the Alab supergiants and the one of the Alb supergiants. These differences suggest a different evolution history of these stars. In fact, Przybilla et al. (2005) found from the abundance analysis of four A-type supergiants (one Ib star and three Ia/lab stars), a blue-loop scenario for the only Ib star studied because of a first dredge up abundance ratios, while the other three objects appear to have evolved directly from the main sequence.

Another very interesting finding from the UV spectrum of A-supergiants which can also be linked with the evolution history of these stars is that there are some luminous stars which present a shortward shifted component at high velocity ($\sim -150 \text{ km s}^{-1}$) but there is not a component at zero velocity (except the interstellar components of the resonance lines) or this component is less intense than the high velocity one. Such behavior has been detected in the Fe II lines of some bright A-supergiants (see Fig. 8). In principle, the absence of a component at 0 km s^{-1} could be due to the fact that the lines of Fe II are only formed in the wind, which would have a lower degree of ionization than the photosphere. However, this phenomenon is only detected in a few stars of our sample. Most of the A-supergiants show a zero velocity component for the lines of this ion. It is possible that this component at 0 km s^{-1} is formed also in the wind. In a low density envelope where shocks could be occurring, the spectra would present a pre-shock component (high velocity) and a post-shock component (low velocity). Therefore, the presence or not of such zero velocity component would be related to the density of the wind.

One of the main predictions of the radiatively driven wind theory is that the terminal velocity of the wind should increase with the escape velocity of the star. However, as shown

Fig. 18 Mg II[uv1] (top) and Fe II[uv1] (bottom) in A-supergiants.



in Fig. 21, the opposite behavior is found in A-supergiants (Talavera and Gómez de Castro, 1987; Verdugo et al., 1997, 2003).

The terminal velocity, v_∞ , is the mean velocity reached by wind material in regions far away from the star, where acceleration has effectively ceased but interaction with the interstellar medium has not yet become important. The terminal velocities of the winds of A-type supergiants can be measured directly from the UV P Cygni profiles.

Traditionally, the terminal velocity of a stellar wind has been observationally defined as the modulus of the largest negative velocity seen in absorption in the P Cygni profiles of UV resonance lines. For a P Cygni profile with a deep absorption (saturated profiles) through and a nearly vertical violet edge, the measured edge velocity (v_{edge}) was considered the terminal velocity of the wind (Abbot 1978). However chaotic motions in the winds may extend and soften the vertical violet edge resulting in an overestimation of v_∞ . The difference $v_{\text{edge}} - v_\infty$ arising from a local velocity field, which has been parameterized as “microturbulence” by Hamann (1980, 1981) and Groenewegen et al. (1989). However, Howarth and Prinja (1989) demonstrate that for saturated ultraviolet line profiles the maximum velocity at which zero residual intensity is recorded (v_{black}) provides an accurate measure of

the wind terminal velocity. For stars without saturated profiles, but with identifiable discrete absorption components, the final central velocity reached by these components, $v_{\text{DAC}}(t \rightarrow \infty)$, also provides a good indicator of v_∞ (e.g. Howarth and Prinja, 1989). However, estimating this quantity observationally requires frequent UV spectra taken over a sufficiently extensive period, and such data are only available for a very few stars. Therefore from a single UV spectrum DACs only provide a lower limit to v_∞ .

In order to determine terminal velocities of A-type supergiants is required to analyze several UV spectra taken over a large period. The wavelength or velocity, v_{edge} , where the violet edge of the Mg II profiles reach the continuum provides an upper limit for the terminal velocities while in most cases the v_{DAC} is a lower limit.

Radiative winds are known to be unstable against small perturbations of the radiative force. However, such small perturbations in the wind cannot account for the aforementioned spectral features. The existence of magnetic fields is a more viable option and has been suggested by many different authors to explain the observations: (1) co-rotating interaction regions have been suggested to explain the presence of the UV DACs (Mullan 1984), (2) Co-rotating weak magnetic surface structures could explain the observed H_α variability

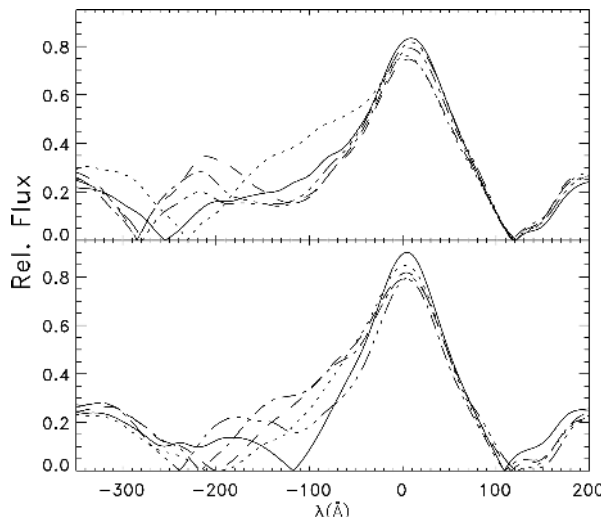


Fig. 19 Cross-correlation function for the Mg II resonance lines of HD46300 (top) and HD87737 (bottom). It is clear The appearance and evolution of a blueshifted component ($\sim -200 \text{ km s}^{-1}$) which migrates through the symmetric profile of the line.

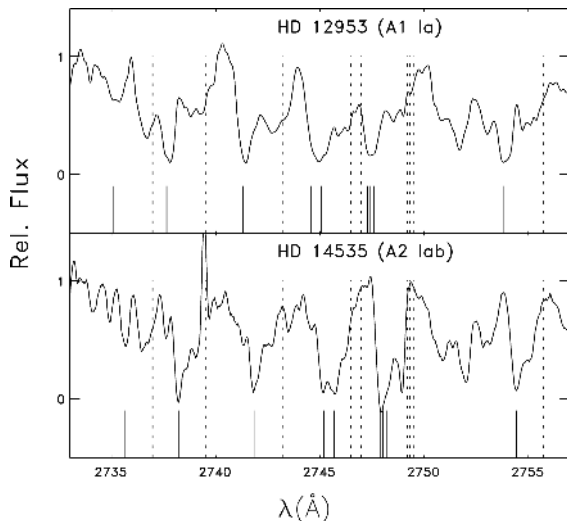


Fig. 20 Fe II [uv62],[uv63] lines in two A-supergiants showing no components at rest (dashed vertical line). The position of a high velocity component ($\sim -150 \text{ km s}^{-1}$) is marked with a solid vertical line

(Kaufer et al., 1996), and (3) The existence of extended cool loops could account for another phenomenon observed in BA supergiants: High Velocity Absorptions (HVA; see Israeli et al., 1997). All these facts have motivated us to undertake a search for magnetic fields in the atmospheres of A-supergiants (Verdugo et al., 2005, 2003). Spectropolarimetric techniques has been drastically improved in the last few years allowing to detect weak magnetic fields (of a few hundred gauss) in massive stars. Magnetic fields have been discovered in 5 OB stars (see Henrichs et al., 2005 for a recent review). Specific behavior of variable stellar wind lines belongs to the well-known indirect indicators of a magnetic field in early-type stars. Typical cyclical variability of the DACs associated

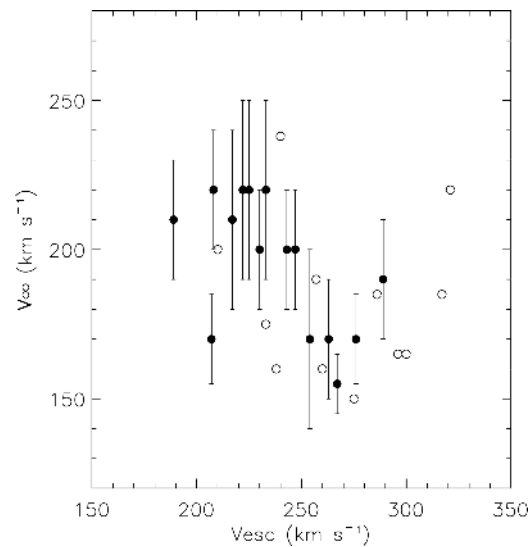


Fig. 21 Terminal velocity of the wind vs. escape velocity for A-type Supergiants. Empty circles correspond to stars for which the measured terminal velocity is uncertain due to the particular shape of the Mg II[uv1] lines

to UV lines are thought to be caused by magnetic fields at the base of the flow. Henceforth, analysis of the UV spectra variability is crucial to identify potential magnetic massive stars.

UV high resolution spectroscopy is therefore instrumental to make progress in the different open questions addressed above:

Is the radiation driven wind theory fully applicable to A-type supergiants? In addition, it seems to exist two different groups of A-type supergiants based on luminosity class but only a few UV spectra of luminosity class Ib stars are available. Therefore, high resolution spectra are needed to measure reliable wind parameters and to confirm the possible existence of two different types of A-supergiants. High resolution spectra are also needed to confirm the lack of UV Fe II resonance lines at rest in some of the brightest stars. Moreover, studies of UV variability are decisive to analyse the stellar winds properties, as well as the relevance of surface magnetic fields.

Acknowledgements

We would like to thank M. Urbaneja for providing some of the figures. F.N. acknowledges PNAYA2003-02785-E grant and the Ramon y Cajal program. This work has been partly supported by the Spanish MEC through PNAYA projects AYA2004-08271-C02-01 and 02.

References

- Aufdenberg, J.P.: Ph.D. Thesis, Arizona State Univ. (2000)
 Aufdenberg, J.P., Hauschildt, P.H., Baron, E., et al.: ApJ **570**, 344 (2002)

- Babel, J.: Astronomy and Astrophysics **301**, 823 (1995)
- Babel, J.: Astronomy and Astrophysics **309**, 867 (1996)
- Bianchi, L., García, M.: The effective temperatures of Mid-O stars. *Astrophysical Journal* **581**, 610 (2002)
- Bouret, J.C., Lanz, T., Hillier, D.J. et al.: Quantitative Spectroscopy of O Stars at Low Metallicity: O Dwarfs in NGC 346. *Astrophysical Journal* **595**, 1182 (2003)
- Bouret, J.-C., Lanz, T., Hillier, D.J.: Lower mass loss rates in O-type stars: Spectral signatures of dense clumps in the wind of two Galactic O4 stars. *Astronomy and Astrophysics* **438**, 301 (2005)
- Bresolin, F., Kudritzki, R.P., Lennon, D.J. et al.: Space Telescope Imaging Spectrograph Ultraviolet Spectroscopy of Early B Supergiants in M31. *Astrophysical Journal* **580**, 213 (2002)
- Castor, J.I., Abbott, D.C., Klein, R.I.: Radiation-driven winds in of stars. *Astrophysical Journal* **195**, 157 (1975)
- Crowther, P.A., Hillier, D.J., Evans, C.J., et al.: *Astrophysical Journal* **579**, 774 (2002)
- Evans, C.J., Crowther, P.A., Fullerton, A.W. Hillier, D.J.: *Astrophysical Journal* **610**, 1021 (2004)
- Eversberg, T., Lépine, S., Moffat, A.F.J.: *Astrophysical Journal* **494**, 799 (1998)
- Fullerton, A.W., Massa, D.L., Prinja, R.K.: *Astrophysical Journal* **637**, 1025 (2006)
- Gabler, R., Gabler, A., Kudritzki, R.P., Puls, J., Pauldrach, A.: Unified NLTE model atmospheres including spherical extension and stellar winds – Method and first results. *Astronomy and Astrophysics* **226**, 162 (1989)
- García, M., Bianchi, L.: The effective temperatures of hot stars. II. The Early-O Types *Astrophysical Journal* **606**, 497 (2004)
- Groenewegen, M.A.T., Lamers, H.J.G.L.M., Pauldrach, A.W.A.: *Astronomy and Astrophysics* **221**, 78 (1989)
- Hamann, W.-R.: *Astronomy and Astrophysics* **84**, 342 (1980)
- Hamann, W.R.: Line formation in expanding atmospheres – on the validity of the Sobolev approximation. *Astronomy Astrophysics* **93**, 353 (1981)
- Haser, S.M., Pauldrach, A.W.A., Lennon, D.J., Kudritzki, R.-P., Lennon, M., Puls, J., Voels, S.A.: Quantitative UV spectroscopy of early O stars in the Magellanic Clouds. The determination of the stellar metallicities. *Astronomy and Astrophysics* **330**, 285 (1998)
- Haser, S.: Ph.D. Thesis, Munich (1995)
- Heap, R.S., Lanz, T., Hubeny, I.: Fundamental properties of O Stars astro-ph/0412345 (2004)
- Henrichs, H.F., Schnerr, R.S., Ten Kulve, E.: ASPC **337**, 114 (2005)
- Hensberge, H., Lamers, H.J.G.L., de Loore, C., Bruhweiler, F.C.: *Astronomy Astrophysics* **106**, 137 (1982)
- Herrero, A., Puls, J., Corral, L.J., Kudritzki, R.P., Villamariz, M.R.: An Analysis of HST UV Spectra of Cyg OB2 stars. *Astronomy and Astrophysics* **366**, 623 (2001)
- Herrero, A., Puls, J., Najarro, F.: Fundamental parameters of Galactic luminous OB stars VI. Temperatures, masses and WLR of Cyg OB2 supergiants *Astronomy and Astrophysics* **396**, 949 (2002)
- Hillier, D.J., Lanz, T., Heap, S., et al.: *Astrophysical Journal* **588**, 1039 (2003)
- Hillier, D.J., Miller, D.L.: *Astrophysical Journal* **496**, 407 (1998)
- Howarth, I.D., Prinja, R.K.: The stellar winds of 203 Galactic O stars - A quantitative ultraviolet survey, *Astrophysical Journal Supplement* **69**, 527 (1989)
- Israelian, G., Chentsov, E., Musaev, F.: *MNRAS* **290**, 521 (1997)
- Kaufer, A., Stahl, O., Wolf, B., et al.: *Astronomy and Astrophysics* **305**, 887 (1996)
- Kudritzki, R.P., Pauldrach, A., Puls, J., Abbott, D.C.: Radiation-driven winds of hot stars. VI – Analytical solutions for wind models including the finite cone angle effect. *Astronomy Astrophysics* **219**, 205 (1989)
- Kudritzki, R.-P.: Quantitative Spectroscopy of the Brightest Blue Supergiant Stars in Galaxies Stellar astrophysics for the local group: VIII Canary Islands Winter School of Astrophysics **149** (1998)
- Kudritzki, R.-P., Puls, J.: Winds from hot stars *Annual Review of Astronomy and Astrophysics* **38**, 613 (2000)
- Kudritzki, R.P., Puls, J., Lennon, D.J., Venn, K.A., Reetz, J., Najarro, F., McCarthy, J.K., Herrero, A.: The wind momentum-luminosity relationship of galactic A- and B-supergiants. *Astronomy and Astrophysics* **350**, 970 (1999)
- Lamers, H.J.G.L.M., Haser, S., de Koter, A., Leitherer, C.: The Ionization in the Winds of O Stars and the Determination of Mass-Loss Rates from Ultraviolet Lines. *Astrophysical Journal* **516**, 872 (1999)
- Lamers, H.J.G.L.M., Snow, T.P., Lindholm, D.M.: *ApJ* **455**, 269 (1995)
- Lamers, H.J.G.L.M., Stalio, R., Kondo, Y.: *ApJ* **223**, 207 (1978)
- Lamers, H.J.G.L.M., Snow, T.P.: *ApJ* **219**, 504 (1978)
- Lépine, S., Moffat, A.F.J. *Astrophysical Journal* **514**, 909 (1999)
- Macfarlane, J.J., Cohen, D.H., Wang, P.: X-ray induced ionization in the winds of near-main-sequence O and B stars *Astrophysical Journal* **437**, 351 (1994)
- Massa, D., Fullerton, A.W., Sonneborn, G., et al.: *Astronomy and Astrophysics* **586**, 996 (2003)
- Markova, N., Puls, J., Repolust, T., et al.: *Astronomy and Astrophysics* **413**, 693 (2004)
- Martins, F., Schaerer, D., Hillier, D.J.: *Astronomy and Astrophysics* **382**, 999 (2002)
- Martins, F., Schaerer, D., Hillier, D.J., Heydari-Malayeri, M.: Puzzling wind properties of young massive stars in SMC-N81 *Astronomy and Astrophysics* **420**, 1087 (2004)
- Martins, F., Schaerer, D., Hillier, D.J.: *Astronomy and Astrophysics* **436**, 1049 (2005)
- Martins, F., Schaerer, D., Hillier, J., Meynadier, F., Heydari-Malayeri, M., Walborn, N.O.: stars with weak winds: the Galactic case *Astronomy and Astrophysics* **441**, 735 (2005)
- Massey, P., Bresolin, F., Kudritzki, R.P., Puls, J., Pauldrach, A.W.A.: *Astrophysical Journal* **608**, 1001 (2004)
- Massey, P., Puls, J., Pauldrach, A.W.A. et al.: The Physical Properties and Effective Temperature Scale of O-Type Stars as a Function of Metallicity. II. Analysis of 20 More Magellanic Cloud Stars and Results from the Complete Sample *Astrophysical Journal* **627**, 477 (2005)
- McErlean, N.D., Lennon, D.J., Dufton, P.L.: *Astronomy and Astrophysics* **349**, 553 (1999)
- Meynet, G., Maeder, A., Schaller, G., et al.: *Astronomy and Astrophysics* **103**, 97 (1994)
- Najarro, F., Kudritzki, R.P., Cassinelli, J.P., Stahl, O., Hillier, D.J.: Stellar winds and the EUV continuum excess of early B-giants. *Astronomy and Astrophysics* **306**, 892 (1996)
- Najarro, F.: Spectroscopy of P Cygni ASP Conf. Ser. 233: P Cygni 2000: 400 Years of Progress p **133** (2001)
- Najarro, F., Figer, D.F., Hillier, D.J., Kudritzki, R.P.: Metallicity in the Galactic Center: The Arches Cluster *Astrophysical Journal Letters*, **611**, L105 (2004)
- Owocki, S.P., Puls, J.: *Astrophysical Journal* **510**, 355 (1999)
- Pauldrach, A.W.A., Kudritzki, R.P., Puls, J., Butler, K., Hunsinger, J.: Radiation-driven winds of hot luminous stars. 12: A first step towards detailed UV-line diagnostics of O-stars. *Astronomy and Astrophysics* **283**, 525 (1994)
- Pauldrach, A.W.A., Hoffmann, T.L., Lennon, M.: *Astronomy and Astrophysics* **375**, 161 (2001)
- Praderie, F., Talavera, A., Lamers, H.J.G.L.M.: *Astronomy and Astrophysics* **86**, 271 (1980)

- Prinja, R.K., Massa, D., Searle, S.C.: *Astronomy and Astrophysics* **430**, L41 (2005)
- Prinja, R.K., Crowther, P.A.: HSTUV measurements of wind structure and velocities in Local Group OB stars, *Monthly Notices of the Royal Astronomical Society* **300**, 828 (1998)
- Przybilla, N., Butler, K., Becker, S.R., Kudritzki, R.P.: *Astronomy and Astrophysics*, astro-ph/0509969 (2005)
- Puls, J., Kudritzki, R.P., Herrero, A. et al.: O-star mass-loss and wind momentum rates in the Galaxy and the Magellanic Clouds Observations and theoretical predictions *Astronomy and Astrophysics* **305**, 171 (1996)
- Puls, J., Kudritzki, R.P., Santolaya-Rey, A.E., Herrero, A., Owocki, S.P.: Proc. 2nd Boulder-Munich Workshop, *PASP* **131**, 245 (1998)
- Puls, J., Springmann, U., Lennon, M.: Radiation driven winds of hot luminous stars. XIV. Line statistics and radiative driving *Astronomy and Astrophysics Supplement Series* **141**, 23 (2000)
- Puls, J., Urbaneja, M.A., Venero, R., et al.: *Astronomy and Astrophysics* **435**, 669 (2005)
- Repolust, T., Puls, J., Herrero, A.: *Astronomy and Astrophysics* **415**, 349 (2004)
- Santolaya-Rey, A.E., Puls, J., Herrero, A.: *Astronomy and Astrophysics* **323**, 488 (1997)
- Springmann, U.W.E., Pauldrach, A.W.A.: *Astronomy and Astrophysics* **262**, 515 (1992)
- Talavera, A., Gómez de Castro, A.I.: *Astronomy and Astrophysics* **181**, 300 (1987)
- Trundle, C., Lennon, D.J., Puls, J., Dufton, P.L.: *Astronomy and Astrophysics* **417**, 217 (2004)
- Trundle, C., Lennon, D.J.: Understanding B-type supergiants in the low metallicity environment of the SMC II *Astronomy and Astrophysics* **434**, 677 (2005)
- Underhill, A.B., Doazan, V.: B stars with and without emission lines, NASA SP-456 (1982)
- Urbaneja, M.A.: Ph.D. Thesis, La Laguna (2004)
- Urbaneja, M.A., Herrero, A., Kudritzki, R.P. et al.: An analysis of STIS HST UV spectra of M 33 early B supergiants. *Astronomy and Astrophysics* **386**, 1019 (2002)
- Vacca, W.D., Garmany, C.D., Shull, J.M.: *ApJ* **460**, 914 (1996)
- Venn, K.A.: *ApJ* **449**, 839 (1995a)
- Venn, K.A.: *ApJSS* **99**, 659 (1995b)
- Verdugo, E., Talavera, A., Gómez de Castro, A.I.: *ESA SP-413* **293** (1997)
- Verdugo, E., Talavera, A., Gómez de Castro, A.I.: *Astronomy and Astrophysics* **346**, 819 (1999a)
- Verdugo, E., Talavera, A., Gómez de Castro, A.I.: *Astronomy and Astrophysics SS* **137**, 351 (1999b)
- Verdugo, E., Talavera, A., Gómez de Castro, A. I., Henrichs, H. F., Geers, V. C., Wiersema, K.: *ASPC* **305**, 364 (2003)
- Verdugo, E., Henrichs, H.F., Talavera, A., Gómez de Castro, A.I., Schnerr, R.S., Geers, V.C.: *ASPC* **337**, 324 (2005)
- Verdugo, E., Talavera, A., Gómez de Castro, A.I.: *Astronomy and Astrophysics*, in preparation (2006)
- Vink, J.S., de Koter, A., Lamers, H.J.G.L.M.: New theoretical mass-loss rates of O and B stars. *Astronomy and Astrophysics* **362**, 295 (2000)
- Vink, J.S., de Koter, A., Lamers, H.J.G.L.M.: Mass-loss predictions for O and B stars as a function of metallicity. *Astronomy and Astrophysics* **369**, 574 (2001)